

LABEL-FREE DETECTION AND DIFFERENTIATION OF FOODBORNE PATHOGENIC  
BACTERIA IN FRESH PRODUCE BY SURFACE-ENHANCED RAMAN SPECTROSCOPY

by

XIAOMENG WU

(Under the Direction of Yao-Wen Huang and Yiping Zhao)

ABSTRACT

Surface-enhanced Raman scattering (SERS) based platform has been previously used for the detection of bacteria. However, these studies had a generally poor sensitivity and specificity that are not practical for the use in food safety applications, and these studies have been conducted with pure lab strains without any consideration of the influence from food samples. This dissertation therefore focuses on the optimization of silver nanorod (AgNR) array substrates to achieve better detection and differentiation of foodborne pathogenic bacteria, as well as its application in the fresh produce.

The origins of the bacterial SERS signal have been studied by thoroughly investigating the impact of cell disruption on SERS signal of bacteria. Important bacterial cell components have been isolated and their SERS spectra are obtained. In addition, the effect of each cell component on the differentiation of the bacteria has also been studied.

The AgNR substrates have been functionalized with vancomycin, and the sensitivity of the functionalized substrates has been optimized. The vancomycin coating on the substrates surface not only captures more bacteria from the solution, but also reduces the distance between bacteria and the substrate surface, resulting in a significant increase on the sensitivity. Such

functionalized substrates also show improved specificity when differentiating bacteria, compared to the pristine AgNR substrates. The differentiation of bacteria between species, strains, and serotypes has been achieved with chemometric analysis, as well as the classification between Gram positive and Gram negative bacteria.

The feasibility of utilizing the vancomycin functionalized AgNR substrates in the detection and differentiation of foodborne pathogenic bacteria from real food samples has also been investigated. Combining with simple filtration methods, low concentration of bacteria have been detected in various fresh produce samples, and the differentiation between bacteria has also been investigated. This SERS based method shows great agreement with conventional bacteria detection method, and the use of bench-top and handheld Raman spectrometers makes the system field-deployable. It has the potential to be used as an on-site pathogen detection method in the food industry.

**INDEX WORDS:** Surface-enhanced Raman spectroscopy, silver nanorods, foodborne bacteria, label-free, culture-free, chemometric analysis, rapid detection, food safety, fresh produce

LABEL-FREE DETECTION AND DIFFERENTIATION OF FOODBORNE PATHOGENIC  
BACTERIA IN FRESH PRODUCE BY SURFACE-ENHANCED RAMAN SPECTROSCOPY

by

XIAOMENG WU

B.S., Purdue University, 2009

B.E., China Agricultural University, China, 2009

A Dissertation Submitted to the Graduate Faculty of The University of Georgia in Partial  
Fulfillment of the Requirements for the Degree

DOCTOR OF PHILOSOPHY

ATHENS, GEORGIA

2014

© 2014

Xiaomeng Wu

All Rights Reserved

LABEL-FREE DETECTION AND DIFFERENTIATION OF FOODBORNE PATHOGENIC  
BACTERIA IN FRESH PRODUCE BY SURFACE-ENHANCED RAMAN SPECTROSCOPY

by

XIAOMENG WU

Major Professor: Yao-Wen Huang  
Yiping Zhao  
Committee: Mark A. Harrison  
Ralph A. Tripp  
Bosoon Park

Electronic Version Approved:

Julie Coffield  
Interim Dean of the Graduate School  
The University of Georgia  
August 2014

## ACKNOWLEDGEMENTS

I would like to express my deepest gratitude to my major advisor Dr. Yao-Wen Huang for taking me as his student and years of guidance and financial supports. His scholarly guidance transferred me from a fresh graduate student to a future food scientist as I am today. I am also grateful to my co-advisor, Dr. Yiping Zhao for treating me as one of his own group members and also offered scientific and financial assistance. Years of training in his lab taught me everything I know and I need to know for being a scientist. I would like to thank my advisory committee members Dr. Ralph Tripp, Dr. Mark Harrison, and Dr. Bosoon Park for their guidance and generosity to allow me to use their facilities over the years.

I also owe special thanks to Dr. Justin L. Abell, who taught me the research techniques that are essential to the completion of this dissertation. I would like to thank Dr. Susu Zughailer, Dr. Rene Alvarez, and Dr. Alexander Burdette for their scientific insights and help in the preparation of this dissertation. Ms. Ruth Ann Morrow and Ms. Gwen Hirsch are also acknowledged for their helpful technical assistance.

I thank my family and friends for years of moral support. I would not have gone this far without their love, encouragement, and sacrifices.

Finally, I would like to acknowledge many of my fellow lab members in Dr. Huang and Dr. Zhao's labs, both past and present, for their help over the years: Ms. Chao Xu, Ms. Jing Chen, Ms. Lu Shen, Dr. Yongjun Liu, Dr. Yuping He, Dr. Jianguo Fan, Dr. Chunyuan Song, Ms. Whitney Ingram, Dr. Caiqin Han, Mr. Monaj Manjare, Mr. George Larson, Mr. Yizhuo He, Mr. Pradip Basnet, Mr. Layne Bradley, Ms. Lu Zhu, and Mr. Funing Chen.

## TABLE OF CONTENTS

	Page
ACKNOWLEDGEMENTS .....	iv
LIST OF TABLES .....	vii
LIST OF FIGURES .....	viii
CHAPTER	
1 INTRODUCTION .....	1
2 LITERATURE REVIEW .....	6
3 UNDERSTANDING BACTERIAL SERS SPECTRA.....	60
4 SERS COUPLED WITH TWO SAMPLING TECHNIQUES FOR DETECTION OF SALMONELLA TYPHIMURIUM.....	97
5 DETECTION AND DIFFERENTIATION OF FOODBORNE PATHOGENIC BACTERIA IN MUNG BEAN SPROUTS USING FIELD DEPLOYABLE LABEL- FREE SERS DEVICES .....	114
6 DIFFERENTIATION AND CLASSIFICATION OF BACTERIA USING SERS SPECTRA AND CHEMOMETRIC ANALYSIS .....	141
7 DETECTION OF PATHOGENIC BACTERIA IN CANTALOUPE CUBES AND LETTUCE USING SERS .....	174
8 CONCLUSIONS AND FUTURE PERSPECTIVES .....	198
APPENDICES	
A SUPPLEMENTARY MATERIAL FOR CHAPTER 5.....	203

B SUPPORTING INFORMATION FOR CHAPTER 6.....212

## LIST OF TABLES

	Page
Table 2.1: Summary of the common food source of outbreaks and the associated bacteria .....	7
Table 2.2: Summary of the current bacteria detection methods .....	16
Table 3.1: SERS/Raman peaks from important cell components that may contribute to the SERS of bacterial cells .....	84
Table 3.2: SERS peaks of important cell components as well as the whole bacterial cells. √ indicates that the peak is present in the SERS spectra of this component .....	95
Table 6.1: A list of bacteria used in this paper. The bacteria isolated from chicken carcass rinses are denoted as USDACR. The isolates from patients at Walter Reed Medical Center are denoted as WRAMC and the isolates from patients at Brooke Army Medical Center are denoted as BAMC.....	167
Table 7.1: The bacteria concentration after each filtration steps for a three-step filtration with HFTS treated PTFE filter.....	197
Table B.1: Literature summary on the use of chemometric analysis to differentiate bacteria based on SERS technique .....	213

## LIST OF FIGURES

	Page
<p>Figure 2.1: The schemes of immunological methods for bacteria detection. In (A) IMS, (i) antibody coated magnetic beads are added to the solution with bacteria and food samples. (ii) Beads bind to the specific antigens on bacteria surface. (ii) Bacteria-bead complexes are isolated by external magnetic field. In (B) ELISAs, (i) antibodies are immobilized on solid plate. (ii) Food samples with bacteria are applied to the solid plate, where bacteria are captured by the immobilized antibodies, while food samples are washed away. (iii) Fluorescence labeled secondary antibodies are conjugated to the complex, and (iv) the signal from the label is read by the detector. ....</p>	10
<p>Figure 2.2: Scheme of the polymerase chain reaction (PCR).....</p>	12
<p>Figure 2.3: The Rayleigh and Raman scattering process. <math>m</math> indicates the ground vibrational state. <math>n</math> indicates the excited vibrational state. The dotted lines indicate the virtual states. Upward arrows indicate the process of the promotion of the molecule, and downward arrows indicate the process the photons being scattered .....</p>	17
<p>Figure 2.4: Morphology of the SERS substrates for bacterial detection. (A) Au-MNPs, (B) AgNCs, (C) AAO. (A adapted with permission from reference 80, Copyright Elsevier 2012; B adapted with permission from reference 72, Copyright ACS 2010; C adapted with permission from reference 73, Copyright John Wiley and Sons 2006).....</p>	27
<p>Figure 2.5: Representative SEM image of the AgNR substrates (<math>\alpha = 86^\circ</math>).....</p>	28

Figure 2.6: SERS spectra of four bacterial species obtained on AgNR substrates. EC = *E. coli* O157:H7; ST = *Salmonella*. Typhimurium; SA = *Staphylococcus aureus* and SE = *Staphylococcus epidermidis*. Incident laser power of 24 mW and collection time of 10 s are used to obtain these spectra. Spectra are offset vertically for display clarity. (Reproduced with permission from reference 70. Copyright SAS 2008).....30

Figure 2.7: SERS spectra of viable *E. coli* O157:H7 and non-viable *E. coli* O157:H7. Incident laser power of 14 mW and collection time of 10 s are used to obtain these spectra. Spectra are offset vertically for display clarity. (Reproduced with permission from reference 70. Copyright SAS 2008).....31

Figure 2.8: The scheme of the immune-SERS platform for multiplexing bacteria detection. (i) Fabrication of immune-conjugated nanoparticles. The core of the nanoparticles can be magnetic. Different nanoparticle have conjugated immune molecules specific to individual bacteria, and are labeled with unique Raman dye. (ii) Adding different immune-conjugated nanoparticles into bacteria mixture solution. (iii) Capture and isolation of nanoparticles with external magnetic field. (iv) Measuring the SERS of the complex to obtain SERS spectra of Raman dyes.....39

Figure 3.1: Cell components of a bacteria cell that may contribute to the overall SERS spectra of bacteria.....86

Figure 3.2: The SERS spectra of *E. Coli* O157:H7 after filtration.....87

Figure 3.3: The SERS spectra of *E. Coli* O157:H7 (EC) undisrupted, after ultrasonic disruption, and the precipitates and supernatants after centrifugation of the disrupted cells .....88

Figure 3.4: PCA scores of the spectra of *Bacillus subtilis* (BS), *E. Coli* O157:H7 (EC), *Listeria monocytogenes* (LM), and *Staphylococcus aureus* (SA) at different conditions. (A)

Undisrupted cells, (B) cells after ultrasonic disruption, (C) supernatants, and (D) precipitates of the disrupted cell after centrifugation. ....	89
Figure 3.5: SERS spectra of NAG, NAM, and two bacteria isolates, <i>E. Coli</i> O157:H7 (EC) and <i>Listeria monocytogenes</i> (LM).....	90
Figure 3.6: SERS spectra of <i>E. Coli</i> O157:H7 (EC) before and after EDTA treatment and the spectra of pure EDTA .....	91
Figure 3.7: SERS spectra of extracted cell wall associated protein from <i>Bacillus subtilis</i> (BS), <i>E. Coli</i> O157:H7 (EC), <i>Listeria monocytogenes</i> (LM), and <i>Staphylococcus aureus</i> (SA) as well as the SERS spectra of the buffer used in the process .....	92
Figure 3.8: (A) SERS spectra of genomic DNA from <i>Bacillus subtilis</i> (BS), <i>E. Coli</i> O157:H7 (EC), <i>Listeria monocytogenes</i> (LM), and <i>Staphylococcus aureus</i> (SA). (B) the 3D PCA score plot of these four spectra .....	93
Figure 3.9: SERS spectra of inner cell water soluble protein from <i>Bacillus subtilis</i> (BS), <i>E. Coli</i> O157:H7 (EC), <i>Listeria monocytogenes</i> (LM), and <i>Staphylococcus aureus</i> (SA).....	94
Figure 4.1: Scheme of centrifugation method with SERS for bacterial detection.....	110
Figure 4.2: (A) SERS spectra of <i>Salmonella Typhimurium</i> prepared by centrifugation method at different concentration. Red number indicated the peaks from the bacteria. (B) Peaks intensity $I_{735}$ as a function of the concentration of <i>Salmonella Typhimurium</i> samples prepared by centrifugation method. Horizontal line indicates the threshold for a positive detection of the bacteria.....	111
Figure 4.3: (A) SEM pictures of $10^9$ CFU/ml <i>Salmonella typhimurium</i> on AgNR prepared by pipette method. The lack of inductance made the bacteria darker in the SEM; while the underneath Ag appeared brighter under SEM view. The more concentrated bacteria form	

a “ring” around the edge of the droplet. (B) The SEM picture of  $10^7$  CFU/ml *Salmonella typhimurium* on AgNR substrate prepared by centrifugation method, showing the even distribution of bacteria throughout the whole substrate surface .....112

Figure 4.4: (A) SERS spectra of *Salmonella Typhimurium* prepared by two-step filtration method at different concentration. Red number indicated the peaks from the bacteria. (B) The SERS peak intensity  $I_{735}$  as a function of the concentration of *Salmonella Typhimurium* samples prepared by filtration method. Horizontal line indicates the threshold for a positive detection of the bacteria .....113

Figure 5.1: Flow chart of the two-step filtration procedure.....135

Figure 5.2: (A) The SERS spectra and (B) the mean and standard deviation of the SERS peak intensity  $I_{728}$  of *E. Coli* O157:H7 at different concentrations ( $C_B = 10^4, 10^5, 10^6$  CFU/ml) and sterile DI water. Significant peaks from the *E. Coli* O157:H7 sample are indicated in red and the significant peaks from the vancomycin coating layer are indicated in black. Spectra were measured by the Enwave Raman system .....136

Figure 5.3: (A) The SERS spectra, and (B) the mean and standard deviation of the SERS peak intensity  $I_{728}$  of *E. Coli* O157:H7 recovered from mung bean sprouts samples inoculated at different rates and sterile DI water inoculated in mung bean sprouts samples (control) followed by a two-step filtration. Spectra were measured by the Enwave Raman system .....137

Figure 5.4: (A) PCA and (B) PLS-DA plot of SERS spectra of *E. coli* O157:H7 recovered from mung bean sprouts samples inoculated at different rates ( $C_B = 10^2, 10^3, 10^4, 10^5$  CFU/ml) and sterile DI water inoculated in mung bean sprouts samples (control) followed by a two-step filtration. Spectra were collected using the Enwave Raman spectrometer .....138

Figure 5.5: (A) SERS spectra, and (B) the mean and standard deviation of the peak intensities  $I_{728}$  from the SERS spectra of six different pathogens inoculated at  $10^2$  CFU/ml on mung bean sprouts samples followed by a two-step filtration: *Salmonella enterica* serotype Anatum (SA), *Salmonella enterica* serotype Cubana (SC), *Salmonella enterica* serotype Stanley (SS), *Salmonella* Enteritidis (SE), *E. coli* O157:H7 (EC), and *Staphylococcus epidermidis* (STE). Spectra were measured by the Enwave Raman system.....139

Figure 5.6: PCA plot of (A) six different pathogens, *Salmonella enterica* serotype Anatum (SA), *Salmonella enterica* serotype Cubana (SC), *Salmonella enterica* serotype Stanley (SS), *Salmonella* Enteritidis (SE), *E. coli* O157:H7 (EC), and *Staphylococcus epidermidis* (STE), and (B) four different *Salmonella* species, SA, SC, SE, and SS inoculated at  $10^2$  CFU/ml on mung bean sprouts samples followed by a two-step filtration.....140

Figure 6.1: SERS of bacteria generated on the pristine substrates. (A) Representative bacterial SERS spectra. The red boxed peaks originate from bacteria, while black boxed peaks are from environmental contamination. (B) The 3D PCA score plot of the SERS spectra on the pristine substrates shows G+ bacteria as unfilled symbols and the G- bacteria are indicated as filled symbols. Bacteria of the same species, regardless of the strains and serotypes, are indicated as symbols of the same color.....168

Figure 6.2: SERS of bacteria generated on the VAN AgNR substrates. (A) Representative bacterial SERS spectra. The red boxed peaks originate from bacteria, while black boxed peaks are from VAN coating. (B) The 3D PCA score plot of the SERS spectra on the VAN AgNR substrates shows G+ bacteria as unfilled symbols and the G- bacteria are indicated as filled symbols. Bacteria of the same species, regardless of the strains and serotypes, are represented by symbols of the same color .....169

Figure 6.3: The HCA dendrogram based on the bacterial SERS spectra generated on the VAN AgNR substrates. Bacterial isolates of the same species are represented by lines of the same color .....170

Figure 6.4: Differentiation of five different serotypes of *Salmonella* species based on the chemometric analysis of the SERS spectra generated on the VAN AgNR substrates. (A) The 3D PCA score plot and (B) HCA plot .....171

Figure 6.5: Differentiation of five different strains of *Staphylococcus aureus* (SA) based on the chemometric analysis of the SERS spectra generated on the VAN AgNR substrates. (A) The 3D PCA score plot and (B) HCA plot .....172

Figure 6.6: Classification between G+ and G- bacteria based on the chemometric analysis of the SERS spectra generated on the VAN AgNR substrates. (A) PCA score plot of PC1 vs. PC3 and (B) PLS-DA score plot. G+ bacteria are indicated as unfilled symbols and the G- bacteria are indicated as filled symbols. Bacteria of the same species, regardless of the strains and serotypes, are represented by symbols of the same color. Black horizontal line in (B) indicates the threshold generated by the model to discriminate G+ and G- bacteria.....173

Figure 7.1: Flow chart of the three-step filtration procedure for the recovery of *Salmonella* Poona from cantaloupe cubes samples .....190

Figure 7.2: Flow chart of the three-step filtration procedure for the recovery of *E. coli* O157:H7 from lettuce samples .....191

Figure 7.3: (A) The SERS spectra, and (B) the mean and standard deviation of the SERS peak intensity  $I_{728}$  of *Salmonella* Poona recovered from cantaloupe cube samples inoculated at

different rates and sterile DI water inoculated in cantaloupe cube samples (control) followed by a two-step filtration.....	192
Figure 7.4: SERS spectra of <i>E. coli</i> O157:H7 recovered from lettuce samples inoculated at $10^4$ CFU/ml and sterile DI water inoculated in lettuce samples followed by a two-step filtration.....	193
Figure 7.5: Chemical structures of (A) adenine and (B) chlorophyll .....	194
Figure 7.6: (A) The UV-Vis absorbance of the lettuce samples processed with different filtration methods. (B) SERS spectra of lettuce samples processed by three-step filtration methods. No bacterium was inoculated on the lettuce samples .....	195
Figure 7.7: (A) The SERS spectra, and (B) the mean and standard deviation of the SERS peak intensity $I_{728}$ of <i>E. coli</i> O157:H7 recovered from lettuce samples inoculated at different rates and sterile DI water inoculated in lettuce samples (control) followed by a three-step filtration method with HFTS treated PTFE filter.....	196
Figure A.1: (A) SERS spectra and (B) the SERS peak intensity $I_{728}$ of $10^8$ CFU/ml <i>E. coli</i> O157:H7 samples on AgNR with QCM thickness $d$ of 200, 300, 400, 500, 600, 700, 800, and 900 nm, respectively. Spectra were measured by Enwave Raman system .....	205
Figure A.2: SEM images of AgNR with 600 nm thickness (QCM reading). (A) Top view. (B) Cross view.....	206
Figure A.3: The change of the SERS peak intensity $I_{728}$ of $10^8$ CFU/ml <i>E. Coli</i> O157:H7 as a function of the Vancomycin concentration $C_v$ . .....	206
Figure A.4: The SERS spectrum of the 1mM Van-coated 600 nm AgNR substrates collected by using Enwave Raman spectrometer. The spectrum is baseline-corrected, and the significant peaks are identified .....	207

Figure A.5: SERS spectra of *E. Coli* O157:H7 recovered from mung bean sprout samples inoculated at different rates ( $C_B = 10^2, 10^3, 10^4, 10^5$  CFU/ml) followed by a two-step filtration, collected using the FirstDefender RM handheld Raman spectrometer .....209

Figure A.6: (A) PCA and (B) PLS-DA plot of SERS spectra of *E. coli* O157:H7 recovered from mung bean sprout samples inoculated at different bacteria concentrations ( $C_B = 10^2, 10^3, 10^4, 10^5$  CFU/ml) and sterile DI water inoculated in mung bean sprout samples (control) followed by a two-step filtration. Spectra were collected by the FirstDefender RM handheld Raman spectrometer.....210

Figure B.1: PCA loading score plot based on the bacterial SERS spectra generated on pristine substrates which corresponds to the PCA plot in Figure 6.1B. The large absolute value on the y-axis suggests heavier weight in the analysis. The SERS peaks with heavy weight in each PC are numbered and the percentages associated with each PC represent the variances explained with that PC.....212

Figure B.2: PCA loading score plot based on the bacterial SERS spectra generated on VAN AgNR substrates which corresponds to the PCA plot in Figure 6.2B. The large absolute value on the y-axis suggests heavier weight in the analysis. The SERS peaks with heavy weight in each PC are numbered and the percentages associated with each PC represent the variances explained with that PC.....215

Figure B.3: PCA loading score plot based on the bacterial SERS spectra of five different serotypes of *Salmonella* species generated on VAN AgNR substrates which corresponds to the PCA plot in Figure 6.4A. The large absolute value on the y-axis suggests heavier weight in the analysis. The SERS peaks with heavy weight in each PC are numbered and

the percentages associated with each PC represent the variances explained with that PC.....216

Figure B.4: PCA loading score plot based on the bacterial SERS spectra of five different strains of *Staphylococcus aureus* (SA) generated on VAN AgNR substrates which corresponds to the PCA plot in Figure 6.5A. The large absolute value on the y-axis suggests heavier weight in the analysis. The SERS peaks with heavy weight in each PC are numbered and the percentages associated with each PC represent the variances explained with that PC.....217

Figure B.5: Differentiation of five different strains of *Acinetobacter baumannii* (AB) based on the chemometric analysis of the SERS spectra generated on the VAN AgNR substrates. (A) The 3D PCA score plot and (B) HCA plot.....218

Figure B.6: PLS-DA loading score plot for classification between G+ and G- bacteria based on the spectra generated on VAN AgNR substrates which corresponds to the PLS-DA plot in Figure 6.6B. The large absolute value on the y-axis suggests heavier weight in the analysis. The SERS peaks with heavy weight are numbered .....219

Figure B.7: PLS-DA based on the bacterial SERS spectra generated on the pristine AgNR substrates. G+ bacteria are indicated as unfilled symbols and the G- bacteria are indicated as filled symbols. Bacteria of the same species, regardless of the strains and serotypes, are represented by symbols of the same color. Black horizontal line indicates the threshold generated by the model to discriminate G+ and G- bacteria.....220

## CHAPTER 1

### INTRODUCTION

As the concept of healthy diet being adopted by the general population, the consumption of the fresh produce has increased worldwide for the past several decades(1). However, the increased consumption of fresh produce is also associated with increased foodborne outbreaks linked to fresh produce(2). The fresh produce items that are often associated with foodborne outbreaks are berries, melons, seed sprouts, and salad-greens, and those outbreaks can be caused by bacteria, virus, and protozoa(3). Among the foodborne pathogenic bacteria, *Salmonella* is the top cause of outbreaks, followed by *E. coli*, *Clostridium*, *Shigella*, *Campylobacter*, *Yersinia*, *Bacillus*, and *Staphylococcus*(3, 4).

To ensure the safety of food processing chain, rapid and accurate bacteria detection methods are highly desired. The traditional culture based methods are sensitive and inexpensive, but their long detection time can not satisfy the demands of the modern food industry. Thus, new technologies such as immunological methods, molecular methods, and biosensors are developed over the past several decades. These methods are rapid and abut have fundamental restrictions limiting their uses in the field or processing plant. For example, PCR is based on nucleic acid amplification and consequently cannot discriminate nucleic acid amplified from viable and nonviable bacteria. Furthermore, PCR-based methods require substantial laboratory equipment and highly skilled personnel. Immunological detection, such as enzyme-linked immunosorbent assay (ELISA), has the advantage of being specific to bacterial type and strain, but it also

requires multiple steps, varied chemical reagents, and incubation time making this method impractical for “real-time” detection in the field.

As one of the feasible way to realize “real-time” detection, Raman spectroscopy has the potential for rapid detection of a wide range of chemical and biological substances (5). Raman spectroscopy is a spectroscopic method based on the inelastic photon scattering from the molecules(6). It can be used to identify the characteristic spectral pattern (often refers as “fingerprints”) of the molecules, and to determine the amount of the substances. Raman and the more advanced surface-enhanced Raman spectroscopy (SERS) are used to detect bacteria from various samples. Many researches have focused on the SERS of bacteria detection. Recent developments include improving its sensitivity, specificity, and detection of bacteria in real food samples. Although the detection and differentiation of bacteria using SERS has been successfully demonstrated, several challenges remain, especially for the detection of bacterial pathogens in real food samples(7). The first challenge is to improve the LOD of SERS. As the second challenge is to identify foodborne bacteria in naturally occurring food commodities, attention needs to be applied to sampling methods that are needed for field detection to separate pathogens from food matrix and concentrate pathogens at the same time. In addition, the heterogeneous distribution of contamination in food samples also needs to consider.

The overall purpose of this dissertation is to provide necessary scientific and technical foundation for the development of label-free SERS platform to detect and differentiate low amount of foodborne pathogenic bacteria in real food samples. In order to realize this goal, four specific research topics will be investigated. (1) Understanding the origins of bacterial SERS spectra. (2) Optimization of SERS substrates for sensitive bacteria detection. (3) Differentiation multiple bacteria between species, strains, and serotypes. (4) Detection of pathogenic bacteria in

fresh produce samples using SERS.

This dissertation is divided into eight chapters. The second chapter will thoroughly review the current detection methods for bacteria to provide a summary of their advantages and disadvantages. The recent research development in the field of SERS of bacteria will also be reviewed, with the emphasis on understanding the origins of the bacterial SERS signals, the development on increasing specificity and sensitivity of the methods, and the detection in food samples. Chapter three will present a thorough investigation on the origins of the bacteria SERS spectra through isolating and analysing each important cell components. Such an investigation will provide us with the foundation to better understand bacterial SERS spectra and to guide the design of bacteria detection methods. Chapter four will explain how to increase SERS detection sensitivity through combining SERS with two pre-concentration methods, the centrifugation and filtration method. Chapter five will also introduce a vancomycin coated silver nanorod array (VAN AgNR) substrate to help improving bacteria capture and SERS sensitivity. It will also demonstrate the use of VAN AgNR substrates for the bacteria detection and differentiation in mung bean sprouts samples, when two-step filtration procedure is used. Chapter six will demonstrate the advantage of VAN AgNR substrates on differentiating the bacteria due to its capability to eliminate the interferences from environmental contamination and the bacterial by-products. Chemometric analyses, i.e. PCA, HCA, and PLS-DA will be applied to the bacterial SERS spectra obtained on VAN AgNR substrates, to allow for the differentiation of 27 bacteria based on their species, serotypes, and strains. This chapter will also validate the classification between Gram positive and Gram negative bacteria. Chapter seven will demonstrate the use of VAN AgNR substrates for the bacteria detection and differentiation in various fresh produce samples, such as cantaloupe cubes and lettuce. Both two-step filtration and three-step filtration

methods with modified filters will be used to eliminate the interferences from the food matrix in order to ensure the success of the SERS detection methods. At last, chapter eight will summarize this dissertation, and provide an outlook for future prospective.

## References

1. **Matthews KR.** 2006. Microorganisms associated with fruits and vegetables, p. 1-19, Microbiology of fresh produce.
2. **Beuchat LR.** 1996. Pathogenic microorganisms associated with fresh produce. *J. Food Prot.* **59**:204-216.
3. **Harris LJ, Farber JN, Beuchat LR, Parish ME, Suslow TV, Garrett EH, Busta FF.** 2003. Outbreaks Associated with Fresh Produce: Incidence, Growth, and Survival of Pathogens in Fresh and Fresh-Cut Produce. *Comprehensive Reviews in Food Science and Food Safety* **2**:78-141.
4. **Doyle MP, Erickson MC.** 2008. Summer meeting 2007 - the problems with fresh produce: an overview. *Journal Of Applied Microbiology* **105**:317-330.
5. **Efrima S, Zeiri L.** 2009. Understanding SERS of bacteria. *J. Raman Spectrosc.* **40**:277-288.
6. **Smith E, Dent G.** 2005. Introduction, Basic Theory and Principles, p. 1-21, *Modern Raman Spectroscopy – A Practical Approach.* John Wiley & Sons, Ltd.
7. **Chu H, Huang Y, Zhao Y.** 2008. Silver Nanorod Arrays as a Surface-Enhanced Raman Scattering Substrate for Foodborne Pathogenic Bacteria Detection. *Appl. Spectrosc.* **62**:922-931.

## CHAPTER 2

### LITERATURE REVIEW

#### **Pathogenic Bacteria in fresh produce**

The consumption of the fresh produce has increased worldwide for the past several decades as the general population adapt to the concept of healthy diet. In the United States, the per capita consumption of fresh fruits and vegetables increase 29% from 254 pound in 1980 to 328 pound in 2000, and further increase is expected through 2020 at a rate of 19% - 27% (1). However, the increased consumption of fresh produce is associated with increased foodborne outbreaks linked to fresh produce (2). In 1990, among outbreaks with an identified food source, 13% (713/5,416 cases) of outbreaks were linked to fresh produce, but such number dramatically increased to 21% (34,049/161,089 cases) in 2005 (1, 3). The frequent imports and exports of fresh produce can also cause multinational foodborne outbreaks (4). For example, the *Salmonella* outbreaks in US and Finland in 2009 traced back to the same alfalfa sprout seeds as their source (1). German outbreak of *E. coli* O104:H4 in 2011 that has been linked to bean sprouts or sprout seeds killed over 50 and sickened really 4000 in 15 European countries, as well as US (5).

The fresh produce items that are often associated with foodborne outbreaks are berries, melons, seed sprouts, and salad-greens, and those outbreaks can be caused by bacteria, virus, and protozoa (6). Among the foodborne pathogenic bacteria, *Salmonella* is the top cause of outbreaks, followed by *E. coli*, *Clostridium*, *Shigella*, *Campylobacter*, *Yersenia*, *Bacillus*, and *Staphylococcus* (6, 7). The common food source of outbreaks and the associated bacteria are summarized in Table 2.1 (6, 8).

Table 2.1 Summary of the common food source of outbreaks and the associated bacteria.

Fresh Produce Commodities	Pathogenic Bacteria
Raw lettuce/ lettuce based salads	<i>E. coli</i> O157:H7, <i>Campylobacter jejuni</i> , <i>Shigella sonnei</i> , <i>Vibrio cholera</i>
Melons	<i>Shigella sonnei</i> , <i>Salmonella</i> Chester/ Saphra/ Poona/ Javiana/ Miami/ Javiana/ Oranienburg, <i>E. coli</i> O157:H7, <i>Shigella sonnei</i> , <i>Vibrio cholera</i>
Onions	<i>Shigella flexneri</i> 6A, <i>Bacillus cereus</i> , <i>Campylobacter jejuni</i>
Cabbages/ coleslaw	<i>E. coli</i> O157:H7, <i>Clostridium botulinum</i> , <i>Listeria monocytogenes</i> , <i>Vibrio cholera</i> , <i>Staphylococcus aureus</i>
Seed sprouts	<i>Bacillus cereus</i> , <i>E. coli</i> O157:H7/ O157:NM , <i>Salmonella</i> Anatum/ Stanley/ Newport/ Montevideo/ Infantis/ Meleagridis/ ftenberg/ Havana/ Cubana/ Mbandaka/ Typhimurium/ Saint Paul/ Muenchen/ Enteritidis/ Kottbus/ Chester
Carrots	<i>Clostridium botulinum</i> , <i>Shigella sonnei</i>
Tomatoes	<i>Salmonella</i> Javiana/ Montevideo, <i>Listeria monocytogenes</i>

Fresh produce are natural vehicles of pathogens as the contamination can happen during cultivation, irrigation, post-harvest handling, and packaging (9). Another reason for high risk of contamination is that the fresh produce often are processed with no heat-treatment, and are consumed raw or with minimal cooking. The foodborne outbreaks in US and other countries are often prevented through implementation of good agricultural practices (GAP), good manufacturing practices (GMP), and hazard analysis critical control points (HACCP) by food companies. The safety of the products are routinely tested by the federal and states agencies. Hence, the food safety highly depends on the accuracy of the testing methods. From a company's point of view, the results of such tests would better be obtained within a shift, e.g. 8 hours, or before the products being shipped outside the food processing plant. So, in order to ensure food safety, it is critical to rapidly identify the foodborne pathogens directly from fresh produce.

## **Current State of Bacteria Detection**

The microbiological tests in food supply chain are critical to ensure the safety and quality of the end-products. For decades, the culture enrichment based tests are used for food testing, and such methods are often referred as the “conventional methods”. These methods generally are consisted of three steps: 1) pre-enrichment, 2) selective enrichment, and 3) identification of the microorganism through biochemical and/or serological tests. The recent advances of the culture-based methods have focused on step 2 and 3. More selective and differential media have been developed to facilitate the simultaneous identification of the microorganism, often using chromogens and fluorogens (10). No matter the identification is based on pH change, redox potential change, enzymatic reaction to the dye, or the production of the chromogens or fluorogens during the growth of the bacteria, these methods all 1) need a pre-enrichment step, 2) rely on the growth of the microorganisms, and 3) happen in a liquid or solid growth media. The strength of the cultural methods, besides inexpensive and good specificity, is that they always give true positive results, and are used by law enforcement agencies as the standards. The weakness the cultural methods is labor-intensive, lab space required, and it often takes several days to obtain confirmative results (11).

The long detection time of the conventional methods can not satisfy the growing needs of the fresh produce industry for rapid detection. Since 1980s, the microbiological tests changed dramatically with many new methods developed. These methods often take less time than the conventional methods, so they are referred as “rapid detection methods”. Based on the principles, they can be generally categorized into the following three classes: 1) immunological methods, 2) nucleic acid based methods (or molecular methods), and 3) biosensors (11).

## The immunological method

The development of the immunological assays is based on the specific binding between antigens and corresponding antibodies, and such assays can rapidly screen and identify the target microorganisms and enterotoxins. The configuration of the system varies from simple mixing the antibodies coated magnetic beads with bacteria in latex agglutination test, to a complicated multiple-step procedure, such as enzyme-linked immunosorbent assays (ELISAs). The schemes of different immunological methods are shown in Figure 2.1.

Immunomagnetic separation (IMS) methods are often used to specifically capture the target bacteria from solution media obtained from samples. The antibody coated magnetic beads bind to the specific antigens on bacteria surface when contacting (Figure 2.1A i& ii), and the resulting bacteria-bead complex can be isolated by applying external magnetic field (Figure 2.1A iii). The IMS methods have been used to detect foodborne pathogens, i.e. *E. coli* O157:H7 (12), *Listeria monocytogenes* (13), and *Salmonella* (14) from various food samples, such as fresh produce, meat, milk, cheese and etc (15-17). The specificity IMS provides is the biggest advantage of this method, and it can be used in almost any food samples. The weakness of the method is that it is only a separation method, and the follow-up identification methods are needed, such as ELISAs, PCR, and sorbital-MacConkey agar, etc.

ELISAs detect the specific antigens using an antibody which is often covalently linked to an enzyme that can yield chromogenic, fluorescent, or chemiluminescent signals. As shown in Figure 2.1 B, ELISAs are often constructed using a "sandwich" format, in which the bacteria with target antigens are captured by the antibody that are immobilized on a solid plate (i &ii). And then the resulting complex is conjugated with a labeled secondary antibody, usually with fluorescence label, via antigen-antibody reaction (iii). The bacterial detection is realized by

measuring the signal from the label molecule on the secondary antibody (iv). ELISAs have been widely used for the detection of bacterial cell, as well as the bacterial enterotoxins in contaminated food samples (18, 19).

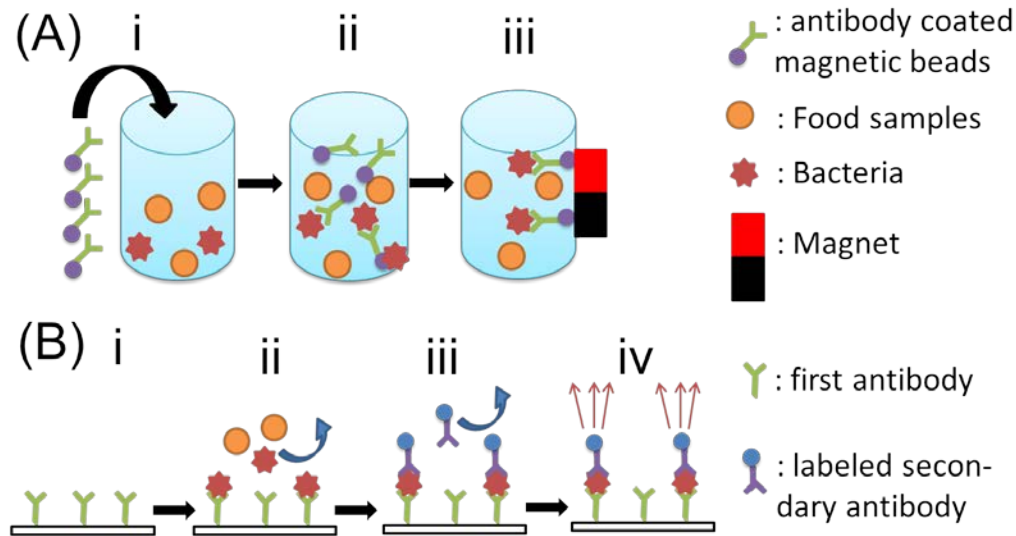


Figure 2.1 The schemes of immunological methods for bacteria detection. In (A) IMS, (i) antibody coated magnetic beads are added to the solution with bacteria and food samples. (ii) Beads bind to the specific antigens on bacteria surface. (ii) Bacteria-bead complexes are isolated by external magnetic field. In (B) ELISAs, (i) antibodies are immobilized on solid plate. (ii) Food samples with bacteria are applied to the solid plate, where bacteria are captured by the immobilized antibodies, while food samples are washed away. (iii) Fluorescence labeled secondary antibodies are conjugated to the complex, and (iv) the signal from the label is read by the detector.

Other immunological methods that have been used for bacteria detection include lateral flow assay (LFA), latex agglutination test, and immunofluorescence staining, dot blot, and etc (20). These immunologically based assays all have the advantage of high specificity owing to the specific binding between antigens and antibodies, along with relative low cost and high-throughput. However, the sensitivity of these assays are usually poor, and at least  $10^4 - 10^6$  CFU/ml of target bacteria are required to show definite results (11). Hence, almost all of these methods require several hours of enrichment to generate positive results.

## **Nucleic acid based methods**

The nucleic acid based methods, known as molecular methods, do not directly detect the whole cell or its metabolic product, rather measure the presence of a specific sequence of nucleic acids, either DNA or RNA. It solves the problem of time consumable enrichment in conventional methods by rapidly amplifying the target sequences through chemical reactions (21).

The molecular methods are based on the polymerase chain reaction (PCR), which often contains three steps: 1) denature the template double-stranded DNA to single strands, 2) annealing of the primers, and 3) extension of the primers, as shown in Figure 2.2. PCR is used to increase the number of the target gene sequence by million fold within hours. The PCR end-product can then be analyzed by agarose gel with stain dyes. PCR saves the time of culture by increase the number of target gens rather than the microorganism cells themselves. The advantage of the PCR is its short run-around time, quantitative results, good sensitivity, and excellent specificity, while its weakness lies within its principle. First, a proper primer needs to be selected for a successful procedure. Secondly, the result only indicates the presence of the gene, no differentiation between viable and dead cells, which will leads to a false positive result. At last, the food samples may contain PCR inhibitor which will limit its use in some food samples(21). A lot of alternatives to the traditional PCR have been developed to be more sensitive, accurate, and rapid; however, some of the strength and weakness of the PCR methods are shared by those alternatives (22).

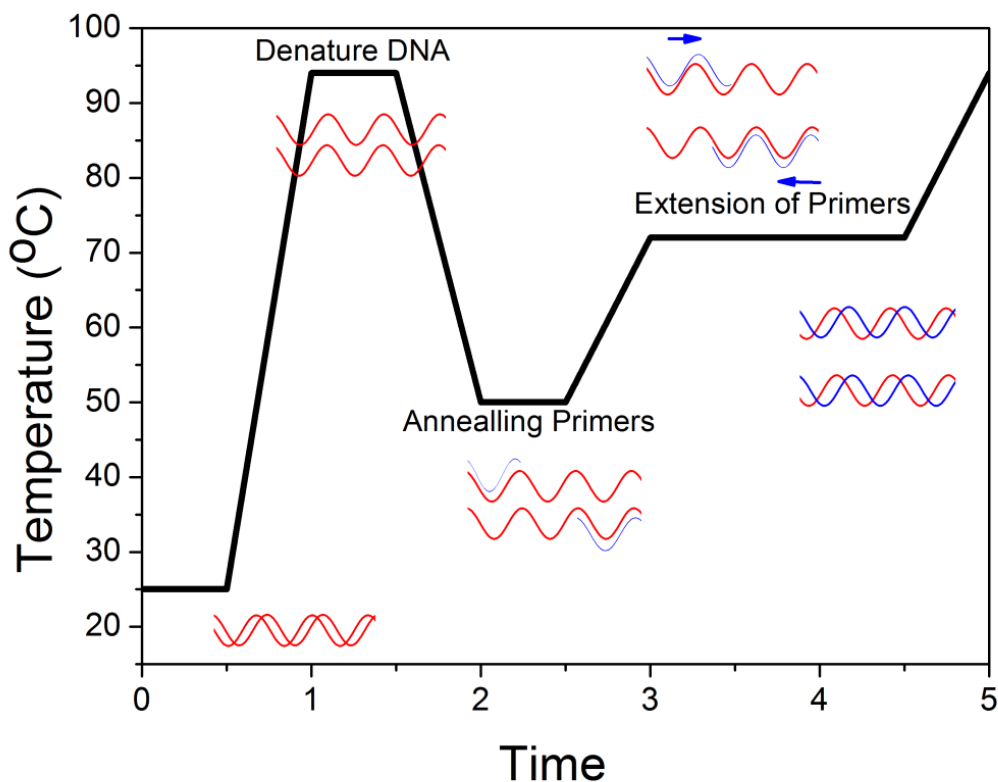


Figure 2.2 Scheme of the polymerase chain reaction (PCR).

Reverse transcription-PCR (RT-PCR) uses target RNA as template to reverse transcribed it to cDNA, and then the resulting cDNA is used as the template for PCR amplification. When using mRNA as template, RT-PCR can differentiate viable cell with non-viable cells, and it has been used to detection viable bacteria in wines, ciders and meat (23-25). But RNAs have short half-life; hence it is easy to be degraded in air, which limits the usage of RT-PCR. Real time PCR (qPCR) follows the basic procedure of the traditional PCR, but the amplicons are analyzed during the process in “real time”, compared to traditional PCR in which the amplicons are analyzed at the end of the amplification procedure. The analysis the amount of amplified products is based on the fluorescent reporter which can be non-specifically bonded to the double-

stranded DNA, or linked to a specific DNA probe which will hybridize with the target DNA sequence. qPCR has the advantage of being quantitative, sensitive and accurate, but the non-specific PCR product often yield a false positive result. It has been applied in the bacteria detection in chees, milk, salmon, and etc (26, 27). Multiplexing has also been achieved using qPCR (28). Microarrays are developed for the high throughput analysis of the DNA samples. In a microarray setting, the probes are immobilized on a solid plate, which contains the complementary sequence to the target DNA. The PRC end-product, often labeled with fluorescent dyes will hybridize with the probe, and the complex will yield fluorescent signals on the plate. Microarrays can detect multiple target genes at once by immobilizing up to millions of probes on the plate. It has the strength to be high throughput, and can be used for screen of multiple bacteria at the same time. The poor reproducibility of the DNA microarray is always a concern, along with its high cost, and requirement for skilled personnel.

## **Biosensors**

Biosensors are often referred to the devices that transfer the biological or chemical signal recognized to an electronic signal. With the development of the nanotechnology, more and more biosensors are used for pathogen detections (29). These biosensors all transfer the chemical or biological signals from bacteria to physical signals that are measurable by the detector, and its applications varies from detection of the signals of the whole cell to the detection of certain chemistry reaction of the bacterial metabolic by-products. Here three types of methods are introduced: impedance-based sensors, transducer-based immunosensors, and spectroscopic methods.

Impedance-based sensors measure the change of the conductance or impedance caused by the bacteria metabolism (30). In a direct impedance system, the electrodes are in direct contact with the growth medium and samples. Bacteria metabolism produce charged end products thus increasing the electrical conductance of the culture medium in the system, and then these changes are detected by the sensor (31). In an indirect impedance sensor setting, the sample is contained in a glass tube, separated from the potassium hydroxide bridge by a headspace (32). This method detects carbon dioxide produced by growing bacteria or fungi. The decrease in conductance is monitored, which is caused by the CO<sub>2</sub> being dissolved into potassium hydroxide to form potassium carbonate. The strength of the technology is that it only measures the viable cells, since only viable cells can have metabolism and produce the end-products. The weakness of the methods is that a cultivation step is necessary because the metabolism of the bacteria is monitored, resulting an increases of the detection time.

Transducers-based immunosensors incorporate the immobilized antibody to capture the bacteria, and such an interaction between antibody and antigens on bacteria produces measurable physical signals that are detected by the sensor. Two examples are surface plasmon resonance (SPR) sensor and piezoelectric sensors. SPR sensor is based on the SPR phenomenon that occurs when the frequency of light photons matches the natural frequency of surface electrons. Such resonance will cause a strong absorbance which depends on the molecules on the surface of the metal. The presence of the bacteria (or the antibody-antigen complex) will cause a shift in the resonance, which leads to the detection (33). Piezoelectric sensors measure the mass change on the surface of a quartz crystal caused by the binding of the bacteria through antibodies (34). These transducers-based immunosensors have the strength of being rapid, low cost with simple system configuration, and label-free. However, the component in sample matrix may interference

with the results, which limits its use in real samples, and their sensitivities sometimes are not good.

The spectroscopic methods measure the intrinsic electromagnetic properties of the bacteria and compare them with the established library to detect the presence of the bacteria, or measure the spectroscopic fingerprints of the extrinsic label on the bacteria. Mass spectroscopy, especially matrix-assisted laser desorption/ionization time-of-flight (MALDI-TOF) mass spectroscopy is an advanced technology used to identify bacteria. In MALDI-TOF, ionized bacteria pass through an electrical field. The time molecules take to arrive the detector is different due to its different mass and charge; therefore such a time spectroscopy can be used as the fingerprint to identify the bacteria with high specificity, even at strain level (35). However, the high capital investment of the equipment limits its application in some industry, and the system requires large lab space. Fourier transform infrared (FT-IR) spectroscopy measures the FT-IR fingerprints of the bacteria when the IR is absorbed or transmitted through the sample (36). It has the advantage of being non-destructive, rapid, and it can differentiate bacteria species. However, it is a qualitative rather than a quantitative method, and interference from the food matrix is great. Raman spectroscopy relies on the inelastic scattering interaction of excitation light and vibrational modes of molecular bonds. These molecular vibrational modes possess unique “fingerprint” peaks which can be used to identify the particular molecule(s) being probed. Raman and the more advanced surface-enhanced Raman scattering (SERS) are used to detect bacteria from various samples, which will be discussed in detail in the following section.

Careful consideration need to be given when choosing the appropriate rapid methods for bacteria detection in food, since they all have their own advantages and drawbacks. Studies have shown that the performance of rapid assays various in different food samples, due the differences

in the bacterial microflora and sample matrix. The advantages and disadvantages of each detection method are summarized in Table 2.2. In addition, the types of information needed determine the choice of the detection methods. For example, molecule methods can not detect specific protein, as they may be important virulence factors. Moreover, the cost of these rapid methods will also need to be considered.

Table 2.2 Summary of the current bacteria detection methods.

Methods	Advantages	Disadvantages
Culture methods	Always true positive, quantitative, accurate, inexpensive	Labor-intensive, slow, lab needed
ELISAs	Easy handling, inexpensive, rapid.	Multiple reagents used low sensitivity, False positive
LFAs	No lab needed. Visual inspection, easy handling	Only works on liquid samples, low sensitivity.
LA	Easy configuration, only need visual inspection	Low sensitivity
PCR methods	Can be quantitative, sensitive,	Cannot differentiate viable cells from dead ones
RT-PCR	Use mRNA as template can differentiate viable cell with non-viable cells	Short half-life, rapidly degraded
qPCR	Quantitative, rapid, accurate.	Non-specific PCR product interference with the results, false positive
Microarrays	Rapid, sensitive, multiplexing, high throughput,	DNA cross-contamination will yield false positive
Impedance-based sensors	Only measures viable cells	Cultivation needed, long detection time
SPR sensor	Real time, label free	Interference from the sample matrix
Piezoelectric biosensors	Low cost, assays can be reusable	Low specificity, only qualitative, not sensitive
MALDI-TOF	Rapid, highly automated, high specificity	High capital investment, pre-enrichment needed
FT-IR spectroscopy	Rapid, non-destructive, sensitive	Qualitative rather quantitative, hard to do multiplexing
Raman spectroscopy	Rapid, non-destructive, sensitive	Qualitative rather quantitative, limited use outside of laboratory

## Raman and Surface-Enhanced Raman Scattering

Raman spectroscopy is a spectroscopic method based on the inelastic photon scattering from the molecules (37). It can be used to identify the characteristic spectral pattern (often refers as “fingerprints”) of the molecules, and to determine the amount of the substances. The Rayleigh and Raman scattering process are illustrated in Figure 2.3. When excitation photon interacts with the target molecular, the molecular is excited from ground vibrational state ( $m$ ) to a “virtual state”, which is unstable, and then the photon is immediately radiate. If the molecular returns to the initial ground vibrational state ( $m$ ), it is called Rayleigh scattering, in which case there is no energy transfer between the excitation photon and the target molecular. However, energy transfers between the photons and molecular will happen, either from photon to molecular or vice versa. Such inelastic scattering of the photon is called Raman scattering. If the target molecular absorbs the energy from the excitation photon, promotes to an excited vibrational state ( $n$ ), it is called Stokes scattering. If the target molecular is initially at the excited state ( $n$ ), it will give energy to the excitation photon and then return to the ground state ( $m$ ) after the scattering, which is called anti-Stokes scattering.

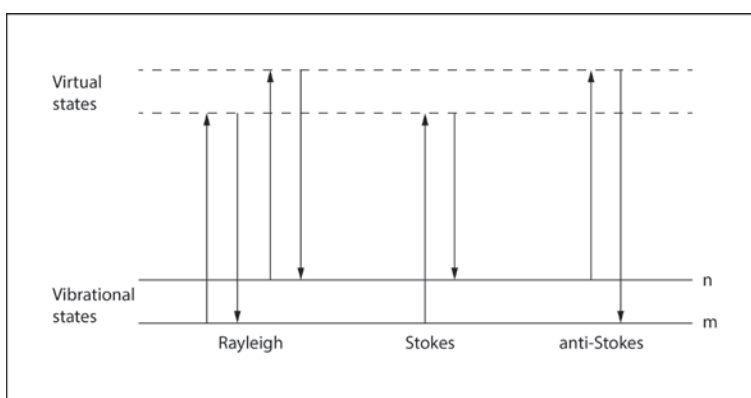


Figure 2.3 The Rayleigh and Raman scattering process.  $m$  indicates the ground vibrational state.  $n$  indicates the excited vibrational state. The dotted lines indicate the virtual states. Upward arrows indicate the process of the promotion of the molecule, and downward arrows indicate the process the photons being scattered.

Raman scattering measures the energy difference between excited vibrational state  $n$  and ground vibrational state  $m$  by measuring the energy differences between the scattered photons and the incident photons. And Raman spectrum is often presented as just the Stokes scattering, and it is expressed as the energy shift, or shift in wavenumber ( $\Delta \text{ cm}^{-1}$ ), often simply as  $\text{cm}^{-1}$ . Raman spectra arise from the vibrational frequencies of molecules and provide ‘molecular fingerprint’ information that is particularly valuable in chemistry. Its narrow peaks have great spectral resolution, and less chance to be interfered by the broad fluorescence from either the target molecular or its surrounding environment. This is the biggest advantage of Raman scattering over IR, and it is very important for detection of biomolecule as such samples often have very high fluorescence background.

However, the intensity of the Raman scattering is relatively weak, due to the small scattering cross-section. In order to obtain a good Raman spectrum, it is essential to use large amount of analyte, preferably Raman active molecules, high laser power, long acquisition time, and highly sensitive instrument. Therefore, these restrictions make Raman scattering itself not a practical sensing technique. However, the discovery of surface enhanced Raman scattering (SERS) phenomenon changes this situation. In 1974, Fleischmann et al in 1974 observed surprisingly strong and potential-dependent Raman signals from pyridine adsorbed on a silver electrode that had been electrochemically roughened in potassium chloride aqueous electrolyte (38). The mechanisms of such dramatic increase of the Raman scattering were explained based on electromagnetic (EM) enhancement and chemical enhancement (39, 40). Later studies have confirmed that the EM enhancement arises from the laser excitation of localized surface plasmons due to the specific local arrangement of nanostructured noble metal morphology, which creates an enhanced electric field (41). Chemical enhancement comes from a charge

transfer mechanism for adsorbed molecules with appropriate acceptor or donor orbitals that interact with the metal substrates (42-44).

In order to optimize the EM effect, the wavelength of the excitation laser should be in resonance with the broad band of the surface plasmon vibrations of the metal. For silver and gold, the surface plasmon bands are typically in the visible (500-700 nm) to near-infrared region (700-1300 nm). The resulting Raman signal enhancement is proportional to  $E^4$ , where  $E$  is the local electric field. Studies have revealed that the most intense electric field is often within the “gaps” between the nanostructured metal particles. Although both of EM and chemical enhancement contribute to the total SERS enhancement, the EM enhancement is believed to play a greater role. A major difference between the EM and chemical enhancement is that the chemical enhancement occurs in a short range (0.1-0.5 nm), where the analyte is directly attached to the nanostructured metal surface; while the EM enhancement can happen in a longer range.

SERS was considered a promising technique to observe Raman signal of very low concentrations of molecules on nanoparticles and nanostructured surfaces since it can increase the intensity of the Raman scattering by million folds. SERS has almost exclusively been associated with three metals, gold silver, and copper, however, recent advances has made on the SERS based on the substrates rather than these three metals, or even on non-metallic substrates (45). Copper is not ideal for biological or chemical detection due to its chemically active nature and it may react with some analyte. Hence, the use of SERS for bacteria detection focused on either Au or Ag nanostructures.

## **SERS of bacteria**

Research on using SERS to detect and differentiate bacteria can be dated back to 1998, when Efrima and Bronk obtained the SERS spectra of *E. coli* with nanocolloidal silver particles deposited on the outer cell wall of the bacteria (46). Since then, this research area has been explored by many researchers, and the SERS-based bacteria detection technique has been greatly advanced. Nowadays, SERS be used to can detect a single bacteria cell or spore (47). The technique has been developed into different kinds of biosensors, that have been used to detect bacteria in numerous real samples, such as environmental samples (45), food samples (48), and clinical samples (49).

For the past decades, great effort has been focused on (1) understanding the SERS signal of bacteria, (2) development of SERS-active substrates with high sensitivity and specificity, (3) combination of SERS with conventional sample processing methods, and (4) detection of bacteria in real samples.

## **Understand bacterial SERS signal**

Bacterial cell is a complex dynamic system, with numerous chemical components that would contribute to the overall SERS signal. Understanding the origins of such SERS signal and subsequently designing appropriate detection strategy for those chemical components is one of the fundamental tasks for researchers. As of today, most of the researchers in the field have convinced that the SERS signals of bacteria are mainly coming from the bacteria cell envelope (50), but there are still controversy on the origins of the bacterial SERS signal.

Since bacteria are grown in the culture media, the effect of media on the Raman or SERS spectra has been investigated by several researchers. Marotta and Bottomley examine the SERS

spectra of fifteen commonly used bacterial growth media and found these spectra are similar to spectra of bacterium (51). Therefore, they suggest that the residues of the bacterial growth media may contribute greatly to the overall SERS response. In response to this hypothesis, Premasiri et al. investigated the SERS spectra of different bacterial species grown in the same growth media, which exhibit different characteristic vibrational spectra, while SERS spectra of the same organism grown in different media displayed the same SERS spectrum (52). They also proved that through several water washing and centrifugation cycles, the growth media can be removed from the samples and result in spectrum of the bacterial cells only. These findings suggest that spectra are indeed intrinsically attributed to the bacterial cells. However, Leyton et al. investigated the bacteria *Acidithiobacillus ferrooxidans* by means of SERS and found out that the SERS spectra displayed physical and chemical variations caused by different growth media(53). Kahraman et al. also found that the features observed in bacterial SERS spectra originate mostly from the bacteria surface with some contributions from metabolic activity or molecular species detached from the bacteria surface during sample preparation(54). From these studies, we know that the bacterial SERS signal is mainly from the whole cell, but different growth condition may alter the metabolism of the bacteria, causing the differences in the chemical composition of the cell, such as the protein synthesized, the amino acids relative abundance on the cell wall, and their configuration (55). Such change in chemical composition is reflected in the bacterial SERS spectra.

Efrima et al (56) did a study to investigate the difference in SERS signal between an "internal colloid" formed inside the *Bacillus megaterium* ( $G^+$ ) and *E. coli* ( $G^-$ ) cells and the nanoparticle layer coating the cell wall. While the AgNP coating on the cell wall generated intense spectra, the internal colloid did not produce appropriate conditions for SERS

enhancement, possibly due to the lack of aggregation of AgNPs within the cells. Combining with the geometry of both bacterial cells and the AgNPs, it seemed that SERS effect is mainly generated on the cell surface, not the cell interior. The analysis of silver-treated bacteria by the same group also revealed that bacterial SERS spectra were dominated by flavin adenine dinucleotide (FAD) (57). FAD is located in the plasma membrane, and it has the largest Raman cross-section of all the constituents of the cell envelope. According to changes in the SERS spectrum, the state of oxidation of the flavins could be tracked. In addition, the redox heme protein of *Shewanella oneidensis* MR1 has been identified as a major component of the cell surface domains.

On the other hands, Zeri et al (58) found that the SERS spectra of four different bacterial species (*E. coli*, *Acinetobacter calcoaceticus*, *Pseudomonas aeruginosa* and *Bacillus megaterium*) were similar, implying that the spectra were greatly attributed to a specific molecule, presumably FAD,. In a follow-up study (59), the group fractionated the cell and collected cell surface debris for SERS measurement. Results confirmed their hypothesis that the spectra of bacteria resembled that of FAD, and the bacterial SERS signal mainly originated from the wall fraction, which was consistent with Efrima et al's findings. They also proposed that the Raman bands at  $\Delta\nu = 735$  and  $1330\text{ cm}^{-1}$  were more probably due to adenine in its denatured form, rather than the nucleic materials. To investigate effect of excitation wavelength and colloid preparation on bacterial SERS signal, Zeri et al (60) did another study in which they compared different types of Raman scattering techniques and sample preparation methods. They found that the bacterial cells remained intact under colloidal preparation conditions and the resonance of the laser with flavins was not essential for their dominance in the SERS spectrum, suggesting that flavins are preferentially located near the colloids.

In the contrary, Leyhton et al. suggests that the peak at  $\Delta\nu = 730 \text{ cm}^{-1}$  is corresponding to the D-glucose, which is attributed to the lipid layer components of the cell walls and membranes. Liu et al (61) pointed out that the origin of the peak at  $\Delta\nu = 730 \text{ cm}^{-1}$  might be attributed to the symmetric O-P-O vibrational mode of the phosphate group, rather than FAD or glucose on the cell surface, based on their observation that  $\text{K}_2\text{HPO}_4$  exhibited the same band. They also suggested that the peak at  $\Delta\nu = 390 \text{ cm}^{-1}$  might be useful for the identification of *L. monocytogenes*, whereas the peak at  $\Delta\nu = 712 \text{ cm}^{-1}$  could be unique to *E. coli*. However, in this study only two types of bacteria were selected, so these conclusions seemed premature. Another group, Sengupta et al (60), also attempted to interpret the bacterial SERS spectra by comparing them with important cell wall components- N-acetyl glucosamine (NAG), L-lysine, D-glutamic acid and D-alanine. They concluded that the main band at  $\Delta\nu = 1370\text{-}1375 \text{ cm}^{-1}$  indicated a strong interaction between carboxylate groups of the amino acids with silver.

Other cell membrane or cell wall components of bacteria were also studied. SERS imaging of fungal hyphae grown on nanostructured SERS active substrates was studied by Szegalmi et al. to present the possibility for the detection of single cell wall components (62). A comparative study of psychro-active arctic marine bacteria and common mesophilic bacteria by SERS revealed that a higher lipid content of unsaturated fatty acids in the outer membranes of marine bacteria could be identified (63).

In all this aforementioned studies, we see the controversy on the origin of SERS peaks, especially on the whether the signal is from the bacterial cell or metabolic products, and the attribution of some peaks, such as the peak at  $\Delta\nu = 730 \text{ cm}^{-1}$ . Identification each and every one of the bacterial SERS peaks and attributed to chemical components in the bacterial cells is a challenging and nearly impossible task. Through the aforementioned studies, we can conclude

that the chemical substances potentially contributing to SERS spectra are mainly from the outer structure of the bacteria cell, such as outer membrane and cell wall. However, some of the inner cell components, such as DNA, RNA, proteins, and some metabolic products may be present in the surrounding environment, and then yield a SERS signal.

### **Development of SERS-based bacteria detection platform: sensitivity**

Since the concentration of pathogenic bacteria in food and clinical samples would be low, the SERS-based biosensors need to be ultra-sensitive. The SERS-active nanostructures can be either a “colloid” type or a “substrate” type. In a “colloid” type of SERS detection, the actual amount of bacteria detected are the ones within the laser focus point. Hence, bulk concentration detection limit of the colloid type SERS method  $C_{LOD}$  is defined by

$$\frac{VC_{LOD}}{f\pi R^2} = N_d f \pi R^2, \text{ so}$$

$$C_{LOD} = \frac{N_d f^2 \pi^2 R^4}{V},$$

where  $V$  is the total volume of bacterial-colloid solution,  $R$  the radius of the laser spot,  $f$  is the depth of focus of the laser, and threshold  $N_d$  is the amount of bacteria detected per volume of the colloid, which reflects the true detectability of a SERS method.

In a “substrate” type of SERS active nanostructure, we must consider that SERS is usually a “surface” detection technique, so the definition of LOD is different. The  $C_{LOD}$  is determined by the amount of bacteria detected within the laser spot on the substrate surface.

$$N_d = \frac{VC_{LOD}\pi R^2}{A_s}, \text{ so}$$

$$C_{LOD} = \frac{N_d A_s}{V\pi R^2},$$

where  $V$  is the volume of bacterial solution applied on the surface,  $A_s$  is the spreading

area of the sample on SERS substrate,  $R$  the radius of the laser spot, threshold  $N_d$  is the amount of bacteria detected per surface area, which reflects the true detectability of a SERS method.

In both “colloid” and “substrate” type of SERS method,  $R$  and  $f$  is limited by the Raman instrument used which can not be tuned once the instrument is fixed, while  $A_0$  could be confined by a narrow well as previously reported (64). Thus, the two strategies to lower  $C_{LOD}$  would be to increase  $V$ , the volume of the samples a, or to decrease  $N_d$ , the true detectability of a SERS method. One way to increase  $V$  is to use pre-concentration methods to load as many bacteria as possible into the small detection range using a large sample volume. Decreasing the  $N_d$  value can be achieved by fabricated better SERS-active substrates, or optimize the substrates for bacteria detection.

### **Development of better SERS-active substrates to decrease $N_d$**

$N_d$  is the minimum number of bacteria needed for a SERS-active substrate to generate enough SERS signal so that the instrument will recognize a positive detection, and it can be viewed as the absolute sensitivity of the SERS-active substrates. The SERS-active substrates usually consist of noble metal fine structure with dimensions in the scale of nanometers. Since the morphology of the metallic structure plays a major role in determining the magnitude of signal enhancement and sensitivity of detection, different types of substrates have been fabricated or synthesized to facilitate sensitive detection of bacteria, such as silver metal deposits (46), silver colloid (65, 66), gold colloid solutions (67), electrochemically roughened metal surfaces (68), silver film over nanosphere (69), silver nanorod array substrates (70), silver nanocrystal assembled silver nanospheres (AgNSs) (71, 72), and array of Ag nanoparticles imbedded in anodic aluminum oxide (AAO) nanochannels substrates (73, 74).

A quantitative way to quantify the absolute sensitivity of the SERS-active substrates is to determine the SERS enhancement factor (EF) of a substrate:

$$EF = \frac{I_{SERS} N_{bulk}}{I_{bulk} N_{SERS}},$$

where  $I_{SERS}$  is the intensity of SERS response due to  $N_{SERS}$ , the number of molecules on SERS substrate surface, while  $I_{bulk}$  is the normal Raman scattering intensity due to  $N_{bulk}$ , the number of molecules being probed in bulk solution. The aforementioned nanostructures have been shown to have an EF ranging from  $10^7$  to  $10^{10}$  for small molecules.

The most common way to fabricate SERS-active nanoparticles is to synthesize gold or silver nanoparticles through chemical reaction, where  $Ag^+$  or  $Au^+$  are reduced by reducing agents. The resulting nanoparticles have a size of 10-30 nm in diameter. To create the so-called “hot spots” for SERS, nanoparticles 10-30 nm in diameter can be further aggregated into assembly 60-80 nm in diameter by adding salt (e.g., NaCl) into the colloid. The aggregated nanoparticles are believed to have enhanced electromagnetic field that results in enormous SERS enhancement factors ( $10^{11}$ - $10^{13}$ ). To generate bacterial SERS spectra, the nanoparticles can form inside the bacterial cells (56, 58-60), or outside the cell wall as an extra-cellular coating (56, 59, 60), or simply be brought into close proximity to the cells by mixing the cells with prepared colloid and then dry on a CaF/glass slide (75-78), or by drying the colloid on the glass slides first, then mounting samples on the dried colloid (79). The lowest LOD of the colloid based SERS detection for bacteria were reported by using AgNSs (diameter = 60 - 80 nm), which is at 10 CFU/mL for *S. aureus* and  $10^2$  CFU/mL for *E. coli* and *Salmonella* Typhimurium (72).

For colloidal SERS, the resonance frequency of the plasmon oscillations is dependent on the size and shape of the particles, as well as the wavelength of the incident radiation. Since the aggregation of the colloids is introduced by the chemical reaction, the reproducibility of

nanostructure is really low. These variations can change the SERS enhancement factors by several orders of magnitude. As a result, the reproducibility of the colloids based SERS bacterial detection is low. To solve the reproducibility problem, several solid phase “substrates” types of nanostructures have been developed. Recently, magnetic–plasmonic Fe<sub>3</sub>O<sub>4</sub>–Au core–shell nanoparticles (Au-MNPs) were reported. Such Au-MNPs can uniformly aggregate to the outside of the bacterial cell with an external point magnetic field. Using this method, *Escherichia coli* K12, *Pseudomonas. aeruginosa*, and *Acinetobacter calcoaceticus* were detected at a LOD of  $2 \times 10^5$  CFU/ml (80). Zhang *et al.* used silver film over nanosphere (AgFON) substrates to acquire the SERS spectra of calcium dipicolinate (CaDPA), a biomarker for bacillus spores, and achieved a LOD of  $2.6 \times 10^3$  spores of bacillus (69). An array of Ag nanoparticles imbedded in anodic aluminum oxide (AAO) nanochannels substrates were fabricated by Liu *et al.*, and such substrates were able to detect the “chemical features” of bacterial cell wall that enables rapid identification of drug resistant bacteria (74). The scanning electron microscope (SEM) images of the some SERS substrates are shown in Figure 2.4.

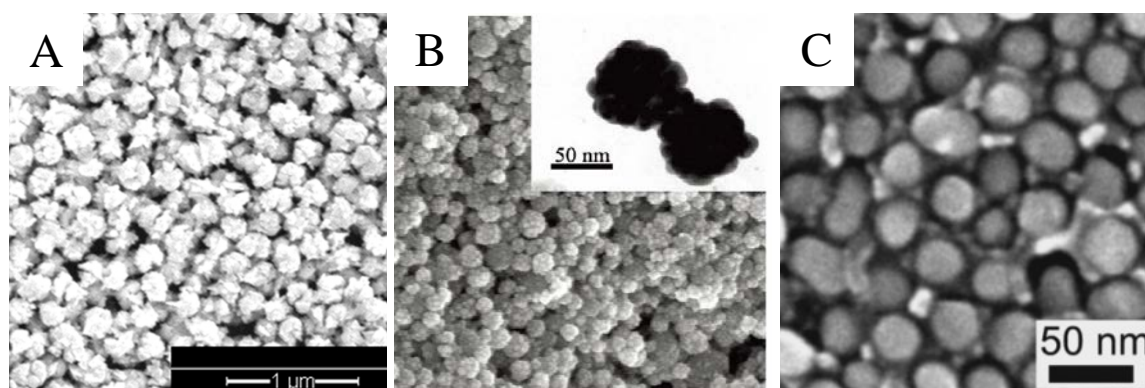


Figure 2.4 Morphology of the SERS substrates for bacterial detection. (A) Au-MNPs, (B) AgNCs, (C) AAO. (A adapted with permission from reference 80, Copyright Elsevier 2012; B adapted with permission from reference 72, Copyright ACS 2010; C adapted with permission from reference 73, Copyright John Wiley and Sons 2006)

The silver nanorod (AgNR) array substrates fabricated by oblique angle deposition (OAD) method have been proven to have a SERS enhancement factor of more than  $10^8$ , and a batch variance below 15%. In addition, these substrates have been shown to markedly enhance the Raman signal of chemical and biological samples including aflatoxins (81), important human viruses such as rotavirus, influenza virus and respiratory syncytial virus (82, 83), foodborne pathogens including *E. coli* O157:H7, *Salmonella* Typhimurium, *Staphylococcus aureus* (70), pesticides like chlorpyrifos and parathion, intentional adulteration agents like melamine (84), and allow for detection and discrimination of microRNA families and family members (8).

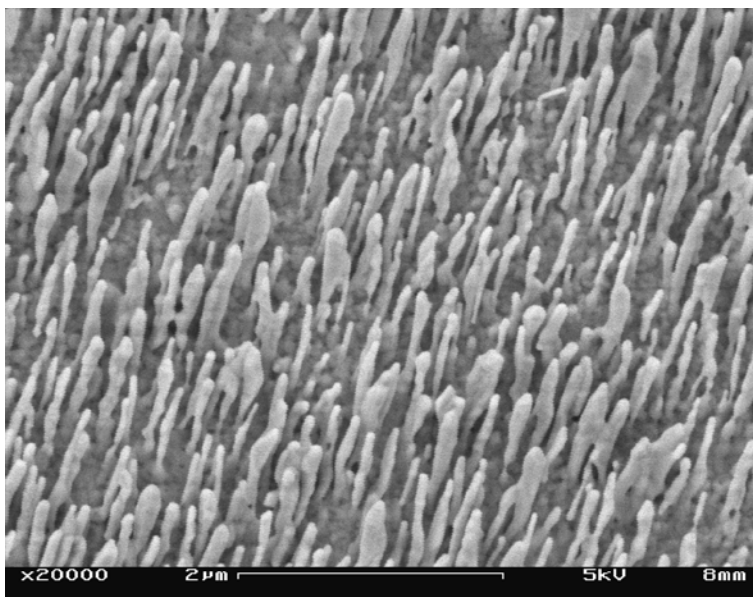


Figure 2.5 Representative SEM image of the AgNR substrates ( $\alpha = 86^\circ$ ).

The morphology of the AgNR substrates fabricated by OAD method is shown in Figure 2.5. The AgNR substrate has the advantage of high uniformity and reproducibility besides its high SERS enhancement. The ability of AgNR as a SERS substrate to rapidly detect pathogenic bacteria has been studied, and its ability to differentiate between different bacterial species,

strains and between viable and nonviable cells based on their characteristic SERS spectra has been demonstrated by Chu et al (70).

In this study by Chu et al (70), the spectral differentiation of bacteria from different species can be easily achieved using SERS by examining the presence or absence of unique peaks for a certain species. In Figure 2.6, highly reproducible SERS spectra of *E. coli* O157:H7, *Salmonella* Typhimurium, *Staphylococcus aureus*, and *Staphylococcus epidermidis* are acquired using a 785 nm excitation laser for 10 s, with relative standard deviations (RSDs) of the peak intensity at  $\Delta\nu = 735 \text{ cm}^{-1}$  and  $1328 \text{ cm}^{-1}$  being less than 6%, and the significant peaks from these species are identified. Although the specific interpretation of the Raman spectra of bacteria is still controversial and debatable in the aforementioned studies, some general Raman peak assignments are accepted by most researchers. The strong SERS bands at  $\Delta\nu = 735$  and  $1330 \text{ cm}^{-1}$ , for example, have been attributed to the nucleic acid base adenine in almost all previous SERS studies of nucleic acids and bacteria. The broad band at  $\Delta\nu = 550 \text{ cm}^{-1}$  can be assigned to carbohydrate; the peak at  $\Delta\nu = 1450 \text{ cm}^{-1}$  can be attributed to the  $\text{CH}_2$  deformation mode of proteins, and the strong band at  $\Delta\nu = 930 \text{ cm}^{-1}$  may be assigned to the C-C stretching modes in proteins. These significant peaks from bacteria are commonly shared by the four species, yet each of the species processes its own unique feature. For example, the protein peak at  $\Delta\nu = 1090 \text{ cm}^{-1}$  appears to be unique for *S. aureus* and *S. epidermidis* but are not present in the spectra of the *E. coli* O157:H7 and *Salmonella* Typhimurium.

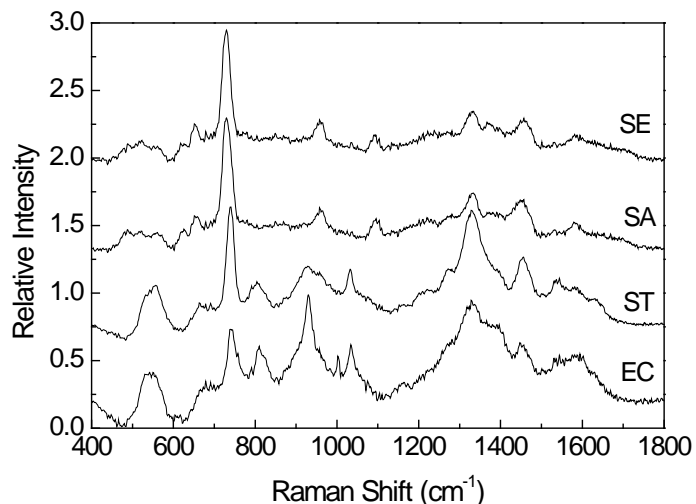


Figure 2.6 SERS spectra of four bacterial species obtained on AgNR substrates. EC = *E. coli* O157:H7; ST = *Salmonella*. Typhimurium; SA = *Staphylococcus aureus* and SE = *Staphylococcus epidermidis*. Incident laser power of 24 mW and collection time of 10 s are used to obtain these spectra. Spectra are offset vertically for display clarity. (Reproduced with permission from reference 70. Copyright SAS 2008)

The detection and identification of viability of bacterial cells are also studied. As discussed before, one disadvantage of the PCR method is that it could give false negative/false positive identification since it is based on DNA detection, which generates the same signals for both the dead and viable bacterial cells. In contrast, SERS spectra of bacteria is based on the chemical structure, so the structure differences on cell surface between dead and alive cells would display in the spectra. Figure 2.7 shows spectra of viable and heat prepared cells of *E. coli* O157:H7, and the dead cells show a significantly reduced SERS response at those characteristic bands at  $\Delta\nu = 550 \text{ cm}^{-1}$ ,  $735 \text{ cm}^{-1}$ ,  $1330 \text{ cm}^{-1}$  and  $1450 \text{ cm}^{-1}$  that are presented in the viable cells, hence the differentiation of live and dead cell can be achieved by SERS.

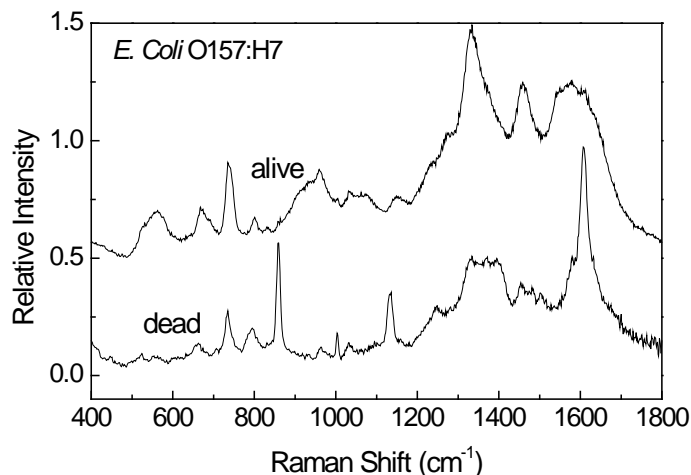


Figure 2.7 SERS spectra of viable *E. coli* O157:H7 and non-viable *E. coli* O157:H7. Incident laser power of 14 mW and collection time of 10 s are used to obtain these spectra. Spectra are offset vertically for display clarity. (Reproduced with permission from reference 70. Copyright SAS 2008)

### **Increase sensitivity by pre-concentration method**

As discussed above, besides decreasing  $N_d$ , another way to decrease  $C_{LOD}$  is to increase  $V$ , which can be achieved by using pre-concentration methods that load as many bacteria as possible into the laser spot with a large sample volume. This is essentially a typical sampling method for bio-detection. Different sampling methods that can concentrate bacteria from complicated samples are reviewed by Stevens and Jaykus(85). These methods can be categorized as chemical (e.g., ion exchange resins, lectins, dielectrophoresis, and aqueous two-phase partitioning), physical (e.g., centrifugations, coagulation, magnetic field, flocculation, filtration methods, flow cytometry, and ultrasound), physicochemical (e.g., metal hydroxides), and biological approaches (e.g., immunomagnetic separation and bacteriophage). These concentration methods can be combined with SERS to assemble a more sensitive and robust detection platform for bacteria.

Chemical sampling methods, such as dielectrophoresis (DEP) and aqueous two-phase partitioning were, also used to combine with SERS detection. Cheng et al constructed a DEP-based microfluidic chip to separate and concentrate of blood cells and bacterial cells using DEP channels, and the sorting efficiencies for red blood cells and *S. aureus* were 98% and 80%, respectively (86). The electrode surface was roughened and coated with 200-300 nm Au/Cr layer for concentration and SERS detection of the bacteria The LOD for *S. aureus* from red blood cells was  $10^6$  CFU/mL after 3 min of concentration and the authors claimed the LOD would be approximately  $10^5$  CFU/mL if the operation was prolonged to 30 min. Walter et al. designed a 6-port microfluidic chip to integrated a Raman system (87). A two-phase segmented constant flow constantly flew during the measurements. During an ongoing flow of droplets that are separated by mineral oil, spectra of bacteria were detected consecutively resulting in Raman spectra of the mineral oil and SERS spectra measured within the droplets. The advantage of this system is that it could save substantial amount of time to collect same amount of spectral information, since it takes only 1 s to collect a single spectra.

Physical methods, such as capillary action and optical tweezers, are used to facilitate the pre-concentration before SERS measurements. Alexander et al. combine the optically trapping of bacteria using optical tweezers with SERS, and single bacterial spores were trapped and the measured by SERS. Strain discrimination of *Bacillus stearothermophilus* spores were also achieved (88). Yang et al., developed a liquid core photonic crystal fiber (LCPCF), which is filled with bacteria solution due to capillary force. Therefore, the effective volume for the sample solution to interact with the excitation light was increased, and the SERS signal was enhanced significantly. A limit of detection at  $10^6$  cells/mL of live bacterial cells of *Shewanella oneidensis MR-1* was achieved in aqueous solution (89). Zhang et al introduced a microfluidic device that

combines the power of convective gas flow, a partial pressure gradient, mass transfer and capillary surface tension to evaporate fluid from the sample and deliver a tiny volume concentrated analyte to a specific area (90). Samples can be concentrated from hundreds of microliters into nanoliters within minutes. This is advantageous over electrophoresis methods because it does not require high salt buffers, therefore preserves the surface charges on the bacteria, which is important to obtain a consistent and intrinsic SERS signal. After evaporation, the SERS signal was significantly increased due to the concentration effect. Intense peaks were resolved from previously negative samples ( $2 \times 10^4$  cfu/mL), and the limit of detection was lowered to  $2 \times 10^3$  cfu/mL.

One of the most commonly used biological method to separate and concentrate bacteria from complicated sample is immunomagnetic separation (IMS (71)). This strategy often includes magnetic nanoparticles that have been linked to antibodies that are specific to target bacteria. After the magnetic nanoparticles capture the target bacteria, they will be separated from the sample matrix by the applied magnetic field. Guven et al reported Gold-coated magnetic spherical nanoparticles prepared by immobilizing biotin-labeled anti-*E. coli* antibodies onto avidin-coated magnetic nanoparticles and these nanoparticles were used in the separation and concentration of the *E. coli* cells. Then Raman-reporter-molecule-labeled gold nanorods were interacted with gold-coated magnetic spherical nanoparticle-antibody-*E. coli* complex. The resulting complex are concentrated and separated from the solution and the LOD and limit of quantification (LOQ) values of the developed method were found to be 8 and 24 CFU/mL (91). Besides antibody, aptamer can also be used as a bacteria capture agent. Aptamer is a kind of synthetic oligonucleotides discriminated by in vitro screening and systematic evolution of exponential enrichment technology (SELEX), which can bind to certain targets, i.e. bacteria with

extremely high specificity. He et al reported a label-free SERS detection platform with aptamer capture concentration method of *Bacillus anthracis* spores (92). This aptamer beads capture and separate the *Bacillus anthracis* spores from orange juice within 40 min, and the LOD using SERS is at  $10^4$  CFU/mL. *B. anthracis* and *B. mycoides* are successfully differentiated from each other.

### **Development of SERS-based bacteria detection platform: specificity**

For SERS-based bacterial detection platform to have great impact in the field, it must have the capability to differentiate bacteria between species, strains, and even serotype, Due to the variety of bacterial pathogens presence in real samples. Such differentiation can be based on the SERS signals of the bacterial whole cells, its DNA, and even biomarkers.

### **Differentiation of bacteria using intrinsic bacteria SERS signals**

It is clear that visualization of differences in the spectra would be very difficult because the chemical structures of different bacterial cell walls are very similar. Since the SERS spectra can be viewed as multi-variant data, the chemometric analysis is often used to reduce the dimensionality of the data set, maximize the variance among spectral fingerprints, and classify different bacteria from the spectra. The chemometric analysis can be used to enhance pattern recognition and facilitate species classification. It can also aid the model calibration of the SERS spectra of bacteria with a variety of statistical format, including principle component analysis (PCA), hierarchical cluster analysis (HCA), partial least square discriminant analysis (PLS-DA), partial least square regression (PLS), discriminant function analysis (DFA), Linear discriminant analysis (LDA), and support vector machine (SVM). PCA is a primary mathematical method to

reduce the data dimensions by identifying correlations amongst a set of variables and then projecting the original set of variables into a new set of uncorrelated variables called principal components (PCs). PCA is an unsupervised chemometric method, and it is often used for pattern recognition purpose, because the PC scores plot may reveal the clusters of the data (48, 52, 82, 93-99). To further improve the grouping of the SERS spectra from different bacteria, HCA is often employed. “Hierarchical”, in contrast to “non-hierarchical”, means that once an object has been assigned to a group, the process cannot be reversed in the analysis. HCA assigns samples to the individual cluster according to the similarity between them, based either on PCA or Mahalanobis distance, and generates a dendrogram (48, 82, 94, 95, 98). In contrary, a supervised method such as PLS-DA can also be used, where prior knowledge of the classes of the bacteria is used to yield more robust discrimination (82). PLS-DA uses a linear combination of the predictor variables to project the original data to a new set of coordinates to generate a positive/negative prediction. It is often used to classify bacteria based on known characteristics, such as Gram stain results, i.e. G+ versus G-. Other methods can also be used, and choosing the appropriate chemometric methods is based on the nature of the data and the objectives of the research.

Jorvis et al., use discriminant function analysis (DFA) and hierarchical cluster analysis (HCA) to group 28 bacterial isolates of 6 different species, and discriminate *Escherichia coli* on strain level, which was validated by projection of test spectra into DFA and HCA space (94). This report showed the promise of using SERS to disseminate bacteria, but the only 5 different bacterial species analyzed together in the study is too small to make a reasonable claim. Patel et al., developed a “barcoding method” which uses binary barcodes based on the sign of the second derivative of the spectrum as input to the followed clustering algorithms (95). Such method effectively processed the raw SERS spectra data, can the resulting data can correctly classify

different bacteria using PCA, HCA or DFA clustering approaches. This study only classify the bacteria for the scenario that 4 different types of bacteria are present together, either 4 different species or 4 different strains of the *cereus* group. Hennigan et al., used PCA and HCA to discriminate the SERS spectra of 3 strains of *Mycoplasma pneumoniae*. The throat swab samples spiked with *M. pneumoniae* and true clinical throat swab samples were correctly classified by using PLS-DA method (82). Fan et al used PCA to differentiate *Staphylococcus epidermidis*, *E. coli* O157:H7, and their 1:1 ratio (93). Premasiri et al., also used PCA to discriminate SERS spectra of 7 different bacteria and the culture media in which they are grown (52). Walter et al developed a microfluidics device to incorporate the SERS detection of nine different strains of *E. coli*. PCA is carried out for the SERS spectra they collected and first 25 PCS is used for calculation. They use half of the spectra collected through a support vector machine (SVM) classifier to predict the other half of the spectra, and achieved high correction rate (97). PCA method is conducted by Pucek et al., in order to seek discrimination between Gram-positive and Gram-negative bacterial genera based on their SERS spectra (96). However the only 4 bacteria (*Enterococcus faecalis* and *Streptococcus pyogenes* for Gram-positive, *Acinetobacter baumannii* and *Klebsiella pneumoniae* for Gram-negative) used in the study makes such statement unreliable. HCA is used by Stephen et al., to distinct molecular differences on the surface of fourteen closely related *Arthrobacter* strains (48). Zhang et al., developed magnetic-plasmonic Fe<sub>3</sub>O<sub>4</sub>-Au core-shell nanoparticles (Au-MNPs) to generate high quality SERS spectra of bacteria and use PCA plot to show the differentiation of three different bacteria, *A. calcoaceticus*, *E. coli* K12 and *P. aeruginosa*. The SERS spectra of seven foodborne bacteria (*Salmonella typhimurium* ATCC 50013, *Salmonella* O7HZ10, *Shigella boydii* CMCC51514, *Shigella sonnei* CMCC51529, *Shigella dysenteriae* CMCC51252, *Citrobacter freundii*

ATCC43864, and *Enterobacter sakazakii* 154) have been generated on gold nanoparticles by Xie et al (98). PCA and HCA have been employed to analyze those spectra and classify those bacteria.

Throughout those literature that are trying to use chemometrics methods to discriminate bacteria species, serotypes and strains, one common problem is that they all lack a large bacteria sample size to make some general statements of their findings. Especially, the maximum number of bacterial species they used is only seven, so none of the publications considered the scenario that large number of bacterial species is present together because. Would the chemometrics methods still be able to differentiate bacteria if large number of bacteria species are considered, and how should one conduct such discrimination analysis in that situation yet need to be answered.

Although intrinsic SERS signal of bacteria can be used to differentiate them among species, strains, and serotypes when chemometric analysis is applied, such chemometric analysis is proven to be limited when the mixture of different bacteria present. When two or more bacteria are mixed together, the spectra of the mixture will show features of all individual bacteria. By using mathematic modeling methods, some separating on the spectra can be achieved, and reveal the individual spectra of the individual bacteria (100). However, such separation of the spectra can only be achieved under the circumstances that 1) the SERS responses of the individual bacteria retain in the same intensity level; 2) the concentrations ratio of the individual bacteria are close to 1. If one of the two conditions is not satisfied, it will result in the SERS intensity of one bacterium much higher than that of the other bacteria and masks the SERS signal of the others, which makes differentiation impossible.

## **Immune-SERS platform for bacteria detection and differentiation**

Since differentiation of bacteria based on their intrinsic SERS spectra poses some challenges, especially for samples with a mixture of different bacteria, a secondary confirmation is often required. Such secondary confirmation is often based on the target bacteria's immunological properties, and immune molecules, such as antibodies and aptamers, are used. The core of the immune-SERS platform is immune-conjugated nanoparticles, as shown in Figure 2.8. The conjugated immune molecules are specific to the target bacteria, while the nanoparticles are used as the SERS-active substrates. These immune molecules are often labeled with Raman reporter molecules, also known as Raman dyes, which are small molecules with strong and distinguishable Raman spectra. The detection and differentiation of the bacteria are achieved through the detection and differentiation of different Raman reporter molecules. Using antibodies, *E. coli* (101, 102), *Staphylococcus aureus* (103, 104) were successfully detected, and multiplexing was achieved by Sun et al (105). Aptamer can also be used in conjunction with SERS for specific bacteria detection and differentiation, as discussed above. Multiplexing detection of bacteria using aptamers were studied by Ravindranath et al (106). The Ag-Au core-shell nanoparticles were functionalized with anti-*Salmonella typhimurium* aptamers, anti-*Staphylococcus aureus* and anti-*Escherichia coli* O157:H7 antibodies, respectively, and were labeled with unique Raman reporter molecules. Specific detection and differentiation between species (*E. coli* O157:H7 vs. *S. typhimurium*) and strains (*E. coli* O157:H7 vs. *E. coli* K12) were achieved at  $10^2$  and  $10^3$  CFU/ml under 45 mins of total detection time.

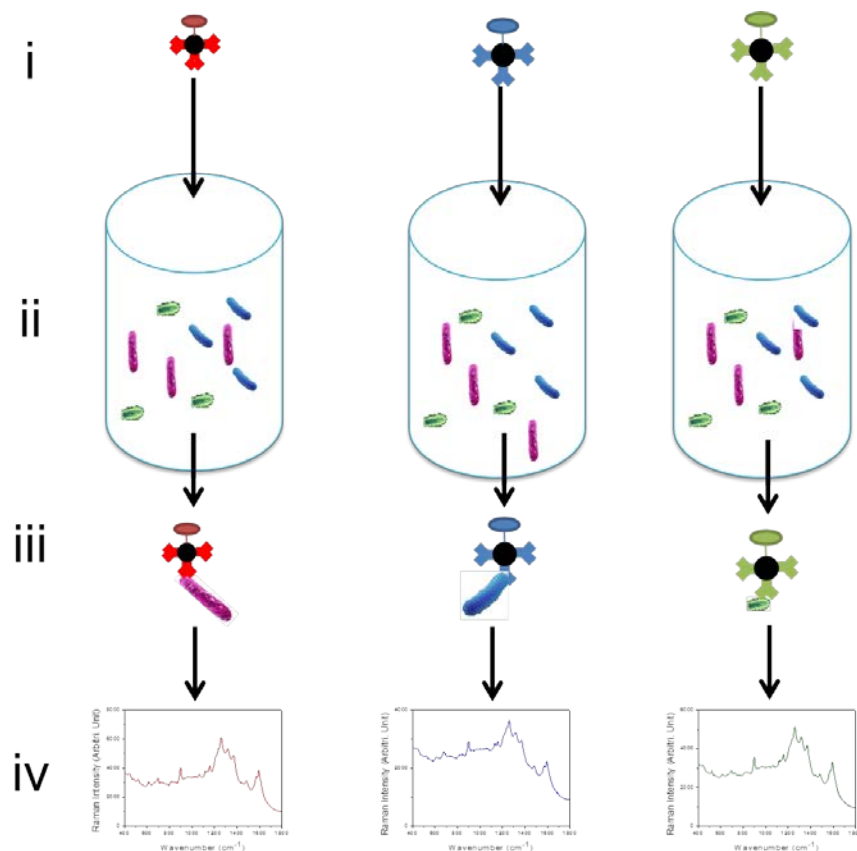


Figure 2.8 The scheme of the immune-SERS platform for multiplexing bacteria detection. (i) Fabrication of immune-conjugated nanoparticles. The core of the nanoparticles can be magnetic. Different nanoparticles have conjugated immune molecules specific to individual bacteria, and are labeled with unique Raman dyes. (ii) Adding different immune-conjugated nanoparticles into a bacteria mixture solution. (iii) Capture and isolation of nanoparticles with an external magnetic field. (iv) Measuring the SERS of the complex to obtain SERS spectra of Raman dyes.

### SERS based bacterial gene probe.

Instead of detection and differentiation of bacterial whole cells, bacterial genomes (DNA or RNA) may be used as alternative means for bacteria detection, since they possess the unique genetic information among bacterial species, strains, and serotypes. The specificity of the SERS-based gene probe relies on the hybridization of the probes with the target bacterial gene sequence, which is complementary to the gene probe. SERS is used to characterize the change before and after the hybridization process, or to detect the Raman dyes attached to the gene probe after the hybridization process. The large amount of genetic material inside the bacterial

cells and their relative smaller size are advantages compared to intrinsic SERS bacteria detection. However, similar to PRC, the drawback of this approach is that it can not differentiate viable cells and dead cells.

SERS based DNA gene probe were reported by Vo-Dinh et al in 1994 (107), and it was used to detect DNA bio-targets via hybridization to DNA sequences complementary to the probe. Nitrocellulose probe containing DNA fragment of interest were subject to hybridization with the the SERS gene probe, which has been labeled with Raman reporter. After hybridization and subsequently washing, only complementary SERS gene probe will be left and detected by SERS, which is the first time the DNA hybridization was monitored by SERS. Over the past 15 years, multiple SERS-based DNA detection assays have been developed, and some of them were used to detect bacterial genomes. Strelau et al. fabricated magnetic nanoparticles (MNPs) for separation of the DNA strands of interest (108). Following the binding of the target DNA, a dye-modified, short synthetic ssDNA was hybridized, which served as label for the SERS detection. The PCR product of the sequences of the bacterium *Mycoplasma mycoides* subspecies *mycoides* small colony type (MmmSC) were amplified and the detected by SERS. To demonstrate the multiplexing capability of SERS, the simultaneous detection of three different PCR products labeled with three dyes was performed. Van Lierop et al. reported a separation free SERS assay with an increase in signal intensity when target DNA was present using a specifically designed SERS primer (109). The presence of specific bacterial DNA from *Staphylococcus epidermidis* was amplified by PCR and then detected by SERS. Multiplexing bacterial DNA detection was achieved by Kang et al. through a Au particle-on-wire system (110). Such a system had a Au nanowire on which the probe DNA was immobilized. After probe DNA was hybridized with the target DNA, another Au nanoparticle linked reporter probe which was also

complementary to the target DNA was then hybridized. Only after the success of these two hybridization steps, the Raman dye on reporter DNA were placed in the SERS enhancement range generated by the coupling of Au nanowire and Au nanoparticles, and then were detected by SERS. Using this SERS platform, PCR products of the four different bacteria from seven clinical isolates (*E. faecium*, 2 isolates; *S. aureus*, 2 isolates; *S. maltophilia*, 2 isolates; *V. vulnificus*, 1 isolate) were successfully identified spontaneously.

Unfortunately, all the findings reported so far were only conducted by using artificially synthesized DNA or PCR products. None of them realized the detection of bacteria in real sample. The time of PCR reaction are added to the total detection time, as well as the associated labor and cost, thus making the SERS gene method not “rapid” enough. The SERS based DNA detection assays also have several drawbacks, besides the inability to differentiate viable and dead cells as discussed above (111). For example, the multiple washing steps are required for all the studies aforementioned, which increase the number of labor intensive handling steps and the risk of sample contamination.

### **Bacterial biomarker detection**

Another alternative method to circumfernce the challenge of whole cell detection is to indirectly detect the presence of bacteria by identifying the biomarkers released by the organism in the matrix fluids. Since these biomarker molecules are unique to bacterial species, detection of specific bacteria from a mixture could easily be accomplished. Zhang *et al* (69) used silver film over nanosphere (AgFON) substrates to acquire the SERS spectra of calcium dipicolinate (CaDPA), a biomarker for bacillus spores, and achieved a limit of detection (LOD) of  $2.6 \times 10^3$  spores of *Bacillus*. Cheng *et al.*, also detected DPA extracted from spores of *Bacillus* using

SERS spectra generated on gold nanoparticles (112), and Cowcher et al measured the DPA SERS spectra used silver colloid (113). Recently Wu et al. reported that pyocyanin (PCN) can be used as a major biomarker for the detection of *Pseudomonas aeruginosa* (114). SERS of PCN were obtained using AgNR substrates as low as 5 ppb or  $2.38 \times 10^{-8}$  mol L<sup>-1</sup> in both aqueous solutions and spiked clinical sputum samples. It has also been used to dynamically monitor the excretion of PCN by *P. aeruginosa* during its growth. The presence of PCN has been detected by SERS in 15 clinical sputum samples, which indicates *P. aeruginosa* infection, with 95.6% sensitivity and 93.3% specificity. However, the studies on the SERS of other bacterial biomarkers are limited due to the difficulties in identifying appropriate biomarkers.

### **Detection of bacteria in food samples**

From a practical point of view, the developed SERS based biosensors must be able detect bacteria in real food samples. However, the greatest challenge comes from the matrix effect in complicated food system (48), and this limit the number of research in this area.

To the best of our knowledge, there are only two studies on the detection of bacteria using SERS from real food samples, due to the complicated nature of food matrix, which contains the molecules similar to target pathogenic bacteria. Other researchers also choose an approach to use extrinsic labels to avoid this problem. Wang et al reported a separation and detection method of multiple pathogens in food matrix by Silica-coated magnetic probes (MNPs@SiO<sub>2</sub>) (71). These probes were functionalized with specific pathogen antibodies to first capture target bacteria directly from a food matrix and another gold nanoparticle integrated with a Raman reporter were functionalized with corresponding antibodies to allow the formation of a sandwich assay. With this assay, *Salmonella enterica* serovar Typhimurium and *Staphylococcus*

*aureus*, were detected in spinach solution, peanut butter as low as  $10^3$  CFU/mL. Orange juice spiked with *Bacillus anthracis* spores was investigated by He et al with aptamer based SERS detection platform (92). A LOD as low as  $10^4$  CFU/mL spores was achieved within 40 mins, and the discrimination between spores *B. anthracis* and *B. mycooides* was also achieved.

## **Conclusions and challenges**

Our discussion thus far has highlighted many aspects of the development on the detection of bacteria using SERS, such as its sensitivity, specificity, and detection in real food samples. Although the detection and differentiation of bacteria using SERS has been successfully demonstrated, several challenges remain, especially for the detection of bacterial pathogens in real food samples (70).

The first challenge is to improve the LOD of SERS. Even though single cell detection is achieved by using a confocal Raman microscope, the concentration of the bacteria in previous studies was high and most of the results are performed only using the pure bacteria strains (70). Therefore, a determination and reduction of the LOD is highly demanded in order to apply the SERS detection methods in real food samples.

As the second challenge is to identify foodborne bacteria in naturally occurring food commodities, attention needs to be applied to sampling methods that are needed for field detection to separate pathogens from food matrix and concentrate pathogens at the same time. The separation method before SERS measurement is crucial to facilitate correctly obtaining bacterial Raman spectra without the interference from other components in food matrix. The food samples often contain macromolecules like protein and polysaccharides that share similar chemical bonds to the target bacteria, which make the detection of intrinsic bacterial SERS

spectra difficult. The small molecules in food samples, such as pigments, may have extremely high SERS intensity, which would interfere the bacterial spectra as well. Therefore, these molecules must be eliminated from the sample matrix prior to the SERS measurement. There is not an easy way to eliminate the interference entirely, but with proper sample pre-processing methods, it is possible to reduce the interference. The sampling methods that can separate bacteria from complicated samples are discussed above. These chemical, physical, physicochemical, or biological approaches can all be combined with SERS for detection of bacteria in complex samples. Another challenge is the low concentration of possible pathogenic bacteria in the food samples. As discussed above, a proper concentration method is also required.

In addition, the heterogeneous distribution of contamination in food samples also needs to consider. In a food system, the pathogenic bacteria are often unevenly distributed, in both concentration level and the types of bacteria present. Pathogens in food samples tend to move and aggregate to the place best for its survival and growth. For example, in cantaloupes, the bacteria concentration is much higher on the outer surface, compared with the inner parts. Such uneven distribution makes the quantitative detection of bacteria from food samples are challenge.

## References

1. **Matthews KR.** 2006. Microorganisms associated with fruits and vegetables, p. 1-19, Microbiology of fresh produce.
2. **Beuchat LR.** 1996. Pathogenic microorganisms associated with fresh produce. *J. Food Prot.* **59**:204-216.
3. **DeWaal CS, Bhuiya F.** 2007. Outbreaks by the numbers: fruits and vegetables 1990-2005.
4. **Lynch MF, Tauxe RV, Hedberg CW.** 2009. The growing burden of foodborne outbreaks due to contaminated fresh produce: risks and opportunities. *Epidemiology and Infection* **137**:307-315.
5. **Buchholz U, Bernard H, Werber D, Böhmer MM, Remschmidt C, Wilking H, Deleré Y, an der Heiden M, Adlhoch C, Dreesman J, Ehlers J, Ethelberg S, Faber M, Frank C, Fricke G, Greiner M, Höhle M, Ivarsson S, Jark U, Kirchner M, Koch J, Krause G, Luber P, Rosner B, Stark K, Kühne M.** 2011. German Outbreak of *Escherichia coli* O104:H4 Associated with Sprouts. *New England Journal of Medicine* **365**:1763-1770.
6. **Harris LJ, Farber JN, Beuchat LR, Parish ME, Suslow TV, Garrett EH, Busta FF.** 2003. Outbreaks Associated with Fresh Produce: Incidence, Growth, and Survival of Pathogens in Fresh and Fresh-Cut Produce. *Comprehensive Reviews in Food Science and Food Safety* **2**:78-141.
7. **Doyle MP, Erickson MC.** 2008. Summer meeting 2007 - the problems with fresh produce: an overview. *Journal Of Applied Microbiology* **105**:317-330.

8. **Driskell JD, Seto AG, Jones LP, Jokela S, Dluhy RA, Zhao YP, Tripp RA.** 2008. Rapid microRNA (miRNA) detection and classification via surface-enhanced Raman spectroscopy (SERS). *Biosensors and Bioelectronics* **24**:917-922.
9. **Berger CN, Sodha SV, Shaw RK, Griffin PM, Pink D, Hand P, Frankel G.** 2010. Fresh fruit and vegetables as vehicles for the transmission of human pathogens. *Environ. Microbiol.* **12**:2385-2397.
10. **Goodridge LD, Bisha B.** 2011. Chromogenic and accelerated cultural methods. *In* Hoorfar J (ed.), *Rapid detection, characterization, and enumeration of foodborne pathogens.* ASM Press, Washington; USA.
11. **Goodridge LD, Fratamico P, Christensen LS, Hoorfar J, Griffiths M, Carter M, Bhumia AK, O'Kennedy R, Goodridge LD, Fratamico P, Christensen LS, Hoorfar J, Griffiths M, Carter M, Bhumia AK, O'Kennedy R.** 2011. Strengths and Shortcomings of Advanced Detection Technologies, p. 15-46, *Rapid Detection, Characterization, and Enumeration of Foodborne Pathogens*, vol. Chapter 2. ASM Press.
12. **De Boer E, Heuvelink AE.** 2000. Methods for the detection and isolation of Shiga toxin-producing *Escherichia coli*. *Journal of Applied Microbiology* **88**:133S-143S.
13. **Bilir Ormanci FS, Erol I, Ayaz ND, Iseri O, Sariguzel D.** 2008. Immunomagnetic separation and PCR detection of *Listeria monocytogenes* in turkey meat and antibiotic resistance of the isolates. *British Poultry Science* **49**:560-565.
14. **Skjerve E, Olsvik Ø.** 1991. Immunomagnetic separation of *Salmonella* from foods. *International Journal of Food Microbiology* **14**:11-17.

15. **Mercanoglu Taban B, Ben U, Aytac SA.** 2009. Rapid detection of Salmonella in milk by combined immunomagnetic separation-polymerase chain reaction assay. *Journal of dairy science* **92**:2382-2388.
16. **Šafaříková M, Šafařík I.** 2001. Immunomagnetic separation of Escherichia coli O26, O111 and O157 from vegetables. *Letters in Applied Microbiology* **33**:36-39.
17. **Notzon A, Helmuth R, Bauer J.** 2006. Evaluation of an Immunomagnetic SeparationReal-Time PCR Assay for the Rapid Detection of Salmonella in Meat. *J. Food Prot.* **69**:2896-2901.
18. **Lakićević B, Janković V, Spirić D, Matekalo-Sverak V, Mitrović R, Borović B, Baltić T.** 2012. Detection of staphylococcal enterotoxins in foodstuffs of animal origin by ELISA method. / Utvrivanje prisustva stafilokoknih enterotoksina u namirnicama animalnog porekla ELISA testom. *Tehnologija Mesa* **53**:50-55.
19. **Jonkuvienė D, Šalomskienė J.** 2009. Rapid methods for the detection and identification of Bacillus cereus in food products (review). / Spartieji Bacillus cereus nustatymo ir identifikavimo maisto produktuose metodai (apzvalga). *Food Chemistry and Technology (Maisto Chemija ir Technologija)* **43**:29-35.
20. **Schlöter M, Aßmus B, Hartmann A.** 1995. The use of immunological methods to detect and identify bacteria in the environment. *Biotechnology Advances* **13**:75-90.
21. **Osek J, Kowalczyk A, Wiczorek K.** 2005. Molecular methods of detecting and identifying bacterial food pathogens. / Molekularne metody wykrywania i identyfikacji chorobotwórczych bakterii w żywności. *Medycyna Weterynaryjna* **61**:5-9.
22. **Rantsiou K, Cocolin L.** 2013. Second-generation polymerase chain reaction (PCR) and DNA microarrays for in vitro and in situ study of foodborne pathogens. *In Sofos J (ed.),*

Advances in microbial food safety, Volume 1. Woodhead Publishing Ltd, Cambridge; UK.

23. **Kántor A, Kačániová M, Petrová J, Medo J, Hleba L, Rovná K.** 2014. Identification of lactic acid bacteria isolated from red wine samples by RT-qPCR. *Journal of Microbiology, Biotechnology and Food Sciences* **3**:235-237.
24. **Cossey J, Thomas K.** 2011. Detection of food poisoning bacteria in ciders using RT PCR. *Aspects of Applied Biology*:69-74.
25. **Dolan A, Burgess CM, Fanning S, Duffy G.** 2010. Application of quantitative reverse-transcription PCR (qRT-PCR) for the determination of the total viable count (TVC) on meat samples. *Journal of Applied Microbiology* **109**:91-98.
26. **Quero GM, Santovito E, Visconti A, Fusco V.** 2014. Quantitative detection of *Listeria monocytogenes* in raw milk and soft cheeses: culture-independent versus liquid- and solid-based culture-dependent real time PCR approaches. *LWT - Food Science and Technology* **58**:11-20.
27. **Macé S, Mamlouk K, Chipchakova S, Prévost H, Joffraud JJ, Dalgaard P, Pilet MF, Dousset X.** 2013. Development of a rapid real-time PCR method as a tool to quantify viable *Photobacterium phosphoreum* bacteria in salmon (*Salmo salar*) steaks. *Applied and Environmental Microbiology* **79**:2612-2619.
28. **Garrido A, Chapela MJ, Román B, Fajardo P, Lago J, Vieites JM, Cabado AG.** 2013. A new multiplex real-time PCR developed method for *Salmonella* spp. and *Listeria monocytogenes* detection in food and environmental samples. *Food Control* **30**:76-85.
29. **Li J, Zhao Z, Jia X, Li J, Zhang Y, Zhao L.** 2013. Advance on detection of foodborne pathogenic bacteria. *Food Research and Development* **34**:110-115.

30. **Samanta N, Kundu O, Chaudhuri CR.** A Simple Low Power Electronic Readout for Rapid Bacteria Detection With Impedance Biosensor.
31. **Shabani A, Marquette CA, Mandeville R, Lawrence MF.** 2013. Carbon microarrays for the direct impedimetric detection of Bacillus anthracis using Gamma phages as probes. *The Analyst* **138**:1434-1440.
32. **Ribeiro T, Romestant G, Depoortere J, Pauss A.** 2003. Development, validation, and applications of a new laboratory-scale indirect impedancemeter for rapid microbial control. *Appl Microbiol Biotechnol* **63**:35-41.
33. **Mejri, Mb, Baccar, Ktari, Aouni, Abdelghani.** - Detection of E.Coli Bacteria Using Impedance Spectroscopy and Surface Plasmon Resonance Imaging Based Biosensor.
34. **Guo X, Lin C-S, Chen S-H, Ye R, Wu VCH.** 2012. A piezoelectric immunosensor for specific capture and enrichment of viable pathogens by quartz crystal microbalance sensor, followed by detection with antibody-functionalized gold nanoparticles. *Biosensors and Bioelectronics* **38**:177-183.
35. **Sandrin TR, Goldstein JE, Schumaker S.** 2013. MALDI TOF MS profiling of bacteria at the strain level: A review. *Mass Spectrometry Reviews* **32**:188-217.
36. **Burgula Y, Khali D, Kim S, Krishnan SS, Cousin MA, Gore JP, Reuhs BL, Mauer LJ.** 2007. REVIEW OF MID-INFRARED FOURIER TRANSFORM-INFRARED SPECTROSCOPY APPLICATIONS FOR BACTERIAL DETECTION. *Journal of Rapid Methods & Automation in Microbiology* **15**:146-175.
37. **Smith E, Dent G.** 2005. Introduction, Basic Theory and Principles, p. 1-21, *Modern Raman Spectroscopy – A Practical Approach*. John Wiley & Sons, Ltd.

38. **Fleischmann M, Hendra PJ, McQuillan AJ.** 1974. Raman spectra of pyridine adsorbed at a silver electrode. *Chemical Physics Letters* **26**:163-166.
39. **Jeanmaire DL, Van Duyne RP.** 1977. Surface raman spectroelectrochemistry: Part I. Heterocyclic, aromatic, and aliphatic amines adsorbed on the anodized silver electrode. *Journal of Electroanalytical Chemistry and Interfacial Electrochemistry* **84**:1-20.
40. **Albrecht MG, Creighton JA.** 1977. Anomalously intense Raman spectra of pyridine at a silver electrode. *J. Am. Chem. Soc.* **99**:5215-5217.
41. **King FW, Van Duyne RP, Schatz GC.** 1978. Theory of Raman scattering by molecules adsorbed on electrode surfaces. *The Journal of Chemical Physics* **69**:4472-4481.
42. **Smith E, Dent G.** 2005. Surface-Enhanced Raman Scattering and Surface-Enhanced Resonance Raman Scattering, p. 113-133, *Modern Raman Spectroscopy – A Practical Approach*. John Wiley & Sons, Ltd.
43. **Ru EL, Etchegoin P.** 2009. *Principles of Surface-Enhanced Raman Spectroscopy: and related plasmonic effects*. Elsevier Science.
44. **Kneipp K, Moskovits M, Kneipp H.** 2006. *Surface-Enhanced Raman Scattering: Physics and Applications*. Springer-Verlag Berlin Heidelberg.
45. **LeytoBrown RJC, Milton MJT.** 2008. Nanostructures and nanostructured substrates for surface—enhanced Raman scattering (SERS). *J. Raman Spectrosc.* **39**:1313-1326.
46. **Efrima S, Bronk BV.** 1998. Silver Colloids Impregnating or Coating Bacteria. *The Journal of Physical Chemistry B* **102**:5947-5950.
47. **Alexander TA, Pellegrino PM, Gillespie JB.** 2003, p 91-100.

48. **Stephen KE, Homrighausen D, DePalma G, Nakatsu CH, Irudayaraj J.** 2012. Surface enhanced Raman spectroscopy (SERS) for the discrimination of *Arthrobacter* strains based on variations in cell surface composition. *Analyst* **137**:4280-4286.
49. **Liu TY, Tsai KT, Wang HH, Chen Y, Chen YH, Chao YC, Chang HH, Lin CH, Wang JK, Wang YL.** 2011. Functionalized arrays of Raman-enhancing nanoparticles for capture and culture-free analysis of bacteria in human blood. *Nature communications* **2**:538.
50. **Biju V, Pan D, Gorby YA, Fredrickson J, McLean J, Saffarini D, Lu HP.** 2006. Combined Spectroscopic and Topographic Characterization of Nanoscale Domains and Their Distributions of a Redox Protein on Bacterial Cell Surfaces. *Langmuir* **23**:1333-1338.
51. **Marotta NE, Bottomley LA.** 2010. Surface-Enhanced Raman Scattering of Bacterial Cell Culture Growth Media. *Appl. Spectrosc.* **64**:601-606.
52. **Premasiri WR, Gebregziabher Y, Ziegler LD.** 2011. On the Difference Between Surface-Enhanced Raman Scattering (SERS) Spectra of Cell Growth Media and Whole Bacterial Cells. *Appl. Spectrosc.* **65**:493-499.
53. **Leyto P, Lizama-Vergara PA, Campos-Vallette MM, Becker MI, Clavijo E, Cordova Reyes I, Vera M, Jerez CA.** 2005. Surface enhanced Raman spectrum of nanometric molecular systems. *Journal of the Chilean Chemical Society* **50**:725-730.
54. **Kahraman M, Kesero, lu K, ulha M.** 2011. On Sample Preparation for Surface-Enhanced Raman Scattering (SERS) of Bacteria and the Source of Spectral Features of the Spectra. *Appl. Spectrosc.* **65**:500-506.

55. **Ramírez P, Toledo H, Guiliani N, Jerez CA.** 2002. An Exported Rhodanese-Like Protein Is Induced during Growth of *Acidithiobacillus ferrooxidans* in Metal Sulfides and Different Sulfur Compounds. *Applied and Environmental Microbiology* **68**:1837-1845.
56. **Efrima S, Bronk B.** 1998. Silver colloids impregnating or coating bacteria. *J. Phys. Chem. B* **102**:5947-5950.
57. **Efrima S, Zeiri L.** 2009. Understanding SERS of bacteria. *J. Raman Spectrosc.* **40**:277-288.
58. **Zeiri L, Bronk B, Shabtai Y, Czege J, Efrima S.** 2002. Silver metal induced surface enhanced Raman of bacteria. *Colloids and Surfaces A: Physicochemical and Engineering Aspects* **208**:357-362.
59. **Zeiri L, Bronk BV, Shabtai Y, Eichler J, Efrima S.** 2004. Surface-enhanced Raman spectroscopy as a tool for probing specific biochemical components in bacteria. *Appl Spectrosc* **58**:33-40.
60. **Zeiri L, Efrima S.** 2005. Surface-enhanced Raman spectroscopy of bacteria: the effect of excitation wavelength and chemical modification of the colloidal milieu. *J. Raman Spectrosc.* **36**:667-675.
61. **Liu Y, Chen Y, Nou X, Chao K.** 2007. Potential of Surface-Enhanced Raman Spectroscopy for the Rapid Identification of *Escherichia Coli* and *Listeria Monocytogenes* Cultures on Silver Colloidal Nanoparticles. *Appl. Spectrosc.* **61**:824-831.
62. **Szeghalmi A, Kaminskyj S, Rösch P, Popp J, Gough KM.** 2007. Time Fluctuations and Imaging in the SERS Spectra of Fungal Hypha Grown on Nanostructured Substrates. *The Journal of Physical Chemistry B* **111**:12916-12924.

63. **Laucks ML, Sengupta A, Junge K, Davis EJ, Swanson BD.** 2005. Comparison of Psychro-active Arctic Marine Bacteria and Common Mesophilic Bacteria Using Surface-Enhanced Raman Spectroscopy. *Appl. Spectrosc.* **59**:1222-1228.
64. **Abell JL, Driskell JD, Dluhy RA, Tripp RA, Zhao YP.** 2009. Fabrication and characterization of a multiwell array SERS chip with biological applications. *Biosensors and Bioelectronics* **24**:3663-3670.
65. **Jarvis R, Clarke S, Goodacre R.** 2006. Rapid Analysis of Microbiological Systems Using SERS, p. 397-408. *In* Kneipp K, Moskovits M, Kneipp H (ed.), *Surface-Enhanced Raman Scattering*, vol. 103. Springer Berlin Heidelberg.
66. **Sengupta A, Mujacic M, Davis EJ.** 2006. Detection of bacteria by surface-enhanced Raman spectroscopy. *Anal. Bioanal. Chem.* **386**:1379-1386.
67. **Premasiri WR, Moir DT, Klempner MS, Krieger N, Jones G, Ziegler LD.** 2004. Characterization of the Surface Enhanced Raman Scattering (SERS) of Bacteria. *The Journal of Physical Chemistry B* **109**:312-320.
68. **Guzelian AA, Sylvia JM, Janni JA, Clauson SL, Spencer KM.** 2002. SERS of whole-cell bacteria and trace levels of biological molecules. *Proc. SPIE 4577, Vibrational Spectroscopy-based Sensor Systems*:182-192.
69. **Zhang X, Young MA, Lyandres O, Van Duyne RP.** 2005. Rapid Detection of an Anthrax Biomarker by Surface-Enhanced Raman Spectroscopy. *J. Am. Chem. Soc.* **127**:4484-4489.
70. **Chu H, Huang Y, Zhao Y.** 2008. Silver Nanorod Arrays as a Surface-Enhanced Raman Scattering Substrate for Foodborne Pathogenic Bacteria Detection. *Appl. Spectrosc.* **62**:922-931.

71. **Wang Y, Ravindranath S, Irudayaraj J.** 2011. Separation and detection of multiple pathogens in a food matrix by magnetic SERS nanoprobe. *Anal Bioanal Chem* **399**:1271-1278.
72. **Wang Y, Lee K, Irudayaraj J.** 2010. Silver Nanosphere SERS Probes for Sensitive Identification of Pathogens. *The Journal of Physical Chemistry C* **114**:16122-16128.
73. **Wang HH, Liu CY, Wu SB, Liu NW, Peng CY, Chan TH, Hsu CF, Wang JK, Wang YL.** 2006. Highly Raman-Enhancing Substrates Based on Silver Nanoparticle Arrays with Tunable Sub-10 nm Gaps. *Advanced Materials* **18**:491-495.
74. **Liu T-T, Lin Y-H, Hung C-S, Liu T-J, Chen Y, Huang Y-C, Tsai T-H, Wang H-H, Wang D-W, Wang J-K, Wang Y-L, Lin C-H.** 2009. A High Speed Detection Platform Based on Surface-Enhanced Raman Scattering for Monitoring Antibiotic-Induced Chemical Changes in Bacteria Cell Wall. *PLoS ONE* **4**:e5470.
75. **Jarvis R, Brooker A, Goodacre R.** 2004. Surface-enhanced Raman spectroscopy for bacterial discrimination utilizing a scanning electron microscope with a Raman spectroscopy interface. *Anal. Chem* **76**:5198-5202.
76. **Çulha M, Adigüzel A, Yazici M, Kahraman M, ahin F, Güllüce M.** 2008. Characterization of thermophilic bacteria using surface-enhanced Raman scattering. *Appl. Spectrosc.* **62**:1226-1232.
77. **LUO B, LIN M.** 2008. A portable Raman system for the identification of foodborne pathogenic bacteria. *Journal of Rapid Methods & Automation in Microbiology* **16**:238-255.

78. **Guicheteau J, Christesen S, Emge D, Tripathi A.** 2010. Bacterial mixture identification using Raman and surface-enhanced Raman chemical imaging. *J. Raman Spectrosc.*:n/a-n/a.
79. **Goeller L, Riley M.** 2007. Discrimination of bacteria and bacteriophages by Raman spectroscopy and surface-enhanced Raman spectroscopy. *Appl. Spectrosc.* **61**:679-685.
80. **Zhang L, Xu J, Mi L, Gong H, Jiang S, Yu Q.** 2012. Multifunctional magnetic-plasmonic nanoparticles for fast concentration and sensitive detection of bacteria using SERS. *Biosens Bioelectron* **31**:130-136.
81. **Wu X, Gao S, Wang J-S, Wang H, Huang Y-W, Zhao Y.** 2012. The surface-enhanced Raman spectra of aflatoxins: spectral analysis, density functional theory calculation, detection and differentiation. *Analyst* **137**:4226-4234.
82. **Neyrolles O, Hennigan SL, Driskell JD, Dluhy RA, Zhao Y, Tripp RA, Waites KB, Krause DC.** 2010. Detection of *Mycoplasma pneumoniae* in Simulated and True Clinical Throat Swab Specimens by Nanorod Array-Surface-Enhanced Raman Spectroscopy. *PLoS ONE* **5**:e13633.
83. **Shanmukh S, Jones L, Zhao YP, Driskell J, Tripp R, Dluhy R.** 2008. Identification and classification of respiratory syncytial virus (RSV) strains by surface-enhanced Raman spectroscopy and multivariate statistical techniques. *Anal. Bioanal. Chem.* **390**:1551-1555.
84. **Du XB, Chu HY, Huang YW, Zhao YP.** 2010. Qualitative and Quantitative Determination of Melamine by Surface-Enhanced Raman Spectroscopy Using Silver Nanorod Array Substrates. *Appl. Spectrosc.* **64**:781-785.

85. **Stevens KA, Jaykus L-A.** 2004. Bacterial separation and concentration from complex sample matrices: a review. *Critical Reviews In Microbiology* **30**:7-24.
86. **Cheng IF, Lin CC, Lin DY, Chang HC.** 2010. A dielectrophoretic chip with a roughened metal surface for on-chip surface-enhanced Raman scattering analysis of bacteria. *Biomicrofluidics* **4**:034104.
87. **Walter A, März A, Schumacher W, Rösch P, Popp J.** 2011. Towards a fast, high specific and reliable discrimination of bacteria on strain level by means of SERS in a microfluidic device. *Lab Chip*.
88. **Alexander TA, Pellegrino PM, Gillespie JB.** 2003. Near-Infrared Surface-Enhanced-Raman-Scattering-Mediated Detection of Single Optically Trapped Bacterial Spores. *Appl. Spectrosc.* **57**:1340-1345.
89. **Yang X, Gu C, Qian F, Li Y, Zhang JZ.** 2011. Highly Sensitive Detection of Proteins and Bacteria in Aqueous Solution Using Surface-Enhanced Raman Scattering and Optical Fibers. *Analytical Chemistry* **83**:5888-5894.
90. **Zhang JY, Do J, Premasiri WR, Ziegler LD, Klapperich CM.** 2010. Rapid point-of-care concentration of bacteria in a disposable microfluidic device using meniscus dragging effect. *Lab Chip* **10**:3265-3270.
91. **Guven B, Basaran-Akgul N, Temur E, Tamer U, Boyac IH.** 2011. SERS-based sandwich immunoassay using antibody coated magnetic nanoparticles for *Escherichia coli* enumeration. *Analyst* **136**:740-748.
92. **He L, Deen B, Pagel AH, Diez-Gonzalez F, Labuza TP.** 2013. Concentration, detection and discrimination of *Bacillus anthracis* spores in orange juice using aptamer based surface enhanced Raman spectroscopy. *Analyst* **138**:1657-1659.

93. **Fan C, Hu Z, Mustapha A, Lin M.** 2011. Rapid detection of food- and waterborne bacteria using surface-enhanced Raman spectroscopy coupled with silver nanosubstrates. *Appl Microbiol Biotechnol* **92**:1053-1061.
94. **Jarvis RM, Goodacre R.** 2004. Discrimination of Bacteria Using Surface-Enhanced Raman Spectroscopy. *Analytical Chemistry* **76**:40-47.
95. **Patel IS, Premasiri WR, Moir DT, Ziegler LD.** 2008. Barcoding bacterial cells: a SERS-based methodology for pathogen identification. *J. Raman Spectrosc.* **39**:1660-1672.
96. **Prucek R, Ranc V, Kvitek L, Panacek A, Zboril R, Kolar M.** 2012. Reproducible discrimination between Gram-positive and Gram-negative bacteria using surface enhanced Raman spectroscopy with infrared excitation. *Analyst* **137**:2866-2870.
97. **Walter A, Marz A, Schumacher W, Rosch P, Popp J.** 2011. Towards a fast, high specific and reliable discrimination of bacteria on strain level by means of SERS in a microfluidic device. *Lab Chip* **11**:1013-1021.
98. **Xie Y, Xu L, Wang Y, Shao J, Wang L, Wang H, Qian H, Yao W.** 2013. Label-free detection of the foodborne pathogens of Enterobacteriaceae by surface-enhanced Raman spectroscopy. *Analytical Methods* **5**:946-952.
99. **Zhang L, Xu J, Mi L, Gong H, Jiang S, Yu Q.** 2012. Multifunctional magnetic-plasmonic nanoparticles for fast concentration and sensitive detection of bacteria using SERS. *Biosensors and Bioelectronics* **31**:130-136.
100. **Cam D, Keseroglu K, Kahraman M, Sahin F, Culha M.** 2010. Multiplex identification of bacteria in bacterial mixtures with surface-enhanced Raman scattering. *J. Raman Spectrosc.* **41**:484-489.

101. **Naja G, Bouvrette P, Hrapovic S, Luong JHT.** 2007. Raman-based detection of bacteria using silver nanoparticles conjugated with antibodies. *Analyst* **132**:679-686.
102. **Guven B, Basaran-Akgul N, Temur E, Tamer U, Boyaci IH.** 2011. SERS-based sandwich immunoassay using antibody coated magnetic nanoparticles for Escherichia coli enumeration. *The Analyst* **136**:740-748.
103. **Huang P-J, Tay L-L, Tanha J, Ryan S, Chau L-K.** 2009. Single-Domain Antibody-Conjugated Nanoaggregate-Embedded Beads for Targeted Detection of Pathogenic Bacteria. *Chemistry – A European Journal* **15**:9330-9334.
104. **Tay L-L, Tanha J, Ryan S, Veres T.** 2007, p 67960C-67960C-67967.
105. **Sun J, Hankus ME, Cullum BM.** 2009, p 73130K-73130K-73110.
106. **Ravindranath SP, Wang Y, Irudayaraj J.** 2011. SERS driven cross-platform based multiplex pathogen detection. *Sensors and Actuators B: Chemical* **152**:183-190.
107. **Vo-Dinh T, Houck K, Stokes DL.** 1994. Surface-Enhanced Raman Gene Probes. *Analytical Chemistry* **66**:3379-3383.
108. **Strelau KK, Brinker A, Schnee C, Weber K, Möller R, Popp J.** 2011. Detection of PCR products amplified from DNA of epizootic pathogens using magnetic nanoparticles and SERS. *J. Raman Spectrosc.* **42**:243-250.
109. **van Lierop D, Faulds K, Graham D.** 2011. Separation Free DNA Detection Using Surface Enhanced Raman Scattering. *Analytical Chemistry* **83**:5817-5821.
110. **Kang T, Yoo SM, Yoon I, Lee SY, Kim B.** 2010. Patterned Multiplex Pathogen DNA Detection by Au Particle-on-Wire SERS Sensor. *Nano Letters* **10**:1189-1193.
111. **van Lierop D, Larmour IA, Faulds K, Graham D.** 2013. SERS Primers and Their Mode of Action for Pathogen DNA Detection. *Analytical Chemistry* **85**:1408-1414.

112. **Cheng H-W, Huan S-Y, Wu H-L, Shen G-L, Yu R-Q.** 2009. Surface-Enhanced Raman Spectroscopic Detection of a Bacteria Biomarker Using Gold Nanoparticle Immobilized Substrates. *Analytical Chemistry* **81**:9902-9912.
113. **Cowcher DP, Xu Y, Goodacre R.** 2013. Portable, Quantitative Detection of Bacillus Bacterial Spores Using Surface-Enhanced Raman Scattering. *Analytical Chemistry* **85**:3297-3302.
114. **Wu X, Chen J, Li X, Zhao Y, Zughair SM.** 2014. Culture-free diagnostics of *Pseudomonas aeruginosa* infection by silver nanorod array based SERS from clinical sputum samples, *Nanomedicine : nanotechnology, biology, and medicine*. Elsevier. DOI: 10.1016/j.nano.2014.04.010.

CHAPTER 3  
UNDERSTANDING BACTERIAL SERS SPECTRA<sup>1</sup>

---

<sup>1</sup>Xiaomeng Wu, Yao-wen Huang, and Yiping Zhao. To be submitted to *Analytical Chemistry*.

## **Abstract**

Successfully application of SERS for bacteria detection relies on the characteristic fingerprints of bacterial SERS spectra. Although numerous efforts have been put into investigation of the origins of the bacterial SERS spectra, there is still great controversy present in the literature. In this report, we performed a systematically investigation on the SERS spectra of important cell components. Cell wall, cell wall associated proteins, inner cell proteins, genomic DNA of four different bacteria were isolated and purified using different biochemical methods. SERS spectra of these important cell components were obtained and compared to reveal the origins of the bacterial SERS spectra. We found that the SERS spectra of bacteria originate from the bacteria cell wall, more specifically the peptidoglycan layer and the cell wall associated proteins. Intrinsic SERS spectra of the genomic DNA of different bacteria showed no differentiation between each other. The inner cell water soluble proteins are not contributing to the SERS spectra of the bacterial whole cells. This information would provide better understanding of the SERS spectra of the bacteria at molecule level, and guide our design of the bacterial detection methods.

## Introduction

For the past decades, the surface-enhanced Raman spectroscopy (SERS) of bacteria has been studied by many researchers as SERS has the potential to be a rapid and sensitive bacteria detection method<sup>1-14</sup>. SERS brings the analyte molecules into close proximity with the appropriate metallic nanostructures, thus significantly increasing the Raman vibrational signals of the analyte. These molecular vibrational modes represent a unique “fingerprint” spectrum consisting of Raman peaks that can be used to identify the particular molecule(s) being probed<sup>15</sup>. This method of enhancement is often employed to facilitate sensitivity so as to allow for the trace detection of molecules, even with single cell sensitivity<sup>16-20</sup>.

The unique feature of SERS detection is to obtain the characteristic fingerprints of specific molecules. However, since bacteria cells are very complicated, the use of intrinsic SERS spectra of bacteria to detect and differentiate bacteria highly relies on the understanding of the bacteria SERS spectra. Bacterial cell is a complex dynamic system, with numerous chemical components that would contribute to the overall SERS signal. Understanding the origins of such SERS signal and subsequently designing appropriate detection strategy for those chemical components is one of the fundamental tasks for researchers. As of today, most of the researchers in the field have convinced that the SERS signals of bacteria are mainly coming from the bacteria cell envelope<sup>21</sup>, but there are still controversy on the origins of the bacterial SERS signal.

Since bacteria are grown in the culture media, the effect of media on the Raman or SERS spectra has been investigated by several researchers. Marotta and Bottomley examine the SERS spectra of fifteen commonly used bacterial growth media and found these spectra are similar to spectra of bacterium<sup>22</sup>. Therefore, they suggest that the residues of the bacterial growth media

may contribute greatly to the overall SERS response. In response to this hypothesis, Premasiri et al. investigated the SERS spectra of different bacterial species grown in the same growth media, suggesting that spectra are indeed intrinsically attributed to the bacterial cells<sup>5</sup>. However, Leyton et al. investigated the bacteria *Acidithiobacillus ferrooxidans* by means of SERS and found out that the SERS spectra displayed physical and chemical variations caused by different growth media<sup>23</sup>. Kahraman et al. also found that the features observed in bacterial SERS spectra originate mostly from the bacteria surface with some contributions from metabolic activity or molecular species detached from the bacteria surface during sample preparation<sup>24</sup>.

Efrima et al.<sup>25</sup> did a study to investigate the difference in SERS signal between an "internal colloid" formed inside the *Bacillus megaterium* ( $G^+$ ) and *E. coli* ( $G^-$ ) cells and the nanoparticle layer coating the cell wall. They reported that that SERS effect is mainly generated on the cell surface, not the cell interior. On the other hands, Zeri et al.<sup>26</sup> found that the SERS spectra of four different bacterial species (*E. coli*, *Acinetobacter calcoaceticus*, *Pseudomonas aeruginosa* and *Bacillus megaterium*) were similar, implying that the spectra were greatly attributed to a specific molecule, presumably FAD,. In a follow-up study<sup>27</sup>, the group fractionated the cell and collected cell surface debris for SERS measurement. Results confirmed their hypothesis that the spectra of bacteria resembled that of FAD, and the bacterial SERS signal mainly originated from the wall fraction, which was consistent with Efrima et al's findings.

Great controversy over the origins of the peak at  $\Delta\nu = 730 \text{ cm}^{-1}$  were found in the literature. Leyhton et al. suggests that the peak at  $\Delta\nu = 730 \text{ cm}^{-1}$  is corresponding to the D-glucose, which is attributed to the lipid layer components of the cell walls and membranes. Liu et al.<sup>28</sup> pointed out that the origin of the peak at  $\Delta\nu = 730 \text{ cm}^{-1}$  might be attributed to the symmetric O-P-O vibrational mode of the phosphate group, rather than FAD or glucose on the cell surface,

based on their observation that  $K_2HPO_4$  exhibited the same band. Another group, Sengupta et al.<sup>29</sup>, also attempted to interpret the bacterial SERS spectra by comparing them with important cell wall components- N-acetyl glucosamine (NAG), L-lysine, D-glutamic acid and D-alanine.

Other cell membrane or cell wall components of bacteria were also studied. SERS imaging of fungal hyphae grown on nanostructured SERS active substrates was studied by Szegalmi et al. to present the possibility for the detection of single cell wall components<sup>30</sup>. A comparative study of psychro-active arctic marine bacteria and common mesophilic bacteria by SERS revealed that a higher lipid content of unsaturated fatty acids in the outer membranes of marine bacteria could be identified<sup>31</sup>.

In all this aforementioned studies, we see the controversy on the origin of SERS peaks, especially on the whether the signal is from the bacterial cell or metabolic products, and the attribution of some peaks, such as the peak at  $\Delta\nu = 730\text{ cm}^{-1}$ . Identification each and every one of the bacterial SERS peaks and attributed to chemical components in the bacterial cells is a challenging and nearly impossible task. Through the aforementioned studies, we can conclude that the chemical substances potentially contributing to SERS spectra are mainly from the outer structure of the bacteria cell, such as outer membrane and cell wall. However, some of the inner cell components, such as DNA, RNA, proteins, and some metabolic products may be present in the surrounding environment, and then yield a SERS signal. The controversy in the origins of the bacterial SERS spectra requires us to thoroughly investigate each may cell components that may contribute to the overall spectra.

Bacteria can be classified as Gram positive (G+) and Gram negative (G-) bacteria. The biggest differences between G+ and G- bacteria are their cell envelopes<sup>32, 33</sup>. Immediately external to the cytoplasmic membrane of G- bacteria is a thin peptidoglycan layer which is made

of N-acetylglucosamine (NAG), N-acetylmuramic acid (NAM), and peptides. External to the peptidoglycan layer is the outer membrane which consists of phospholipids with saturated fatty acids and contains an additional periplasmic space, which is absent in the G+ bacteria. The cell wall of G+ bacteria has multiple layers, consisting mainly of a thick peptidoglycan layer within which may also include teichoic acids, lipoteichoic acids, complex polysaccharides, and proteins. These molecules are common surface antigens that distinguish bacterial serotypes and promote attachment to other bacteria as well as to specific receptors on mammalian cell surfaces<sup>34</sup>. Inside of cell wall, the differences between G+ and B- bacteria cells are limited. They both consist of chromosome (naked DNA), soluble proteins, ribosomes, and small molecules such as nucleotides, carbohydrate, and lipids. These Raman and SERS spectra of these substances have been previously studied<sup>2, 24, 35-40</sup>, and their Raman/SERS signature peaks are summarized in Table 3.1.

In this report, we performed a systematic investigation on the SERS spectra of important cell components. Cell wall, cell wall associated proteins, inner cell proteins, genomic DNA of four different bacteria were isolated and purified using different biochemical methods. SERS spectra of these important cell components were obtained and compared to reveal the origins of the bacterial SERS spectra.

## **Materials and Methods**

### **Chemicals**

N-acetylglucosamine (NAG) and N-acetylmuramic acid (NAM) were purchased from Sigma Aldrich Ltd. (St. Louis, MO), and they were diluted by using ultra-pure water (18M $\Omega$ ) to 1 mM.

### **AgNR SERS substrate fabrication**

The bacterial SERS spectra were acquired using AgNR array substrates fabricated by the oblique angle deposition (OAD) technique in a custom-designed electron beam evaporation (e-beam) system<sup>41-43</sup>. Briefly, glass microscopic slides (Gold Seal® Catalog No.3010, Becton, Dickinson and Company, Portsmouth, NH) were cleaned with piranha solution (80% sulfuric acid, 20% hydrogen peroxide in volume) and rinsed with deionized (DI) water. The substrates were then dried with a stream of nitrogen gas before being loaded into the deposition system. In the deposition system, the substrate surface was held perpendicular to the incident vapor direction while a 20-nm titanium film and then a 200-nm silver film were evaporated onto the glass slides at a rate of ~ 0.2 nm/s and 0.3 nm/s, respectively. Monitoring of this process was performed *in situ* by a quartz crystal microbalance (QCM). The substrates were then rotated to an angle of 86° with respect to the incident vapor and AgNRs were grown with a deposition rate of ~ 0.3 nm/s until the thickness reading of QCM reached 2000 nm.

### **Bacteria strains and growth**

Four bacterial isolates were used in this study, *Bacillus subtilis* (BS), *E. Coli* O157:H7 salami isolate (EC), *Listeria monocytogenes* 301 (LM), and *Staphylococcus aureus* ATCC 12600 (SA). Bacterial isolates were stored at -80°C in 15-20 % glycerol for long-term storage. For short-term storage, bacterial isolates were stored in trypticase soy agar (TSA) slants at 4°C. Bacterial cultures were prepared by inoculating pure isolates from agar slants into trypticase soy broth (TSB) tubes and incubated at 35 ± 2°C for 18 - 24 hours. The overnight cultures of all isolates were centrifuged at 5000 rpm for 10 minutes and washed three times with sterilized DI water before being resuspended in DI water.

### **Ultrasonic disruption**

One mL of bacteria solution was placed in micro centrifuge tubes and ultrasonicated at power of 20 W with ice batch. The samples were ultrasonicated for 30 sec, and then cool for 30 sec to prevent the overheating of the samples. The total effective ultrasonic disruption time is 6 minutes. After ultrasonic disruption, the disrupted samples were centrifuged at 12000 rpm for 10 minutes. The resulting precipitate contained the large insoluble fragments of cell envelope, such as cell wall and outer membranes. And the supernatant contained soluble constituents of the bacterial cell, such as water soluble proteins, and DNA.

### **Cell wall associated protein extraction**

The cell wall associated protein were extracted using the methods previously described by Tavares and Sellstedt<sup>44</sup>. Briefly, cells from bacterial culture were washed with 62.5 mM Tris–HCl (pH 6.8) buffer to remove traces of extracellular proteins, then the bacteria were thoroughly mixed with the same buffer supplemented with 0.1% (v/v) Triton X-100 in order to solubilize the proteins associated to the cell wall. The suspension was finally centrifuged at 20,000 g for 5 min at 4 C, and the supernatant was collected for SERS measurements.

### **Bacterial genomic DNA extraction and dialysis**

Bacterial genomic DNAs were extracted using a commercial DNA extraction kit, QIAamp DNA Mini Kit (Qiagen Sciences Inc., Germantown, MD), following the instruction provided with the kit. In order to remove the buffer used in the extraction procedure and to improve the spectra quality, dialysis were performed using Slide-A-Lyzer Dialysis Kit, 3500 molecular weight (Thermo Scientific Inc., Waltham, MA), following the instruction provided with the kit.

### **SERS Measurements and Data Analysis**

To prepare the bacteria coated SERS substrates, a 2  $\mu$ l droplet of a single species

bacterial sample was applied to the pristine AgNR substrate and allowed to dry. The SERS spectra were acquired using Enwave Raman system (Model ProRaman-L 785A2, Enwave Optronics Inc., Irvine, CA), with a 785 nm near-IR diode laser as the excitation source. The power of the laser at the sample was set to be ~ 30 mW. SERS spectra over a range of ~ 400 – 1800  $\text{cm}^{-1}$  were collected from nine to ten spots across the substrate surface over a five second exposure time. All data analysis was performed using Origin software 8.5 version (OriginLab Corporation, Northampton, MA). Statistical data analysis was conducted with Matlab 2010b (The MathWorks, Inc., Natick, MA) using the PLS toolbox (Eigenvector Research, Inc., Wenatchee, WA).

## **Results and Discussion**

### **SERS spectra of bacteria surrounding solution**

In this report, we divide the possible origins of SERS signal into following cell components groups, as demonstrated in Figure 3.1. We have designed a systematic experiment to investigate the SERS spectra of different cell components, based on the chemical components of bacteria cells shown in Figure 3.1. These important cell components are isolated and purified using different biochemical methods, and their individual SERS spectra are obtained based on AgNR SERS substrates. First, we will investigate the bacteria surround solution.

As aforementioned, in the studies on SERS of bacteria, almost all of them were conducted in a way that bacteria were suspended in aliquot solution, i.e. DI water. This may cause the bacteria cell to be disrupted in the solution due to osmotic pressure. In addition, during the bacterial metabolism, the by-products may be released by bacterial cells to their

surroundings. Hence, it is critical to first establish whether the SERS signals are coming from the bacterial whole cell or the metabolic by-products.

In order to separate the bacterial whole cell from its surrounding solution, the solution of *E. coli* O157:H7 was filtered through centrifugal filter with pore size of 0.22  $\mu\text{m}$ . The filtrate may contain cell by-products or any small inner cell constituents that are leaked out from inside if the cells are disrupted, such as nucleotides. The intact bacterial whole cells remain on the filters, which were then resuspended into its original concentration. The SERS spectra of filtrate and filter resuspended of the *E. Coli* O157:H7 (EC) are shown in Figure 3.2. We can see that filtrate (cell leak) share most of the SERS signature peaks with the filter resuspended solution (whole cells), indicated with red number in Figure 3.2. Both of the filtrate and filters showed peaks at  $\Delta\nu = 735$  and  $1330\text{ cm}^{-1}$ , which corresponds to the adenine structure, and such adenine may come from the DNA that are leaked into solution. However, at  $\Delta\nu = 735\text{ cm}^{-1}$ , the whole cell showed much greater Raman intensity than the filtrate. The filtrate has  $I_{735} = 2200 \pm 50$ ,  $I_{1330} = 1150 \pm 35$ ; and the whole cell has  $I_{735} = 6300 \pm 750$ ,  $I_{1330} = 7800 \pm 530$ . This suggests that peaks at  $\Delta\nu = 735$  and  $1330\text{ cm}^{-1}$  may from both inner cell constituents, mainly DNA, and surface genetic materials. Also in Figure 3.2, the filtrate spectrum does not have the peak at  $\Delta\nu = \sim 1034\text{ cm}^{-1}$ , which is the most intense peak in the whole cell spectrum. It suggested that this peak may come from the cell surface, which can not be leaked into the solution. The peak at  $\Delta\nu = 1034\text{ cm}^{-1}$  is corresponding to the in-plane C–H bending of the protein, which proves that this peak is mainly from cell wall protein rather than inner part of the cell.

## **The effect of cell disruption on SERS spectra of bacteria**

Now that we prove the both cell wall and inner cell components contribute to the total SERS signal of the bacteria although outer cell components weigh more in the differentiation, we need to further analyze the SERS spectra of some important cell components.

As shown in Figure 3.1, in a rough view, a bacteria cell can be viewed as two parts, cell envelope (cell wall, outer membrane, capsule, and etc.), and the inner cell constituents, such as chromosomes, water soluble proteins, and etc. Thus, breaking up the rigid cell wall and isolating outer cell envelope components are essential. There are several ways to break up the rigid bacterial cell wall, both physically and chemically. Boiling the bacterial cell, followed by cooling with ice can effectively disrupt the cell. Cell lysis can also be conducted with enzymatic permeabilization. In this procedure, EDTA is often used in order to destabilize the outer membrane of Gram negative cells, making the peptidoglycan layer accessible to the enzyme used. And the cell lysing enzymes, such as beta(1-3) glycanases, proteases, and mannase, can be employed to permeabilize cells. One of the easiest ways to disrupt bacterial cells is through mechanical methods, such as homogenizers, ball mills, blenders, and ultrasonic disruption. We choose to use ultrasonic disruption due to its high effectiveness and the fact that no foreign chemicals are introduced during the process, which will benefit the later SERS measurements.

The representative SERS spectra of EC in its original condition, after ultrasonic disruption, the precipitates and supernatants after centrifugation of the disrupted cells are shown in Figure 3.3. We can see that the disrupted sample has an overall higher Raman intensity than that of the original undisrupted sample due to the fact that more SERS active compounds are released into the solution after cell disruption. The peaks at  $\Delta\nu = 630, 735, \text{ and } 1330 \text{ cm}^{-1}$ , attributed to adenine in previous SERS studies, have higher peak intensity in the spectrum of the

disrupted cell. The spectrum of the disrupted cell also exhibit some additional peaks, such as the peaks at  $\Delta\nu = 808, 1140, \text{ and } 1540 \text{ cm}^{-1}$ . These new peaks may be attributed to the inner cell constituents such as water-soluble proteins and genomic DNA, which will be discussed later.

In fact, the supernatant spectrum looks almost identical to the spectrum of the disrupted cell, in both peak position and peak intensity, as shown in Figure 3.3. This spectrum not only has peaks at  $\Delta\nu = 630, 735, \text{ and } 1330 \text{ cm}^{-1}$ , but also processes peaks  $\Delta\nu = 808, 1140, \text{ and } 1540 \text{ cm}^{-1}$ . It suggests that majority SERS active components in the disrupted cell are not from cell surface, but from inner cell components, such as DNAs and water soluble proteins. However, two peaks at  $\Delta\nu = 655, 858 \text{ cm}^{-1}$  from the disrupted cells are absent in the supernatant, which are probably from the cell wall. The origins of these two peaks are due to NAG, which will be discussed later. The precipitate spectrum looks similar to the spectrum of the undisrupted cell, with similar peak position and peak intensity. It suggests that the SERS peaks of intact whole cell are mainly from the bacterial cell envelope.

Disruption of the bacterial cell seems to increase the absolute Raman intensity of the spectra, which may result in better detection. However, to merely increase the SERS intensity is not the only criterion to judge a detection method; it must at least be successful in differentiating bacteria from different species. In order to validate the differentiation between spectra, the SERS spectra of the four aforementioned bacteria, BS, EC, LM, and SA from undisrupted cells, cells after ultrasonic disruption, supernatants and precipitates of the disrupted cell after centrifugation. at different condition are subject to PCA analysis. The 3D PCA score plots of the spectra of these four bacteria at different conditions are shown in Figure 3.4. The differentiation between four bacterial isolates is achieved in undisrupted cells (Figure 3.4A) and precipitates (Figure 3.4B). In both disrupted cells and supernatants, the LM and SA are hard to be distinguished from each

other. This is because the inner cell components, DNA and water soluble proteins, have little differences in molecular structures, therefore the SERS spectra between species are very similar. Thus, cell disruption releases similar inner cell components, which dominates the SERS spectra and result in the loss of differentiation between bacteria species. It also proves that the differentiation between bacterial species using intrinsic SERS spectra is attributed to the cell envelopes, such as cell wall and surface protein.

Another way to determine the quality of the differentiation is through the variance of the PC score. The first three PC in undisrupted cells account for 83.86% of the total variance; while this value is 90.31% in precipitates, 64.58% in disrupted cells, and 73.68% in supernatants, respectively. Hence, the best discrimination is found using the spectra of precipitates, which are primarily outer cell components. It further proves that these outer cell components are critical in differentiation between different bacteria.

### **SERS spectra of cell wall**

As discussed above, the cell wall of the bacteria contributes heavily to the intrinsic SERS spectra of bacteria, and it can be used to differentiate between bacteria species and strains. The major components of the cell wall are layers of peptidoglycan, which is a polymer consisting of sugars and amino acids, and cell wall associated proteins are embedded in it. The sugar component consists of alternating residues of  $\beta$ -(1,4) linked N-acetylglucosamine (NAG) and N-acetylmuramic acid (NAM). Therefore, it is interesting to investigate how NAG and NAM contribute to the bacterial SERS spectra.

Comparing the spectra of NAG, NAM to LM (Gram positive) and EC (Gram negative) in Figure 3.5, we can conclude that the bacterial peak at  $\Delta\nu = 960$  and  $1327\text{ cm}^{-1}$  are from NAG,

bacterial peak at  $\Delta\nu = 797 \text{ cm}^{-1}$  are from NAM, and the bacterial peaks at  $\Delta\nu = 655$  and  $858 \text{ cm}^{-1}$  are from of both NAM and NAG. It is also noted that compared to EC, the NAM and NAG peaks at  $\Delta\nu = 960, 797$  and  $655 \text{ cm}^{-1}$  in LM have higher relative peak intensity. This is due to the G+ and G- bacteria structure difference, where LM has a cell wall directly exposed to environment, but EC has an additional outer membrane outside the cell wall. The outer membrane separates the cell wall away from AgNR surface, and weakens the signal from the peptidoglycan.

SERS spectrum of NAG has been previously reported Jarvis et al <sup>2</sup>. Such spectrum presents an intense peak  $\Delta\nu = 730 \text{ cm}^{-1}$ , and the authors attributed to a vibrational mode of the glycosidic ring. This conclusion is contradicted to our findings here, since this peak is absent in our spectrum of NAG, as shown in Figure 3.5. However, in a similar study conducted by Kahraman et al <sup>24</sup>, they isolated the peptidoglycan layers of four different bacteria, and found the peak  $\Delta\nu = 730 \text{ cm}^{-1}$  is absent in the SERS spectra of all four samples. These result suggested that the intense bacterial SERS peak at  $\Delta\nu = 730 \text{ cm}^{-1}$  may not originate from either peptidoglycan or NAG. but from the cell wall associated proteins. In the study by Kahraman et al <sup>24</sup>, the peptidoglycan layers are isolated using EDTA to disrupt the bacteria cell wall, so we propose that the diminishing of the peak at  $\Delta\nu = 730 \text{ cm}^{-1}$  is associated with the EDTA treatment to cell.

SERS spectra of the bacterial solution before and after EDTA treatment, and the EDTA solution were obtained using AgNR substrates, as shown in Figure 3.6. The most important change of the spectra is that the peaks at  $\Delta\nu = 730$  and  $1450 \text{ cm}^{-1}$  disappears after incubation with EDTA, but the peak at  $\Delta\nu = 1330 \text{ cm}^{-1}$  remains. The mechanism of antibacterial effectiveness by EDTA is not fully understood. Studies have suggested it is associated with EDTA's ability to divalent cation of  $\text{Ca}^{++}$ ,  $\text{Mg}^{++}$ , to release the lipopolysaccharides on G- bacteria surface, which

result in increased permeability areas of the cell <sup>45, 46</sup>. However, this hypothesis would not explain its antibacterial property against several G+ bacteria, such as LM and SA <sup>47, 48</sup>. Regardless of the mechanism, EDTA does disorient the bacteria surface, hence we can conclude that the signature bacterial peak at  $\Delta\nu = 730 \text{ cm}^{-1}$  is originated from the cell wall.

To further analyze the origins of this peak, we isolate the cell wall associated protein using the methods previously described by Tavares and Sellstedt <sup>44</sup>. The SERS spectra of the cell wall associated proteins extracted from four bacteria isolates, BS, EC, LM, and SA, are shown in Figure 3.7. The buffer shows intense SERS signature while the proteins only give low signal-to-noise ratio (S/N). For the protein spectra, one can also see that buffer spectral features dominate the SERS spectra, but the peaks from bacteria at  $\Delta\nu = 730$  and  $1320 \text{ cm}^{-1}$  are observed. These two peaks are stronger in the two Gram positive bacteria, LM and SA, as the cell wall associated proteins are easier to be extracted in G+ bacteria. The possible origins of the peak  $\Delta\nu = \sim 730 \text{ cm}^{-1}$  will be discussed later.

### **SERS spectra of inner cell components**

The inner cell components contain primarily nucleic acids, and water soluble proteins. It is also possible that the inner cell components are associated with the SERS spectra of bacteria as well. Therefore, the four aforementioned bacteria isolates, BS, EC, LM, and SA are used, and the DNA of these four bacteria were extracted. In order to remove the buffer used in the extraction procedure and to improve the spectra quality, dialysis were performed on the extracted DNA. The SERS spectra of the genomic DNA after dialysis are obtained, as shown in Figure 3.8A. The SERS spectra of the genomic DNA have identical characteristic peaks across the four different types of bacteria. Further analysis by PCA, as shown in Figure 3.8B can not differentiate the

bacteria from each other, especially between EC and BS. Thus, direct differentiation of bacterial genomic DNA is hard to achieved, but one can use the DNA probe to circumference this challenge.

Note that the spectra of genomic DNA have a peak at  $\Delta\nu = \sim 737 \text{ cm}^{-1}$ , which is slightly shifted compared with the similar peaks at  $\Delta\nu = \sim 730 \text{ cm}^{-1}$  in the spectra of bacteria whole cell. Comparing the results we present so far, the significant bacterial SERS peak  $\Delta\nu = \sim 730 \text{ cm}^{-1}$  is presented in the spectra of the whole cell, disrupted cells, supernatants, and precipitates (all shown in Figure 3.3), as well as the spectra of cell wall associated proteins (Figure 3.7) and genome DNA. It is not presented in the spectra of NAG/NAM (Figure 3.5), or the spectra of EDTA treated cells (Figure 3.6). Therefore, we conclude the possible contribution to this particular peak is from two parts. One part is the adenine in bacterial genomes, which, and the other part is the wall associated proteins. It may actually be two peaks with really close or identical peak position. The Raman spectrometer used in this dissertation has a spectral resolution of  $7 \text{ cm}^{-1}$ , which will be able to differentiate these two peaks. Another possible explanation is that peak at  $\Delta\nu = \sim 730 \text{ cm}^{-1}$  from genomic DNA and cell wall proteins are the same vibrational modes in different chemicals.

The water soluble protein inside bacteria cells are obtained by using the protein precipitation agents in the DNA extraction kit, followed by the same dialysis procedure. SERS spectra of the water soluble protein of four bacteria after dialysis are obtained, as shown in Figure 3.9. The spectra of the water soluble proteins showed signature peak at  $\Delta\nu = 616, 689, 769, 808, 931, 960, 1048, 1140, 1273 \text{ cm}^{-1}$  which are not present in the spectra of the whole bacterial cells (Figure 3.3). However, the peaks at  $\Delta\nu = 808$  and  $1140 \text{ cm}^{-1}$  are presented in the

spectra of disrupted cell and supernatants (Figure 3.3). Hence, we conclude that the inner cell water soluble proteins are not contributing to the SERS spectra of the bacterial whole cells.

## Conclusions

In this report, we have thoroughly investigated the SERS spectra of important bacterial cell components as well as their contribution to the overall SERS spectra of the bacterial whole cell. The possible bacterial peak in each component and their assignments are summarized in Table 3.2.

Cell filtration experiments demonstrated that the majority of the bacterial SERS peaks are from the bacterial cell itself, with possible contribution from the cell metabolic by-products. After ultrasonic disruption, the SERS features change dramatically, and the overall SERS intensity increases. This is caused by the release of nucleic acids and proteins, which dominate the SERS spectra. This result in the loss of differentiation between species at the same time, which suggests detection and differentiation of bacteria can not be performed on disrupted cells. A more detailed study on the SERS of cell components shows that the peptidoglycan layer and proteins of cell wall contribute greatly to the SERS spectra of bacterial whole cell. On the other hand, the inner cell water soluble proteins have little or no contribution. The genomic DNAs of the bacteria show similar spectra to the whole cell, but there is no differentiation capability between DNA from different types of bacteria. The possible origins of some SERS peaks, especially the one at  $\Delta\nu = \sim 730\text{cm}^{-1}$  are discussed, and we find that it may be originated from both genomic DNA and cell wall associated proteins. In conclusion, it is plausible to state that the SERS spectra of bacteria originate from the bacteria cell wall. This information would

provide better understanding of the SERS spectra of the bacteria at molecule level, and guide our design of the bacterial detection methods.

## References

1. Fan, C., Hu, Z., Mustapha, A. & Lin, M. Rapid detection of food- and waterborne bacteria using surface-enhanced Raman spectroscopy coupled with silver nanosubstrates. *Appl Microbiol Biotechnol* **92**, 1053-1061 (2011).
2. Jarvis, R.M. & Goodacre, R. Discrimination of Bacteria Using Surface-Enhanced Raman Spectroscopy. *Analytical Chemistry* **76**, 40-47 (2004).
3. Neyrolles, O. et al. Detection of *Mycoplasma pneumoniae* in Simulated and True Clinical Throat Swab Specimens by Nanorod Array-Surface-Enhanced Raman Spectroscopy. *PLoS ONE* **5**, e13633 (2010).
4. Patel, I.S., Premasiri, W.R., Moir, D.T. & Ziegler, L.D. Barcoding bacterial cells: a SERS-based methodology for pathogen identification. *J. Raman Spectrosc.* **39**, 1660-1672 (2008).
5. Premasiri, W.R., Gebregziabher, Y. & Ziegler, L.D. On the Difference Between Surface-Enhanced Raman Scattering (SERS) Spectra of Cell Growth Media and Whole Bacterial Cells. *Appl. Spectrosc.* **65**, 493-499 (2011).
6. Prucek, R. et al. Reproducible discrimination between Gram-positive and Gram-negative bacteria using surface enhanced Raman spectroscopy with infrared excitation. *Analyst* **137**, 2866-2870 (2012).
7. Stephen, K.E., Homrighausen, D., DePalma, G., Nakatsu, C.H. & Irudayaraj, J. Surface enhanced Raman spectroscopy (SERS) for the discrimination of *Arthrobacter* strains based on variations in cell surface composition. *Analyst* **137**, 4280-4286 (2012).

8. Walter, A., Marz, A., Schumacher, W., Rosch, P. & Popp, J. Towards a fast, high specific and reliable discrimination of bacteria on strain level by means of SERS in a microfluidic device. *Lab Chip* **11**, 1013-1021 (2011).
9. Xie, Y. et al. Label-free detection of the foodborne pathogens of Enterobacteriaceae by surface-enhanced Raman spectroscopy. *Analytical Methods* **5**, 946-952 (2013).
10. Zhang, L. et al. Multifunctional magnetic-plasmonic nanoparticles for fast concentration and sensitive detection of bacteria using SERS. *Biosensors and Bioelectronics* **31**, 130-136 (2012).
11. Wu, X., Xu, C., Tripp, R.A., Huang, Y.-w. & Zhao, Y. Detection and differentiation of foodborne pathogenic bacteria in mung bean sprouts using field deployable label-free SERS devices. *Analyst* **138**, 3005-3012 (2013).
12. Efrima, S. & Zeiri, L. Understanding SERS of bacteria. *J. Raman Spectrosc.* **40**, 277-288 (2009).
13. Wu, X., Chen, J., Park, B., Huang, Y.-w. & Zhao, Y. in *Advances in Applied Nanotechnology for Agriculture*, Vol. 1143 85-108 (American Chemical Society, 2013).
14. Jarvis, R.M. & Goodacre, R. Characterisation and identification of bacteria using SERS. *Chemical Society Reviews* **37**, 931-936 (2008).
15. Kneipp, K., Kneipp, H., Itzkan, I., Dasari, R.R. & Feld, M.S. Ultrasensitive Chemical Analysis by Raman Spectroscopy. *Chemical Reviews* **99**, 2957-2976 (1999).
16. Campion, A. & Kambhampati, P. Surface-enhanced Raman scattering. *Chemical Society Reviews* **27**, 241-250 (1998).
17. Kneipp, K. et al. Single Molecule Detection Using Surface-Enhanced Raman Scattering (SERS). *Physical Review Letters* **78**, 1667-1670 (1997).

18. Nie, S.M. & Emery, S.R. Probing single molecules and single nanoparticles by surface-enhanced Raman scattering. *Science* **275**, 1102-1106 (1997).
19. Xu, H., Aizpurua, J., Käll, M. & Apell, P. Electromagnetic contributions to single-molecule sensitivity in surface-enhanced Raman scattering. *Physical Review E* **62**, 4318-4324 (2000).
20. Xu, H., Bjerneld, E.J., Käll, M. & Börjesson, L. Spectroscopy of Single Hemoglobin Molecules by Surface Enhanced Raman Scattering. *Physical Review Letters* **83**, 4357-4360 (1999).
21. Biju, V. et al. Combined Spectroscopic and Topographic Characterization of Nanoscale Domains and Their Distributions of a Redox Protein on Bacterial Cell Surfaces. *Langmuir* **23**, 1333-1338 (2006).
22. Marotta, N.E. & Bottomley, L.A. Surface-Enhanced Raman Scattering of Bacterial Cell Culture Growth Media. *Appl. Spectrosc.* **64**, 601-606 (2010).
23. Leyto, P. et al. Surface enhanced Raman spectrum of nanometric molecular systems. *Journal of the Chilean Chemical Society* **50**, 725-730 (2005).
24. Kahraman, M., Kesero, lu, K. & ulha, M. On Sample Preparation for Surface-Enhanced Raman Scattering (SERS) of Bacteria and the Source of Spectral Features of the Spectra. *Appl. Spectrosc.* **65**, 500-506 (2011).
25. Efrima, S. & Bronk, B. Silver colloids impregnating or coating bacteria. *J. Phys. Chem. B* **102**, 5947-5950 (1998).
26. Zeiri, L., Bronk, B., Shabtai, Y., Czege, J. & Efrima, S. Silver metal induced surface enhanced Raman of bacteria. *Colloids and Surfaces A: Physicochemical and Engineering Aspects* **208**, 357-362 (2002).

27. Zeiri, L., Bronk, B.V., Shabtai, Y., Eichler, J. & Efrima, S. Surface-enhanced Raman spectroscopy as a tool for probing specific biochemical components in bacteria. *Appl Spectrosc* **58**, 33-40 (2004).
28. Liu, Y., Chen, Y., Nou, X. & Chao, K. Potential of Surface-Enhanced Raman Spectroscopy for the Rapid Identification of *Escherichia Coli* and *Listeria Monocytogenes* Cultures on Silver Colloidal Nanoparticles. *Appl. Spectrosc.* **61**, 824-831 (2007).
29. Zeiri, L. & Efrima, S. Surface-enhanced Raman spectroscopy of bacteria: the effect of excitation wavelength and chemical modification of the colloidal milieu. *J. Raman Spectrosc.* **36**, 667-675 (2005).
30. Szeghalmi, A., Kaminskyj, S., Rösch, P., Popp, J. & Gough, K.M. Time Fluctuations and Imaging in the SERS Spectra of Fungal Hypha Grown on Nanostructured Substrates. *The Journal of Physical Chemistry B* **111**, 12916-12924 (2007).
31. Laucks, M.L., Sengupta, A., Junge, K., Davis, E.J. & Swanson, B.D. Comparison of Psychro-active Arctic Marine Bacteria and Common Mesophilic Bacteria Using Surface-Enhanced Raman Spectroscopy. *Appl. Spectrosc.* **59**, 1222-1228 (2005).
32. Beveridge, T.J. Structures of Gram-Negative Cell Walls and Their Derived Membrane Vesicles. *Journal of Bacteriology* **181**, 4725-4733 (1999).
33. Navarre, W.W. & Schneewind, O. Surface Proteins of Gram-Positive Bacteria and Mechanisms of Their Targeting to the Cell Wall Envelope. *Microbiology and Molecular Biology Reviews* **63**, 174-229 (1999).
34. Wicken, A. & Knox, K. Lipoteichoic acids: a new class of bacterial antigen. *Science* **187**, 1161-1167 (1975).

35. Liu, T.-T. et al. A High Speed Detection Platform Based on Surface-Enhanced Raman Scattering for Monitoring Antibiotic-Induced Chemical Changes in Bacteria Cell Wall. *PLoS ONE* **4**, e5470 (2009).
36. Wang, T., Hu, X. & Dong, S. Surfactantless Synthesis of Multiple Shapes of Gold Nanostructures and Their Shape-Dependent SERS Spectroscopy. *The Journal of Physical Chemistry B* **110**, 16930-16936 (2006).
37. Vogel, H. & Jähnig, F. Models for the structure of outer-membrane proteins of *Escherichia coli* derived from raman spectroscopy and prediction methods. *Journal of Molecular Biology* **190**, 191-199 (1986).
38. Barhoumi, A., Zhang, D., Tam, F. & Halas, N.J. Surface-Enhanced Raman Spectroscopy of DNA. *J. Am. Chem. Soc.* **130**, 5523-5529 (2008).
39. Uchiyama, T. et al. Raman optical activity of flagellar filaments of Salmonella: Unusually intense ROA from L-type self-assembled protein filaments and their possible higher level chiral organization. *Vib. Spectrosc.* **48**, 65-68 (2008).
40. Latteyer, F., Peisert, H., Göhring, N., Peschel, A. & Chassé, T. Vibrational and electronic characterisation of *Staphylococcus aureus* wall teichoic acids and relevant components in thin films. *Analytical & Bioanalytical Chemistry* **397**, 2429-2437 (2010).
41. Chaney, S.B., Shanmukh, S., Dluhy, R.A. & Zhao, Y.P. Aligned silver nanorod arrays produce high sensitivity surface-enhanced Raman spectroscopy substrates. *Appl. Phys. Lett.* **87**, 031908 (2005).
42. Driskell, J.D. et al. The use of aligned silver nanorod Arrays prepared by oblique angle deposition as surface enhanced Raman scattering substrates. *J. Phys. Chem. C* **112**, 895-901 (2008).

43. Liu, Y.J., Chu, H.Y. & Zhao, Y.P. Silver Nanorod Array Substrates Fabricated by Oblique Angle Deposition: Morphological, Optical, and SERS Characterizations. *The Journal of Physical Chemistry C* **114**, 8176-8183 (2010).
44. Tavares, F. & Sellstedt, A. A simple, rapid and non-destructive procedure to extract cell wall-associated proteins from Frankia. *Journal of Microbiological Methods* **39**, 171-178 (2000).
45. GRAY, G.W. & WILKINSON, S.G. The Effect of Ethylenediaminetetra-acetic Acid on the Cell Walls of Some Gram-Negative Bacteria. *Journal of General Microbiology* **39**, 385-399 (1965).
46. Alakomi, H.-L., Saarela, M. & Helander, I.M. Effect of EDTA on Salmonella enterica serovar Typhimurium involves a component not assignable to lipopolysaccharide release. *Microbiology* **149**, 2015-2021 (2003).
47. Ko, K.Y., Mendonca, A.F. & Ahn, D.U. Effect of Ethylenediaminetetraacetate and Lysozyme on the Antimicrobial Activity of Ovotransferrin Against *Listeria monocytogenes*. *Poultry Science* **87**, 1649-1658 (2008).
48. Root, J.L., McIntyre, O.R., Jacobs, N.J. & Daghlian, C.P. Inhibitory effect of disodium EDTA upon the growth of *Staphylococcus epidermidis* in vitro: relation to infection prophylaxis of Hickman catheters. *Antimicrobial Agents and Chemotherapy* **32**, 1627-1631 (1988).

Table 3.1 SERS/Raman peaks from important cell components that may contribute to the SERS of bacterial cells.

Chemicals	Peak position (cm <sup>-1</sup> )	Raman or SERS	Tentative peak assignments	Ref	
Peptidoglycan	699	SERS	N/A	24	
	815	SERS	N/A	24	
	964	SERS	N/A	24	
	1059	SERS	N/A	24	
	1236	SERS	N/A	24	
	1279	SERS	N/A	24	
	1374	SERS	N/A	24	
	1394	SERS	N/A	24	
	1536	SERS	N/A	24	
	1638	SERS	N/A	24	
Teichoic Acid	964	Raman	POH $\delta$	40	
	1250	Raman	PO- $\nu$	40	
	1212	Raman	CN $\delta$	40	
	1322	Raman	CHOH $\delta$	40	
	1452	Raman	CH	40	
	1646	Raman	Amid II	40	
	1761	Raman	C=O $\nu$	40	
Outer Membrane Proteins (Porins, OmpA)	1553	Raman	Trp	37	
	1579	Raman	Trp	37	
	1602	Raman	Phe	37	
	1613	Raman	Tyr	37	
	1669	Raman	Amide	37	
	1734	Raman	N/A	37	
	Lipopolysaccharide	1612	Raman	N/A	37
		1652	Raman	N/A	37
		1726	Raman	N/A	37
	Flagellum	903	Raman	N/A	39
945		Raman	Skeletal CCN deformation	39	
1003		Raman	Phe	39	
1246		Raman	Helix	39	
1320		Raman	N/A	39	
1453		Raman	CH <sub>2</sub> rocking vibrational mode	39	
1662		Raman	Amide I	39	
Spheroplast		735	SERS	N/A	35
	1330	SERS	N/A	35	

	780	SERS	N/A	35
	1050	SERS	N/A	35
	1125	SERS	N/A	35
	1170	SERS	N/A	35
	1230	SERS	N/A	35
	1435	SERS	N/A	35
Inner cell proteins	1250	SERS	Amide III	2
	1322	SERS	Adenine, guanine, Tyr	2
	1003	SERS	C(CC)aromatic ring (Phe)	2
	1081	SERS	V(PO) in oligonucleotides	2
DNA/RNA	546	SERS	CO, POC bending	38
	730	SERS	glycosidic ring	38
	795	SERS	V(PO <sub>2</sub> ), v(CC) ring breathing	38
	816	SERS	CO, POC	38
	853	SERS	1,4 glycosidic link	38

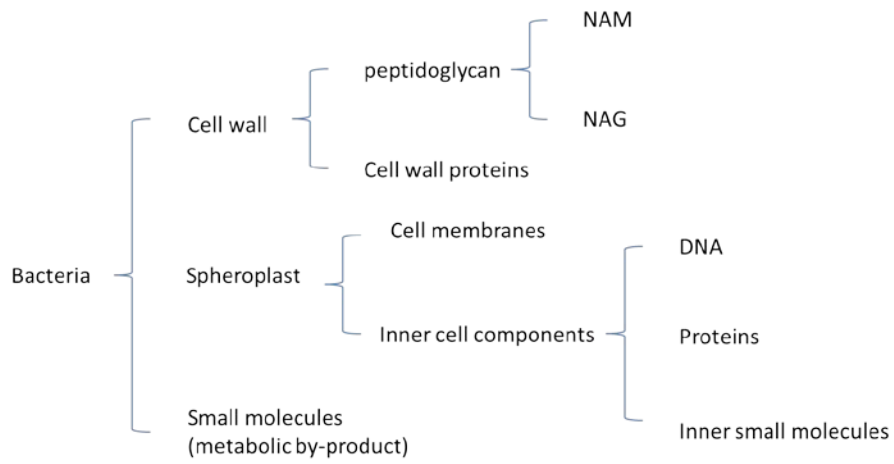


Figure 3.1 Cell components of a bacteria cell that may contribute to the overall SERS spectra of bacteria.

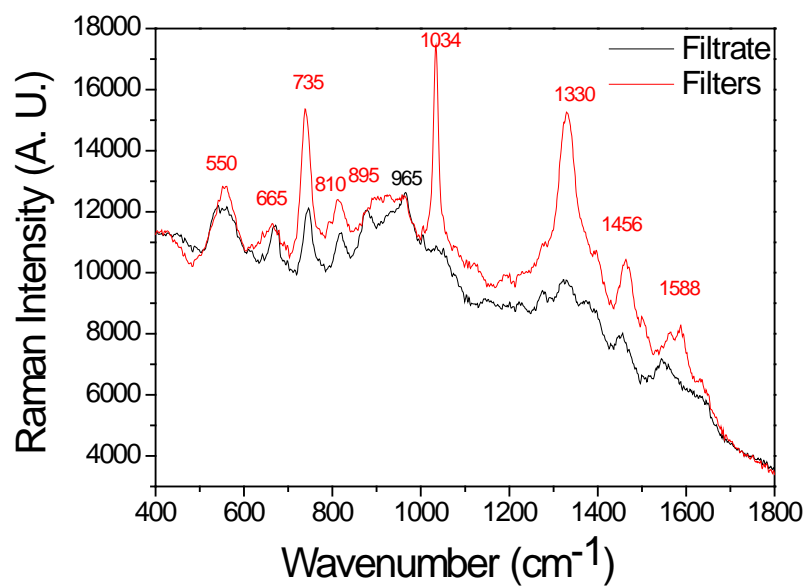


Figure 3.2 The SERS spectra of *E. Coli* O157:H7 after filtration.

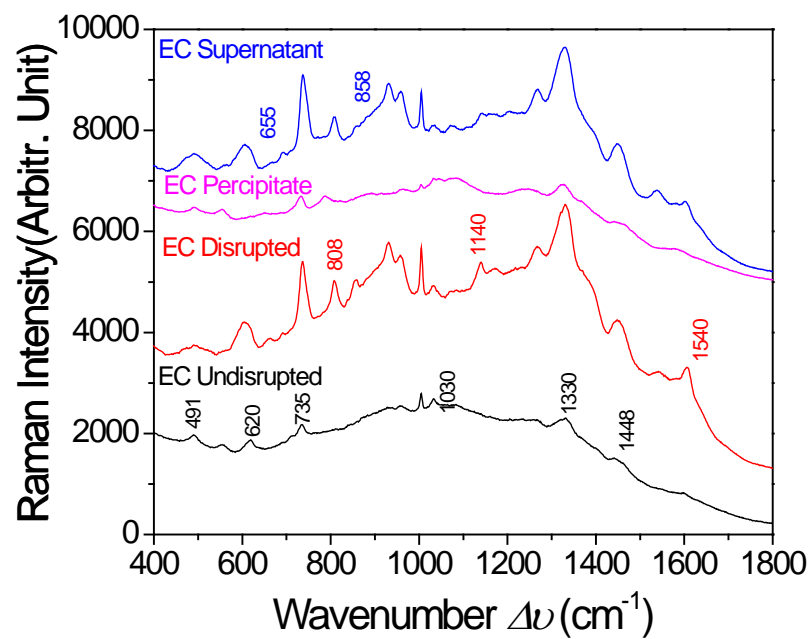


Figure 3.3 The SERS spectra of *E. Coli* O157:H7 (EC) undisrupted, after ultrasonic disruption, and the precipitates and supernatants after centrifugation of the disrupted cells.

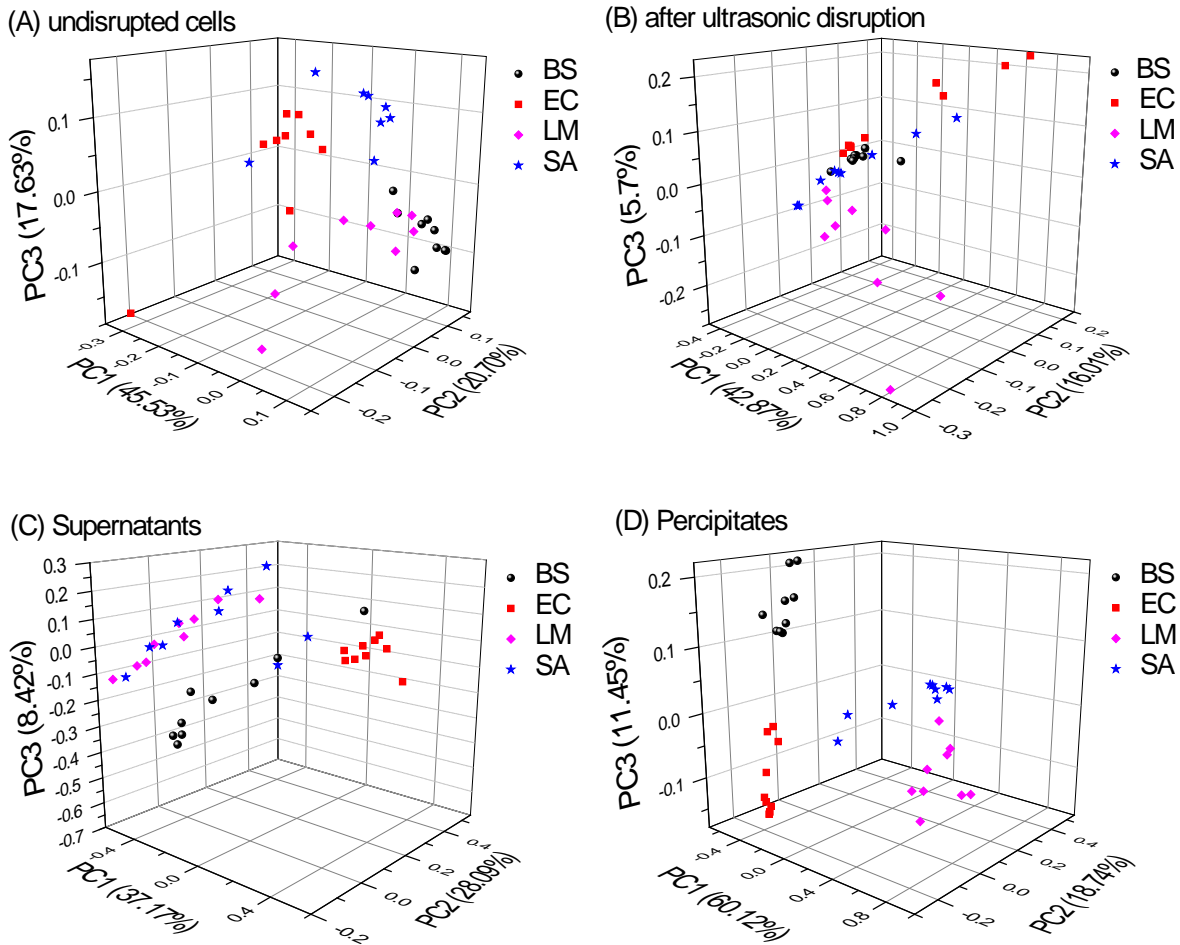


Figure 3.4 PCA scores of the spectra of *Bacillus subtilis* (BS), *E. Coli* O157:H7 (EC), *Listeria monocytogenes* (LM), and *Staphylococcus aureus* (SA) at different conditions. (A) Undisrupted cells, (B) cells after ultrasonic disruption, (C) supernatants, and (D) precipitates of the disrupted cell after centrifugation.

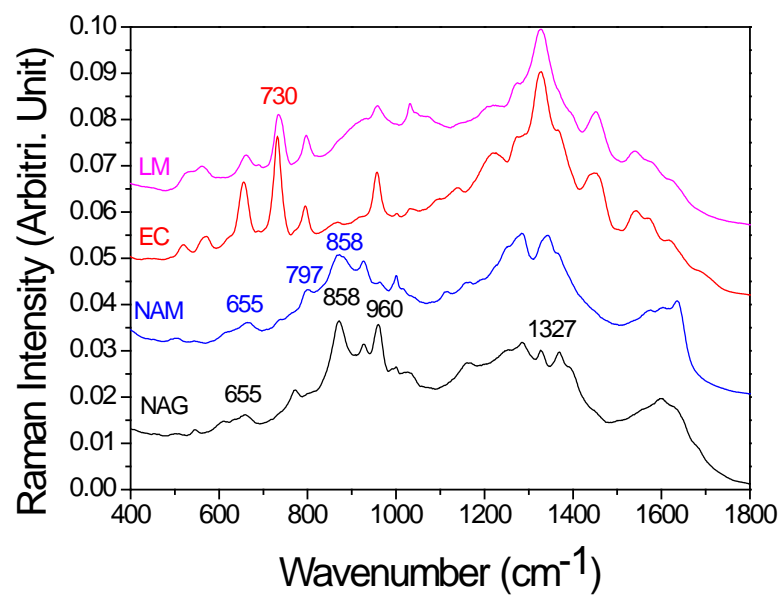


Figure 3.5 SERS spectra of NAG, NAM, and two bacteria isolates *E. Coli* O157:H7 (EC) and *Listeria monocytogenes* (LM).

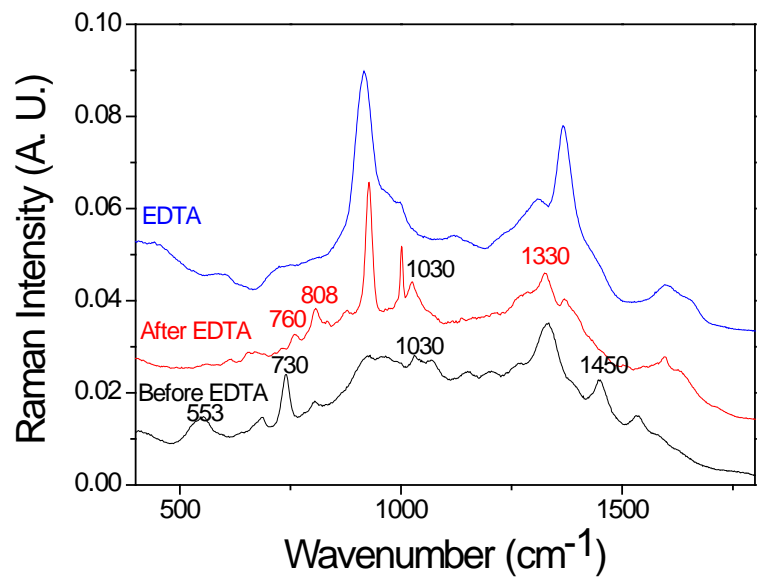


Figure 3.6 SERS spectra of *E. Coli* O157:H7 (EC) before and after EDTA treatment and the spectra of pure EDTA.

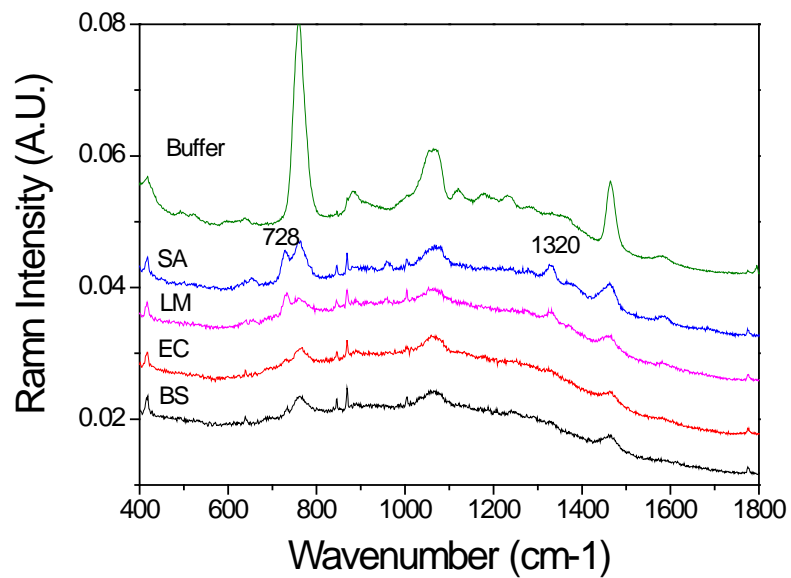


Figure 3.7 SERS spectra of extracted cell wall associated protein from *Bacillus subtilis* (BS), *E. Coli* O157:H7 (EC), *Listeria monocytogenes* (LM), and *Staphylococcus aureus* (SA) as well as the SERS spectra of the buffer used in the process.

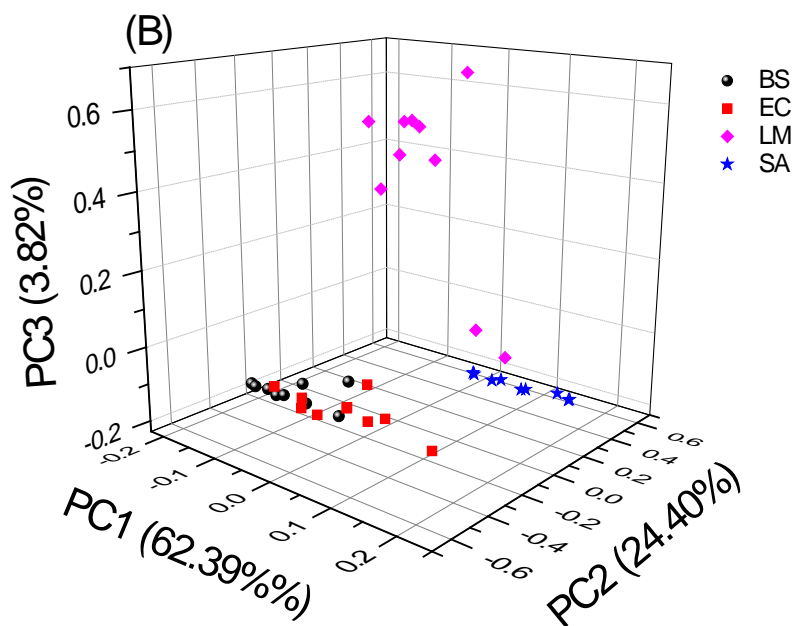
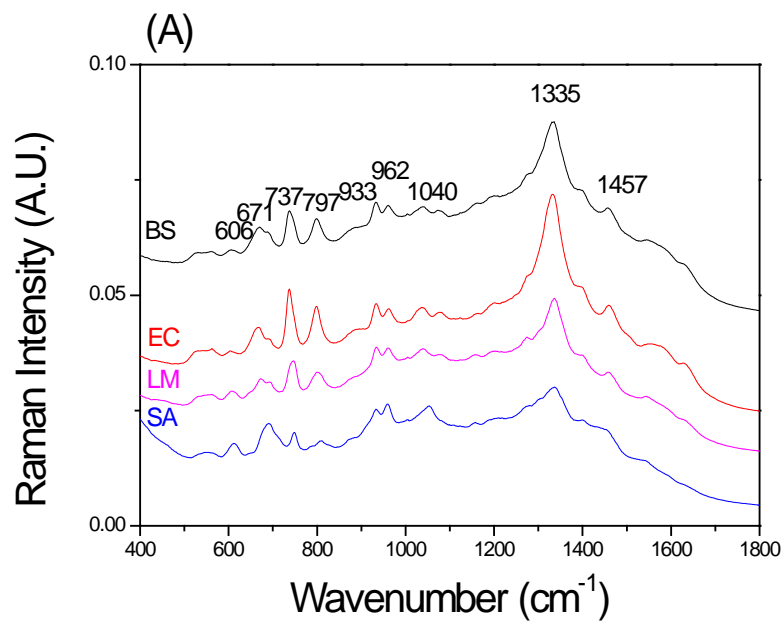


Figure 3.8 (A) SERS spectra of genomic DNA from *Bacillus subtilis* (BS), *E. Coli* O157:H7 (EC), *Listeria monocytogenes* (LM), and *Staphylococcus aureus* (SA). (B) The 3D PCA score plot of these four spectra.

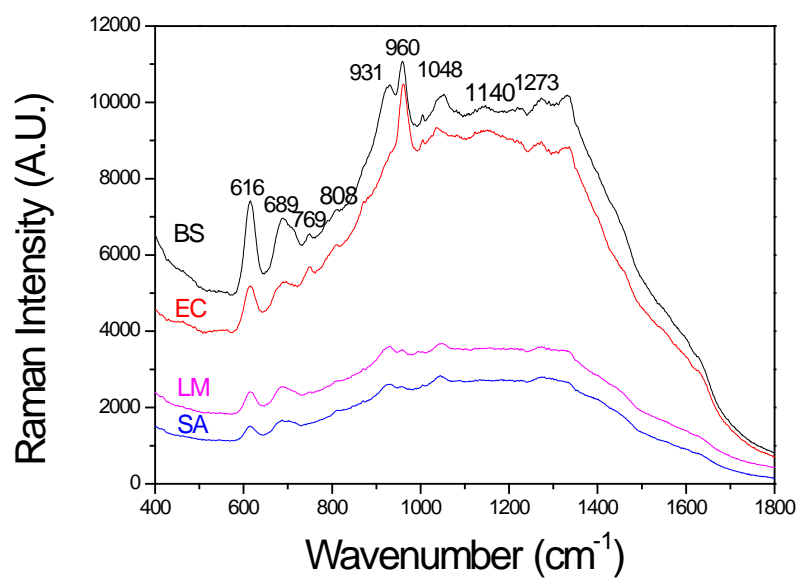


Figure 3.9 SERS spectra of inner cell water soluble protein from *Bacillus subtilis* (BS), *E. Coli* O157:H7 (EC), *Listeria monocytogenes* (LM), and *Staphylococcus aureus* (SA).

Table 3.2 SERS peaks of important cell components as well as the whole bacterial cells.  $\checkmark$  indicated that the peak is present in the SERS spectra of this component.

SERS Peaks (cm-1)	Peak assignments	Corresponding chemicals	Bacterial whole cells	Cell wall	NAG	NAM	Cell wall associated protein	Water soluble proteins	Genomic DNA
550	S-S stretch	Protein	$\checkmark$	$\checkmark$					
606	CO	Nucleic acids							$\checkmark$
620	POC bending	Proteins						$\checkmark$	
655	C-O-C stretch	Carbohydrates	$\checkmark$	$\checkmark$	$\checkmark$	$\checkmark$			
671	$\delta$ (guanine)	Nucleic acids							$\checkmark$
689	$\nu$ (C-S)	Protein						$\checkmark$	
735	Adenine	Nucleic acids	$\checkmark$	$\checkmark$			$\checkmark$		$\checkmark$
769	C-C bending	Protein						$\checkmark$	$\checkmark$
797	C-C bending	Carbohydrates	$\checkmark$	$\checkmark$		$\checkmark$			$\checkmark$
810	Cytosine, uracil (ring, stretch)	Nucleic acids						$\checkmark$	
858	1,4 glycosidic link	Carbohydrates; Nucleic acids			$\checkmark$	$\checkmark$			
890	COC stretch	Carbohydrates	$\checkmark$						
933	Skeletal CCN deformation	Proteins						$\checkmark$	$\checkmark$
960	$\delta$ (C=C)	Carbohydrates	$\checkmark$		$\checkmark$			$\checkmark$	$\checkmark$
982	C-O	Nucleic acids backbone							$\checkmark$
1030	Phenylalanine (in-plane C-H bending)	Protein	$\checkmark$	$\checkmark$					$\checkmark$

1048	CN stretching	Tryptophan						√	
1140	$\delta$ C-H2 (amide II)	Proteins						√	
1273	Amide III	Proteins						√	
1330	Adenine, guanine, Tryptophan	Nucleic acids	√	√	√		√		√
1455	C-O-H	Oligosaccharides	√						√
1540	N-acetyl related vibration	Nucleic acids							√
1588	$\delta$ N-H & $\nu$ C-N (amide II)	Proteins	√	√			√		

CHAPTER 4

SERS COUPLED WITH TWO SAMPLING TECHNIQUES FOR DETECTION OF  
SALMONELLA TYPHIMURIUM<sup>1</sup>

---

<sup>1</sup> Xiaomeng Wu, Yao-wen Huang, and Yiping Zhao. To be submitted to *International Journal of Food Protection*.

## Abstract

The recent outbreaks of foodborne illness have raised the requests of rapid detection methods for pathogens. Surface-enhanced Raman spectroscopy (SERS), as a sensitive and rapid detection method, had long been used in detection of biological and chemical substances. Due to the low number of pathogenic bacteria contaminated with food samples, a proper sampling technique becomes challenge in rapid detection methods. We have been developing better sampling procedures including centrifuge and two-step filtration techniques, followed by SERS measurement using silver nanorod array substrates. The centrifugation method concentrated the bacteria onto the surface of the SERS-active substrate. It conquered the problem of uneven sample distribution and undesired distance between target bacteria and the substrate surface. The entire procedure from sampling to quantization took 30 min; it increased the limit of detection (LOD) of *Salmonella* Typhimurium to  $10^6$  CFU/ml. Two-step filtration method concentrates 250 ml sample solution to a final volume to 50 $\mu$ l. The LOD of *Salmonella* Typhimurium reached to  $10^5$  CFU/ml. This method also demonstrates the potential in separating the bacteria from food matrix by adding one initial filtration step to remove contaminations from food samples. This study has contributed to the development of a rapid and sensitive detection method of foodborne pathogenic bacteria without the need of sample enrichment. It has potential for the application in an on-line detection for food industry.

## Introduction

The Centers for Disease Control (CDC) estimated that foodborne diseases cause approximately 76 million illnesses, 325,000 hospitalizations, and 5,000 deaths in the United States each year. Known pathogens account for an estimated 14 million illnesses, 60,000 hospitalizations, and 1,800 deaths (1). Recent foodborne outbreaks include the *E. coli* O157:H7 contaminated spinach and *Salmonella* outbreak linked to Peter Pan<sup>®</sup> peanut butter in 2006. The recent outbreaks of foodborne illness have raised the requests of rapid detection methods for pathogens. Although conventional culturing of foodborne pathogens recommended by USDA is the most sensitive detection methodology available, it is time-consuming and requires extensive manual labor. The similar situation is for toxins detection.

Similar to infrared (IR) spectroscopy, Raman spectroscopy provides detailed information about the material under investigation, often at the molecular level. Raman spectroscopy has advantages over IR such as less interference from water bands in aqueous samples and selection rules that result in fewer spectral bands and thus simpler spectra. It has been used to obtain highly structured information on bacteria (2, 3), even at the single bacterial cell level(4) . Although Raman sensitivity is low in comparison to IR spectroscopy, it can be greatly increased by the surface-enhanced Raman scattering.

The effect of drastically enhanced Raman signals rely on either the adsorption or close proximity of a molecule to a metal substrate (5) . When the analyte is in close proximity to the metal, the energy from the plasmon resonance may be coupled into bonds of the molecule of interest resulting in an enhancement of the Raman signal of several orders of magnitude (6, 7). Surface-enhanced Raman spectroscopy (SERS) has been used as an analytical tool to observe trace amount of chemical and biological molecules due to its capability of giving real-time

molecular vibrational information under ambient conditions. In addition to signal enhancement, SERS has a fluorescence-quenching effect (8) . This is extremely valuable when investigating microorganisms, which often exhibit a fluorescence background under excitation in the near-infrared to visible regions.

The morphology of the metallic structure plays a major role in determining the magnitude of signal enhancement and sensitivity of detection(9) . Substrate preparation methods are either expensive or time consuming, and it is not easy to make reproducible substrates of the correct surface morphology to provide maximum SERS enhancements. Without uniformity and good reproducibility of the metal substrates, the attainment of reproducible spectra remains a major challenge for SERS. Silver nanorod (AgNR) array substrates fabricated by oblique angle deposition (OAD) overcome some of the difficulties and disadvantages of the other SERS substrates (10-13). These substrates have been shown to markedly enhance the detection of chemical and biological samples, including aflatoxins (14), important human viruses such as rotavirus, influenza virus and respiratory syncytial virus (15, 16), foodborne pathogens like *E. coli* O157:H7, *Salmonella* Typhimurium, *Staphylococcus aureus* (17), pesticides like chlorpyrifos and parathion, intentional adulteration agents like melamine (17), and allow for detection and discrimination of microRNA families and family members (18). Hence, it shows a great potential to identify and detect a wide range of chemical and biological samples that are related to food safety issues.

The detection of bacteria such as *E. coli* O157:H7, *Salmonella* Typhimurium, and *Staphylococcus aureus* using AgNR substrate has been explored by Chu et al (17). In their study, they use a “pipette method”, where 2  $\mu$ L of bacteria solution was pipetted onto the AgNR substrates, and then let dried. They examined the SERS spectra of Gram positive and Gram

negative bacteria obtained from this novel SERS substrate. Spectral difference between Gram types, species and strains were also observed. However, the limit of detection (LOD) of this study is only at  $10^8$  CFU/ml, which is far above the possible pathogen level in a food sample. Moreover, the study only includes pure bacteria culture, not the bacteria inoculated in food. Hence, two challenges remain for detecting bacterial pathogens in food samples. The first challenge is to lower the LOD of the bacteria and the second challenge is to detect foodborne bacteria in its natural environment and not a laboratory culture.

In food detection settings, 25 g of food in 225 mL of water is required, so there is often a need to detect foodborne bacteria in a bulk sample with large volume. The relationship between the bulk concentration detection limit and the surface detection limit is determined by (1) the volume  $V$  of bacterial solution applied; (2) the spreading area of the sample on SERS substrate  $A_0$ ; (3) the size of the laser spot  $\pi R^2$  with  $R$  the radius of the laser spot, and (4) the bulk concentration  $C$ . The amount of bacteria detected is  $N_d = VC\pi R^2/A_0$ , so  $C = N_d A_0 / V\pi R^2$ , where threshold  $N_d$  reflects the true detectability of a SERS method, and  $C$  represents the bulk LOD of such detection. Thus, for a fixed surface detection method, the reduction of  $C$  can be achieved by decreasing  $A_0$ , increasing  $V$ , and increasing  $R$ . In the equation,  $R$  is limited by the Raman instrument used while  $A_0$  could be confined by a narrow well as previously reported (19). Thus, the best strategy to lower  $C$  would be to increase  $V$ , the volume of the samples put on the substrates. One way to increase  $V$  is to use pre-concentration methods that capture as many bacteria as possible in a fixed surface area using a large sample volume.

Hence, in this report, we will develop better sampling procedures including centrifugation and two-step filtration techniques, followed by SERS measurement using AgNR substrates, to target the problem of uneven sample distribution and undesired distance between

target bacteria and the substrate surface, and to develop a rapid and sensitive detection method of foodborne pathogenic bacteria without the need of sample enrichment.

## **Materials and Methods**

### **Bacterial Samples and Sampling Methods**

*Salmonella* Typhimurium 1925-1 (poultry isolate) was stored at -80°C in 15-20 % glycerol for long-term storage. For short-term storage, bacterial isolate was stored in trypticase soy agar (TSA) slants at 4°C. Bacterial cultures were prepared by inoculating pure isolates from agar slants into trypticase soy broth (TSB) tubes and incubated at  $35 \pm 2^\circ\text{C}$  for 18 - 24 hours. The overnight cultures of all isolates were centrifuged at 5000 rpm for 10 minutes and washed three times with sterilized DI water before being resuspended in DI water.

### **SERS Substrates Fabrication**

The SERS active substrate used to obtain spectra will be AgNR arrays fabricated by OAD technique using a custom-designed electron beam evaporation system that has been previously described.<sup>26</sup> Glass microscopic slides (Gold Seal®) will be used as the base platform for AgNR arrays deposition. The glass slides will be cleaned with Piranha solution (80% sulfuric acid, 20% hydrogen peroxide), and rinsed with DI water. The substrates then will be dried with a stream of nitrogen gas before loading into the deposition system. A base layer of Ti (20nm) and silver film (500 nm) are first evaporated onto the glass slides at a normal angle to the substrate surface at a rate of  $\sim 0.1$  nm/s and 0.3-0.4 nm/s, respectively. The substrates are then rotated by a computer controlled stepper motor to  $86^\circ$  with respect to the vapor incident direction. Ag nanorods are grown at this oblique angle with a nominal deposition rate of  $\sim 0.3$  nm/s, and a deposition pressure of  $\sim 1 \times 10^{-6}$  Torr.

### **Centrifugation method**

The centrifugation method utilizes the centrifugation force to move bacteria tightly onto the substrates and evenly distributed, and the scheme is shown in Figure 4.1. First, a standard 15 ml centrifuge tube was prepared by filling with Polydimethylsiloxane (PDMS) to provide a flat bottom surface, and then a regular AgNR substrate was placed on the flat surface in the centrifuge tube. Ten mL *Salmonella* Typhimurium solution at  $10^4$ ,  $10^5$ ,  $10^6$ , and  $10^7$  CFU/mL, respectively, was carefully added into the centrifuge tube, and then centrifuged at 7000 rpm using Microcentrifuge (Eppendorf, Hauppauge NY) for 10 mins. The substrate was measured for SERS after it was dried using nitrogen gun.

### **Two-step Filtration Method**

Two-step filtration method started with a conventional vacuum filtration of 250 ml *Salmonella* Typhimurium sample solution through filters with pore size of 0.22  $\mu\text{m}$ , and *Salmonella* cells were collected by the filters. The bacteria cells were collected from the filter by vortexing in 2 ml of DI water, and then further subjected to second step of centrifugal filtration to lower the volume to 50  $\mu\text{l}$  with centrifuge at 7000 rpm for 10 minutes using centrifugal filters with pore size of 0.22 $\mu\text{m}$  as well. A 15  $\mu\text{L}$  aliquot of final bacterial samples after filtration was pipetted onto the AgNR SERS substrate and allowed to bind at room temperature prior to spectrum acquisition.

### **SERS Measurements and Data Analysis**

SERS spectra were acquired using a portable Enwave Raman system (Model HRC-10HT, Enware Optronics Inc., Irvine, CA), with a 785 nm near-IR diode laser as the excitation source. The power of the laser at the sample was set to be  $\sim 30$  mW. SERS spectra over a range of  $\sim 400 - 1800$   $\text{cm}^{-1}$  were used over a 10 sec exposure time. SERS spectra were collected from 9 spots (3

× 3 array) across the substrate surface and multiple substrates were measured. All data analysis was performed using Origin software 8.5 version (OriginLab Corporation, Northampton, MA) and WIRE2.0 software (Renishaw, United Kingdom).

## RESULTS AND DISCUSSION

### Centrifugation method

The SERS spectra of *Salmonella* Typhimurium at concentration of  $10^4$ ,  $10^5$ ,  $10^6$ , and  $10^7$  CFU/mL after centrifugation are shown in Figure 4.2A. It clearly demonstrates that after centrifugation, the spectra clearly shows signature peaks of *Salmonella* Typhimurium at  $\Delta\nu = 552, 735, 950, 1030, 1330, \text{ and } 1450 \text{ cm}^{-1}$ , which are the signature bacterial peaks previously discussed. In order to determine the LOD, we quantify the intensity of the SERS spectra by using the peak intensity at  $\Delta\nu = 735 \text{ cm}^{-1}$  ( $I_{735}$ ), which corresponds to the adenine in bacteria. The DI water samples are treated as the background, and the baseline subtracted data are used to calculate the average standard deviation. The LOD of the SERS detection is defined as the lowest concentration at which a distinguished bacterial SERS spectrum can be obtained. In our experiment, the LOD is the lowest concentration at which  $I_{735}$  is significantly different from the sterile DI water which is used to dilute the bacteria samples. It is shown in Figure 4.2B that at concentration of  $10^6$  and  $10^7$  CFU/ml all data points yield positive detection; while below that there is no significant difference between the bacteria sample and the background. It suggests that with centrifuge method the LOD can reach  $10^6$  CFU/ml, which increases a magnitude of 2 fold over the “pipette method” previously reported by Chu et al (17).

One indispensable advantage the centrifugation method, as an effective sampling method, is capability to provide more even distribution of the bacteria on the substrates by preventing the

“coffee ring” effect during drying of the solution. When bacteria solution was directly pipette onto the substrate used the same “pipette method” as previously performed by Chu et al (17), the surface tension of the water droplet will migrate the bacteria to the edge of the droplet, and form a “coffee ring”, as shown in Figure 4.3A; while the samples with centrifugation method shows even bacteria distribution in Figure 4.3B. The bacteria are concentrated to the edge of the droplet in “pipette method”, so it has lower bacteria concentration in the center, where majority of the SERS measurements will be taken. With the even distribution of the bacteria by the centrifugation method, the amount of bacteria yield by is higher than that yield by the “pipette method” within the same surface area, which explains why that samples prepared by centrifuge method give stronger SERS signals than those prepared by pipette method.

### **Filtration Method**

The spectra of *Salmonella* Typhimurium samples prepared by filtration method, shown in Figure 4.4A, exhibit great similarity with the ones prepared by “pipette method” (17) and centrifugation method (Figure 4.2A). The same peak analysis procedure is used, and the  $I_{735}$  is plotted against bacteria concentration in Figure 4.4B. The filtration method concentrates the initial bacterial solution of 250 mL to a final solution of 50  $\mu$ L, so theoretically it will decrease the LOD by 5000 times. In Figure 4.4B, all the spectra at concentration of  $10^5$  CFU/ml yield positive detection; while  $10^4$  and  $10^3$  samples are not significantly different from the background samples, which suggests the LOD of filtration method reaches at least  $10^5$  CFU/ml. The difference between the real LOD and the theoretical LOD is coming from the bacteria loss during the procedure. Besides reducing the LOD by 1000 times, filtration method has the potential to be used in real food sample for separation bacteria from the food matrix. It can be

realized by adding another initial filtration step using filter membrane with pore size bigger than bacteria to remove the interference substances in the food samples.

## **Conclusions**

In this report, we have investigated better sampling procedures for bacteria detection including centrifugation and filtration techniques, followed by SERS measurement using regular AgNR. The centrifuge method concentrates the bacteria onto the surface of the SERS-active substrate, solving the problems of uneven sample distribution, and reducing the undesired distance between target bacteria and the substrate surface. The entire procedure from sampling to quantization takes 30 min; it improves the LOD of *Salmonella* Typhimurium to  $10^6$  CFU/ml. The filtration method concentrates the sample volume from 250ml to 50 $\mu$ l, so the LOD of *Salmonella* Typhimurium reaches to  $10^5$  CFU/ml. This method also demonstrates the potential in separating the bacteria from food matrix by adding one initial filtration step. This study has contributed to the development of a rapid and sensitive detection method of foodborne pathogenic bacteria without the need of sample enrichment. It has potential for the application in an on-line detection for food industry.

## References

1. **Mead PS, Slutsker L, Dietz V, McCaig LF, Bresee JS, Shapiro C, Griffin PM, Tauxe RV.** 1999. Food-related illness and death in the United States. *Emerg. Infect. Dis* **5**:607.
2. **Nelson WH, Manoharan R, Sperry JF.** 1992. UV resonance Raman studies of bacteria. *Appl. Spectrosc. Rev.* **27**:67.
3. **Wu Q, Hamilton T, Nelson WH, Elliott S, Sperry JF, Wu M.** 2001. UV Raman spectral intensities of E.coli and other bacteria excited at 228.9, 224 and 248.2 nm. *Anal. Chem.* **73**:3432.
4. **Alexander TA, Pellegrion PM, Gillespie JB.** 2003. Near-infrared surface-enhanced Raman scattering mediated detection of single optically trapped bacterial spores. *Appl. Spectrosc.* **57**:1340.
5. **Fleischmann M, Hendra PJ, McQuillan AJ.** 1974. Raman spectra of pyridine adsorbed at a silver electrode. *Chem. Phys. Lett.* **26**:163.
6. **Moskovits M.** 1985. Surface-enhanced spectroscopy. *Rev. Mod. Phys.* **57**:783.
7. **Campion A, Kambhampati P.** 1998. Surface-enhanced Raman scattering. *Chem. Soc. Rev.* **4**:241.
8. **Kneipp K, Haka AS, Kneipp H, Badizadegan K, Yoshizawa N, Boone C, Shafer-Peltier KE, Motz JT, Dasari RR, Feld MS.** 2002. Surface-enhanced Raman spectroscopy in single living cells using gold nanoparticles. *Appl. Spectrosc.* **56**:150.
9. **Tian ZQ, Ren B, Wu DY.** 2002. Surface-enhanced Raman scattering: From noble to transition metals and from rough surfaces to ordered nanostructures. *Journal of Physical Chemistry B* **106**:9463-9483.

10. **Chaney SB, Shanmukh S, Dluhy RA, Zhao Y-P.** 2005. Aligned silver nanorod arrays produce high sensitivity surface-enhanced Raman spectroscopy substrates. *Applied Physics Letters* **87**.
11. **Driskell JD, Shanmukh S, Liu Y, Chaney SB, Tang X-J, Zhao Y-P, Dluhy RA.** 2008. The use of aligned silver nanorod arrays prepared by oblique angle deposition as SERS substrates. *J. Phys. Chem. C*:jp075288u.
12. **Shanmukh S, Jones L, Driskell J, Zhao Y-P, Dluhy R, Tripp RA.** 2006. Rapid and sensitive detection of respiratory virus molecular signatures using a silver nanorod array SERS substrate. *Nano Lett.* **6**:2630.
13. **Zhao YP, Chaney, S.B., Shanmukh, S., Dluhy, R.A.** 2006. Polarized Surface Enhanced Raman and Absorbance Spectra of Aligned Silver Nanorod Arrays. *Journal of Physical Chemistry B* **110**:3153-3157.
14. **Wu X, Gao S, Wang J-S, Wang H, Huang Y-W, Zhao Y.** 2012. The surface-enhanced Raman spectra of aflatoxins: spectral analysis, density functional theory calculation, detection and differentiation. *Analyst* **137**:4226-4234.
15. **Driskell JD, Zhu Y, Kirkwood CD, Zhao Y, Dluhy RA, Tripp RA.** 2010. Rapid and sensitive detection of rotavirus molecular signatures using surface enhanced Raman spectroscopy. *PloS one* **5**:e10222.
16. **Shanmukh S, Jones L, Zhao YP, Driskell J, Tripp R, Dluhy R.** 2008. Identification and classification of respiratory syncytial virus (RSV) strains by surface-enhanced Raman spectroscopy and multivariate statistical techniques. *Analytical and bioanalytical chemistry* **390**:1551-1555.

17. **Chu H, Huang Y, Zhao Y.** 2008. Silver Nanorod Arrays as a Surface-Enhanced Raman Scattering Substrate for Foodborne Pathogenic Bacteria Detection. *Appl. Spectrosc.* **62**:922-931.
18. **Driskell JD, Seto AG, Jones LP, Jokela S, Dluhy RA, Zhao YP, Tripp RA.** 2008. Rapid microRNA (miRNA) detection and classification via surface-enhanced Raman spectroscopy (SERS). *Biosensors and Bioelectronics* **24**:917-922.
19. **Abell JL, Driskell JD, Dluhy RA, Tripp RA, Zhao YP.** 2009. Fabrication and characterization of a multiwell array SERS chip with biological applications. *Biosensors and Bioelectronics* **24**:3663-3670.

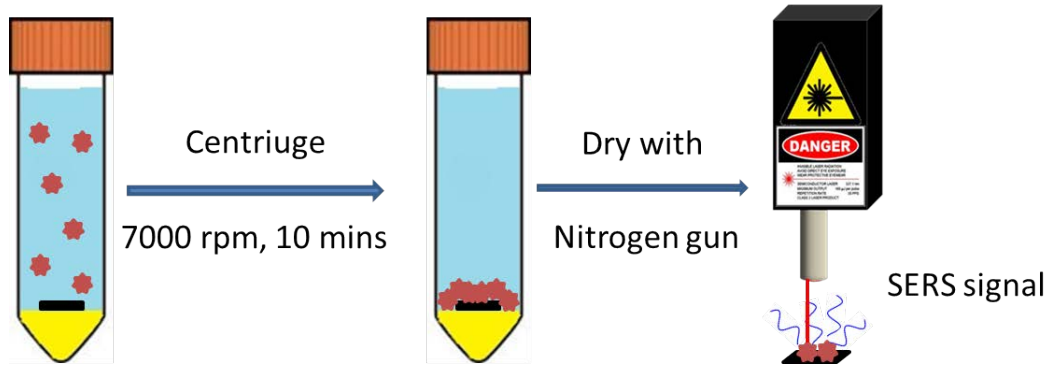


Figure 4.1 Scheme of centrifugation method with SERS for bacterial detection.

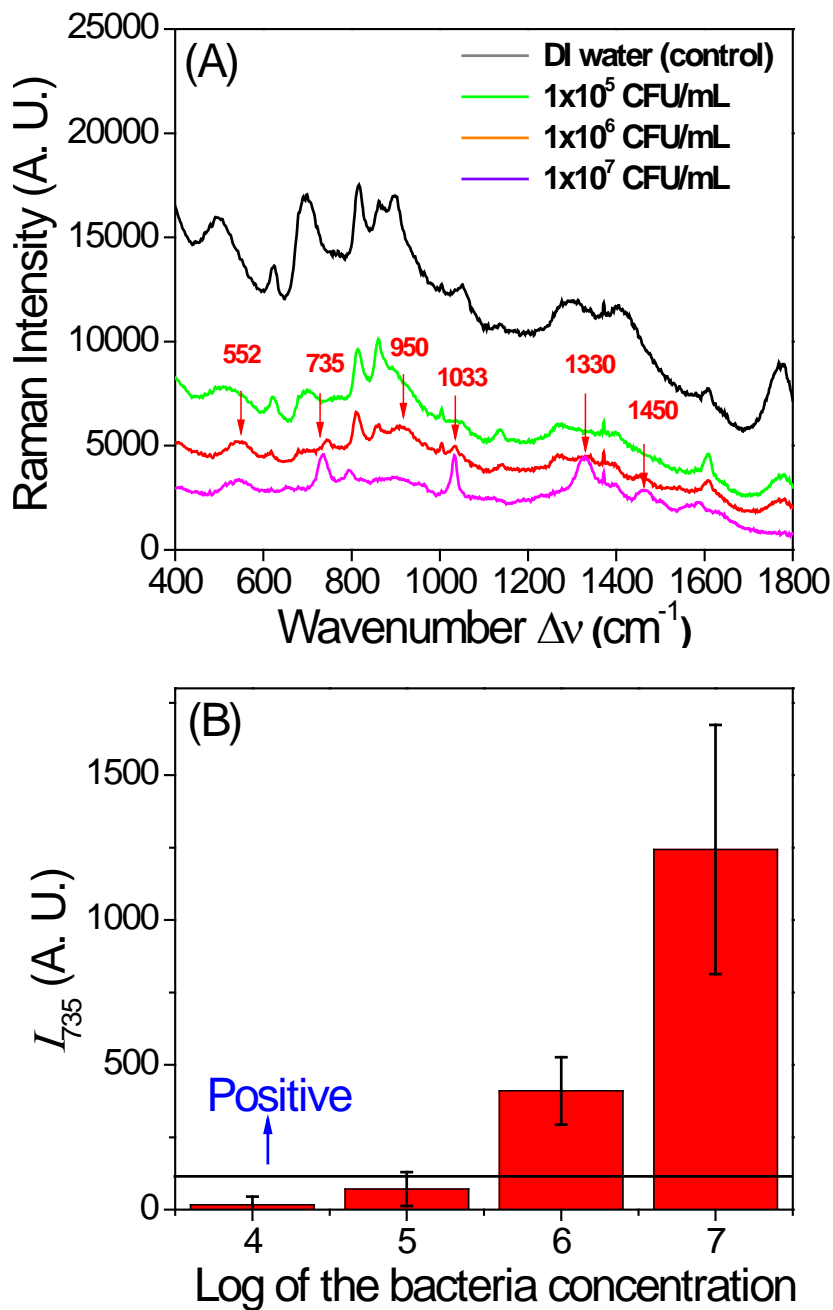


Figure 4.2 (A) SERS spectra of *Salmonella* Typhimurium prepared by centrifugation method at different concentration. Red number indicated the peaks from the bacteria. (B) Peaks intensity  $I_{735}$  as a function of the concentration of *Salmonella* Typhimurium samples prepared by centrifugation method. Horizontal line indicates the threshold for a positive detection of the bacteria.

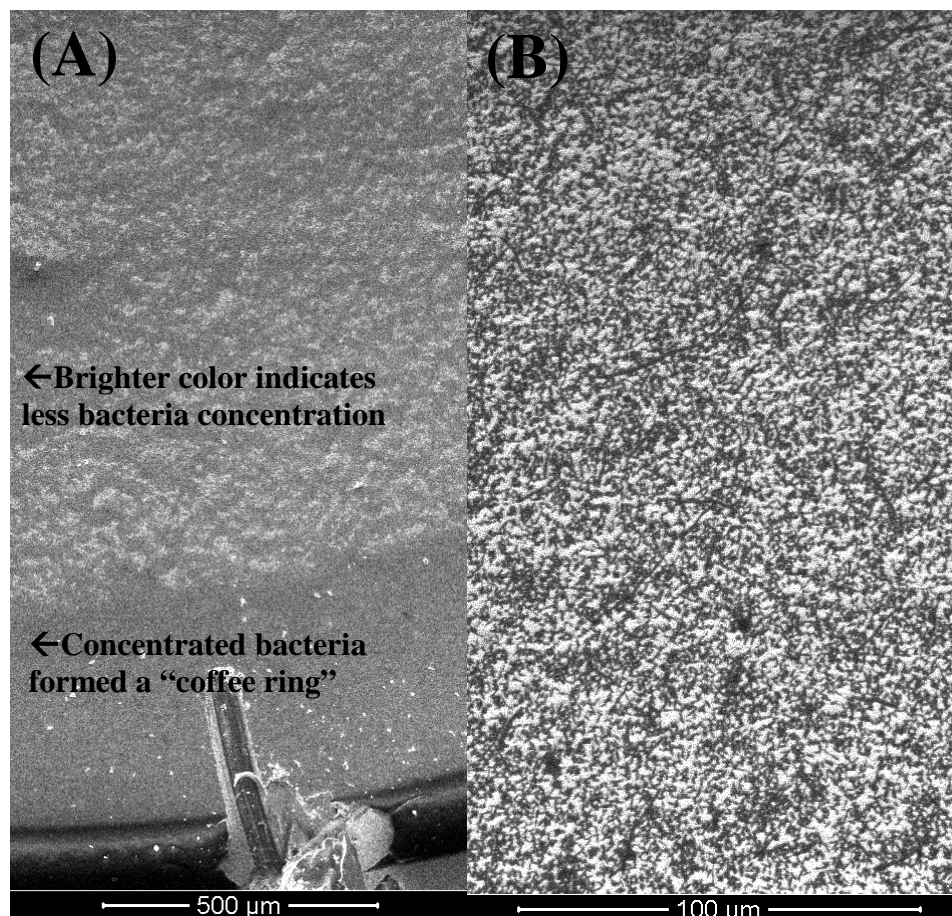


Figure 4.3 (A) SEM pictures of  $10^9$  CFU/ml *Salmonella* Typhimurium on AgNR prepared by pipette method. The lack of inductance made the bacteria darker in the SEM; while the underneath Ag appeared brighter under SEM view. The more concentrated bacteria form a “coffee ring” around the edge of the droplet. (B) The SEM picture of  $10^7$  CFU/ml *Salmonella* Typhimurium on AgNR substrate prepared by centrifugation method, showing the even distribution of bacteria throughout the whole substrate surface.

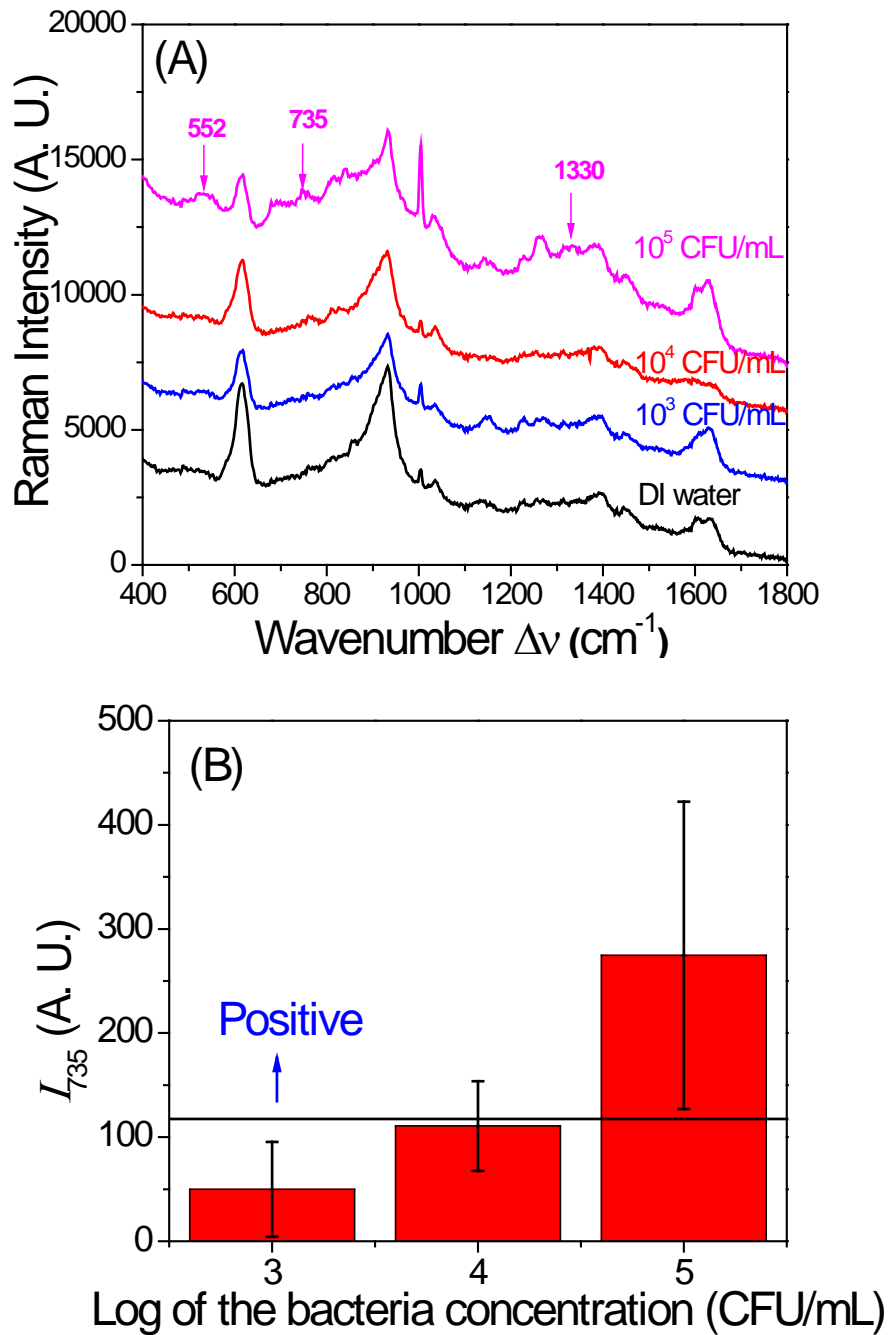


Figure 4.4 (A) SERS spectra of *Salmonella* Typhimurium prepared by two-step filtration method at different concentration. Red number indicated the peaks from the bacteria. (B) The SERS peak intensity  $I_{735}$  as a function of the concentration of *Salmonella* Typhimurium samples prepared by filtration method. Horizontal line indicates the threshold for a positive detection of the bacteria.

## CHAPTER 5

### DETECTION AND DIFFERENTIATION OF FOODBORNE PATHOGENIC BACTERIA IN MUNG BEAN SPROUTS USING FIELD DEPLOYABLE LABEL-FREE SERS DEVICES<sup>1</sup>

---

<sup>1</sup> Xiaomeng Wu, Chao Xu, Ralph A. Tripp, Yao-wen Huang, Yiping Zhao. 2013. *Analyst* 138 (10), 3005-3012

Reprinted it here with permission of publisher

## Abstract

Vancomycin functionalized silver nanorod arrays substrates were used to obtain the surface enhanced Raman scattering (SERS) signals of six foodborne pathogenic bacteria in mung bean sprouts samples using both a portable and a handheld Raman system. The silver nanorod arrays substrates were optimized to facilitate quantitative, rapid, and sensitive detection of *Salmonella enterica* serotype Anatum, *Salmonella enterica* serotype Cubana, *Salmonella enterica* serotype Stanley, *Salmonella* Enteritidis, *Escherichia coli* O157:H7, and *Staphylococcus epidermidis*. Substrate optimization was achieved by varying the nanorod length and vancomycin incubation concentration. By combining these substrates with a two-step filtration process we found that the foodborne pathogenic bacteria used in this study can be identified in mung bean sprouts with a limit of detection as low as 100 CFU/ml in less than 4 hrs using both portable and handheld Raman systems. The results show that SERS spectra can be used to differentiate between bacterial species and serotypes when chemometric methods are employed. The low detection limit and rapid detection time of this biosensing platform for foodborne pathogenic bacteria could be a valuable field detection method for the fresh produce and food processing industries.

## Introduction

Foodborne diseases are increasingly reported as substantial public health problems worldwide, particularly in areas where fresh fruits and vegetables have been the major vehicles of foodborne outbreaks <sup>1</sup>. In the United States, green salads, sprouts, potatoes, and lettuce have been reported to be main sources of produce-associated foodborne outbreaks <sup>2</sup>. The presence of pathogens in produce and other ready-to-eat products is a serious concern because consumers may not perform any treatment to reduce bacterial load prior to consumption.

Mung bean sprouts are widely consumed in Asia, and their consumption in the USA has increased rapidly as Asian dishes gain more favour in the market <sup>3, 4</sup>. Mung bean sprouts are commonly consumed raw or with minimal thermal processing and have acted as a vector for several outbreaks <sup>5</sup>. Most sprouts-related outbreaks have been linked to contamination by *Salmonella* and *Escherichia coli* O157:H7, followed by *Listeria monocytogenes*, *Staphylococcus aureus*, *Bacillus cereus*, and *Aeromonas hydrophila* <sup>6</sup>.

To overcome illness linked to foodborne pathogens, particularly in raw foods, it is important to develop rapid and specific pathogen detection methods to prevent contaminated food from entering the food supply. Bacterial culture-based methods are the conventional way to detect bacterial pathogens in food. These methods often include incubation and enrichment steps requiring 6-24 hours with an additional 1-3 days for confirmation by biochemical tests <sup>7, 8</sup>. Though these methods are sensitive, relatively inexpensive, and provide both qualitative and quantitative information on the number and the nature of the microorganisms, their lengthy duration makes them unsuitable to satisfy today's food industry requirements for rapid detection. Newer technologies that incorporate polymerase chain reaction (PCR) and immunological detection are faster than culture-based methods <sup>9, 10</sup>, but have fundamental restrictions limiting

their uses in the field or processing plant. For example, PCR is based on nucleic acid amplification and consequently cannot discriminate nucleic acid amplified from viable and nonviable bacteria. Furthermore, PCR-based methods require substantial laboratory equipment and highly skilled personnel. Immunological detection, such as enzyme-linked immunosorbent assay (ELISA), has the advantage of being specific to bacterial type and strain, but it also requires multiple steps, varied chemical reagents, and incubation time making this method impractical for “real-time” detection in the field. To overcome such disadvantages, researches on the development of rapid, highly sensitive, high throughput, and “real time” biosensors have been intensively conducted <sup>11</sup>, especially with nanomaterial based sensors <sup>12,13</sup>. Several studies have used microfluidic devices to combine the separation/concentration capabilities for bacteria detection, such as fluorescence imaging <sup>14</sup>, immune assay <sup>15</sup>, optical analysis <sup>16</sup>, DNA hybridization assay <sup>17</sup>, surface enhanced Raman scattering <sup>18</sup>. Impedance biosensors have also been developed to use interdigitated microelectrodes to conduct chip-based impedance bacteria detections <sup>19-21</sup>. Dynamic staining of the bacterial endospores is also used to monitor the fluorescence images of bacteria <sup>22</sup>.

As one of the feasible way to realize “real-time” detection, Raman spectroscopy has the potential for rapid detection of a wide range of chemical and biological substances <sup>23</sup>. Traditional Raman spectroscopy relies on the inelastic scattering interaction of excitation light and vibrational modes of molecular bonds. These molecular vibrational modes possess unique “fingerprint” peaks which can be used to identify the particular molecule(s) being probed. Surface-enhanced Raman spectroscopy (SERS) is a highly sensitive Raman detection technique based on metallic nanostructured substrates <sup>24,25</sup>. The nanostructure-induced signal enhancement is sensitive enough to detect even trace levels of molecules. Several forms of nanostructures have

been developed and used to facilitate SERS spectra of bacteria including silver metal deposits<sup>26</sup>, silver colloid<sup>27,28</sup>, gold colloid solutions<sup>29</sup>, and electrochemically roughened metal surfaces<sup>30</sup>. Although silver or gold colloids have been used to detect bacteria with a limit of detection (LOD) of  $10^3$  CFU/ml for *E. coli*<sup>28</sup> for example, methods incorporating these colloids often lack reproducibility due to slight variations in cluster size and shape introduced by the colloidal solution. These variations can change the SERS enhancement factors by several orders of magnitude. To solve the reproducibility problem, several solid phase substrates have been developed. Recently, magnetic-plasmonic nanoparticles were used to detect *Escherichia coli* K12, *Pseudomonas. aeruginosa*, and *Acinetobacter calcoaceticus* at a LOD of  $2 \times 10^5$  CFU/ml<sup>31</sup>. Wang *et al.* used silver nanocrystal assembled silver nanospheres (AgNSs) to detect *E. coli* O157:H7, *S. Typhimurium*, and *S. aureus* with a LOD as low as 10 CFU/ml and were able to detect bacteria in a food matrix when the nanospheres were used in conjunction with antibodies<sup>32, 33</sup>. Zhang *et al.* used silver film over nanosphere (AgFON) substrates to acquire the SERS spectra of calcium dipicolinate (CaDPA), a biomarker for bacillus spores, and achieved a LOD of  $2.6 \times 10^3$  spores of bacillus<sup>34</sup>. An array of Ag nanoparticles imbedded in anodic aluminum oxide (AAO) nanochannels substrates were fabricated by Liu *et al.*, and such substrates were able to detect the “chemical features” of bacterial cell wall that enables rapid identification of drug resistant bacteria<sup>35</sup>.

For SERS to be a viable and sensitive detection platform for pathogens in a food system, it is necessary to fabricate reproducible and practical SERS substrates with high signal to-noise-ratio. Silver nanorod (AgNR) array substrates fabricated by oblique angle deposition (OAD) method have been shown to have a SERS enhancement factor of  $> 10^8$  and a batch variability  $< 15\%$ <sup>36, 37</sup>. In addition, these substrates have been shown to markedly enhance the detection of

chemical and biological samples including aflatoxins<sup>38</sup>, human viruses such as rotavirus, influenza virus and respiratory syncytial virus<sup>39, 40</sup>, as well as allow for detection and discrimination of microRNA families and family members<sup>41</sup>. The detection of bacteria such as *E. coli* O157:H7, *S. Typhimirium*, and *S. aureus* using AgNR substrate has also been demonstrated<sup>42</sup>. However, two challenges remain for detecting bacterial pathogens in food samples. The first challenge is to lower the LOD of the bacteria and the second challenge is to detect foodborne bacteria in its natural environment and not a laboratory culture<sup>42</sup>. There is often a need to detect foodborne bacteria in a bulk sample with large volume. The relationship between the bulk concentration detection limit and the surface detection limit is determined by (1) the volume  $V$  of bacterial solution applied; (2) the spreading area of the sample on SERS substrate  $A_0$ ; (3) the size of the laser spot  $\pi R^2$  with  $R$  the radius of the laser spot, and (4) the bulk concentration  $C$ . The amount of bacteria detected is  $N_d = VC\pi R^2/A_0$ , so  $C = N_d A_0 / V\pi R^2$ , where threshold  $N_d$  reflects the true detectability of a SERS method, and  $C$  represents the bulk LOD of such detection. Thus, for a fixed surface detection method, the reduction of  $C$  can be achieved by decreasing  $A_0$ , increasing  $V$ , and increasing  $R$ . In the equation,  $R$  is limited by the Raman instrument used while  $A_0$  could be confined by a narrow well as previously reported<sup>43</sup>. Thus, the best strategy to lower  $C$  would be to increase  $V$ , the volume of the samples put on the substrates. One way to increase  $V$  is to use pre-concentration methods that capture as many bacteria as possible in a fixed surface area using a large sample volume. Another strategy to lower the  $C$  would be to optimize the substrates, hence decreasing the  $N_d$  value. Liu *et al.* reported that the functionalization of silver nanoparticles with vancomycin increased the bacteria capture ability of the nanoparticle by 3 folds of magnitude and greatly reduced the distance between the bacteria and the substrate surface thereby increasing its SERS intensity dramatically

<sup>44</sup>. A similar capture agent coating procedure is adapted in this study to coat the AgNR substrates with vancomycin, in order to decrease the  $N_d$  value.

In order to identify bacterial pathogens in food using SERS, it is necessary to develop field sampling methods that simultaneously detect, separate and concentrate pathogens from the food matrix. Conventional culture based methods rely on selective and differential plating to separate the pathogens from the background and background microflora. However, such cultural enrichment and selective plating result in a lengthy procedure up to four days. Other sampling methods that separate and concentrate bacteria from food matrices were developed, and well-reviewed by Stevens and Jaykus <sup>45</sup>. These methods can be categorized as chemical (e.g., ion exchange resins, lectins, dielectrophoresis, and aqueous two-phase partitioning), physical (e.g., centrifugations, coagulation, flocculation, filtration methods, flow cytometry, and ultrasound), physicochemical (e.g., metal hydroxides), or biological approaches (e.g., immunomagnetic separation and bacteriophage). An effective field sampling method is crucial to facilitate identification of bacterial Raman spectra without interference from the food matrix. The main interference in food samples comes from macromolecules like protein and polysaccharides that contain similar chemical bonds to the target bacteria. There is not an easy way to eliminate the interference entirely from the sample, but with proper separation methods it is possible to reduce the interference. Due to the size difference of bacteria and macromolecules in food samples filtration is used to physically separate the bacteria from the interfering molecules. Wolffs reported a two-step filtration method prior to PCR to detect *S. enterica* and *L. monocytogenes* in chicken rinse and yogurt with 79.1% recovery rate and only 29 minutes of filtration time <sup>46</sup>. A similar filtration procedure was adopted in this study to separate and concentrate pathogens from mung bean sprouts samples.

In order for the SERS detection method to be used in the field, the size and weight of the instrument has to be reasonable. The Enwave Raman system (model HRC-10HT) is a bench top Raman spectrometer that can be transported into the field. Another system, FirstDefender RM, is an even smaller and lighter handheld Raman spectrometer, weighing 2 lb (919g) with a size of  $19.6 \times 11.4 \times 6.1$  cm and designed for easy transportation. Since the resolution and sensitivity of such small Raman spectrometers are limited, the feasibility of using these two devices as field instruments is tested in this study.

In this study, we used the vancomycin functionalized AgNR array substrates to study the SERS spectra of foodborne pathogens in mung bean sprouts samples. The SERS spectra were acquired using both bench top and handheld Raman systems. We also used the functionalized AgNR array substrates to differentiate pathogens from different species and different serotypes of the same species.

## **Material and methods**

### **AgNR fabrication**

SERS spectra were acquired using AgNR array substrates fabricated by the oblique angle deposition (OAD) technique using a custom-designed electron beam/sputtering evaporation (e-beam) system<sup>36, 37, 47</sup>. Briefly, glass microscopic slides (Gold Seal® Catalog No.3010, Becton, Dickinson and Company, Portsmouth, NH) used for AgNR arrays deposition were cleaned with piranha solution (80% sulfuric acid, 20% hydrogen peroxide in volume) and rinsed with deionized water. The substrates were then dried with a stream of nitrogen gas before being loaded into the e-beam deposition system. A 20-nm titanium film and then a 200-nm silver film layer were evaporated onto the glass slides at a rate of  $\sim 0.2$  nm/s and 0.3 nm/s, respectively,

while the substrate surface was held perpendicular to the incident vapor direction. The substrates were then rotated to 86° with respect to the incident vapor and AgNRs were grown at this oblique angle with a deposition rate of ~0.3 nm/s. The film thickness was monitored *in situ* by a quartz crystal microbalance (QCM) positioned at normal incidence to the vapor source direction. We varied the thickness of the AgNR layer from 200 nm to 900 nm to optimize the substrate for bacteria detection.

### **AgNR functionalization**

Vancomycin (VAN) was purchased from Sigma Aldrich Ltd. (St. Louis, MO), and was diluted by using ultra-pure water (18MΩ) to 0.05, 0.1, 0.2, 0.5, 1, 2, 5, 10, and 20 mM. The AgNR array substrates were immersed in the VAN solutions overnight (> 12 hrs), rinsed three times with DI water, and then dried with nitrogen.

### **Food samples preparation and bacteria incubation**

Six different bacteria were used in this study. *Salmonella enterica* serotype Anatum (H3536), *Salmonella enterica* serotype Cubana (H7976), *Salmonella enterica* serotype Stanley (H1256), *Salmonella* Enteritidis (ATCC# 13076), *E. coli* O157:H7 (salami isolate), and *Staphylococcus epidermidis* (ATCC# 14990), were obtained from the Department of Food Science and Technology of The University of Georgia (Athens, GA). These bacteria were grown in trypticase soy broth (TSB, Difco, Detroit, MI) overnight at 37 °C to yield ~10<sup>9</sup> CFU/ml culture. Bacterial populations were determined by conventional surface plate count method using plate count agar (PCA, Difco®, Detroit, MI). Following incubation, the cultures were washed three times with sterilized deionized (DI) water before re-suspending in sterilized DI water. Desired dilutions were made in sterilized DI water as well.

The mung bean sprouts samples were cleaned by using 1000 ppm house bleach (acidified hyperchlorine, EverydayLiving) for at least 20 min to ensure no bacteria survival on the surface. The food samples were then carefully rinsed with sterilized DI water to remove any chemical residue, and dried in a biosafety hood with laminar flow. Ten grams of mung bean sprouts were inoculated with 100 $\mu$ l of bacterial culture with different concentrations for 1 hr to ensure the attachment of the bacteria. The inoculated sprouts samples were then mixed with 100 ml of sterile DI water and massaged with a stomacher for 1 min at 200 rpm. Next, these solutions underwent a filtration procedure adapted from the method of Wolffs *et al.*<sup>46</sup> as illustrated in Figure 5.1. This method is a two-step filtration: 1) a crude pre-filtration step through VWR® # 417 filters (pore size 40  $\mu$ m) to remove larger sample particles, and 2) a second filtration to recover the target bacteria from the filtrate using Durapore® filter membranes (pore size 0.22 $\mu$ m). The filter membrane containing the bacteria was vortexed with 0.5 ml sterile DI water for 15 sec. The bacteria will be re-suspended in this 0.5 ml solution, and the vancomycin treated AgNR substrate (VAN substrate) was immersed in this solution for 2 hrs at 37 °C with shaking at 200 rpm. The inoculated substrates were then rinsed with DI water, followed by drying with Nitrogen. The entire process, from filtration to spectrum acquisition, took approximately 4 hrs.

### **SERS measurements and data analysis**

For most of this study, SERS spectra were acquired using a portable Enwave Raman system (Model HRC-10HT, Enware Optronics Inc., Irvine, CA), with a 785 nm near-IR diode laser as the excitation source. The power of the laser at the sample was set to be ~ 30 mW. SERS spectra over a range of ~ 400 – 1800  $\text{cm}^{-1}$  were used over a 10 sec exposure time. SERS spectra were collected from 9 spots (3  $\times$  3 array) across the VAN substrate surface and multiple substrates were measured. The spectra acquired by using FirstDefender RM (Thermo Fisher

Scientific, Tewksbury, MA) are specially indicated in the study, which were acquired under low power and auto exposure time setting. All data analysis was performed using Origin software 8.5 version (OriginLab Corporation, Northampton, MA) and WIRE2.0 software (Renishaw, United Kingdom). Statistical data analysis was conducted with Matlab 2000b (The MathWorks, Inc., Natick, MA) using the PLS toolbox (Eigenvector Research, Inc., Wenatchee, WA).

## **Results and discussion**

### **LOD of pure bacteria using optimized VAN substrates**

The length of the AgNR will affect the SERS enhancement of bacteria, and we have conducted a systematic study on how the thickness of the AgNR affects bacteria SERS signal detailed in Appendix A.1.1. The SERS intensity of *E. coli* O157:H7 reaches a maximum intensity at 600 nm AgNR thickness (QCM reading) as shown in Figure A.1 in Appendix A. In addition, as demonstrated by Liu *et al.*, coating the Ag nanoparticles with vancomycin provides a capture layer for bacteria which can increase the detection sensitivity of bacteria<sup>44</sup>. We have also performed a systematic investigation on vancomycin coating conditions for the AgNR substrates to achieve the best SERS sensitivity detailed in Appendix A.1.2. By investigating the SERS spectra as a function of the AgNR thickness and vancomycin concentration, we established that 1mM vancomycin coated AgNR substrate with thickness (QCM reading) of 600 nm yielded the most intense bacteria SERS signal. Therefore, substrates with these optimized conditions were used to detect the pure bacteria. The SERS spectra of *E. coli* O157:H7 at different concentrations ( $10^4$ ,  $10^5$ , and  $10^6$  CFU/ml) and the sterile DI water as a control are shown in Figure 5.2A. The optimized vancomycin coated AgNR substrate is considered as the background sample and its SERS spectrum is illustrated in Figure A.4 in Appendix A. By comparing the SERS spectra of

the control with those from *E. coli* O157:H7, we see that the control sample has no obvious peaks in the region of 400-1200  $\text{cm}^{-1}$ , suggesting that vancomycin coating does not introduce much interference in this spectral region. However, in the region of 1200-1700  $\text{cm}^{-1}$ , the control has several peaks in common with the *E. coli* O157:H7 ( $\Delta\nu = 1243, 1321, 1369, 1476, \text{ and } 1595 \text{ cm}^{-1}$ ). Therefore, spectra in the region of 400 to 1200  $\text{cm}^{-1}$  were used for the remainder of this study. Also note that in Figure 5.2A the peaks at  $\Delta\nu = 652, 728, 893, \text{ and } 955 \text{ cm}^{-1}$  only present in the *E. coli* O157:H7 samples, but not in the control sample. The intensities of these peaks increase with bacterial concentration. In addition, these peaks were previously reported by several other groups for bacteria<sup>27, 28, 42, 48</sup>. Hence, we conclude that the peaks at  $\Delta\nu = 652, 728, 893, \text{ and } 955 \text{ cm}^{-1}$  are signature peaks from *E. coli* O157:H7 samples and their corresponding vibrational modes of these SERS peaks are assigned in Appendix A.1.1.

In order to establish the LOD of VAN substrates for *E. coli* O157:H7 samples, we plotted the SERS peak intensity at  $\Delta\nu = 728 \text{ cm}^{-1}$  ( $I_{728}$ ) against the bacterial concentration (Figure 5.2B). At each concentration, at least 9 spectra from two different substrates were measured and analyzed by peak fitting, and the mean and standard deviation of the peak intensities  $I_{728}$  are shown in Figure 5.2B. The LOD of the SERS detection is defined as the lowest concentration at which a distinguished bacterial SERS spectrum can be obtained. In our experiment, the LOD is the lowest concentration at which the peak intensity of the bacteria at  $\Delta\nu = 728 \text{ cm}^{-1}$  is significantly different from the sterile DI water (control) which is used to dilute the bacteria samples. Using the same peak fitting method, the  $I_{728}$  of the DI water sample was  $149 \pm 96$  arbitrary units (AU). The value of average plus three times the standard deviation of the sterile DI water was set as the limit for determining a positive detection from a negative detection. In this experiment 427 AU ( $149 + 3 \times 96$ ) was found to be the limit. This means that when a

spectrum has an  $I_{728}$  greater than 427 AU, the peak is significantly different from the control, resulting in a positive detection of the *E. coli* O157:H7 sample. Using the VAN substrates, shown in Figure 5.2B, the lowest concentration of pure *E. coli* O157:H7 that yielded all positive detections (LOD) was approximately  $10^4$  CFU/ml.

### **Detection of *E. coli* O157:H7 in mung bean sprouts using the VAN substrates**

To test the feasibility of using VAN substrates as a real-time bacteria detection method in food, we inoculated mung bean sprouts, performed a two-step filtration, and then measured the SERS response. The two-step filtration procedure served as both a separation method to isolate bacteria from the food samples, and as a concentration method. The efficiency of the filtration method was 74.6% as determined by conventional surface plate count method using plate count agar. Although the filtration method resulted in loss of target bacteria, it effectively concentrated the solution from 100 ml to 0.5 ml. This means that 100 ml of a  $10^2$  CFU/ml solution can be concentrated to  $1.49 \times 10^4$  CFU/ml in 0.5 ml ( $10^2$  CFU/ml  $\times$  100 ml  $\times$  74.6%  $\div$  0.5 ml =  $1.49 \times 10^4$  CFU/ml) which is detectible using our SERS technique as previously demonstrated.

Figure 5.3A compares the SERS spectra of *E. coli* O157:H7 recovered from inoculated mung bean sprouts ( $10^2$ ,  $10^3$ ,  $10^4$ , and  $10^5$  CFU/ml) with a sterile DI water inoculated sample as a control. The control sample shows a “flat” background with no obvious peak present. In the  $10^2$  CFU/ml inoculated samples (equivalent to  $10^3$  CFU/g of mung bean sprouts), the spectra has all the features of the standard *E. coli* O157:H7 SERS spectra as previously established with peaks at  $\Delta\nu = 652, 728, 893, \text{ and } 955 \text{ cm}^{-1}$ . Again we see that peak intensity increases as inoculation rates increase. To quantify the SERS intensity, we employed the same peak fitting method as

before (using peak at  $\Delta\nu = 728 \text{ cm}^{-1}$ ) and  $I_{728}$  of these samples are plotted in Figure 5.3B. The result is similar to that obtained in Figure 5.2B.

As before, an  $I_{728}$  value considered positive for bacterial detection was set as the average value plus three times the standard deviation of the control sample (sterile DI water inoculated mung bean sprouts sample), which is 782 AU ( $635 + (3 \times 49)$ ). From Figure 5.3B we can see that samples with inoculation rates as low as  $10^2$  CFU/ml yield  $I_{728}$  higher than 782 AU. Therefore, the LOD of *E. coli* O157:H7 in mung bean sprouts sample using this method is  $10^2$  CFU/ml in initial solution or  $10^3$  CFU/g of mung bean sprouts. This result is consistent with our above-mentioned calculation.

To confirm the LOD, chemometric analysis of the experimental data was also explored. When the spectra data is viewed as multi-variant data, chemometric analysis can be used to reduce the dimensionality of the dataset, maximize the variance among spectral fingerprints, and provide a measure of method sensitivity. Both principal component analysis (PCA) and partial least-squares discriminatory analysis (PLS-DA) were performed on the spectra of *E. coli* O157:H7 samples and the control samples, as shown in Figure 5.4. PCA is a well-known unsupervised method to reduce dimensionality of multivariate data while preserving most of the variance. It is used to identify correlations amongst a set of variables and to transform the original set of variables into a new set of uncorrelated variables called principal components (PCs). When these PCs are plotted, the data of similar spectra can be grouped for classification based on the PC scores. In Figure 5.4A, comparison of processed spectra, PC1 and PC2, can clearly differentiate *E. coli* O157:H7 samples at different concentration from the control where each data point corresponds to a single SERS spectrum.

PLS-DA is a full-spectrum, multivariate, supervised method whereby prior knowledge of the classes (i.e. *E. coli* O157:H7 sample or control) is used to yield more robust discrimination, while emphasizing latent variables between or among classes (positive or negative detection). PLS-DA was applied to establish the statistical significance of differences between the SERS spectra of *E. coli* O157:H7 samples and the control. In Figure 5.4B, PLS-DA generated a model from 50 spectra (10 spectra per sample; same spectra as in Figure 5.4A), differentiating the positive detection of *E. coli* O157:H7 samples from the control with 100% sensitivity and specificity. In both PCA and PLS-DA method, there is a clear discrimination between the control samples and the *E. coli* O157:H7 samples above the established LOD, which provides another level of confirmation to our results.

To further improve the mobility and easy handle of the system, FirstDefender RM, a handheld Raman spectrometer, is also used to acquire SERS spectra from the *E. coli* O157:H7 recovered from mung bean sprouts samples followed by a two-step filtration. The detailed results are described in Appendix A.2. Similar to the portable fiber Raman system, the FirstDefender RM handheld Raman spectrometer is able to detect  $10^2$  CFU/ml or  $10^3$  CFU/g *E. coli* O157:H7 from mung bean sprouts samples, and this result is confirmed by PCA and PLS-DA in Figure A.6 in Appendix A.

### **Discrimination of different bacteria in mung bean sprouts samples.**

Sprouts-associated outbreaks between 1996 and 2009 were linked to several pathogens including *Salmonella* and *E. coli* O157:H7<sup>49</sup>. Due to the variety of bacterial pathogens that may pose a threat to a particular food, it is essential for a detection platform to not only detect different pathogens but to discriminate them by species or even specific serotype. To test the

ability of our detection method to differentiate various pathogen, we chose *Salmonella enterica* serotype Anatum (SA), *Salmonella enterica* serotype Cubana (SC), *Salmonella enterica* serotype Stanley (SS), *Salmonella* Enteritidis (SE), *E. coli* O157:H7 (EC), and *Staphylococcus epidermidis* (STE) to study. The first five pathogens were chosen because they have all been linked to previous sprouts outbreaks<sup>49</sup> and STE was chosen because it is a common foodborne pathogen and used here as a representative Gram positive pathogen. These six pathogens were inoculated onto mung bean sprouts prior to recovery by the two-step filtration as described above. The SERS spectra from the six pathogens inoculated at a rate of  $10^2$  CFU/ml were acquired by the Enwave Raman spectrometer and compared (see Figure 5.5A). The  $I_{728}$  of these spectra are compared in Figure 5.5B. In Figure 5.5B, it is clear that all six pathogens have  $I_{728}$  values larger than 728 AU (the threshold value used to determine a positive detection) which indicates that the LODs for all these pathogens are at least  $10^2$  CFU/ml or  $10^3$  CFU/g in the mung bean sprouts samples using the bench-top Enwave Raman spectrometer.

The SERS spectra of different pathogens are expected to be distinctive because of differences in cell structures and antigens, but the spectral disparity between them is expected to be small since the majority of cell wall components are similar. In Figure 5A, spectra from the six pathogens look similar with peaks at  $\Delta\nu = 652, 728, \text{ and } 893 \text{ cm}^{-1}$  present for each bacteria. In order to differentiate minute differences in the SERS spectra, PCA was employed. The plot of PC1 versus PC2 of the six pathogens is shown in Figure 5.6A with the components forming three clusters based on bacterial species. The four *Salmonella* species (SA, SC, SE, and SS) form a big and complicated cluster while the *Staphylococcus epidermidis* (STE) and *E. coli* O157:H7 (EC) both form individual and distinguished clusters. This plot suggests that bacterial species from mung bean sprouts can be discriminated with their SERS spectra using a PCA plot. A PCA plot

of PC1 versus PC2 of the four different serotypes of the *Salmonella spp.* (SA, SC, SE, SS) are shown in Figure 5.6B with components separating into four clusters. This indicates that this label-free SERS detection method can be used to distinguish serotypes of the same species.

## **Conclusions**

In this study we demonstrate the sensitivity and specificity of SERS for detection of foodborne pathogens from mung bean sprouts samples using the vancomycin functionalized AgNR substrates. The LOD of this system reaches  $10^2$  CFU/ml in initial solution or  $10^3$  CFU/g of mung bean sprouts when combined with a two-step filtration process. To the best of our knowledge, this is the lowest LOD reported for the SERS technique using real food samples and in the absence of external SERS reporters. The LOD was determined using both bench-top and handheld Raman spectrometers indicating that the method lends itself to application in the field. Six different pathogens were detected and differentiated by their species and serotypes using PCA. We believe the SERS detection technique based on AgNR is a powerful platform to detect low amounts of foodborne pathogens with the potential to be used as an on-site pathogen detection method in the food industry. Further studies focused on using the technique on more food commodities, as well as more robust pre-processing methods, are needed.

## **Acknowledgments**

This work is supported in part by USDA CSREES Grant #2009-35603-05001 and the University of Georgia College of Agricultural and Environmental Sciences Experimental Station. X. Wu would like to thank Jessica Just for her help in the preparation of the manuscript.

## References

1. M. P. Doyle and M. C. Erickson, *Journal Of Applied Microbiology*, 2008, **105**, 317-330.
2. M. C. Erickson, *Comprehensive Reviews in Food Science and Food Safety*, 2010, **9**, 602-619.
3. S. Y. Lee, K. M. Yun, J. Fellman and D. H. Kang, *J. Food Prot.*, 2002, **65**, 1088-1092.
4. P. J. Taormina, L. R. Beuchat and L. Slutsker, *Emerg. Infect. Dis*, 1999, **5**, 626-634.
5. J. C. Mohle-Boetani, J. Farrar, P. Bradley, J. D. Barak, M. Miller, R. Mandrell, P. Mead, W. E. Keene, K. Cummings, S. Abbott and S. B. Werner, *Epidemiology and Infection*, 2009, **137**, 357-366.
6. M. L. Bari, M. I. Al-Haq, T. Kawasaki, M. Nakauma, S. Todoriki, S. Kawamoto and K. Isshiki, *J. Food Prot.*, 2004, **67**, 2263-2268.
7. K. S. Gracias and J. L. McKillip, *Can. J. Microbiol.*, 2004, **50**, 883-890.
8. B. Swaminathan and P. Feng, *Annual Review of Microbiology*, 1994, **48**, 401-426.
9. O. Lazcka, F. J. D. Campo and F. X. Muñoz, *Biosensors and Bioelectronics*, 2007, **22**, 1205-1217.
10. P. Leonard, S. Hearty, J. Brennan, L. Dunne, J. Quinn, T. Chakraborty and R. O'Kennedy, *Enzyme and Microbial Technology*, 2003, **32**, 3-13.
11. D. Ivnitski, I. Abdel-Hamid, P. Atanasov and E. Wilkins, *Biosensors and Bioelectronics*, 1999, **14**, 599-624.
12. K. S. Hwang, S.-M. Lee, S. K. Kim, J. H. Lee and T. S. Kim, *Annual Review of Analytical Chemistry*, 2009, **2**, 77-98.
13. P. J. Vikesland and K. R. Wigginton, *Environ. Sci. Technol.*, 2010, **44**, 3656-3669.

14. J. P. Diao, L. Young, S. Kim, E. A. Fogarty, S. M. Heilman, P. Zhou, M. L. Shuler, M. M. Wu and M. P. DeLisa, *Lab Chip*, 2006, **6**, 381-388.
15. J. S. Kim, G. P. Anderson, J. S. Erickson, J. P. Golden, M. Nasir and F. S. Ligler, *Analytical Chemistry*, 2009, **81**, 5426-5432.
16. P. N. Floriano, N. Christodoulides, D. Romanovicz, B. Bernard, G. W. Simmons, M. Cavell and J. T. McDevitt, *Biosens. Bioelectron.*, 2005, **20**, 2079-2088.
17. R. Lenigk, R. H. Liu, M. Athavale, Z. J. Chen, D. Ganser, J. N. Yang, C. Rauch, Y. J. Liu, B. Chan, H. N. Yu, M. Ray, R. Marrero and P. Grodzinski, *Anal. Biochem.*, 2002, **311**, 40-49.
18. I. F. Cheng, H. C. Chang, D. Hou and H. C. Chang, *Biomicrofluidics*, 2007, **1**, 21503.
19. M. Varshney, Y. B. Li, B. Srinivasan and S. Tung, *Sens. Actuator B-Chem.*, 2007, **128**, 99-107.
20. L. Yang and R. Bashir, *Biotechnology Advances*, 2008, **26**, 135-150.
21. D. A. Boehm, P. A. Gottlieb and S. Z. Hua, *Sens. Actuator B-Chem.*, 2007, **126**, 508-514.
22. B. Xia, S. Upadhyayula, V. Nuñez, P. Landsman, S. Lam, H. Malik, S. Gupta, M. Sarshar, J. Hu, B. Anvari, G. Jones and V. I. Vullev, *Journal of Clinical Microbiology*, 2011, **49**, 2966-2975.
23. S. Efrima and L. Zeiri, *J. Raman Spectrosc.*, 2009, **40**, 277-288.
24. K. Kneipp, Y. Wang, H. Kneipp, L. T. Perelman, I. Itzkan, R. R. Dasari and M. S. Feld, *Physical Review Letters*, 1997, **78**, 1667-1670.
25. S. M. Nie and S. R. Emery, *Science*, 1997, **275**, 1102-1106.
26. S. Efrima and B. V. Bronk, *The Journal of Physical Chemistry B*, 1998, **102**, 5947-5950.

27. R. Jarvis, S. Clarke and R. Goodacre, in *Surface-Enhanced Raman Scattering*, eds. K. Kneipp, M. Moskovits and H. Kneipp, Springer Berlin Heidelberg, 2006, vol. 103, pp. 397-408.
28. A. Sengupta, M. Mujacic and E. J. Davis, *Anal. Bioanal. Chem.*, 2006, **386**, 1379-1386.
29. W. R. Premasiri, D. T. Moir, M. S. Klempner, N. Krieger, G. Jones and L. D. Ziegler, *The Journal of Physical Chemistry B*, 2004, **109**, 312-320.
30. A. A. Guzelian, J. M. Sylvia, J. A. Janni, S. L. Clauson and K. M. Spencer, *Proc. SPIE 4577, Vibrational Spectroscopy-based Sensor Systems*, 2002, 182-192.
31. L. Zhang, J. Xu, L. Mi, H. Gong, S. Jiang and Q. Yu, *Biosens Bioelectron*, 2012, **31**, 130-136.
32. Y. Wang, S. Ravindranath and J. Irudayaraj, *Anal Bioanal Chem*, 2011, **399**, 1271-1278.
33. Y. Wang, K. Lee and J. Irudayaraj, *The Journal of Physical Chemistry C*, 2010, **114**, 16122-16128.
34. X. Zhang, M. A. Young, O. Lyandres and R. P. Van Duyne, *J. Am. Chem. Soc.*, 2005, **127**, 4484-4489.
35. T.-T. Liu, Y.-H. Lin, C.-S. Hung, T.-J. Liu, Y. Chen, Y.-C. Huang, T.-H. Tsai, H.-H. Wang, D.-W. Wang, J.-K. Wang, Y.-L. Wang and C.-H. Lin, *PLoS ONE*, 2009, **4**, e5470.
36. S. B. Chaney, S. Shanmukh, R. A. Dluhy and Y. P. Zhao, *Appl. Phys. Lett.*, 2005, **87**, 031908.
37. J. D. Driskell, S. Shanmukh, Y. Liu, S. B. Chaney, X. J. Tang, Y. P. Zhao and R. A. Dluhy, *J. Phys. Chem. C*, 2008, **112**, 895-901.
38. X. Wu, S. Gao, J.-S. Wang, H. Wang, Y.-W. Huang and Y. Zhao, *Analyst*, 2012, **137**, 4226-4234.

39. O. Neyrolles, S. L. Hennigan, J. D. Driskell, R. A. Dluhy, Y. Zhao, R. A. Tripp, K. B. Waites and D. C. Krause, *PLoS ONE*, 2010, **5**, e13633.
40. S. Shanmukh, L. Jones, Y. P. Zhao, J. Driskell, R. Tripp and R. Dluhy, *Anal. Bioanal. Chem.*, 2008, **390**, 1551-1555.
41. J. D. Driskell, A. G. Seto, L. P. Jones, S. Jokela, R. A. Dluhy, Y. P. Zhao and R. A. Tripp, *Biosensors and Bioelectronics*, 2008, **24**, 917-922.
42. H. Chu, Y. Huang and Y. Zhao, *Appl. Spectrosc.*, 2008, **62**, 922-931.
43. J. L. Abell, J. D. Driskell, R. A. Dluhy, R. A. Tripp and Y. P. Zhao, *Biosensors and Bioelectronics*, 2009, **24**, 3663-3670.
44. T. Y. Liu, K. T. Tsai, H. H. Wang, Y. Chen, Y. H. Chen, Y. C. Chao, H. H. Chang, C. H. Lin, J. K. Wang and Y. L. Wang, *Nature communications*, 2011, **2**, 538.
45. K. A. Stevens and L.-A. Jaykus, *Critical Reviews In Microbiology*, 2004, **30**, 7-24.
46. P. F. G. Wolffs, K. Glencross, R. Thibaudeau and M. W. Griffiths, *Applied and Environmental Microbiology*, 2006, **72**, 3896-3900.
47. Y. J. Liu, H. Y. Chu and Y. P. Zhao, *The Journal of Physical Chemistry C*, 2010, **114**, 8176-8183.
48. C. Fan, Z. Hu, A. Mustapha and M. Lin, *Appl Microbiol Biotechnol*, 2011, **92**, 1053-1061.
49. M. L. Bari, K. Enomoto, D. Nei and S. Kawamoto, *Japan Agricultural Research Quarterly: JARQ*, 2011, **45**, 153-161.

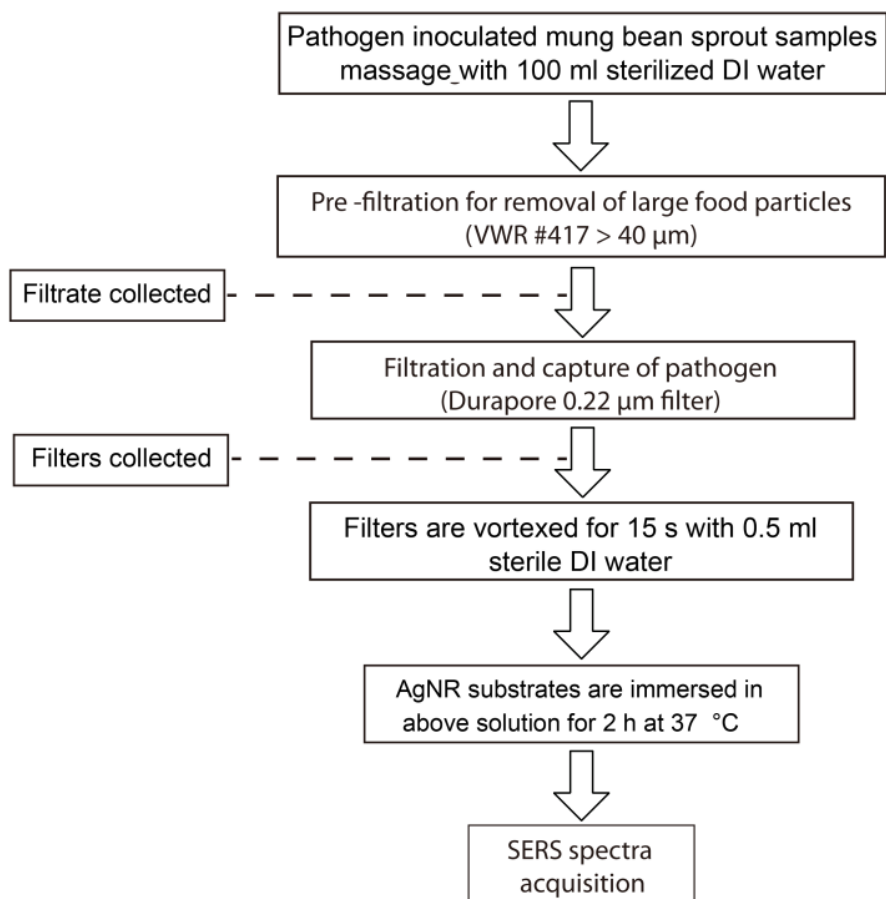


Figure 5.1 Flow chart of the two-step filtration procedure.

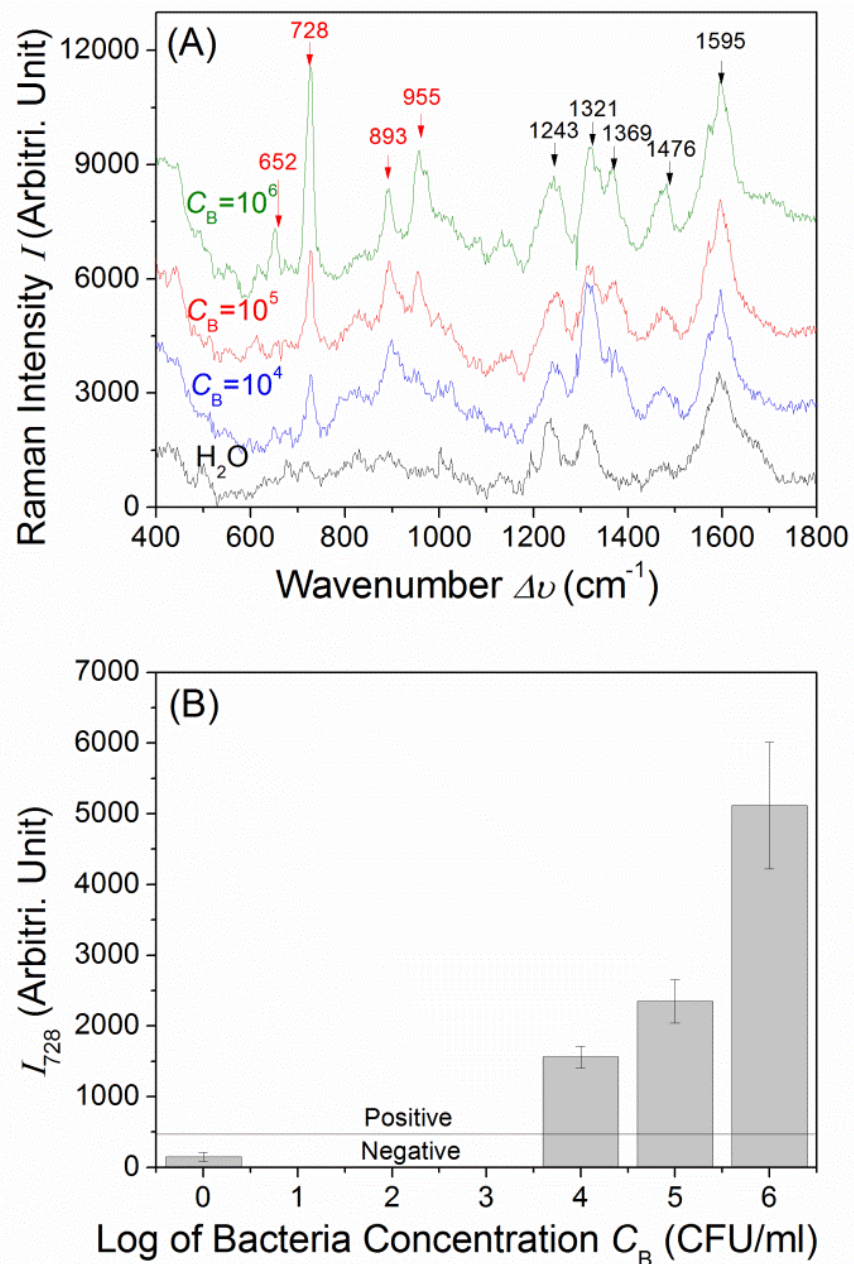


Figure 5.2 (A) The SERS spectra and (B) the mean and standard deviation of the SERS peak intensity  $I_{728}$  of *E. Coli* O157:H7 at different concentrations ( $C_B = 10^4, 10^5, 10^6$  CFU/ml) and sterile DI water. Significant peaks from the *E. Coli* O157:H7 sample are indicated in red and the significant peaks from the vancomycin coating layer are indicated in black. Spectra were measured by the Enwave Raman system.

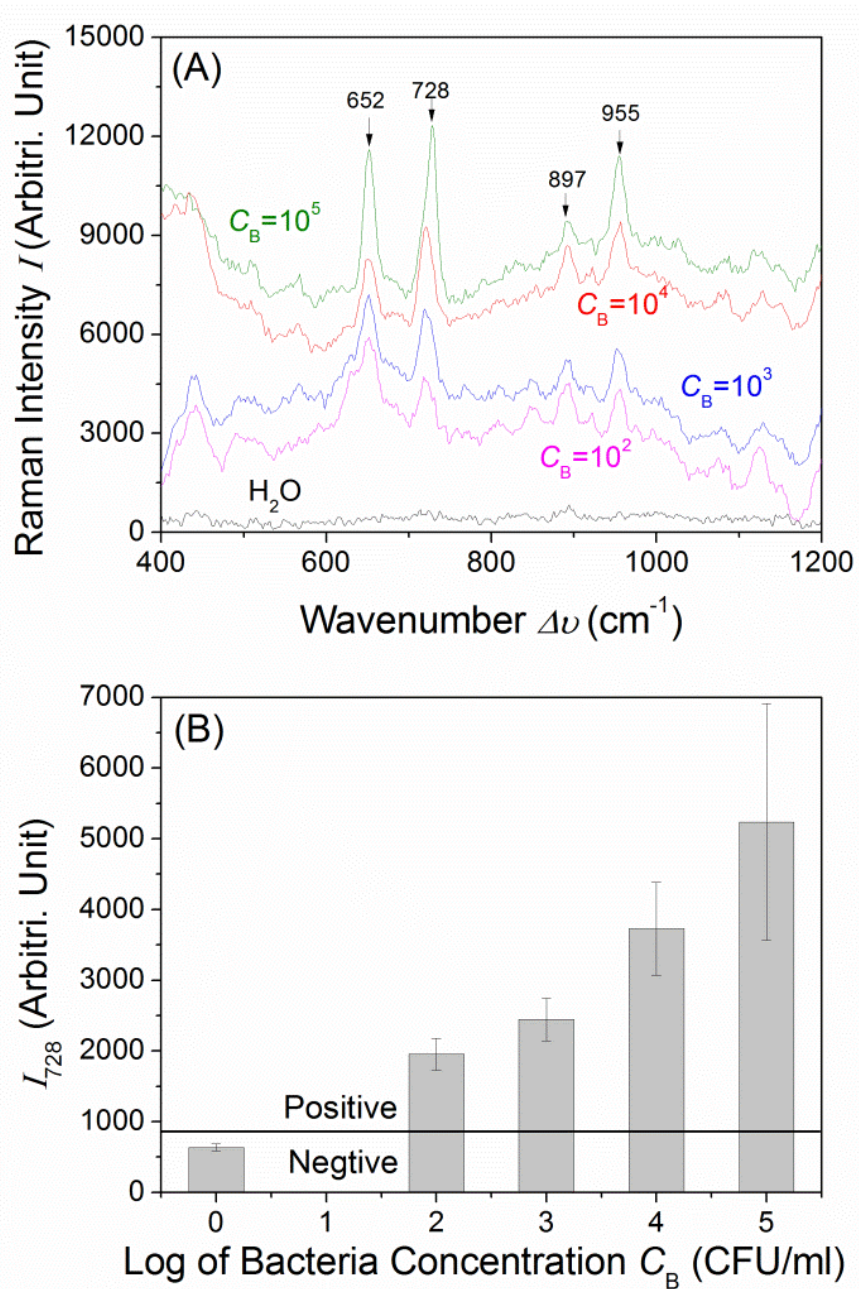


Figure 5.3 (A) The SERS spectra, and (B) the mean and standard deviation of the SERS peak intensity  $I_{728}$  of *E. Coli* O157:H7 recovered from mung bean sprouts samples inoculated at different rates and sterile DI water inoculated in mung bean sprouts samples (control) followed by a two-step filtration. Spectra were measured by the Enwave Raman system.

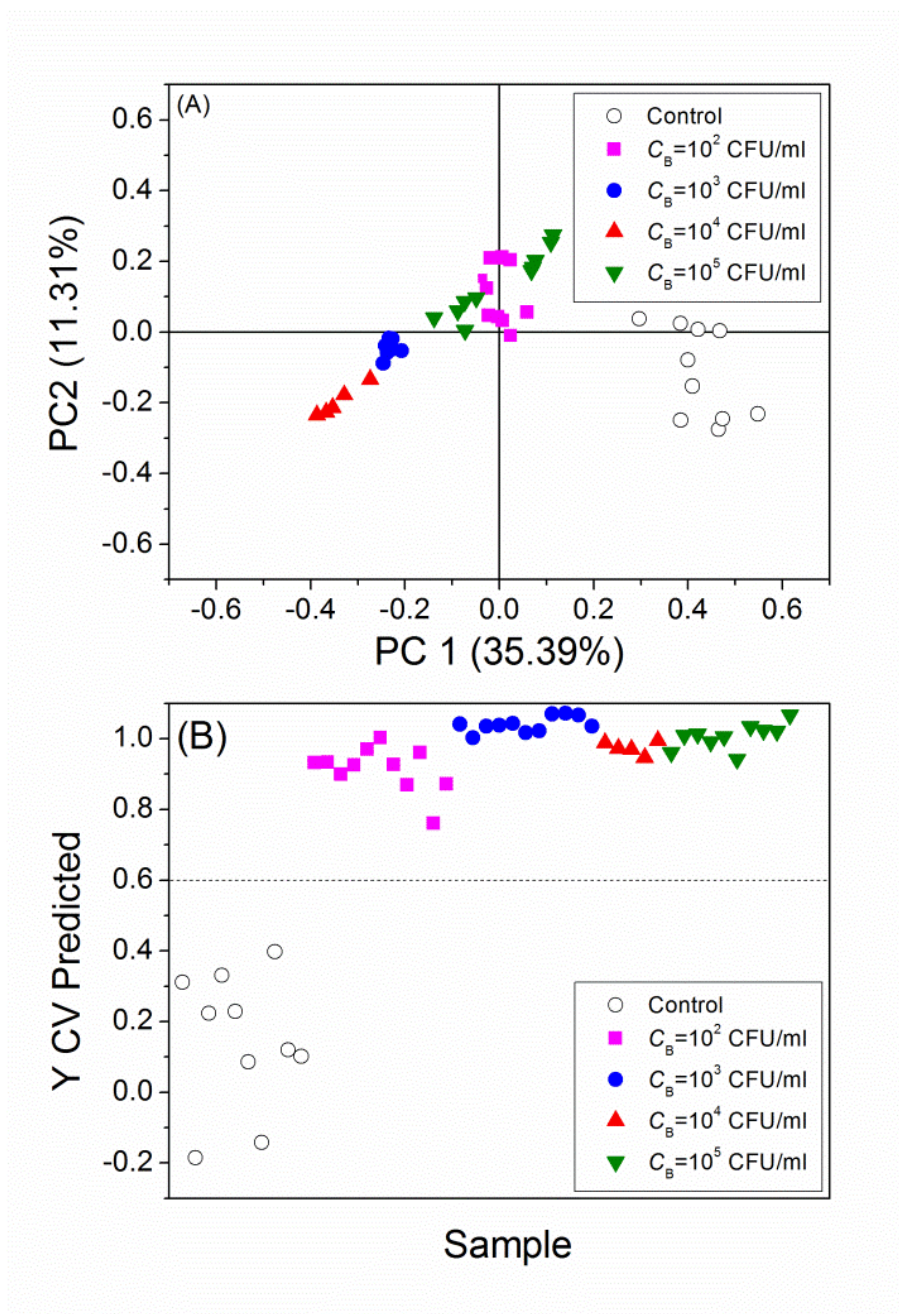


Figure 5.4 (A) PCA and (B) PLS-DA plot of SERS spectra of *E. coli* O157:H7 recovered from mung bean sprouts samples inoculated at different rates ( $C_B = 10^2, 10^3, 10^4, 10^5$  CFU/ml) and sterile DI water inoculated in mung bean sprouts samples (control) followed by a two-step filtration. Spectra were collected using the Enwave Raman spectrometer.

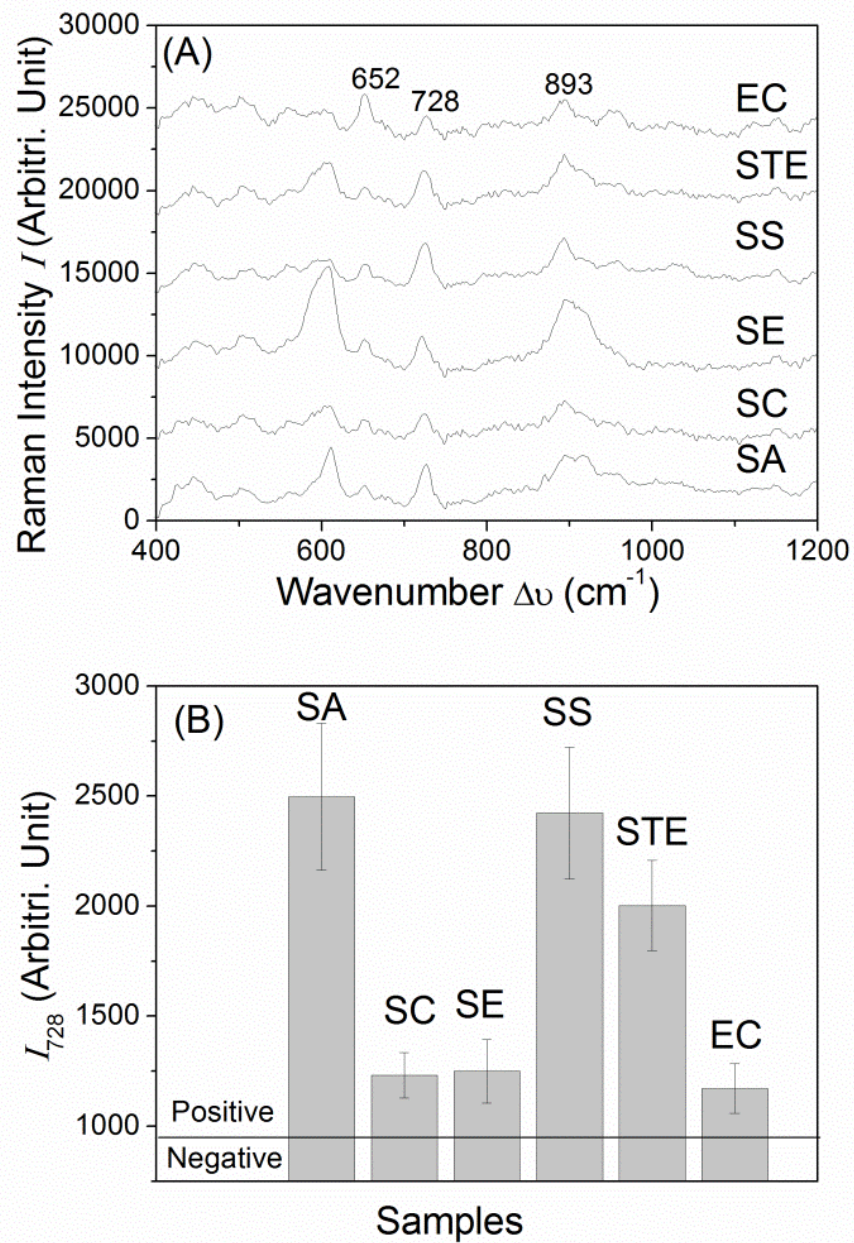


Figure 5.5 (A) SERS spectra, and (B) the mean and standard deviation of the peak intensities  $I_{728}$  from the SERS spectra of six different pathogens inoculated at  $10^2$  CFU/ml on mung bean sprouts samples followed by a two-step filtration: *Salmonella enterica* serotype Anatum (SA), *Salmonella enterica* serotype Cubana (SC), *Salmonella enterica* serotype Stanley (SS), *Salmonella Enteritidis* (SE), *E. coli* O157:H7 (EC), and *Staphylococcus epidermidis* (STE). Spectra were measured by the Enwave Raman system.

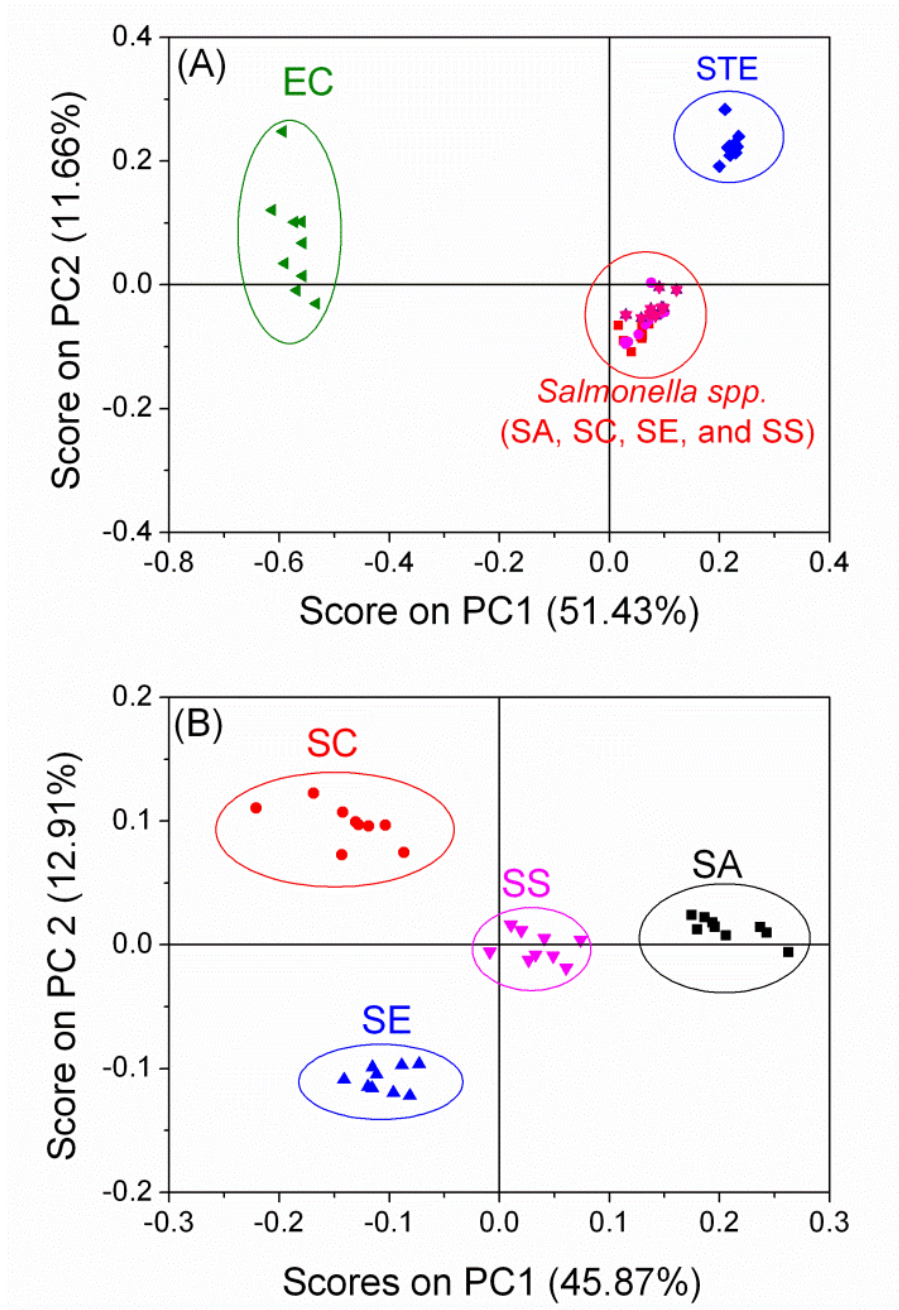


Figure 5.6 PCA plot of (A) six different pathogens, *Salmonella enterica* serotype Anatum (SA), *Salmonella enterica* serotype Cubana (SC), *Salmonella enterica* serotype Stanley (SS), *Salmonella* Enteritidis (SE), *E. coli* O157:H7 (EC), and *Staphylococcus epidermidis* (STE), and (B) four different *Salmonella* species, SA, SC, SE, and SS inoculated at  $10^2$  CFU/ml on mung bean sprouts samples followed by a two-step filtration.

CHAPTER 6  
DIFFERENTIATION AND CLASSIFICATION OF BACTERIA USING SERS SPECTRA  
AND CHEMOMETRIC ANALYSIS <sup>1</sup>

---

<sup>1</sup>Xiaomeng Wu, Yao-Wen Huang, Bosoon Park, Ralph A. Tripp, Rene Alvarez, Alexander J. Burdette, and Yiping Zhao. To be submitted to *Applied and Environmental Microbiology*.

## **Abstract**

In the past decade, the intrinsic surface-enhanced Raman scattering (SERS) spectra has been used for the differentiation and classification of bacterial species using chemometric analysis. Such differentiation has often been conducted with an insufficient sample population and strong interference from the sample matrix. To address these problems, 27 different bacteria isolates from 12 species were analyzed using SERS with recently developed vancomycin coated silver nanorod (VAN AgNR) substrates. The VAN AgNR substrates could generate reproducible SERS spectra of the bacteria with little to no interference from the environment or bacterial by-products as compared to the pristine substrates. By taking advantage of the structural composition of the cellular wall which varies from species to species, the differentiation of bacterial species is demonstrated by using chemometric analyses on those spectra. A second chemometric analysis step within the species cluster is able to differentiate serotypes and strains. The spectral features used for serotype differentiation arises from the surface proteins, while Raman peaks from genetic materials dominate the differentiation of strains. In addition, due to the intrinsic structural differences in the cell walls, the SERS spectra can distinguish Gram-positive from Gram-negative bacteria with high sensitivity and specificity. Our results provide important insights for using SERS as a bacterial diagnostic tool and further guide the design of a SERS-based detection platform.

## **Introduction**

Over the past decade, surface-enhanced Raman scattering (SERS) has been considered a powerful platform for the rapid and sensitive detection of bacteria (1-14). SERS brings the analyte molecules into close proximity with the appropriate metallic nanostructures, thus significantly increasing the Raman vibrational signals of the analyte. These molecular vibrational modes represent a unique “fingerprint” spectrum consisting of Raman peaks that can be used to identify the particular molecule(s) being probed (15). This method of enhancement is often employed to facilitate sensitivity so as to allow for the trace detection of molecules, even with single molecular sensitivity (16-20).

For SERS based bacterial detection, two of the most important tasks are (1) to detect bacteria with high sensitivity from complex media such as food matrices or clinical samples, and (2) to distinguish between bacterial species using their intrinsic SERS spectra. In fact, researchers have put forth great effort to answer two critical questions which include whether or not the intrinsic SERS spectra arising from the bacteria whole cell can be used for differentiation and classification of bacteria, and what would be the most effective strategy to utilize chemometric analysis to achieve such a differentiation. Although the origin of the SERS signal which arises from the bacteria is still not clearly understood, the majority of researchers agree that it primarily originates from the external structure of the bacterial cell, i.e. cell wall and proteins (12). Hence, it is hypothesized that the spectral differences in SERS that occurs between bacterial isolates reflect these external structural differences between bacteria. However, the chemical makeup of the bacterial cell wall is very similar between species, so it is difficult to differentiate between bacterial species through visual inspection of the SERS spectra alone. Since the SERS spectra can be viewed as multi-variant data, chemometric analysis is often used

to differentiate bacteria by reducing the dimensionality of the data set and maximizing the variance among spectral fingerprints.

Various chemometric methods have been adapted to analyze the bacterial SERS spectra, including principle component analysis (PCA), hierarchical cluster analysis (HCA), partial least square discriminant analysis (PLS-DA), partial least square regression (PLS), discriminant function analysis (DFA), linear discriminant analysis (LDA), and support vector machine (SVM). PCA is a primary mathematical method that reduces the data dimensions by identifying correlations amongst a set of variables and then projects the original set of variables into a new set of uncorrelated variables called principal components (PCs). PCA is an unsupervised chemometric method often used for the purpose of pattern recognition (1-10). To further improve the grouping of the SERS spectra from different bacteria, HCA is often employed. HCA assigns samples to the individual cluster according to the similarity between them, based either on PCA or Mahalanobis distance, and generates a dendrogram (2-4, 7, 9). If the classes of which the bacterial species being analyzed are already known, supervised methods such as PLS-DA can be used in order to yield more robust discrimination (3, 11). PLS-DA uses a linear combination of the predictor variables to project the original data into a new set of coordinates to generate a positive/negative prediction. It is often used to classify bacteria based on known characteristics, such as Gram stain results, i.e. Gram positive (G+) versus Gram negative (G-). Choosing the appropriate chemometric method is based on the nature of the data and the objectives of the research.

The literature on the differentiation of bacteria based on their intrinsic SERS spectra is summarized in Table B.1 in Appendix B. The discrimination between bacterial species has been achieved by several authors using PCA, HCA, LDA, etc., with sample sizes of up to eight

individual bacterial species. Such differentiation is easy to achieve since the structural differences between species is significant (1, 2, 4, 5, 9, 10, 21). Researchers have also explored the ability to discriminate between bacteria at the sub-species level using up to four individual serotypes of *Salmonella* (11) or 14 individual strains of *Arthrobacter* (7). Unfortunately, all those results were analyzed by chemometric methods on the individually measured spectra of bacterial isolates, and the bacterial mixtures were not yet well studied. We still lack a comprehensive understanding on what molecular structures or components contribute to the differences observed between bacterial spectra. In addition, the reproducibility of the spectra obtained has not been able to support any specific claims, and the molecular principle behind such differentiation was not well comprehended.

In order to reliably combine chemometrics with SERS as a bacterial detection platform, the SERS spectra generated needs to be reproducible and reliable. Thus, three important factors should be carefully considered: (1) reproducibility of the SERS-active nanostructures, (2) contamination from the environment, and (3) interference from the bacterial metabolic by-products. SERS-active nanostructures with high reproducibility can generate spectra with less variance from experiment to experiment, and from sample to sample. Researchers have used different types of nanostructures to study the SERS of bacteria such as silver metal deposits (22, 23), silver colloid solutions (2, 24, 25), gold colloid solutions (26, 27), electrochemically roughened metal surfaces (28), Ag nanocrystal assembled Ag nanospheres (AgNSs) (29, 30), silver film over nanospheres (AgFON) (31), and silver nanorod array substrates (11, 13, 32). Gold or silver colloids are the most widely used SERS active substrates due to the easy manufacturing process and low cost. However, they often lack reproducibility due to large variations in cluster size and shape. The nanostructure involved in the other “substrate” types

tends to have more reproducibility due to their highly uniform structures. Among them, silver nanorod (AgNR) array substrates fabricated by the oblique angle deposition (OAD) method have been shown to have a SERS enhancement factor  $> 10^8$  and a batch-to-batch variability  $< 15\%$  (33, 34). The detection of bacteria using AgNR substrates has been demonstrated with high sensitivity and specificity (11). However, the use of silver nanostructures, such as AgNR, AgNSs, or AgFON for bacterial SERS detection poses some disadvantages, including cytotoxicity, so the binding between silver and bacteria is not favoured. In addition, silver is relatively chemically active, so it can react with the sulphur that is present in the environment. The reaction with sulphur will interfere with the SERS signal, thus preventing one from obtaining clear and reproducible SERS spectra.

Finally, it is possible that the by-products synthesized by the bacteria may be detected by the highly sensitive SERS substrates thus interfering with the bacterial SERS spectra. To overcome these disadvantages, the surface of AgNR substrates can be modified by a coating that can actively capture the bacteria, yet protect the surface from reacting with unwanted substances. The use of a vancomycin (VAN) coating on the silver nanostructure has been explored by different research groups to illustrate its ability to capture bacteria and subsequently improve sensitivity (11, 35). However, the ability of VAN coated substrates to protect the silver nanostructure surface and improve the reproducibility of the spectra has not yet been explored. A VAN coating on the AgNR substrate may protect the silver surface from reacting with environmental contaminants, thus resulting in a low to completely absent background signal. Furthermore, because VAN selectively binds to the bacterial cell wall, other biomolecules such as bacterial by-products will have a lower chance of binding to the SERS substrate surface (36). Thus, the vancomycin coated silver nanorod (VAN AgNR) substrates will ensure that the SERS

signal obtained are from the outer structures of the bacteria, thus providing insight into the molecular principles involved in differentiating between bacteria using SERS. Overall, the high reproducibility and sensitivity of the AgNR substrates in combination with the protection and selectivity given by the VAN coating will generate reliable SERS measurements when analyzing bacterial cells.

In order to design a better differentiation strategy and validate the ability of chemometric methods to differentiate between bacteria in a large bacterial sample, this study used three conventional multivariate analysis methods, PCA, HCA, and PLS-DA, to differentiate and classify the SERS spectra of 27 bacterial isolates from 12 species with various strains and serotypes. The results reveal the advantages of using the VAN AgNR SERS substrates to (1) protect the substrate's surface from environmental contamination and bacterial metabolic products, (2) generate reproducible SERS spectra of bacteria, and (3) to consequently improve the differentiation of bacteria. PCA and HCA methods are employed to illustrate the feasibility of using simple multivariate analysis methods to differentiate bacteria between species, serotypes, and strains. The discrimination between G<sup>+</sup> and G<sup>-</sup> bacteria are tested by PLS-DA methods. These results provide insights for the future application of SERS as a bacterial diagnostic platform.

## **Materials and methods**

### **AgNR SERS substrate fabrication**

The bacterial SERS spectra were acquired using AgNR array substrates fabricated by the oblique angle deposition (OAD) technique in a custom-designed electron beam evaporation (e-beam) system (33, 34, 37). Briefly, glass microscopic slides (Gold Seal® Catalog No.3010,

Becton, Dickinson and Company, Portsmouth, NH) were cleaned with piranha solution (80% sulfuric acid, 20% hydrogen peroxide in volume) and rinsed with deionized (DI) water. The substrates were then dried with a stream of nitrogen gas before being loaded into the deposition system. In the deposition system, the substrate surface was held perpendicular to the incident vapor direction while a 20-nm titanium film and then a 200-nm silver film were evaporated onto the glass slides at a rate of  $\sim 0.2$  nm/s and 0.3 nm/s, respectively. Monitoring of this process was performed *in situ* by a quartz crystal microbalance (QCM). The substrates were then rotated to an angle of  $86^\circ$  with respect to the incident vapor and AgNRs were grown with a deposition rate of  $\sim 0.3$  nm/s until the thickness reading of QCM reached 2000 nm for pristine AgNR substrates and 800 nm for VAN AgNR substrates.

### **AgNR functionalization**

Vancomycin was purchased from Sigma Aldrich Ltd. (St. Louis, MO), and was diluted by ultra-pure water ( $18\text{M}\Omega$ ) to a concentration of 1 mM. The VAN AgNR substrates were produced by immersing AgNR array substrates into the VAN solutions overnight ( $> 12$  hours), rinsing three times with DI water, and then dried with nitrogen as previously reported (11).

### **Bacteria strains and growth**

The details of the bacteria used in this study and their respective codes are summarized in Table 6.1. The bacterial isolates with the strain code labeled as USDACR were isolated from chicken carcass rinses obtained from the Poultry Microbiological Safety and Processing Research Unit of the USDA, Agricultural Research Service, Athens, GA. The rest of the bacteria were a kind gift from Dr. Abercrombie at Brooke Army Medical Center. Strain WRAMC #13 is a primary isolate obtained from patients at Walter Reed Medical Center. Strain BAMC 07-18 is a primary isolate obtained from patients at Brooke Army Medical Center. Bacterial isolates were

stored at  $-80^{\circ}\text{C}$  in 15-20 % glycerol for long-term storage. For short-term storage, bacterial isolates were stored in trypticase soy agar (TSA) slants at  $4^{\circ}\text{C}$ . Bacterial cultures were prepared by inoculating pure isolates from agar slants into trypticase soy broth (TSB) tubes and incubated at  $35 \pm 2^{\circ}\text{C}$  for 18 - 24 hours. The overnight cultures of all isolates were centrifuged at 5000 rpm for 10 minutes and washed three times with sterilized DI water before being resuspended in DI water.

### **SERS Measurements and Data Analysis**

To prepare the bacteria coated SERS substrates, a 2  $\mu\text{l}$  droplet of a single species bacterial sample was applied to the pristine AgNR substrate and allowed to dry. The VAN coated substrates were immersed in 2 ml of a single species bacterial culture for two hours at  $37^{\circ}\text{C}$  with 250 rpm of shaking then rinsed with DI water and dried. The SERS spectra were acquired using a portable Enwave Raman system (Model ProRaman-L 785A2, Enwave Optronics Inc., Irvine, CA), with a 785 nm near-IR diode laser as the excitation source. The power of the laser at the sample was set to be  $\sim 30$  mW. SERS spectra over a range of  $\sim 400 - 1800$   $\text{cm}^{-1}$  were collected from nine to ten spots across the VAN substrate surface over a five second exposure time. All data analysis was performed using Origin software 8.5 version (OriginLab Corporation, Northampton, MA). Statistical data analysis was conducted with Matlab 2010b (The MathWorks, Inc., Natick, MA) using the PLS toolbox (Eigenvector Research, Inc., Wenatchee, WA).

## Results and Discussions

### Reproducible VAN substrates facilitate better bacterial differentiation

To illustrate the effect of the substrate surface on spectral reproducibility and differentiation, the SERS spectra of the bacteria listed in Table 6.1 was generated on both pristine and VAN AgNR substrates. Representative spectra of the bacteria generated on pristine AgNR SERS substrates are shown in Figure 6.1A. The spectra share some common significant peaks at  $\Delta\nu = 550, 730, 795, 1030,$  and  $1330 \text{ cm}^{-1}$ , indicated in red in Figure 6.1A, which are well documented bacterial peaks (9, 11, 12). However, the spectrum of water from the AgNR substrate exhibits strong interference from environmental contamination and bacterial metabolic products. For example, the peaks at  $\Delta\nu = 930, 1000,$  and  $1140 \text{ cm}^{-1}$ , indicated in black in Figure 6.1A, were found in the water control spectra which, as stated above, is due to the contaminating sulfur that is in the air. These contaminants are competing with the bacteria for the SERS “hot spots” on the substrate surface. The resulting contamination peaks may not significantly affect discrimination analysis when the signal from the bacteria is strong enough to mask them, however, when the bacteria concentration is low or the SERS signal from the bacteria is weak, the contamination peaks can dominate and affect the interpretation of the results.

For example, as shown in Figure 6.1A, the peak at  $\Delta\nu = 1000 \text{ cm}^{-1}$  is not present in the spectra of *Citrobacter koseri* (CK), but is in the spectra of *Klebsiella pneumoniae* BAMC 07-18 (KP2), since KP2 generates an overall lower SERS signal as compared to CK. The peak at  $\Delta\nu = 1352 \text{ cm}^{-1}$  is a significant peak only found in the *Pseudomonas aeruginosa* (PA) spectrum. This peak originates not from the bacterial cell, but from pyocyanin, a pigment that the bacteria produces during its growth, which acts as a quorum sensing molecule as recently reported (38). Unfortunately, pyocyanin is not eliminated by the washing steps, thus, it introduces interference

into the bacterial spectra. The strong SERS signal from pyocyanin distinguishes the PA spectra from the rest of the bacteria although the pyocyanin peaks are not intrinsic SERS spectra which arise from the bacterial whole cell.

Such an inconsistency in the spectral measurements is also reflected when PCA is performed, as shown in Figure 6.1B. The PC score plot of the SERS spectra on pristine substrates showed little discrimination between different types of bacteria. This could be due to environmental contaminants and/or the secreted bacterial by-products interfering with the SERS signal. As the intensities of the interference peaks are not consistent from sample to sample, the PCA results mainly reflect those non-bacterial whole cell related changes. For example, the PP cluster in Figure 6.1B separates away from the other bacterial clusters and becomes an outlier due to the strong contamination peaks present in their spectra. Additionally, different serotypes of the *Salmonella* species are clustered together with CK and *E. coli* (EC). Finally, the effect of the bacterial by-products is demonstrated in Figure 6.1A, as shown by the substantial peak at  $\Delta\nu = 1352 \text{ cm}^{-1}$ , which represents the metabolic by-product, pyocyanin. This peak is absent for every other bacteria. The result is that the two strains of PA, PA1 and PA2, have very different spectral features. This causes these strains to separate far from each other as shown in Figure 6.1B. The interference from the environmental contamination and bacterial by-products are also revealed by the loadings of the PCA, as shown in Figure B.1 in Appendix B, where the contamination peak at  $\Delta\nu = 1000 \text{ cm}^{-1}$  weighs heavily in both PC1 and PC2, and the pyocyanin peak at  $\Delta\nu = 1352 \text{ cm}^{-1}$  weighs heavily in PC3. The inconsistencies in spectra caused by the environmental contamination and bacterial by-products on the pristine AgNR SERS substrates reduces the reproducibility of the SERS spectra and lessens its ability to discriminate between bacteria using chemometric analysis.

Both issues of environmental contamination and bacterial by-products for SERS spectral measurements can be resolved by coating VAN on the AgNR substrates. In Figure 6.2A, the representative SERS spectra of some bacteria generated on VAN AgNR substrates is shown, along with the spectrum of a water control VAN AgNR substrate. When the AgNR substrate is coated by vancomycin, it not only works as a capture agent for the bacteria which increases the SERS signal, but also serves as a protective layer which keeps off environmental contaminants (11, 35). The control (water) sample in Figure 6.2A shows the peaks which originate from the vancomycin layer (peaks in black boxes). The contamination peaks which were found on the pristine substrates such as  $\Delta\nu = 1000 \text{ cm}^{-1}$ , are absent in all the spectra when using VAN AgNR substrates. Importantly, the common bacterial SERS peaks on VAN AgNR substrates which occur at  $\Delta\nu = 650, 730, 795, 900, \text{ and } 960 \text{ cm}^{-1}$  are retained (11). The PA2 spectra in Figure 6.2A showed no peak at  $\Delta\nu = 1352 \text{ cm}^{-1}$ , which suggests little to no interference from pyocyanin. This is expected as pyocyanin should not bind vancomycin. Hence, the use of the VAN AgNR substrates increases the reproducibility of the SERS spectra from sample to sample, and prevents interference from environmental contamination and bacterial by-products.

When PCA was performed on the SERS spectra from VAN AgNR substrates, as shown in Figure 6.2B, the discrimination between different types of bacteria is more obvious. First of all, the top three PCs combined represents 81.4% of the total variance, which is greater than those in Figure 6.1B (62.14%). This suggests that when using VAN AgNR substrates, more variance and bacterial information is represented in the 3D PCA plot. In Figure 6.2B, the different serotypes of *Salmonella* species are clustered closely together, but this cluster is indistinguishable from the *Enterobacter cloacae* (ENC) group due to the similarity between these two types of bacteria. The different strains of KP also form a cluster. Similar clustering is

also found in the samples of *Staphylococcus aureus* (SA) and PA, where samples of different strains of the same species are clustered together. Hence, if we considered the bacteria from the same species, regardless of the strains and serotypes, they all form individual clusters according to their species in Figure 6.2B, except for the PP and the KP groups which are hard to visualize in the 3D plot. The loadings of the PCA plot is shown in Figure B.2 in Appendix B, and in all three PCs we considered, the discrimination weighs heavily at  $\Delta\nu = 650, 730, 795, 900,$  and  $960 \text{ cm}^{-1}$ , which all are the intrinsic bacterial Raman peaks. Comparing Figure 6.1B with Figure 6.2B, it is clear that the SERS spectra generated on VAN AgNR substrates can easily cluster different types of bacteria using PCA. Thus, VAN AgNR substrates not only capture the bacteria specifically, but also eliminate the interference that occurs from both environmental contamination and bacterial by-products, as well as facilitate a better discrimination between the different bacteria.

### **Bacterial species differentiation using a combined PCA and HCA analysis approach on VAN AgNR substrates**

As shown in Figure 6.2B, the differentiation between bacterial species can be achieved by simply performing PCA on the SERS spectra obtained from VAN AgNR substrates. However, such discrimination between bacteria based on the visual inspection of the PCA score plot is ambiguous and lacks quantitative measurement. Hence, HCA is performed on the same spectra from Figure 6.2B to better identify bacterial clustering. The specific HCA method used here is the k-means method which starts by dividing the sample points (the spectra) into k clusters, and then each individual point (a single spectrum) is assigned to the cluster whose centroid is nearest. The centroid is recalculated when a cluster loses or gains a data point, and the

process is continued until each point is in the cluster whose centroid is nearest. The dendrogram generated by the k-means method is shown in Figure 6.3 with each color representing an individual isolate of bacteria. Similar to PCA analysis, different serotypes of *Salmonella* are hard to distinguish from each other when other species are present suggesting that the spectral differences within the species are much smaller than those between species. In addition, as demonstrated by the PA, SA, and KP clusters, the different strains of the same species are also impossible to distinguish. Thus, when combining SERS and a single step chemometric analysis, one can only differentiate bacteria from species to species, rather than strain to strain or serotype to serotype.

### **Differentiating bacteria between serotypes and strains of the same species**

From a microbiology point of view, the cell structural differences between species are more obvious than those that occur between strains or serotypes. Thus, the structural differences between species will dominate the classification when different species are present, making the discrimination of different serotypes and strains for a particular species not feasible. Therefore, in order to classify strains or serotypes, one may need to confine the chemometric analysis only to those strains and serotypes within the same species, i.e. a second chemometric analysis may be needed to differentiate strains or serotypes.

To validate such a strategy, the spectra from *Salmonella* species obtained on VAN AgNR substrates, namely SalE, SalH, SalI, SalK, SalT, were analyzed. In Figure 6.4, the 3D PCA plot and the HCA plot of the *Salmonella* species is shown. In Figure 6.4A, each serotype of the *Salmonella* species forms a close cluster, and each cluster can be visually distinguished. The loadings of the PCA are shown in Figure B.3 in Appendix B. The peaks used to discriminate

between *Salmonella* serotypes are at  $\Delta\nu = 650$  and  $730\text{ cm}^{-1}$  in all three PCs, which originate from guanine and adenine, as reported previously (39). Unlike the loadings for species discrimination, the bacteria peaks between  $\Delta\nu = 1330$  and  $1380\text{ cm}^{-1}$  were given more weight in PC2, which is assigned to tryptophan, an essential amino acid in bacterial proteins (9). This suggests that the spectral differences between the serotypes come mainly from the different bacterial surface proteins. The bacteria peak at  $\Delta\nu = 950\text{ cm}^{-1}$  weighs less in all three PCs, which is assigned to the deformation of C=C bond, and it most likely comes from the carbohydrates of the bacterial cell wall. These results suggest that when differentiating *Salmonella* serotypes, the protein differences that occur between serotypes contributes more to the variation in the SERS spectra than the cell wall structural differences. The HCA dendrogram in Figure 6.4B further demonstrates the discrimination between each serotype. The samples from the same serotypes, indicated by the same color, are clustered closer than those from other serotypes.

Similar results are also observed for different strains. Figure 6.5 shows the analysis of five strains of SA on VAN AgNR substrates using PCA and HCA. In Figure 6.5A, each strain of SA forms a close cluster, and each cluster is visually distinguished. This result is confirmed by an HCA plot shown in Figure 6.5B. The loadings of the PCA plot, as shown in Figure B.4 in Appendix B, suggests that besides the peaks at  $\Delta\nu = 650$  and  $730\text{ cm}^{-1}$ , the peak at  $\Delta\nu = 900\text{ cm}^{-1}$  also weighs heavily when discriminating between different strains of SA. As stated above, peaks at  $\Delta\nu = 650$  and  $730\text{ cm}^{-1}$  are assigned to guanine and adenine respectively, and the peak at  $\Delta\nu = 900\text{ cm}^{-1}$  is assigned the stretching mode of the C-N bond and C-O-N bond. The peaks from proteins, such as the peaks at  $\Delta\nu = 1330$  and  $1380\text{ cm}^{-1}$ , weigh lightly in the loading, which suggests that surface proteins do not play an important role in strain discrimination. Different strains may differ slightly from one another in many ways, such as different sequences in

sections of their genome, and the amount of materials they synthesize. From the PCA loadings of the SERS spectra, we cannot conclude exactly what components contribute most to the spectral differences observed between strains. They may come from adenine, which is present in molecules such as FAD and FADH, or the genetic material presented on the cell surface. Similarly, the discrimination between different strains of the AB (*Acinetobacter baumannii*) samples obtained on VAN AgNR substrates can also be achieved, as shown in the Figure B.5 in Appendix B.

Based on the above results, a “two-step” chemometric analysis is proposed to analyze the SERS spectra of bacteria when large amounts of bacteria are present. When the bacterial collection has sub-species level differences, either by serotype or strain, the PCA or HCA method will be performed on all the spectral data to first discriminate the bacteria based on their species. Then the spectra from each subset (cluster) with potential serotype or strain differences will be further analyzed by PCA or HCA.

### **Classification between G+ and G- bacteria**

As stated above, the majority of researchers agree that the SERS spectrum that is generated by bacteria originates from the external structure of the bacterial cell. The structure of the cell wall between G+ and G- bacteria is very different, so the SERS spectra of the G+ and G- bacteria could be significantly different. The discrimination between G+ and G- bacteria based on their SERS spectra has been reported by Pucek *et al.* (6) and Liu *et al.* (40). Pucek *et al.* was able to discriminate two G+ bacteria from two G- bacteria, while Liu *et al.* only used one G+ bacteria, one G- bacteria, and one *Mycobacterium* to demonstrate the ability of SERS to discriminate between G+ and G- bacteria. Since we have obtained reproducible SERS spectra

without the interference from environmental contamination and bacterial by-products, it is reasonable to believe that those spectra can be used to differentiate between bacterial Gram +/- types. In our collection, we have 19 G- and 8 G+ isolates as shown in Table 6.1.

In Figure 6.6A, the PC1 vs. PC3 scores of the bacterial SERS spectra, which was generated on VAN AgNR substrates, demonstrates the grouping of the G+ and G- bacteria. In general, G+ bacteria have PC1 scores from 0.2 to 0.5 and PC3 scores from -0.5 to 0.2, while G- bacteria have PC1 scores smaller than 0.4 and PC3 scores bigger than -0.2. To obtain a quantitative discrimination between those bacteria, PLS-DA was performed based on the same 27 sets of spectra. These isolates were assigned to their respective group based on their Gram stain properties, in which 19 are G- and 8 are G+. The PLS-DA model gives a Y CV predicted score by projecting the original variables of the SERS spectral data using the class information provided. The Y CV predicted scores of these 27 spectra generated with the PLS-DA model are shown in Figure 6.6, with the black horizontal line indicating the threshold for classification of G+ from G-. The bacteria from the G+ and G- groups are successfully separated and classified with 98.9% sensitivity and 100% specificity. Only one sample of *Salmonella* Infantis (SalI) and one sample of PA Xen-41 (PA1) in the G- samples are misclassified as G+. All the G+ samples are correctly classified. Figure B.6 in Appendix B shows the loadings of the PLS-DA model where the peaks mainly used to discriminate between bacterial G+ and G- groups are at  $\Delta\nu = 650, 730, \text{ and } 950 \text{ cm}^{-1}$ , which are the same peaks primarily used to differentiate bacteria between species. However, when the SERS spectra of the same bacteria are generated on pristine AgNR substrates, the discrimination is not obvious, with only 86.3% sensitivity and 84.6% specificity, as shown in Figure B.7 in Appendix B. This further demonstrates the advantages of using the VAN AgNR substrates.

The ability to correctly discriminate between G<sup>+</sup> and G<sup>-</sup> samples when their SERS spectra is generated on VAN AgNR substrates is due to the structural differences between their cell walls (41, 42). Immediately external to the cytoplasmic membrane of G<sup>-</sup> bacteria is a thin peptidoglycan layer which is made of N-acetylglucosamine (NAG), N-acetylmuramic acid (NAM), and peptides. External to the peptidoglycan layer is the outer membrane which consists of phospholipids with saturated fatty acids and contains an additional periplasmic space, which is absent in the G<sup>+</sup> bacteria. The cell wall of G<sup>+</sup> bacteria has multiple layers, consisting mainly of a thick peptidoglycan layer within which may also include teichoic acids, lipoteichoic acids, complex polysaccharides, and proteins. These molecules are common surface antigens that distinguish bacterial serotypes and promote attachment to other bacteria as well as to specific receptors on mammalian cell surfaces (43). The VAN coating on the AgNR substrate works as a capture agent for bacteria by forming hydrogen bonds with the terminal D-alanyl-D-alanine moieties of the NAM/NAG-peptides on the cell wall (11, 35). Thus, the VAN coating layer more readily captures the G<sup>+</sup> bacteria than the G<sup>-</sup> bacteria which consequently, further enhances the SERS signal originating from the cell wall structural differences between the G<sup>+</sup> and G<sup>-</sup> bacteria. This data altogether demonstrates the ability of SERS to differentiate G<sup>+</sup> from G<sup>-</sup> bacteria.

## **Conclusions**

In this report, we have demonstrated the capability and advantages of using VAN AgNR substrates to differentiate bacterial species, strains, and serotypes using chemometric methods. This is the first time more than 27 different bacteria isolates were collected and analyzed simultaneously. Furthermore, the large sample size gives more insight on the use of SERS for bacteria detection. We observed that the spectra generated on pristine substrates suffer from the

interferences of both the environment and the bacterial metabolic by-products due to the active chemical nature of silver. VAN AgNR substrates protect the silver surface from such interferences, generate more reproducible bacterial SERS spectra, and can be used to differentiate bacteria using chemometric methods. The results of the species, serotypes, and strains differentiation obtained in our study show that a two-step chemometric approach can be applied to differentiate bacteria at the sub-species level. The first step is to apply chemometric analysis on all the spectral data to discriminate the bacteria based on their species. The second step is to analyze the spectra from each subset (cluster) for potential serotypes or strains. The classification between serotypes was demonstrated using five different serotypes of *Salmonella* species, while the classification between strains was demonstrated using five different strains of *Staphylococcus aureus* and five different strains of *Acinetobacter baumannii*. We also demonstrated that for the 27 bacteria we studied, the discrimination between G+ and G- bacteria was achieved with high sensitivity and specificity based on the SERS technique. These results will provide insights to future studies on using SERS as a bacterial diagnostic tool and guide the design for a SERS based detection platform.

### **Acknowledgements**

This work was partly supported by USDA CSREES Grant #2009-35603-05001, National Institute of Health grant R21-AI096364, National Science Foundation under contract number grant CBET-1064228, and University of Georgia College of Agricultural and Environmental Sciences Experiment Station. The authors would like to thank Dr. Arthur Hinton, Jr. for providing the bacterial strains and Dr. Nasreen Bano for bacterial sample preparation.

## **Declaration of Interest**

Mention of trade names or commercial products in this article is solely for the purpose of providing specific information and does not imply recommendation or endorsement by the U.S. Department of Agriculture. The views expressed in this article are those of the authors and do not necessarily reflect the official policy or position of the Department of the Navy, Department of Defense, nor the U.S. Government. This work was funded by work unit number G1021. Rene Alvarez and Alexander J. Burdette are employees of the US Government. This work was prepared as part of their official duties. Title 17 USC §105 provides that ‘copyright protection under this title is not available for any work of the US Government.’ Title 17 USC §101 defines a US Government work as a work prepared by a military service member or employee of the US Government as part of that person’s official duties.

## References

1. **Fan C, Hu Z, Mustapha A, Lin M.** 2011. Rapid detection of food- and waterborne bacteria using surface-enhanced Raman spectroscopy coupled with silver nanosubstrates. *Appl Microbiol Biotechnol* **92**:1053-1061.
2. **Jarvis RM, Goodacre R.** 2004. Discrimination of Bacteria Using Surface-Enhanced Raman Spectroscopy. *Analytical Chemistry* **76**:40-47.
3. **Neyrolles O, Hennigan SL, Driskell JD, Dluhy RA, Zhao Y, Tripp RA, Waites KB, Krause DC.** 2010. Detection of *Mycoplasma pneumoniae* in Simulated and True Clinical Throat Swab Specimens by Nanorod Array-Surface-Enhanced Raman Spectroscopy. *PLoS ONE* **5**:e13633.
4. **Patel IS, Premasiri WR, Moir DT, Ziegler LD.** 2008. Barcoding bacterial cells: a SERS-based methodology for pathogen identification. *J. Raman Spectrosc.* **39**:1660-1672.
5. **Premasiri WR, Gebregziabher Y, Ziegler LD.** 2011. On the Difference Between Surface-Enhanced Raman Scattering (SERS) Spectra of Cell Growth Media and Whole Bacterial Cells. *Appl. Spectrosc.* **65**:493-499.
6. **Prucek R, Ranc V, Kvitek L, Panacek A, Zboril R, Kolar M.** 2012. Reproducible discrimination between Gram-positive and Gram-negative bacteria using surface enhanced Raman spectroscopy with infrared excitation. *Analyst* **137**:2866-2870.
7. **Stephen KE, Homrighausen D, DePalma G, Nakatsu CH, Irudayaraj J.** 2012. Surface enhanced Raman spectroscopy (SERS) for the discrimination of *Arthrobacter* strains based on variations in cell surface composition. *Analyst* **137**:4280-4286.

8. **Walter A, Marz A, Schumacher W, Rosch P, Popp J.** 2011. Towards a fast, high specific and reliable discrimination of bacteria on strain level by means of SERS in a microfluidic device. *Lab Chip* **11**:1013-1021.
9. **Xie Y, Xu L, Wang Y, Shao J, Wang L, Wang H, Qian H, Yao W.** 2013. Label-free detection of the foodborne pathogens of Enterobacteriaceae by surface-enhanced Raman spectroscopy. *Analytical Methods* **5**:946-952.
10. **Zhang L, Xu J, Mi L, Gong H, Jiang S, Yu Q.** 2012. Multifunctional magnetic-plasmonic nanoparticles for fast concentration and sensitive detection of bacteria using SERS. *Biosensors and Bioelectronics* **31**:130-136.
11. **Wu X, Xu C, Tripp RA, Huang Y-w, Zhao Y.** 2013. Detection and differentiation of foodborne pathogenic bacteria in mung bean sprouts using field deployable label-free SERS devices. *Analyst* **138**:3005-3012.
12. **Efrima S, Zeiri L.** 2009. Understanding SERS of bacteria. *J. Raman Spectrosc.* **40**:277-288.
13. **Wu X, Chen J, Park B, Huang Y-w, Zhao Y.** 2013. The Use of Silver Nanorod Array-Based Surface-Enhanced Raman Scattering Sensor for Food Safety Applications, p. 85-108, *Advances in Applied Nanotechnology for Agriculture*, vol. 1143. American Chemical Society.
14. **Jarvis RM, Goodacre R.** 2008. Characterisation and identification of bacteria using SERS. *Chemical Society Reviews* **37**:931-936.
15. **Kneipp K, Kneipp H, Itzkan I, Dasari RR, Feld MS.** 1999. Ultrasensitive Chemical Analysis by Raman Spectroscopy. *Chemical Reviews* **99**:2957-2976.
16. **Campion A, Kambhampati P.** 1998. Surface-enhanced Raman scattering. *Chemical Society Reviews* **27**:241-250.

17. **Kneipp K, Wang Y, Kneipp H, Perelman LT, Itzkan I, Dasari RR, Feld MS.** 1997. Single Molecule Detection Using Surface-Enhanced Raman Scattering (SERS). *Physical Review Letters* **78**:1667-1670.
18. **Nie SM, Emery SR.** 1997. Probing single molecules and single nanoparticles by surface-enhanced Raman scattering. *Science* **275**:1102-1106.
19. **Xu H, Aizpurua J, Käll M, Apell P.** 2000. Electromagnetic contributions to single-molecule sensitivity in surface-enhanced Raman scattering. *Physical Review E* **62**:4318-4324.
20. **Xu H, Bjerneld EJ, Käll M, Börjesson L.** 1999. Spectroscopy of Single Hemoglobin Molecules by Surface Enhanced Raman Scattering. *Physical Review Letters* **83**:4357-4360.
21. **Liu Y, Chen Y-R, Nou X, Chao K.** 2007. Potential of Surface-Enhanced Raman Spectroscopy for the Rapid Identification of Escherichia Coli and Listeria Monocytogenes Cultures on Silver Colloidal Nanoparticles. *Appl. Spectrosc.* **61**:824-831.
22. **Zeiri L, Bronk BV, Shabtai Y, Czege J, Efrima S.** 2002. Silver metal induced surface enhanced Raman of bacteria. *Colloids and Surfaces A: Physicochemical and Engineering Aspects* **208**:357-362.
23. **Efrima S, Bronk BV.** 1998. Silver Colloids Impregnating or Coating Bacteria. *The Journal of Physical Chemistry B* **102**:5947-5950.
24. **Jarvis RM, Brooker A, Goodacre R.** 2004. Surface-Enhanced Raman Spectroscopy for Bacterial Discrimination Utilizing a Scanning Electron Microscope with a Raman Spectroscopy Interface. *Analytical Chemistry* **76**:5198-5202.
25. **Sengupta A, Laucks ML, Davis EJ.** 2005. Surface-Enhanced Raman Spectroscopy of Bacteria and Pollen. *Appl. Spectrosc.* **59**:1016-1023.

26. **Montoya JR, Armstrong RL, Smith GB.** 2003. Detection of salmonella using surfaced enhanced Raman scattering. Proc. SPIE 5085, Chemical and Biological Sensing IV:144-152.
27. **Premasiri WR, Moir DT, Klempner MS, Krieger N, Jones G, Ziegler LD.** 2004. Characterization of the Surface Enhanced Raman Scattering (SERS) of Bacteria. The Journal of Physical Chemistry B **109**:312-320.
28. **Guzelian AA, Sylvia JM, Janni JA, Clauson SL, Spencer KM.** 2002. SERS of whole-cell bacteria and trace levels of biological molecules. Proc. SPIE 4577, Vibrational Spectroscopy-based Sensor Systems:182-192.
29. **Wang Y, Ravindranath S, Irudayaraj J.** 2011. Separation and detection of multiple pathogens in a food matrix by magnetic SERS nanoprobe. Anal Bioanal Chem **399**:1271-1278.
30. **Wang Y, Lee K, Irudayaraj J.** 2010. Silver Nanosphere SERS Probes for Sensitive Identification of Pathogens. The Journal of Physical Chemistry C **114**:16122-16128.
31. **Zhang X, Young MA, Lyandres O, Van Duyne RP.** 2005. Rapid Detection of an Anthrax Biomarker by Surface-Enhanced Raman Spectroscopy. J. Am. Chem. Soc. **127**:4484-4489.
32. **Chu H, Huang Y, Zhao Y.** 2008. Silver Nanorod Arrays as a Surface-Enhanced Raman Scattering Substrate for Foodborne Pathogenic Bacteria Detection. Appl. Spectrosc. **62**:922-931.
33. **Chaney SB, Shanmukh S, Dluhy RA, Zhao YP.** 2005. Aligned silver nanorod arrays produce high sensitivity surface-enhanced Raman spectroscopy substrates. Appl. Phys. Lett. **87**:031908.
34. **Driskell JD, Shanmukh S, Liu Y, Chaney SB, Tang XJ, Zhao YP, Dluhy RA.** 2008. The use of aligned silver nanorod Arrays prepared by oblique angle deposition as surface enhanced Raman scattering substrates. J. Phys. Chem. C **112**:895-901.

35. **Liu TY, Tsai KT, Wang HH, Chen Y, Chen YH, Chao YC, Chang HH, Lin CH, Wang JK, Wang YL.** 2011. Functionalized arrays of Raman-enhancing nanoparticles for capture and culture-free analysis of bacteria in human blood. *Nature communications* **2**:538.
36. **Liu TY, Tsai KT, Wang HH, Chen Y, Chen YH, Chao YC, Chang HH, Lin CH, Wang JK, Wang YL.** 2011. Functionalized arrays of Raman-enhancing nanoparticles for capture and culture-free analysis of bacteria in human blood. *Nature communications* **2**:538.
37. **Liu YJ, Chu HY, Zhao YP.** 2010. Silver Nanorod Array Substrates Fabricated by Oblique Angle Deposition: Morphological, Optical, and SERS Characterizations. *The Journal of Physical Chemistry C* **114**:8176-8183.
38. **Wu X, Chen J, Li X, Zhao Y, Zughair SM.** 2014. Culture-free diagnostics of *Pseudomonas aeruginosa* infection by silver nanorod array based SERS from clinical sputum samples. *Nanomedicine : nanotechnology, biology, and medicine*.
39. **Abell JL, Garren JM, Driskell JD, Tripp RA, Zhao Y.** 2012. Label-Free Detection of Micro-RNA Hybridization Using Surface-Enhanced Raman Spectroscopy and Least-Squares Analysis. *J. Am. Chem. Soc.* **134**:12889-12892.
40. **Liu TY, Chen Y, Wang HH, Huang YL, Chao YC, Tsai KT, Cheng WC, Chuang CY, Tsai YH, Huang CY, Wang DW, Lin CH, Wang JK, Wang YL.** 2012. Differentiation of Bacteria Cell Wall Using Raman Scattering Enhanced by Nanoparticle Array. *Journal of Nanoscience and Nanotechnology* **12**:5004-5008.
41. **Beveridge TJ.** 1999. Structures of Gram-Negative Cell Walls and Their Derived Membrane Vesicles. *Journal of Bacteriology* **181**:4725-4733.

42. **Navarre WW, Schneewind O.** 1999. Surface Proteins of Gram-Positive Bacteria and Mechanisms of Their Targeting to the Cell Wall Envelope. *Microbiology and Molecular Biology Reviews* **63**:174-229.
43. **Wicken A, Knox K.** 1975. Lipoteichoic acids: a new class of bacterial antigen. *Science* **187**:1161-1167.

Table 6.1 A list of bacteria used in this paper. The bacteria isolated from chicken carcass rinses are denoted as USDACR. The isolates from patients at Walter Reed Medical Center are denoted as WRAMC and the isolates from patients at Brooke Army Medical Center are denoted as BAMC.

<b>Abbr.</b>	<b>Bacteria speciesserotypes</b>	<b>Strains</b>	<b>Serotypes</b>	<b>Gram</b>
AB1	<i>Acinetobacter baumannii</i>	ATCC 19606	N/A	-
AB2	<i>Acinetobacter baumannii</i>	ATTC BAA-1605	N/A	-
AB3	<i>Acinetobacter baumannii</i>	ATTC 17961	N/A	-
AB4	<i>Acinetobacter baumannii</i>	ATTC 19003	N/A	-
AB6	<i>Acinetobacter baumannii</i>	WRAMC #13	N/A	-
CK	<i>Citrobacter koseri</i>	USDACR	N/A	-
PP	<i>Pseudomonas putida</i>	USDACR	N/A	-
EC	<i>Escherichia coli</i>	USDACR	N/A	-
EF	<i>Enterococcus faecalis</i>	USDACR	N/A	+
ENC	<i>Enterobacter cloacae</i>	USDACR	N/A	-
KP1	<i>Klebsiella pneumoniae</i>	IA- 525	N/A	-
KP2	<i>Klebsiella pneumoniae</i>	BAMC 07-18	N/A	-
KP3	<i>Klebsiella pneumoniae</i>	Xen- 39	N/A	-
PA1	<i>Pseudomonas aeruginosa</i>	Xen-41	N/A	-
PA2	<i>Pseudomonas aeruginosa</i>	PA 01	N/A	-
SalE	<i>Salmonella enterica</i>	USDACR	Enteritidis	-
SalH	<i>Salmonella enterica</i>	USDACR	Heidelberg	-
SalI	<i>Salmonella enterica</i>	USDACR	Infantis	-
SalK	<i>Salmonella enterica</i>	USDACR	Kentucky	-
SalT	<i>Salmonella enterica</i>	USDACR	Typhimurium	-
SA1	<i>Staphylococcus aureus</i>	IQ 0070	N/A	+
SA2	<i>Staphylococcus aureus</i>	Xen 40	N/A	+
SA3	<i>Staphylococcus aureus</i>	ATCC 33591	N/A	+
SA4	<i>Staphylococcus aureus</i>	TCH 1516	N/A	+
SA5	<i>Staphylococcus aureus</i>	USDACR	N/A	+
SH	<i>Staphylococcus hyicus</i>	USDACR	N/A	+
SK	<i>Staphylococcus kloosii</i>	USDACR	N/A	+

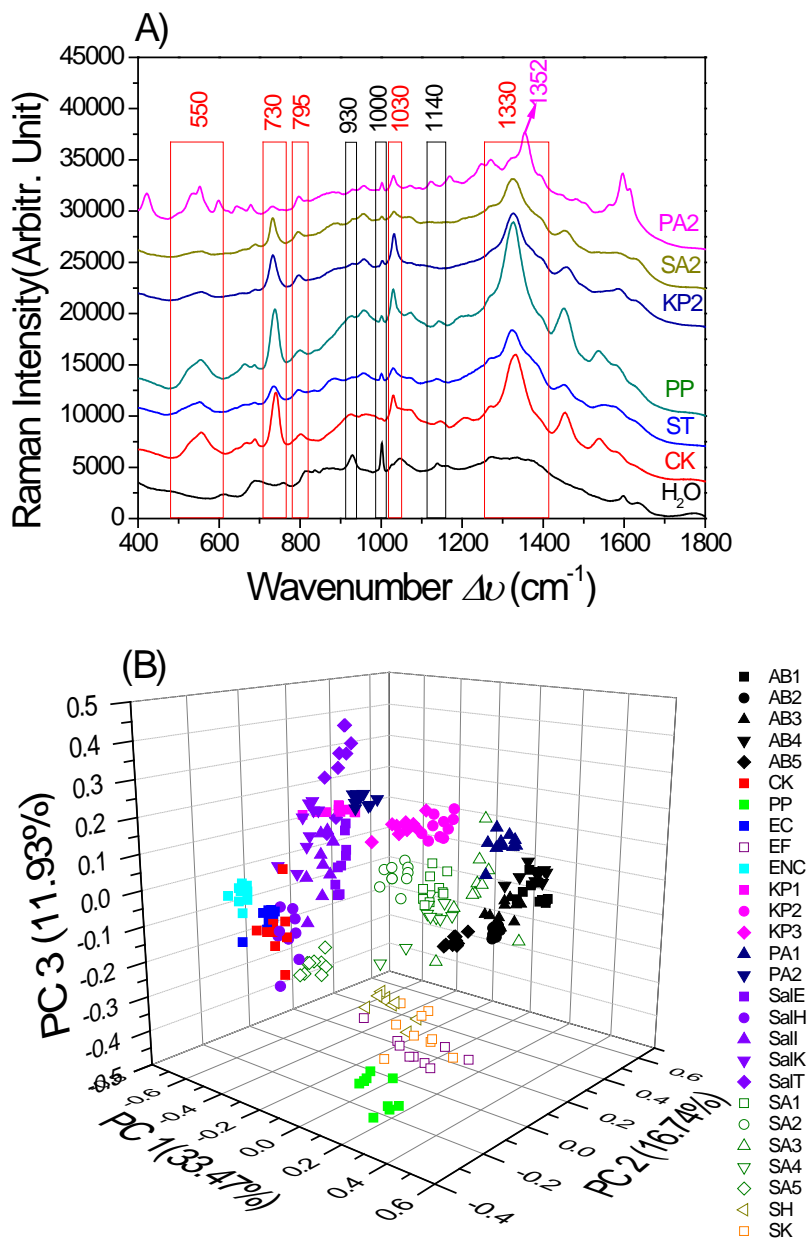


Figure 6.1 SERS of bacteria generated on the pristine substrates. (A) Representative bacterial SERS spectra. The red boxed peaks originate from bacteria, while black boxed peaks are from environmental contamination. (B) The 3D PCA score plot of the SERS spectra on the pristine substrates shows G+ bacteria as unfilled symbols and the G- bacteria are indicated as filled symbols. Bacteria of the same species, regardless of the strains and serotypes, are indicated as symbols of the same color.

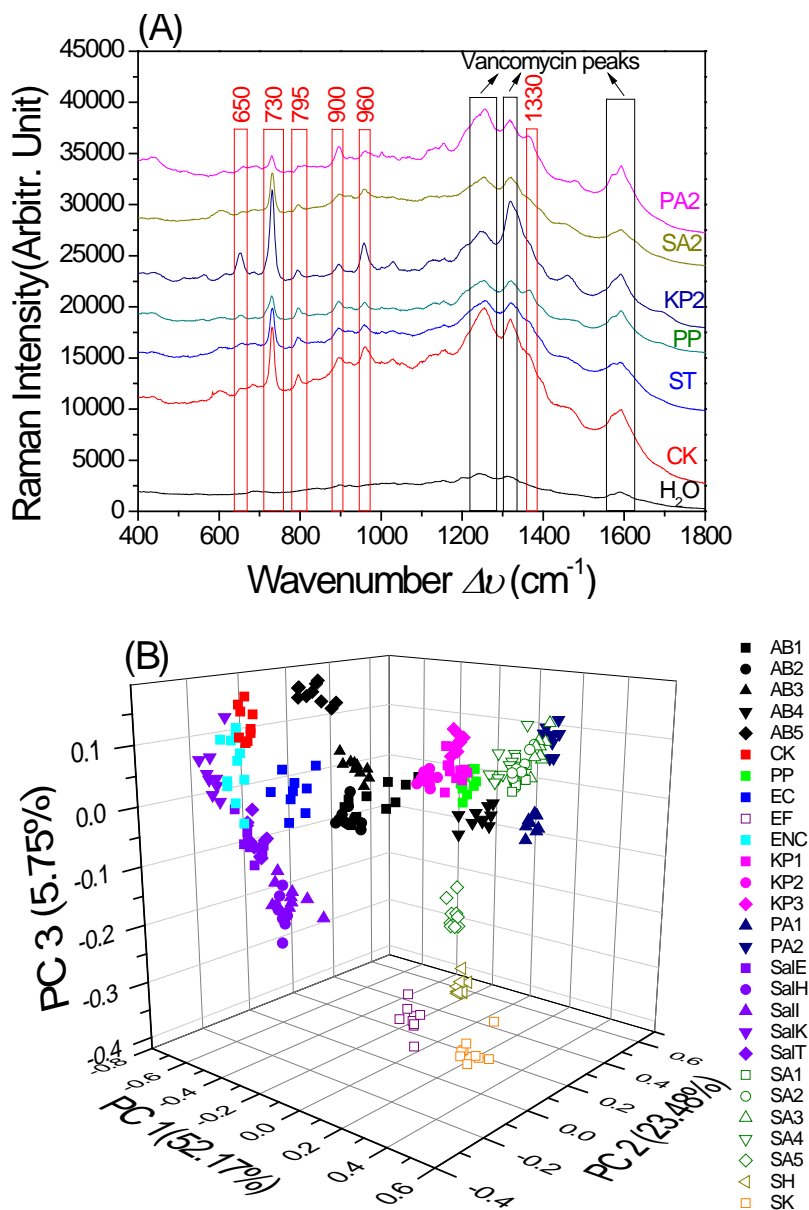


Figure 6.2 SERS of bacteria generated on the VAN AgNR substrates. (A) Representative bacterial SERS spectra. The red boxed peaks originate from bacteria, while black boxed peaks are from VAN coating. (B) The 3D PCA score plot of the SERS spectra on the VAN AgNR substrates shows G+ bacteria as unfilled symbols and the G- bacteria are indicated as filled symbols. Bacteria of the same species, regardless of the strains and serotypes, are represented by symbols of the same color.

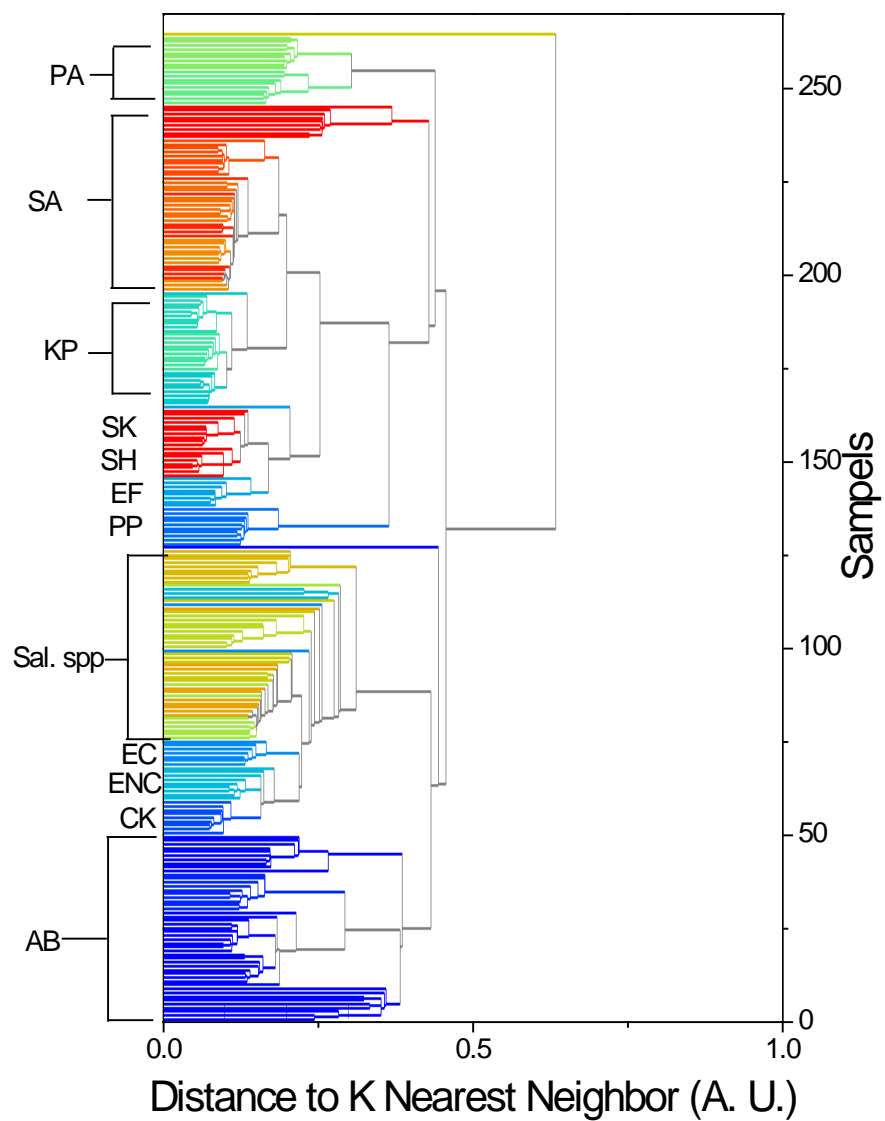


Figure 6.3 The HCA dendrogram based on the bacterial SERS spectra generated on the VAN AgNR substrates. Bacterial isolates of the same species are represented by lines of the same color.

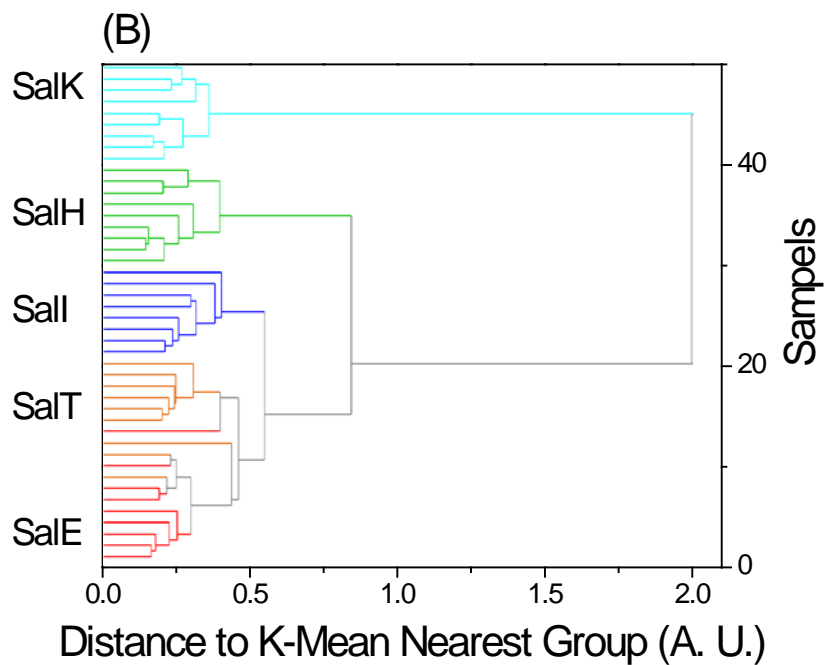
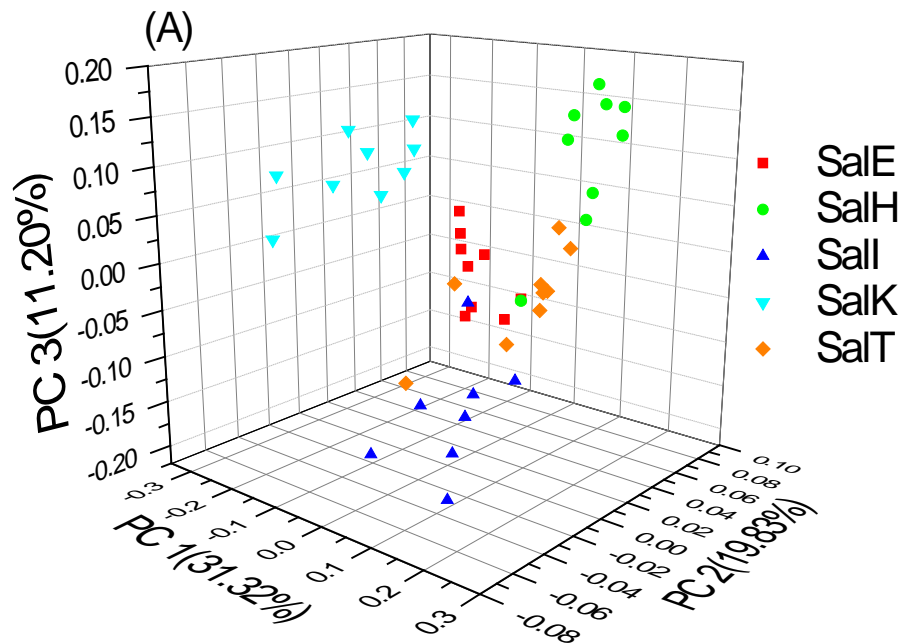


Figure 6.4 Differentiation of five different serotypes of *Salmonella* species based on the chemometric analysis of the SERS spectra generated on the VAN AgNR substrates. (A) The 3D PCA score plot and (B) HCA plot.

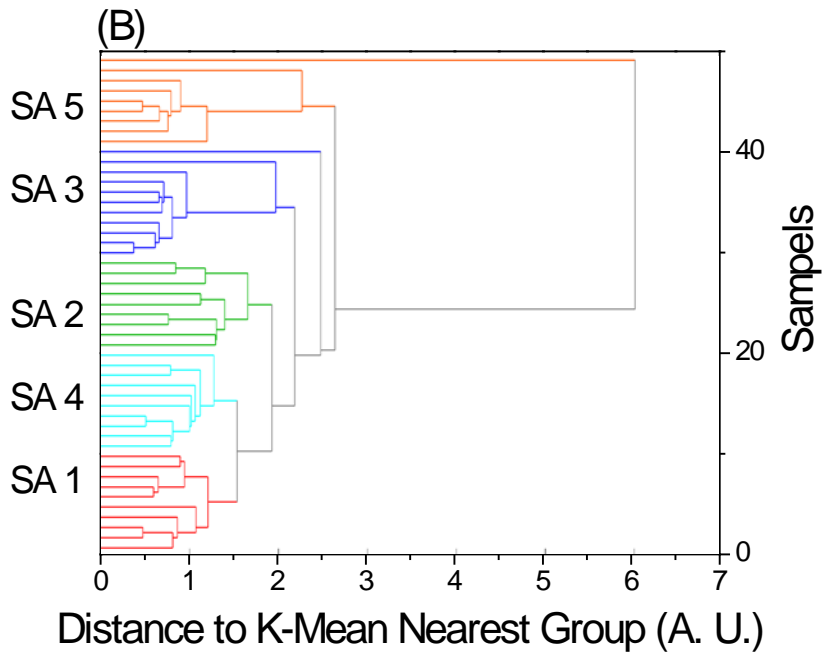
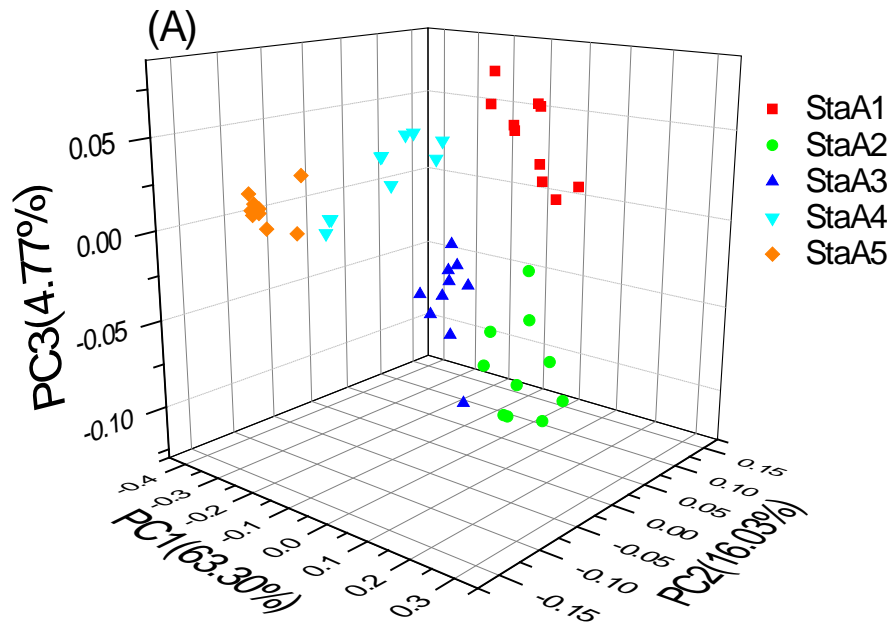


Figure 6.5 Differentiation of five different strains of *Staphylococcus aureus* (SA) based on the chemometric analysis of the SERS spectra generated on the VAN AgNR substrates. (A) The 3D PCA score plot and (B) HCA plot.

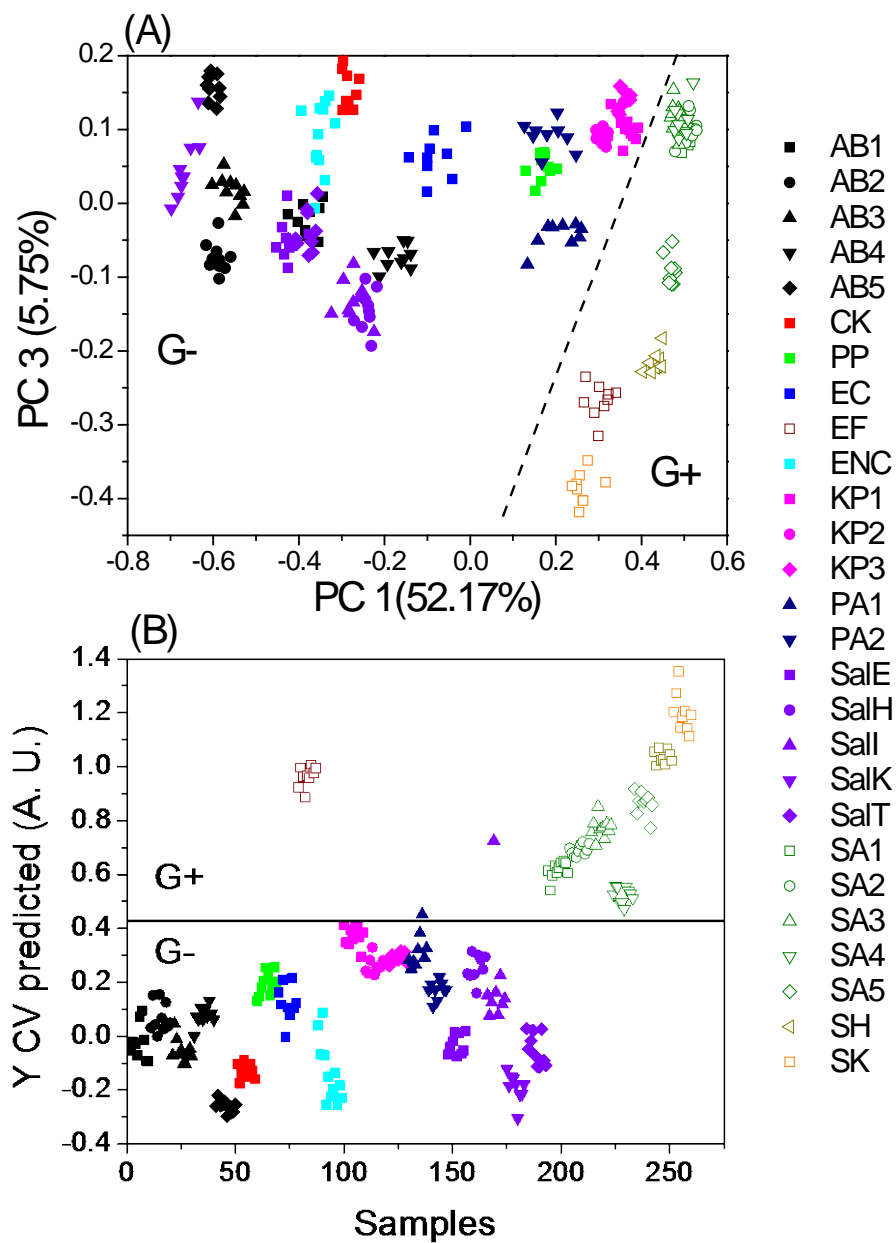


Figure 6.6 Classification between G+ and G- bacteria based on the chemometric analysis of the SERS spectra generated on the VAN AgNR substrates. (A) PCA score plot of PC1 vs. PC3 and (B) PLS-DA score plot. G+ bacteria are indicated as unfilled symbols and the G- bacteria are indicated as filled symbols. Bacteria of the same species, regardless of the strains and serotypes, are represented by symbols of the same color. Black horizontal line in (B) indicates the threshold generated by the model to discriminate G+ and G- bacteria.

CHAPTER 7

DETECTION OF PATHOGENIC BACTERIA IN CANTALOUPE CUBES AND LETTUCE  
USING SERS<sup>1</sup>

---

<sup>1</sup>Xiaomeng Wu, Yao-wen Huang, and Yiping Zhao. To be submitted to *International Journal of Food Protection*.

## **Abstract**

Vancomycin functionalized silver nanorod arrays substrates were used to obtain the surface enhanced Raman scattering (SERS) spectra of *Salmonella* Poona in cantaloupe cube and *E. coli* O157:H7 in lettuce samples. By combining these substrates with a two-step filtration process we found that *Salmonella* Poona can be identified in cantaloupe cube samples with a limit of detection as low as 100 CFU/ml in less than 4 hrs. On the other hand, a three-step filtration method with the HTFS treated PTFE filters can effectively eliminated the interferences from the lettuce samples, namely the chlorophyll. *E. coli* O157:H7 in lettuce samples at 1000 CFU/ml was successfully detected within 5 hours. The low detection limit and rapid detection time of this biosensing platform for foodborne pathogenic bacteria could be a valuable field detection method for the fresh produce and food processing industries.

## Introduction

Although the U.S. food supply is generally considered to be one of the safest in the world, foodborne diseases continue to be a concern for consumers, governmental agencies and industries. The safety of fresh produce is of great concern as the number of foodborne outbreaks linked to fresh produce has increased over the past decades (1). In 1990, among outbreaks with an identified food source, 13% (713/5,416 cases) of outbreaks were linked to fresh produce, but such number dramatically increased to 21% (34,049/161,089 cases) in 2005 (2, 3). The frequent imports and exports of fresh produce can also cause multinational foodborne outbreaks (4). For example, the *Salmonella* outbreaks in US and Finland in 2009 traced back to the same alfalfa sprout seeds as their source (2). German outbreak of *E. coli* O104:H4 in 2011 that has been linked to bean sprouts or sprout seeds killed over 50 and sickened really 4000 in 15 European countries, as well as US (5).

Fresh produce by nature or by accident is vulnerable to contamination by pathogenic microorganisms at any point from farm to table since they are natural vehicles of pathogens. Contamination can happen during cultivation, irrigation, post-harvest handling, and packaging (6). Another reason for high risk of contamination is that the fresh produce often are processed with no heat-treatment, and are consumed raw or with minimal cooking. The fresh produce items that are often associated with foodborne outbreaks are berries, melons, seed sprouts, and salad-greens, and those outbreaks can be caused by bacteria, virus, and protozoa (7). Among the foodborne pathogenic bacteria, *Salmonella* is the top cause of outbreaks, followed by *E. coli*, *Clostridium*, *Shigella*, *Campylobacter*, *Yersinia*, *Bacillus*, and *Staphylococcus* (7, 8). In recent years, consumption of fresh cantaloupe melons has been associated with many outbreaks of foodborne illness, especially salmonellosis. For example, *Salmonella* Chester caused 245

illnesses in 30 states in 1990; an outbreak of *Salmonella* Poona involving 400 infections in 23 states in 1991; a 1997 outbreak of *Salmonella* Saphra was attributed to the consumption of cantaloupes imported from Mexico; three outbreaks of *Salmonella* Poona in 2000- 2002 have resulted in 154 cases of illness .

To prevent the potential disaster in food and drink supplies, a rapid and portable detection technique for pathogens is needed. Currently, the detection technique used for foodborne pathogen relies heavily on conventional microbiological culturing methods. They are labor intensive and time consuming. Newly developed molecular techniques have improved performance, but they still lack sensitivity, require time for enrichment procedure, or need expensive and non-mobile equipment.

In order to realize “real-time” detection with mobile device, bacterial detection using Raman spectroscopy and more sensitive Surface-enhanced Raman spectroscopy (SERS) has been studied. Traditional Raman spectroscopy relies on the inelastic scattering interaction of excitation light and vibrational modes of molecular bonds. These molecular vibrational modes possess unique “fingerprint” peaks which can be used to identify the particular molecule(s) being probed(9). Surface-enhanced Raman spectroscopy (SERS) is a highly sensitive Raman detection technique based on metallic nanostructured substrates (10, 11). Silver nanorod (AgNR) array substrates fabricated by oblique angle deposition (OAD) overcome some of the difficulties and disadvantages of the other SERS substrates. (12-15) These substrates have been shown to markedly enhance the detection of chemical and biological samples, including aflatoxins (16), important human viruses such as rotavirus, influenza virus and respiratory syncytial virus (17, 18), foodborne pathogens like *E. coli* O157:H7, *Salmonella* Typhimurium, *Staphylococcus aureus* (19), pesticides like chlorpyrifos and parathion, intentional adulteration agents like

melamine (19), and allow for detection and discrimination of microRNA families and family members (20). Vancomycin coated AgNR (VAN AgNR) substrates have been used to detect pathogenic bacteria in mung bean sprout samples(21). The limit of detection (LOD) of this SERS based detection platform reaches 100 CFU/ml in initial solution or  $10^3$  CFU/g food samples in mung bean sprout, combined with a two-step filtration process. The LOD was determined using both bench-top and handheld Raman spectrometers indicating that the method lends itself to application in the field. Six different pathogens in mung bean sprout samples have been detected and differentiated by their species and serotypes using principle component analysis.

In this report, we will utilize the same VAN AgNR to detect pathogenic bacteria in cantaloupe cubes and lettuce samples as representative of fresh produce samples. Two-step filtration and three-step filtration procedure with modified filters are developed to better process the fresh produce sample, in order to eliminate the interferences from the food matrix.

## **MATERIAL AND METHODS**

### **AgNR fabrication and functionalization**

SERS spectra were acquired using AgNR array substrates fabricated by the oblique angle deposition (OAD) technique using a custom-designed electron beam/sputtering evaporation (e-beam) system (22-24). Briefly, glass microscopic slides (Gold Seal® Catalog No.3010, Becton, Dickinson and Company, Portsmouth, NH) used for AgNR arrays deposition were cleaned with piranha solution (80% sulfuric acid, 20% hydrogen peroxide in volume) and rinsed with deionized water. The substrates were then dried with a stream of nitrogen gas before being loaded into the e-beam deposition system. A 20-nm titanium film and then a 200-nm silver film layer were evaporated onto the glass slides at a rate of  $\sim 0.2$  nm/s and 0.3 nm/s, respectively,

while the substrate surface was held perpendicular to the incident vapor direction. The substrates were then rotated to 86° with respect to the incident vapor and AgNRs were grown at this oblique angle with a deposition rate of ~0.3 nm/s. The film thickness was monitored *in situ* by a quartz crystal microbalance (QCM) positioned at normal incidence to the vapor source direction until the reading reaches 600nm.

The AgNR are functionalized by Vancomycin as described before(21). The AgNR array substrates were immersed in the 1 mM VAN solutions overnight (> 12 hrs), rinsed three times with DI water, and then dried with nitrogen.

### **PTFE filter modification**

Fluoropore® filter (EMD Millipore, Billerica, MA) is used, which is made of polytetrafluoroethylene (PTFE). In order to further improve the hydrophobicity, the PTFE filter was modified with (HeptadecaFluoro - 1, 1,2, 2 - tetra-hydrodecyl) TrichloroSilane (HFTS) as described before(25). Briefly, the PTFE filters were placed in a chemical evaporation chamber, while 30 µl of HFTS is applied. Under vacuum condition, the vapour of HFTS formed a monolayer on the surface of the filter.

### **Food samples preparation and bacteria incubation**

*Salmonella* Poona and *E. coli* O157:H7 (salami isolate) were obtained from the Department of Food Science and Technology of The University of Georgia (Athens, GA). These bacteria were grown in trypticase soy broth (TSB, Difco, Detroit, MI) overnight at 37 °C to yield ~10<sup>9</sup> CFU/ml culture. Bacterial populations were determined by conventional surface plate count method using plate count agar (PCA, Difco®, Detroit, MI). Following incubation, the cultures were washed three times with sterilized deionized (DI) water before re-suspending in sterilized DI water. Desired dilutions were made in sterilized DI water as well.

The fresh cut cantaloupe cubes and lettuce samples were cleaned by using 1000 ppm house bleach (acidified hyperchlorine, EverydayLiving) for at least 20 min to ensure no bacteria survival on the surface. The food samples were then carefully rinsed with sterilized DI water to remove any chemical residue, and dried in a biosafety hood with laminar flow. Ten grams of cantaloupe cubes were inoculated with 100 $\mu$ l of bacteria culture with different concentrations for 1 hr to ensure the attachment of the bacteria. The inoculated samples were then mixed with 100 ml of sterile DI water and massaged with a stomacher for 1 min at 200 rpm.

Next, these solutions underwent either two-step or three-step filtration procedure. The two-step filtration are described by Wu et al (21) as illustrated in Figure 7.1. This method is a two-step filtration: 1) a crude pre-filtration step through VWR® # 417 filters (pore size 40  $\mu$ m) to remove larger sample particles, and 2) a second filtration to recover the target bacteria from the filtrate using Durapore® filter membranes (pore size 0.22 $\mu$ m). The filter membrane containing the bacteria was vortexed with 0.5 ml sterile DI water for 15 sec. The bacteria will be re-suspended in this 0.5 ml solution, and the vancomycin treated AgNR substrate (VAN substrate) was immersed in this solution for 2 hrs at 37 °C with shaking at 200 rpm. The inoculated substrates were then rinsed with DI water, followed by drying with Nitrogen. The entire process, from filtration to spectrum acquisition, took approximately 4 hrs.

The three-step filtration produce is illustrated in Figure 7.2. The first two step of the filtration is identical to those in the two-step filtration procedure. After second filtration step, the 0.5 mL bacteria containing solution was filtered through the PTFE filter (0.22  $\mu$ m pore size, HTFS treated or untreated), and 3 mL of DI water was applied to wash the filter repeatedly to remove any residues of the chlorophyll. Then the PTFE filter was collected, and resuspended with 0.5 mL of DI water. VAN AgNR substrates were immersed in 0.5mL solution, dried, and

measured for SERS in the same way as in two-step filtration method. The entire process, from filtration to spectrum acquisition, took approximately 4.5 hrs.

### **SERS measurements and data analysis**

SERS spectra were acquired using a portable Enwave Raman system (Model ProRaman 785A2, Enware Optronics Inc., Irvine, CA), with a 785 nm near-IR diode laser as the excitation source. The power of the laser at the sample was set to be  $\sim 30$  mW. SERS spectra over a range of  $\sim 400 - 1800$   $\text{cm}^{-1}$  were used over a 10 sec exposure time. SERS spectra were collected from 9 spots ( $3 \times 3$  array) across the VAN AgNR substrate surface and multiple substrates were measured. All data analysis was performed using Origin software 8.5 version (OriginLab Corporation, Northampton, MA) and WIRE2.0 software (Renishaw, United Kingdom). Statistical data analysis was conducted with Matlab 2000b (The MathWorks, Inc., Natick, MA) using the PLS toolbox (Eigenvector Research, Inc., Wenatchee, WA).

## **Results and Discussion**

### **Detection of *Salmonella* Poona in cantaloupe cubes**

The SERS spectra of *Salmonella* Poona recovered from inoculated cantaloupe cube samples ( $10^2$  and  $10^3$  CFU/ ml) are shown in Figure 7.3A. Significant peaks for *Salmonella* were found at  $\Delta\nu = 616, 697, \text{ and } 728$   $\text{cm}^{-1}$ , with peak intensity increasing as the bacterial concentration increased, while the vancomycin peaks dominate the region of  $1200 - 1800$   $\text{cm}^{-1}$ . It is interesting to note that the control samples ( $\text{H}_2\text{O}$ ) also has a peak at  $\Delta\nu = 895$   $\text{cm}^{-1}$ , which may come from the cantaloupes samples. However, this peak does not affect the detection of bacteria as significant peak at  $\Delta\nu = 728$   $\text{cm}^{-1}$  will be used to establish the LOD of *Salmonella* in cantaloupe cubes samples/

We plotted the SERS peak intensity at  $\Delta\nu = 728 \text{ cm}^{-1}$  ( $I_{728}$ ) against the bacterial concentration (Figure 7.3B). At each concentration, at least 9 spectra from two different substrates were measured and analyzed by peak fitting, and the mean and standard deviation of the peak intensities  $I_{728}$  are shown in Figure 7.3B. The LOD of the SERS detection is defined as the lowest concentration at which a distinguished bacterial SERS spectrum can be obtained. In our experiment, the LOD is the lowest concentration at which the peak intensity of the bacteria at  $\Delta\nu = 728 \text{ cm}^{-1}$  is significantly different from the sterile DI water (control) which is used to dilute the bacteria samples. The value of average plus three times the standard deviation of the sterile DI water was set as the limit for determining a positive detection from a negative detection. From Figure 7.3B we can see that samples with inoculation rates as low as  $10^2$  CFU/ml yield  $I_{728}$  higher than the threshold determined. Therefore, the LOD of *Salmonella* Poona in cantaloupe cube samples using this method is 100 CFU/ml in initial solution or  $10^3$  CFU/g of cantaloupe cube samples.

### **Detection of *E. coli* O157:H7 in lettuce**

The SERS platform for detection of pathogenic bacteria in both mung bean sprout (21) and cantaloupe cubes has been validated, but these two food samples have relatively simple contents and have little background in sample solutions. On the other hands, leafy green vegetables have large amount of chlorophyll that may cause significant inference to the SERS spectra. Here we will test our detection method for a typical leafy green, lettuce (mixture of Romaine lettuce and iceberg lettuce). The same two-step filtration procedure was used to process the *E. coli* O157:H7 inoculated lettuce, followed by the 2 hour incubation with VAN AgNR substrates for bacteria capture. The SERS spectra of *E. coli* O157:H7 recovered from lettuce

samples inoculated at  $10^4$  CFU/ml and sterile DI water inoculated in lettuce samples (control) followed by a two-step filtration are shown in Figure 7.4. Both the *E. coli* O157:H7 inoculated samples and the control showed significant peaks at  $\Delta\nu = 728, 895, \text{ and } 955 \text{ cm}^{-1}$ , which limits the differences between these two spectra.

The SERS peaks shown in control samples  $\Delta\nu = 728, 895, \text{ and } 955 \text{ cm}^{-1}$  may result from the chlorophyll residues in the final solution. The peak at  $\Delta\nu = \sim 730 \text{ cm}^{-1}$  is corresponding to adenine vibrational mode. If we compare the molecule structure of adenine and chlorophyll in Figure 7.5, we can see that they share the similar ring structure, which would result in similar SERS spectra. During the message processing, the leaf cells are disrupted by the mechanic force, and the chlorophyll is released to the solution. It is then absorbed onto the filter, which is made of cellulose, and then re-suspended into the final solution along with the bacteria.

In order to overcome the interference from the chlorophyll, a third filtration step is added after the second filtration, and before AgNR substrates were immersed in the solution, as shown in Figure 7.2. In the third filtration step, a hydrophobic filter is desired, so the chlorophyll will not be absorbed onto it. We use a hydrophobic PTFE filter in the third step. In order to make it more hydrophobic, PTFE filters are treated with HFTS. To investigate the effect of three-step filtration method, and the use of HFTS treated filter, ten grams of lettuce samples were messaged with 100 mL of DI water, and evenly divided into three parts. The first part of the solution was processed with the two-step filtration procedure as described in Figure 7.1. The second part of the solution was processed with the three-step filtration procedure with untreated PTFE filter; while the third part of the solution was processed with the three-step filtration procedure with HFTS treated PTFE filter, as shown in Figure 7.2. The absorbance of the three final solutions is measured by UV-VIS to determine the concentration of chlorophyll in each sample, as shown in

Figure 7.6. Based on the equation formulated by Arnon, the concentration of total chlorophyll  $C_{ch}$  (chlorophyll a & chlorophyll b) can be determined by:  $C_{ch} = 1000 \times A_{652} / 34.5$ , where  $A_{652}$  is the absorbance at 652 nm (26). So, in Figure 7.6A, we can see that the additional filtration step significantly decrease chlorophyll concentration to 50.3% with untreated PTFE filter and 8.9% with HTFS treated PTFE filter, respectively, compared to the two-step filtration method. Such decreases in chlorophyll concentration effectively eliminate the interference from the lettuce samples, as shown in Figure 7.6B. The SERS spectra of the lettuce after filtration do show interference peaks at  $\Delta\nu = 523, 697, \text{ and } 898 \text{ cm}^{-1}$ , but not at  $\Delta\nu = 728 \text{ cm}^{-1}$ , which can be used as the representative peaks of the bacteria.

The three-step filtration method with HTFS treated PTFE filter is the best way to eliminate the interference from the food pigments. We obtained the SERS spectra of *E. coli* O157:H7 recovered from lettuce samples inoculated with bacteria and the sterile DI water as control followed by a three-step filtration method with HTFS treated PTFE filter, as shown in Figure 7.7A, and the  $I_{728}$  of these samples are plotted in Figure 7.7B. The samples at 100 CFU/ml showed no significant differences between the control, in either spectral features or  $I_{728}$ . The samples with bacteria concentration of  $10^3$  CFU/ml or higher are successfully be determined as positive, which suggests that the LOD of SERS for detection of *E. coli* O157:H7 in lettuce samples using three-step filtration procedure is at  $10^3$  CFU/ml. This LOD is 10 times of that obtained using two-step filtration procedure in both mung bean sprout and cantaloupe cube samples, and the reason is the loss of bacteria during the additional third filtration step. We determine the bacteria concentration after each filtration step by inoculating the sample on plate counting agar with 24 hour incubation at 37 °C, and the results are shown in Table 7.1. A significant amount of bacteria (nearly 50%) is lost during the third filtration step due to the

repeated washing in this step. The additional third step of filtration adds 30 minutes to the total detection time. The bacteria can be detected within 4.5 hours in lettuce samples using this three-step filtration procedure, which is less than a shift (normally 8 hours) in food processing plants.

## **Conclusions**

In this report, we demonstrate the sensitivity and specificity of SERS for detection of foodborne pathogens from different fresh produce samples using the VAN AgNR substrates. The LOD of this system reaches 100 CFU/ml in initial solution or  $10^3$  CFU/g food samples in cantaloupe cube samples, combined with a two-step filtration process. In lettuce samples, due to the inference from chlorophyll, a three-step filtration procedure with a specialized PTFE filter is used and the LODs reach  $10^3$  CFU/ml in initial solution or  $10^4$  CFU/g food samples. To the best of our knowledge, this is the lowest LOD reported for the SERS technique using real food samples and in the absence of external SERS reporters. We believe that the SERS detection technique based on AgNR is a powerful platform to detect low amounts of foodborne pathogens with the potential to be used as an on-site pathogen detection method in the fresh produce industry.

## REFERENCES

1. **Beuchat LR.** 1996. Pathogenic microorganisms associated with fresh produce. *J. Food Prot.* **59**:204-216.
2. **Matthews KR.** 2006. Microorganisms associated with fruits and vegetables, p. 1-19, *Microbiology of fresh produce.*
3. **DeWaal CS, Bhuiya F.** 2007. Outbreaks by the numbers: fruits and vegetables 1990-2005.
4. **Lynch MF, Tauxe RV, Hedberg CW.** 2009. The growing burden of foodborne outbreaks due to contaminated fresh produce: risks and opportunities. *Epidemiology and Infection* **137**:307-315.
5. **Buchholz U, Bernard H, Werber D, Böhmer MM, Remschmidt C, Wilking H, Deleré Y, an der Heiden M, Adlhoch C, Dreesman J, Ehlers J, Ethelberg S, Faber M, Frank C, Fricke G, Greiner M, Höhle M, Ivarsson S, Jark U, Kirchner M, Koch J, Krause G, Lubert P, Rosner B, Stark K, Kühne M.** 2011. German Outbreak of *Escherichia coli* O104:H4 Associated with Sprouts. *New England Journal of Medicine* **365**:1763-1770.
6. **Berger CN, Sodha SV, Shaw RK, Griffin PM, Pink D, Hand P, Frankel G.** 2010. Fresh fruit and vegetables as vehicles for the transmission of human pathogens. *Environ. Microbiol.* **12**:2385-2397.
7. **Harris LJ, Farber JN, Beuchat LR, Parish ME, Suslow TV, Garrett EH, Busta FF.** 2003. Outbreaks Associated with Fresh Produce: Incidence, Growth, and Survival of Pathogens in Fresh and Fresh-Cut Produce. *Comprehensive Reviews in Food Science and Food Safety* **2**:78-141.

8. **Doyle MP, Erickson MC.** 2008. Summer meeting 2007 - the problems with fresh produce: an overview. *Journal Of Applied Microbiology* **105**:317-330.
9. **Efrima S, Zeiri L.** 2009. Understanding SERS of bacteria. *J. Raman Spectrosc.* **40**:277-288.
10. **Kneipp K, Wang Y, Kneipp H, Perelman LT, Itzkan I, Dasari RR, Feld MS.** 1997. Single Molecule Detection Using Surface-Enhanced Raman Scattering (SERS). *Physical Review Letters* **78**:1667-1670.
11. **Nie SM, Emery SR.** 1997. Probing single molecules and single nanoparticles by surface-enhanced Raman scattering. *Science* **275**:1102-1106.
12. **Chaney SB, Shanmukh S, Dluhy RA, Zhao Y-P.** 2005. Aligned silver nanorod arrays produce high sensitivity surface-enhanced Raman spectroscopy substrates. *Applied Physics Letters* **87**.
13. **Driskell JD, Shanmukh S, Liu Y, Chaney SB, Tang X-J, Zhao Y-P, Dluhy RA.** 2008. The use of aligned silver nanorod arrays prepared by oblique angle deposition as SERS substrates. *J. Phys. Chem. C*:jp075288u.
14. **Shanmukh S, Jones L, Driskell J, Zhao Y-P, Dluhy R, Tripp RA.** 2006. Rapid and sensitive detection of respiratory virus molecular signatures using a silver nanorod array SERS substrate. *Nano Lett.* **6**:2630.
15. **Zhao YP, Chaney, S.B., Shanmukh, S., Dluhy, R.A.** 2006. Polarized Surface Enhanced Raman and Absorbance Spectra of Aligned Silver Nanorod Arrays. *Journal of Physical Chemistry B* **110**:3153-3157.

16. **Wu X, Gao S, Wang J-S, Wang H, Huang Y-W, Zhao Y.** 2012. The surface-enhanced Raman spectra of aflatoxins: spectral analysis, density functional theory calculation, detection and differentiation. *Analyst* **137**:4226-4234.
17. **Driskell JD, Zhu Y, Kirkwood CD, Zhao Y, Dluhy RA, Tripp RA.** 2010. Rapid and sensitive detection of rotavirus molecular signatures using surface enhanced Raman spectroscopy. *PloS one* **5**:e10222.
18. **Shanmukh S, Jones L, Zhao YP, Driskell J, Tripp R, Dluhy R.** 2008. Identification and classification of respiratory syncytial virus (RSV) strains by surface-enhanced Raman spectroscopy and multivariate statistical techniques. *Analytical and bioanalytical chemistry* **390**:1551-1555.
19. **Chu H, Huang Y, Zhao Y.** 2008. Silver Nanorod Arrays as a Surface-Enhanced Raman Scattering Substrate for Foodborne Pathogenic Bacteria Detection. *Appl. Spectrosc.* **62**:922-931.
20. **Driskell JD, Seto AG, Jones LP, Jokela S, Dluhy RA, Zhao YP, Tripp RA.** 2008. Rapid microRNA (miRNA) detection and classification via surface-enhanced Raman spectroscopy (SERS). *Biosensors and Bioelectronics* **24**:917-922.
21. **Wu X, Xu C, Tripp RA, Huang Y-w, Zhao Y.** 2013. Detection and differentiation of foodborne pathogenic bacteria in mung bean sprouts using field deployable label-free SERS devices. *Analyst* **138**:3005-3012.
22. **Chaney SB, Shanmukh S, Dluhy RA, Zhao YP.** 2005. Aligned silver nanorod arrays produce high sensitivity surface-enhanced Raman spectroscopy substrates. *Appl. Phys. Lett.* **87**:031908.

23. **Driskell JD, Shanmukh S, Liu Y, Chaney SB, Tang XJ, Zhao YP, Dluhy RA.** 2008. The use of aligned silver nanorod Arrays prepared by oblique angle deposition as surface enhanced Raman scattering substrates. *J. Phys. Chem. C* **112**:895-901.
24. **Liu YJ, Chu HY, Zhao YP.** 2010. Silver Nanorod Array Substrates Fabricated by Oblique Angle Deposition: Morphological, Optical, and SERS Characterizations. *The Journal of Physical Chemistry C* **114**:8176-8183.
25. **Manjare M, Ting Wu Y, Yang B, Zhao Y-P.** 2014. Hydrophobic catalytic Janus motors: Slip boundary condition and enhanced catalytic reaction rate. *Appl. Phys. Lett.* **104**:-
26. **Arnon DI.** 1949. COPPER ENZYMES IN ISOLATED CHLOROPLASTS. POLYPHENOLOXIDASE IN BETA VULGARIS. *Plant Physiology* **24**:1-15.

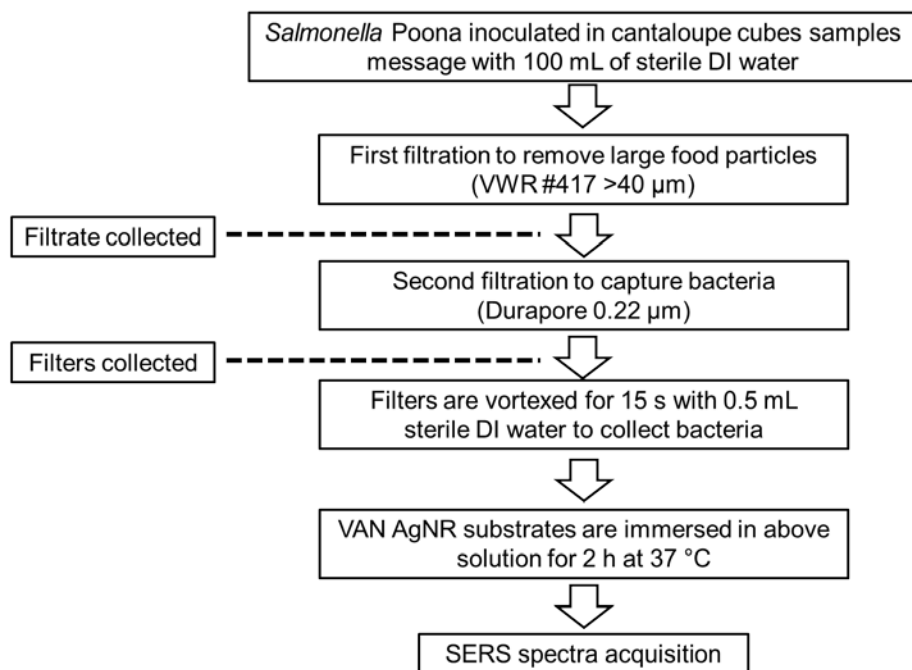


Figure 7.1 Flow chart of the three-step filtration procedure for the recovery of *Salmonella* Poona from cantaloupe cubes samples.

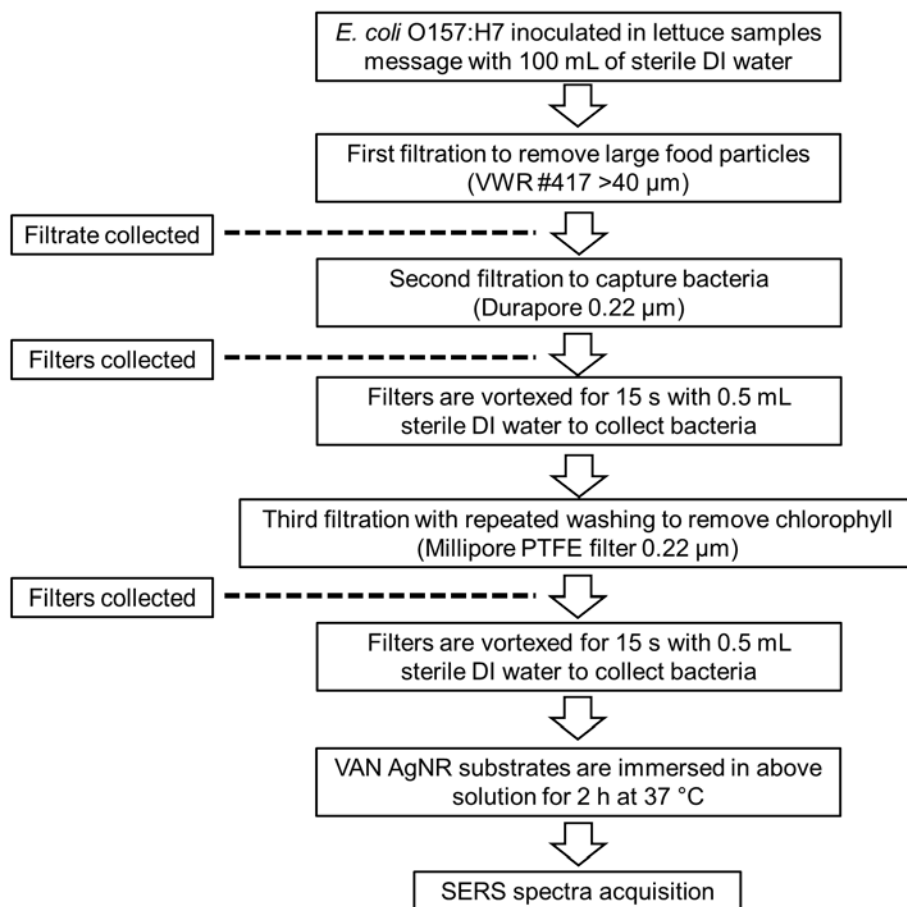


Figure 7.2 Flow chart of the three-step filtration procedure for the recovery of *E. coli* O157:H7 from lettuce samples.

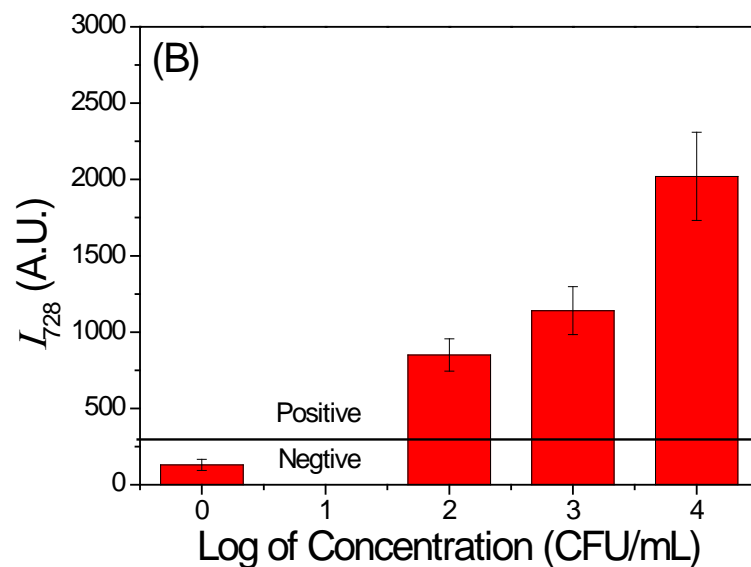
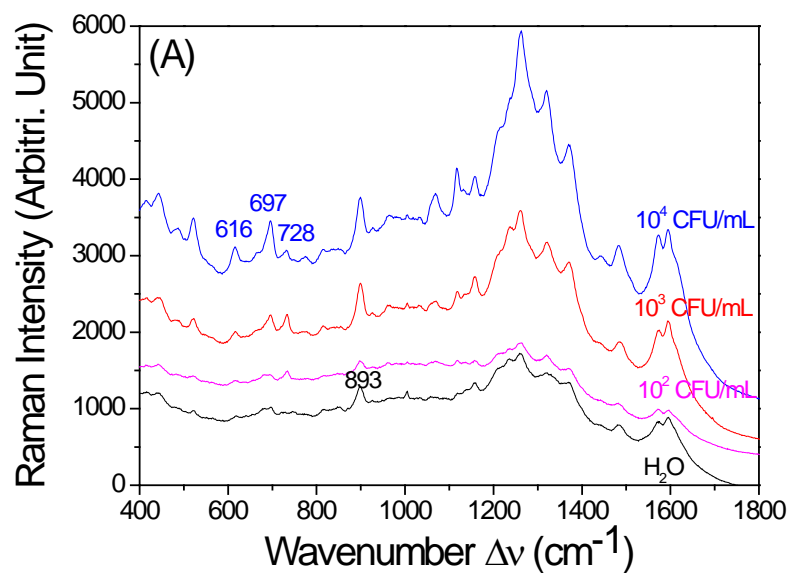


Figure 7.3 (A) The SERS spectra, and (B) the mean and standard deviation of the SERS peak intensity  $I_{728}$  of *Salmonella* Poona recovered from cantaloupe cube samples inoculated at different rates and sterile DI water inoculated in cantaloupe cube samples (control) followed by a two-step filtration.

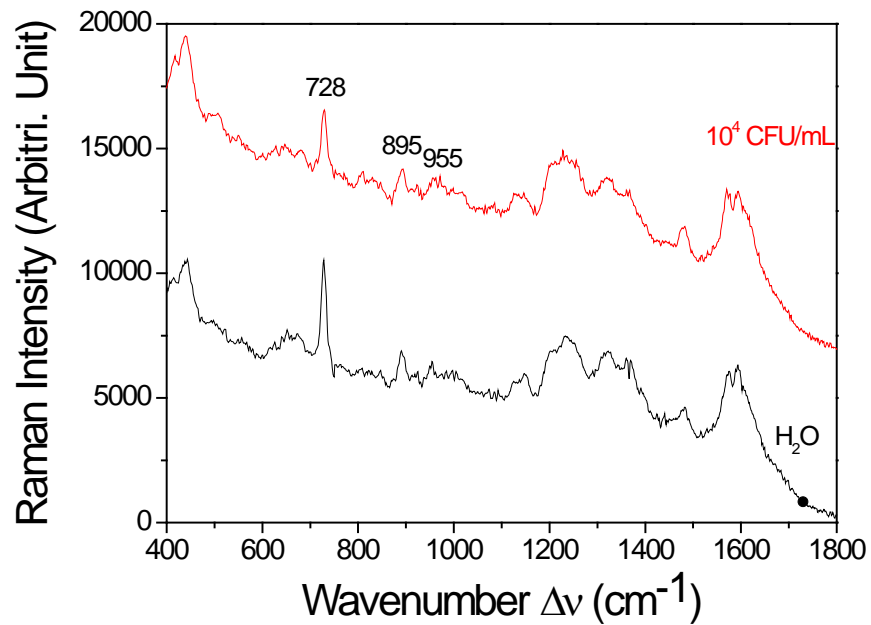


Figure 7.4 SERS spectra of *E. coli* O157:H7 recovered from lettuce samples inoculated at  $10^4$  CFU/ml and sterile DI water inoculated in lettuce samples followed by a two-step filtration.



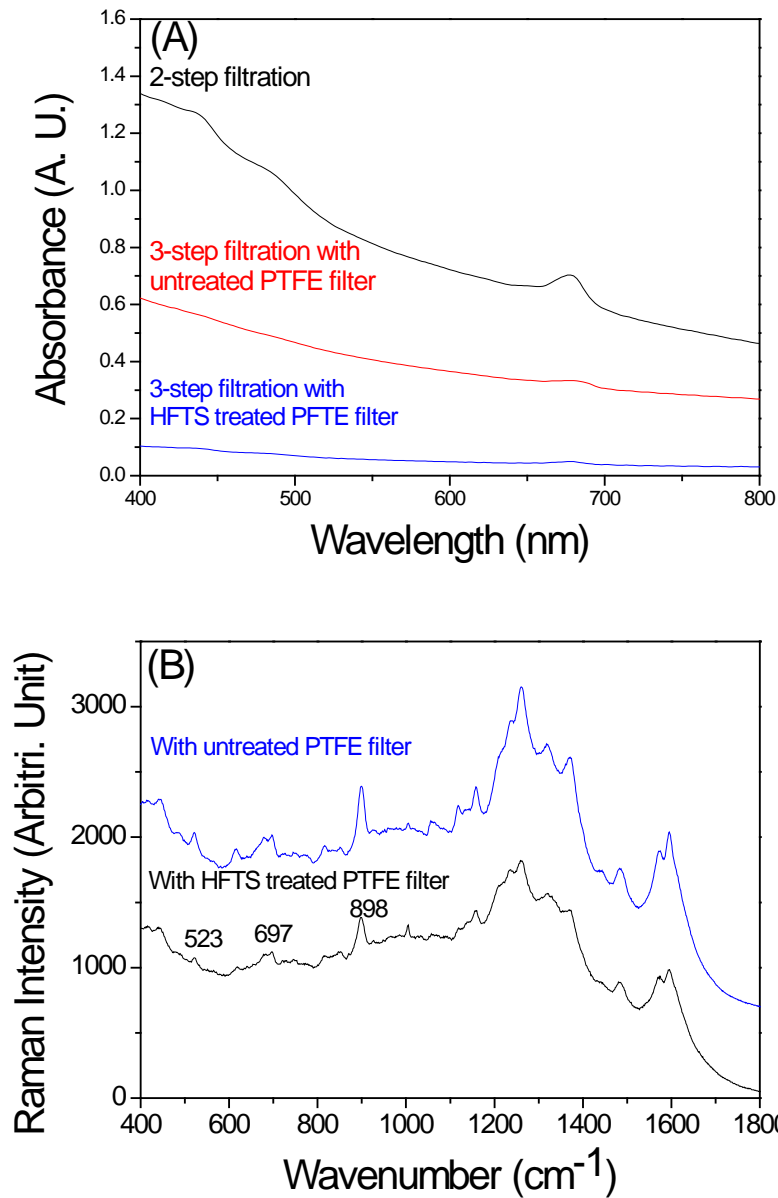


Figure 7.6 (A) The UV-Vis absorbance of the lettuce samples processed with different filtration methods. (B) SERS spectra of lettuce samples processed by three-step filtration methods. No bacterium was inoculated on the lettuce samples.

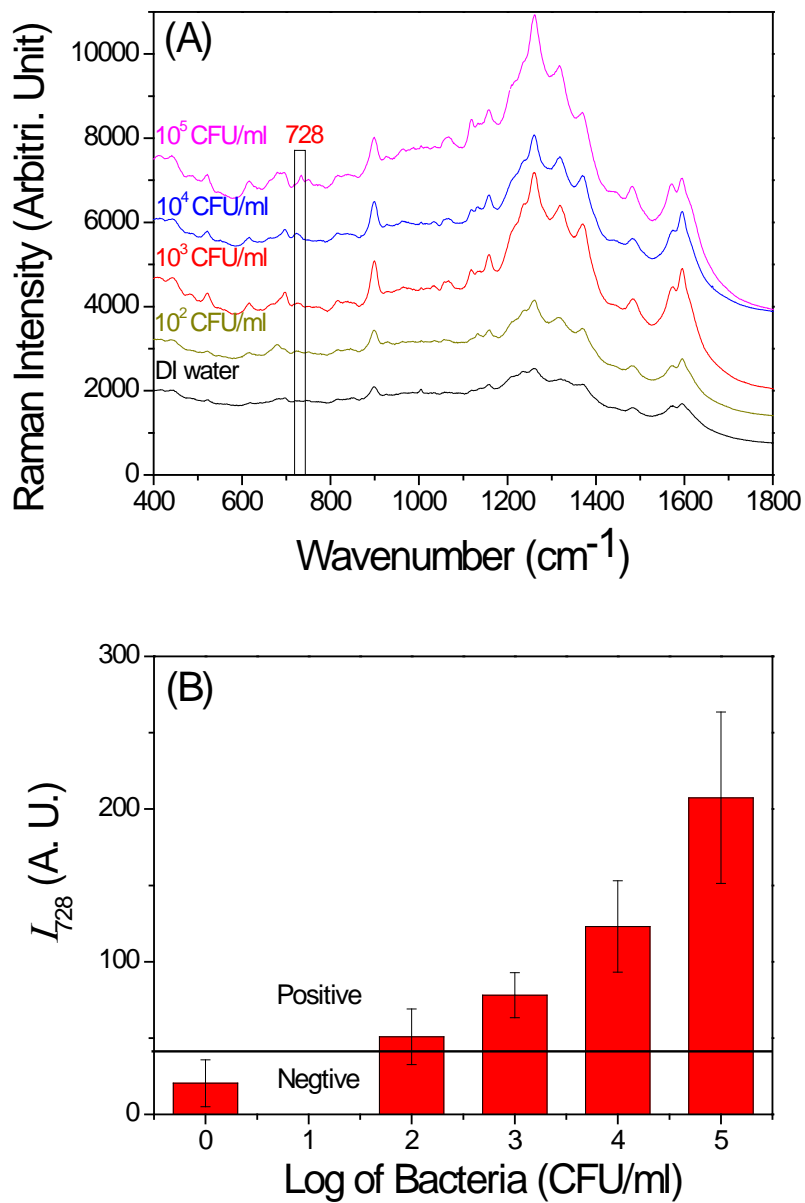


Figure 7.7 (A) The SERS spectra, and (B) the mean and standard deviation of the SERS peak intensity  $I_{728}$  of *E. coli* O157:H7 recovered from lettuce samples inoculated at different rates and sterile DI water inoculated in lettuce samples (control) followed by a three-step filtration method with HFTS treated PTFE filter.

Table 7.1 The bacteria concentration after each filtration steps for a three-step filtration with HFTS treated PTFE filter.

	Bacteria concentration (CFU/mL)	Recovery rate in this step (%)	Total recovery rate (%)
Initial	1.64E+09		
1st filtration	1.49E+09	90.85	90.85
2nd filtration	1.24E+09	83.22	75.61
3rd filtration	6.05E+08	48.79	36.89

## CHAPTER 8

### CONCLUSIONS AND FUTURE PERSPECTIVES

This dissertation has investigated the use of SERS as an analytical platform for culture free and label-free detection and differentiation of pathogenic bacteria based on the AgNR substrates. Through cell component experiments, we have obtained the fundamental understanding of the origin of the bacterial SERS spectra. Such understanding leads to a surface modification of the AgNR substrates with antibiotic, which result in better sensitivity as well as specificity. Such functionalized substrates, combined with simple filtration method can effectively detect and differentiate pathogenic bacteria from various fresh produce samples.

We have discussed the current controversy found in the scientific literature on the origins of the bacterial SERS signal, i.e. whether the signal is from bacteria cell or metabolic by-products, and where exactly the signal is coming from. Thorough investigation of each important cell component, we have concluded that the majority bacterial SERS signal are indeed from the bacterial cell itself, more specifically from the cell wall components, such as NAM, NAG, cell wall associated proteins. The genomic DNA may contribute to the bacterial SERS signal, if the bacteria cells are disrupted, but it would reduce the differentiation between different bacteria isolates. Inner cell proteins have little or none contribution to the SERS signal. In addition, the cell wall components are also critical in the differentiation of bacteria between different species. This knowledge leads us to develop a method to specifically enhance the signal from the bacteria cell wall, so as to improve the detection sensitivity and specificity.

We combined the SERS detection with two pre-concentration methods, filtration and centrifugation to detect bacteria in a large volume. These two methods effectively reduce the volume of the initial solution; therefore improve the sensitivity of the detection dramatically. Moreover, the centrifugation method achieved even distribution of the bacteria on AgNR substrates.

We have then systematically optimized the bacteria detection sensitivity by functionalizing the AgNR substrates with vancomycin. Such optimization was achieved by alternating the length of the AgNR and the concentration of the VAN coating on the substrate surface. The VAN coating on the AgNR substrates not only provides a layer to effectively capture the bacteria from the solution, with four times of more bacteria surface coverage, but also reduces the distance between bacteria and the AgNR surface to further enhance the SERS signal.

Such optimized VAN AgNR substrates have shown not only the improvement in bacteria detection sensitivity with LOD at  $10^4$  CFU/mL, but also in specificity, through the simultaneous analysis of 27 different bacteria isolates. VAN AgNR substrates protect the silver surface from the interferences of both the environment and the bacterial metabolic by-products, generate more reproducible bacterial SERS spectra, and can be used to differentiate bacteria using chemometric methods. The differentiation between different species, serotypes, and strains are obtained using VAN AgNR substrates with chemometric analysis. The discrimination between G+ and G- bacteria was also demonstrated with high sensitivity and specificity based on this SERS technique.

Since the sensitivity and the specific of the functionalized AgNR have been optimized, such substrates are used in detecting bacteria from real food samples, combined with filtration

method to pre-concentrate and separate the bacteria from the food matrix. The LOD of the system reaches 100 CFU/ml in initial solution or  $10^3$  CFU/g food samples in mung bean sprout and cantaloupe cube samples. Six different pathogens in mung bean sprout samples were detected and differentiated by their species and serotypes using PCA. For lettuce samples, due to the interference from chlorophyll, a more complicated three-step filtration procedure are used to eliminate the interferences from the food matrix and the LOD reaches  $10^3$  CFU/ml in initial solution or  $10^4$  CFU/g food samples. Such low LODs were achieved using both bench-top and handheld Raman spectrometers for mung bean sprout samples, suggesting the detection system is field deployable. Detection of pathogenic bacteria from fresh produce using both two-step filtration and three step filtration method is performed under 5 hours, indicating that the method is suitable for field applications

This dissertation presents the necessary technical foundation for the future development of SERS platform to detect low amounts of foodborne pathogens, with the potential to be used as an on-site pathogen detection method in the food industry. Equipped with the understanding and knowledge bestowed in this dissertation, such a proposition can be realized and possible future developments are below presented.

The detection of bacteria using SERS is performed based on the knowledge of standard spectra of target bacteria. So a library of pathogenic bacteria that are often associated with foodborne outbreaks needs to be established. In this dissertation, although we try our best to cover as many common pathogenic bacteria as possible, it is impossible to perform the detection on each and every one of them. However, the established method in this dissertation can be easily expanded to the detection of other bacteria of interests beyond the scope of this dissertation. Similarly, more fresh produce samples can also be tested use the same procedure.

However, when the food samples are expanded to meat and poultry products, careful consideration of the pre-processing methods are required. Meat samples are far more complicated matrix than fresh produce, and the large molecules in meat, such as lipids, proteins, and carbohydrates, may easily block the pore of the filter. Hence, the filtration methods to process the sample developed in this dissertation may not be successful in detecting bacteria in meat samples, and one need to investigate and develop a more appropriate processing method prior to SERS detection.

In order to makes the SERS detection platform ready for commercial use, the system needs to be integrated into a miniature assay. An appropriate way to integrate pre-processing method with SERS detection is to develop a microfluidic device. A dielectrophoresis (DEP) based microfluidic separation/ concentration may be a promising method to effectively separate and concentrate the pathogenic bacteria from food samples. Combining sensitive detection of SERS and the cell sorting capability of DEP may lead to the development of commercial ready lab-on-chip device.

Although the SERS system we developed with VAN AgNR is highly sensitive, rapid, and field deployable, one thing needs to be considered is the cost of the test if a new method wants to compete with the current detection methods. The commercial AgNR substrates are sold for \$65 a piece by Argent Diagnostics, which is far more expensive than the culture media or commercial ELISAs. Since the AgNR substrates are made of pure silver, the cost of fabrication depends on the price of silver, which keeps increasing for the past several years. One way to lower the cost of fabrication is to lower the silver contents in the substrates. Since SERS only happens at the nanostructure surface, one can fabricate the inner core of the nanorod with SiO<sub>2</sub>, and then coat

the nanostructure with silver shell later. Systematically investigations of the core-shell nanorod structure are required to achieve the maximum Raman enhancement factor.

In this dissertation, all the bacteria detection and differentiation are performed with individual bacteria isolates, and no bacterial cocktail are tested. Such detection and differentiation are based on the intrinsic bacterial SERS signal. As discussed in Chapter 1, the intrinsic SERS detection of bacteria is more complicated in bacterial mixtures. The detection and differentiation of bacteria isolates in a bacterial mixture can be realized by the combination of SERS and immunological reaction, such as antibody and aptamer, or by the SERS DNA probe. Unlike the Immune-SERS sensor discussed in the Chapter 2, which all used external Raman labels, one can detect the bacteria by monitoring the SERS spectral change before and after the immunological reaction between antibody and the antigens of the bacteria. This will provide a more specific detection and differentiation of the bacteria.

## APPENDIX A

### SUPPLEMENTARY MATERIAL FOR CHAPTER 5

#### A.1 Optimizing AgNR substrates for detection of bacteria

##### A.1.1 Optimizing AgNR length

Conventionally, AgNR substrates have been developed with a length maximized for chemical detection and sensing, e.g. BPE (Trans-1,2-bis(4-pyridyl)ethylene) and Rhodamine 6G (R6G), which allows small chemical molecules to diffuse in between the nanorods and reside in the small gap<sup>1</sup>. Compared to small chemical molecules, bacteria are much larger and the conventional AgNR substrates produce a relatively weak SERS signal of bacteria due to limited contact between bacteria and substrate surface which only takes place on the tips of the Ag nanorods. Therefore the length of the AgNR may need to be optimized in order to acquire the maximum SERS intensity and improve the LOD for bacteria. The length of the AgNR is proportional to the thickness the AgNR layer which is monitored by the QCM *in situ* during the deposition. To optimize the SERS substrates, AgNR of 200, 300, 400, 500, 600, 700, 800, and 900 nm QCM reading were deposited. Then a droplet of 10  $\mu\text{L}$   $10^8$  CFU/ml *E. coli* O157:H7 was applied to each of the substrates and their SERS spectra were collected under the same conditions and compared, as shown in Figure A.1A. The spectra of *E. coli* has significant peaks at  $\Delta\nu = 652\text{ cm}^{-1}$  (C-O-C from tyrosine),  $728\text{ cm}^{-1}$  (ring breathing and N-H wagging mode from adenine),  $893\text{ cm}^{-1}$  (C-O-C stretch from carbohydrates), and  $955\text{ cm}^{-1}$  (C-C stretching), which are consistent with previous reports<sup>2,3</sup>. These peaks for *E. coli* O157:H7 samples are present for all

AgNR substrates with thickness from 400 nm to 900 nm, but not for 200 nm and 300 nm substrates. For the 200 and 300 nm substrates, the shorter AgNR length makes the shape of the substrate more like an islanded film rather than nanorods and the SERS signal enhancement is limited. In order to determine the optimal AgNR length for bacteria detection, we quantified the intensity of the SERS spectra by using the peak intensity at  $\Delta\nu = 728 \text{ cm}^{-1}$  ( $I_{728}$ ), which is the most significant peak from *E. coli* O157:H7 samples. The  $I_{728}$ , obtained by peak fitting, was plotted against the AgNR thickness in Figure A.1B. As the length of the AgNR increased, the SERS intensity of *E. coli* O157:H7 increased, and it reached a maximum intensity at 600 nm AgNR thickness (QCM reading). The SEM images of the 600 nm AgNR are shown in Figure S.2. At 600 nm, the AgNR has an average diameter of 52 nm, an average length of 487 nm, and an average density of 18 rods/ $\mu\text{m}^2$ . The diameter of the bacteria is generally around 0.5  $\mu\text{m}$ , so this AgNR length does not exceed the diameter of the bacteria. This morphology has enough “hot spots” to generate strong SERS signal, yet not too long to decrease the SERS signal. The morphology of the AgNR at other different thickness was previously reported <sup>4</sup>. Thus, the 600 nm-thick AgNR layer was found to be the optimal substrate for bacterial detection.

### **A.1.2 Optimizing AgNR functionalization using vancomycin**

The mechanism of affinity capture of bacteria by vancomycin modified nanoparticles is studied by Kell *et al* <sup>5</sup>. And Liu *et al.*, demonstrated that coating the Ag nanoparticles with vancomycin (VAN) provides a layer of capture agent for bacteria which increases the detection sensitivity of bacteria <sup>6</sup>. Theoretically, coating the AgNR substrates with vancomycin would play the same role, and the optimal condition of such a coating on AgNR was explored in this study. The 600 nm AgNR substrates were coated with six different concentrations of vancomycin (0.05, 0.1, 0.2, 0.5, 1, 2, 5, 10, and 20 mM). After vancomycin coating, these functionalized substrates

was immersed in 0.5 ml of  $10^8$  CFU/ml *E. coli* O157:H7 solution for 2 hours at 37 °C with shaking at 200 rpm. The inoculated substrates were then rinsed with DI water, followed by drying with Nitrogen. SERS measurements were carried out under the same conditions after drying. In order to determine which concentration of vancomycin would yield the greatest SERS intensity of bacteria, again we used the  $I_{728}$  peak from *E. coli* O157:H7 to quantify the SERS response of the bacteria on the VAN substrates, and Figure A.3 shows  $I_{728}$  as a function of the vancomycin concentration  $C_v$ . Similar to results from Liu *et al.*,<sup>6</sup> the SERS intensity of the bacteria increased as the concentration of vancomycin increased until it reached a maximum at 1 mM. Ellipsometry was performed on a Ag thin film with 600 nm thickness (data not shown), and we found that at 1mM, the surface coverage of the vancomycin was close to 1. Therefore when the concentration of vancomycin is less than 1mM, the amount of bacteria captured on the AgNR surface will be determined by the amount of vancomycin on the surface, i.e., the surface coverage of vancomycin, so the SERS intensity increases with vancomycin concentration initially as shown in Figure A.3.

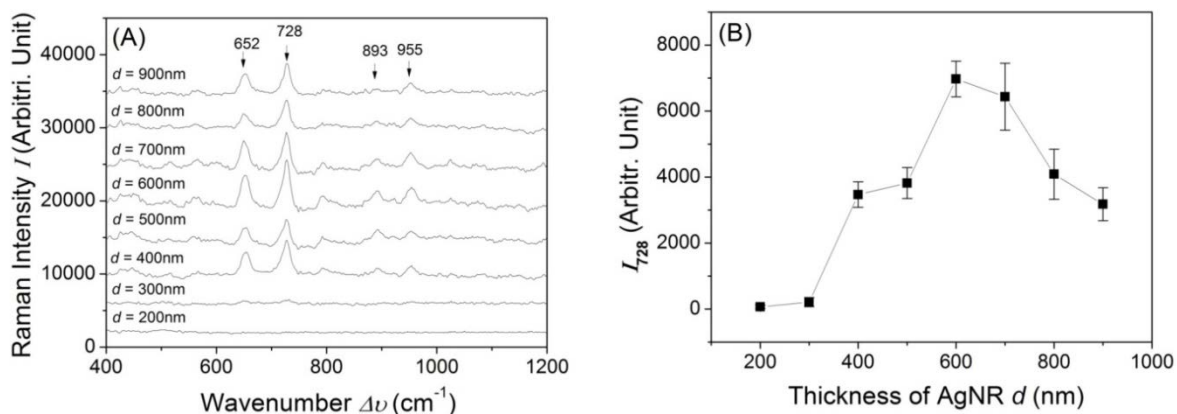


Figure A.1 (A) SERS spectra and (B) the SERS peak intensity  $I_{728}$  of  $10^8$  CFU/ml *E. coli* O157:H7 samples on AgNR with QCM thickness  $d$  of 200, 300, 400, 500, 600, 700, 800, and 900 nm, respectively. Spectra were measured by Enwave Raman system.

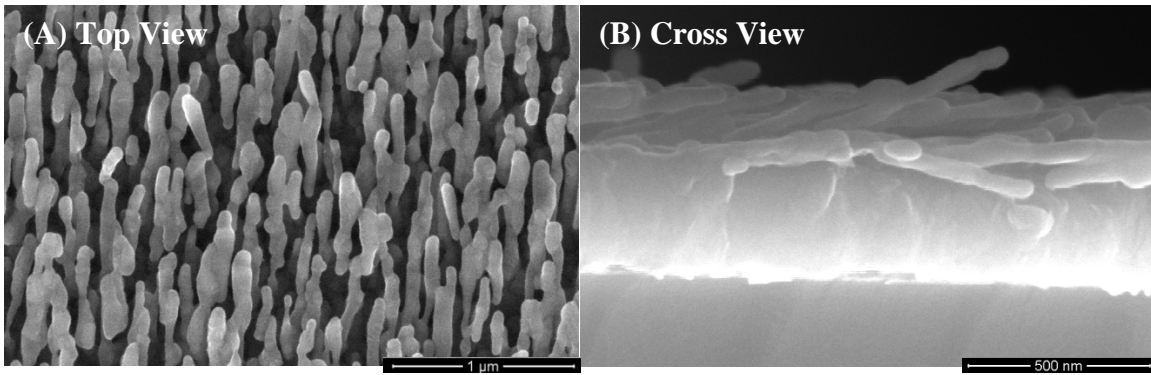


Figure A.2 SEM images of AgNR with 600 nm thickness (QCM reading). (A) Top view. (B) Cross view.

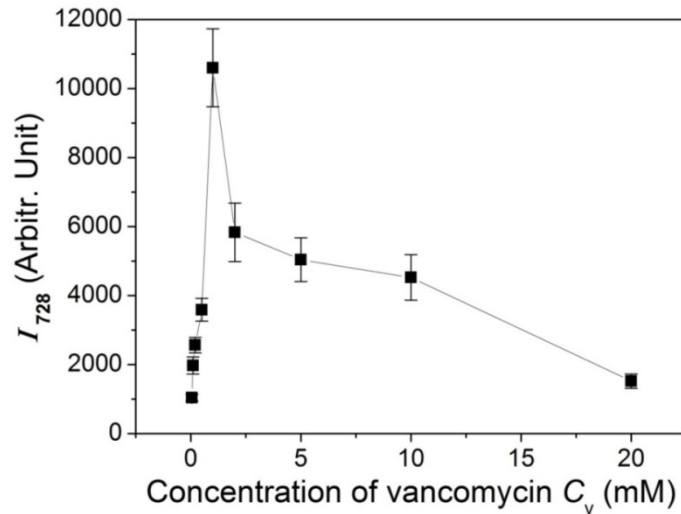


Figure A.3 The change of the SERS peak intensity  $I_{728}$  of  $10^8$  CFU/ml *E. Coli* O157:H7 as a function of the Vancomycin concentration  $C_v$ .

When the concentration of the vancomycin exceeds the 1mM, there will be multilayer vancomycin coating on AgNR surface. Although the amount of bacteria captured could stay the same, but some of them are captured by vancomycin molecules on the second layer. The SERS signal is very sensitive to the distance, and their relationship is approximately  $I \propto (1/R)^{12}$ , where  $I$

is the SERS intensity,  $R$  is the distance between the Ag surface and the absorbed molecule(s) <sup>7</sup>. Thus the bacteria captured by second layer would contribute less SERS intensity compared to those from the first layer. Thus, with the increase of the vancomycin concentration, more vancomycin molecules are on the second layer, less are on the first layer, then the effective SERS signal decreases. If third layer or fourth layer of vancomycin is built, the SERS signal will become even weaker. Thus, the maximum  $I_{728}$  is found when 1 mM vancomycin was used, and is determined to be the optimal vancomycin treatment for the 600 nm AgNR.

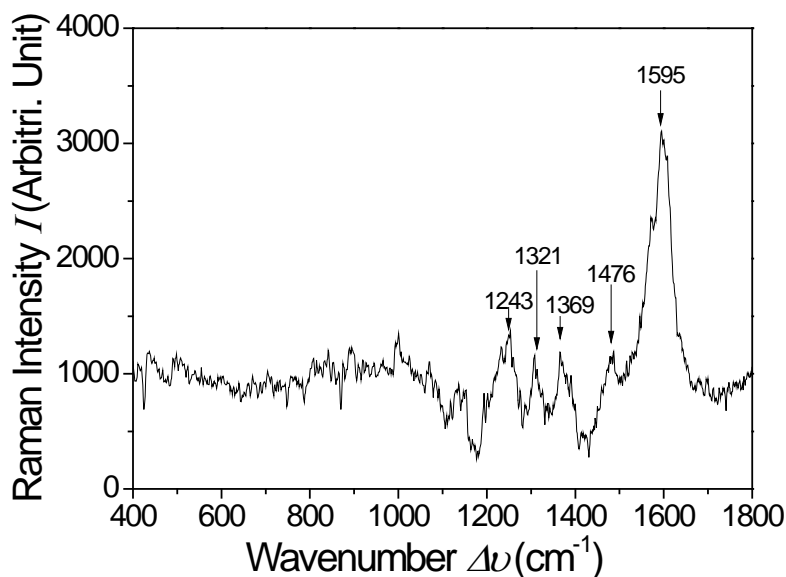


Figure A.4 The SERS spectrum of the 1mM Van-coated 600 nm AgNR substrates collected by using Enwave Raman spectrometer. The spectrum is baseline-corrected, and the significant peaks are identified.

### **A.1.3 Background of the optimized AgNR substrates**

The background SERS spectrum of the optimized vancomycin coating (1mM) on 600 nm-thick AgNR substrates is shown in Figure A.4. The SERS peaks of the VAN-coated substrates are identified at  $\Delta\nu = 1243, 1321, 1369, 1476, 1595 \text{ cm}^{-1}$ , respectively, and these peaks are consistent with previously reported Raman peaks of vancomycin<sup>8</sup>. Those peaks should be excluded from any bacteria SERS spectra on the VAN-coated substrates.

### **A.2 Detection of *E. Coli* O157:H7 in mung bean sprouts using a handheld Raman spectrometer**

In order to use our detection platform in field applications, the system should be light-weight and portable. The FirstDefender RM is a handheld Raman spectrometer that is easy to handle and suitable for field use because of its tough design and ease of mobility. To validate the use of this handheld Raman spectrometer we used it to acquire SERS spectra in conjunction with the previously described procedures for inoculation and filtration. Figure A.5 shows the SERS spectra of *E. coli* O157:H7 recovered from inoculated mung bean sprout samples ( $10^2, 10^3, 10^4$ , and  $10^5$  CFU/ ml) using the handheld Raman spectrometer. Similar to the results acquired using the Enwave spectrometer in Figure 5.3A (see Chapter 5), significant peaks for *E. coli* O157:H7 SERS spectra collected by FirstDefender RM were found at  $\Delta\nu = 654, 730, 797, 895, \text{ and } 957 \text{ cm}^{-1}$ , with peak intensity increasing as the bacterial concentration increased. For the  $10^2$  CFU/ml sample, the spectrum has all these signature peaks of the *E. coli* O157:H7, thus the LOD for *E. coli* O157:H7 using the handheld Raman spectrometer should also be  $10^2$  CFU/ml.

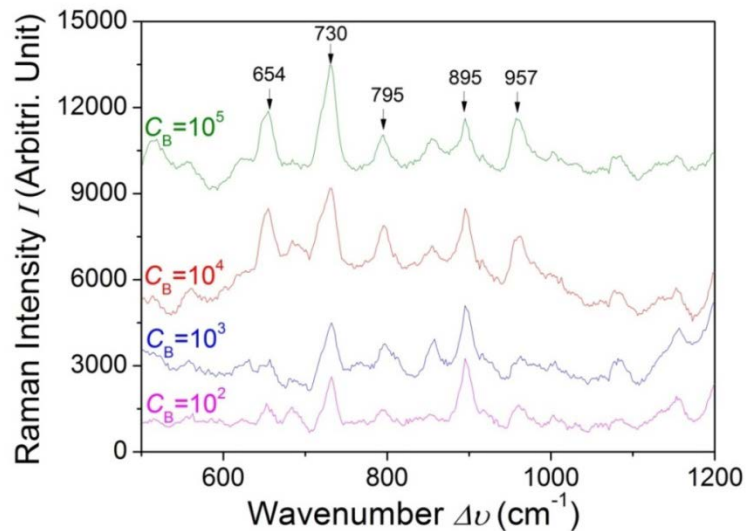


Figure A.5 SERS spectra of *E. Coli* O157:H7 recovered from mung bean sprout samples inoculated at different rates ( $C_B = 10^2, 10^3, 10^4, 10^5$  CFU/ml) followed by a two-step filtration, collected using the FirstDefender RM handheld Raman spectrometer.

In order to see the spectral differences statistically, we also performed PCA and PLS-DA analysis. Figure A.6A shows the plot of PC1 versus PC2. Samples inoculated with *E. coli* O157:H7 at rates as low as  $10^2$  CFU/ml formed a cluster separate from the control samples. As shown in Figure A.6B, PLS-DA also confirmed the differences between the bacteria sample spectra and the control. Furthermore, the PLS-DA plot discriminates spectra between the control and bacterial samples inoculated over  $10^2$  CFU/ml with 100% sensitivity and specificity. PCA and PLS-DA indicate that VAN-coated substrates can detect as low as  $10^2$  CFU/ml or  $10^3$  CFU/g *E. coli* O157:H7 in mung bean sprout samples using the handheld Raman spectrometer.

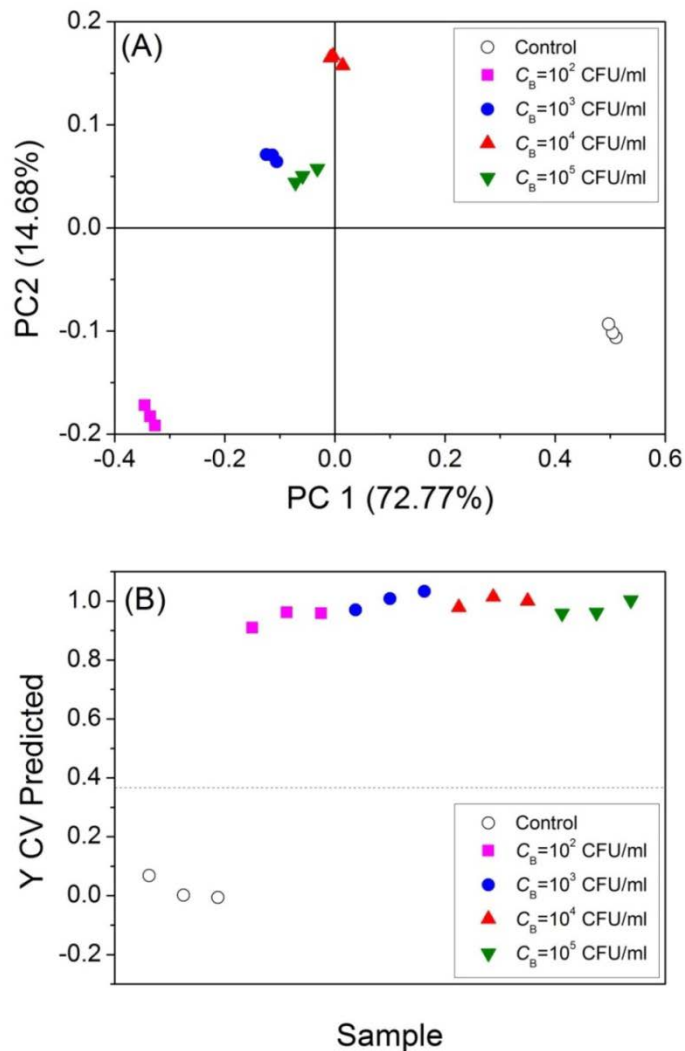


Figure A.6 (A) PCA and (B) PLS-DA plot of SERS spectra of *E. coli* O157:H7 recovered from mung bean sprout samples inoculated at different bacteria concentrations ( $C_B = 10^2, 10^3, 10^4, 10^5$  CFU/ml) and sterile DI water inoculated in mung bean sprout samples (control) followed by a two-step filtration. Spectra were collected by the FirstDefender RM handheld Raman spectrometer.

## References

1. J. D. Driskell, S. Shanmukh, Y. Liu, S. B. Chaney, X. J. Tang, Y. P. Zhao and R. A. Dluhy, *J. Phys. Chem. C*, 2008, **112**, 895-901.
2. C. Fan, Z. Hu, A. Mustapha and M. Lin, *Appl Microbiol Biotechnol*, 2011, **92**, 1053-1061.
3. H. Chu, Y. Huang and Y. Zhao, *Appl. Spectrosc.*, 2008, **62**, 922-931.
4. Y. Liu and Y. Zhao, Proc. SPIE 7757, Plasmonics: Metallic Nanostructures and Their Optical Properties VIII, 2010.
5. A. J. Kell, G. Stewart, S. Ryan, R. Peytavi, M. Boissinot, A. Huletsky, M. G. Bergeron and B. Simard, *ACS Nano*, 2008, **2**, 1777-1788.
6. T. Y. Liu, K. T. Tsai, H. H. Wang, Y. Chen, Y. H. Chen, Y. C. Chao, H. H. Chang, C. H. Lin, J. K. Wang and Y. L. Wang, *Nature communications*, 2011, **2**, 538.
7. E. C. Le Ru and P. G. Etchegoin, *Principles of Surface-Enhanced Raman Spectroscopy and Related Plasmonic Effects*, Elsevier Science, 2009.
8. R. C. Lora, L. Silveira, S. R. Zamuner and M. T. T. Pacheco, *Spectroscopy*, 2011, **25**, 103-112.

## APPENDIX B

### SUPPORTING INFORMATION FOR CHAPTER 6

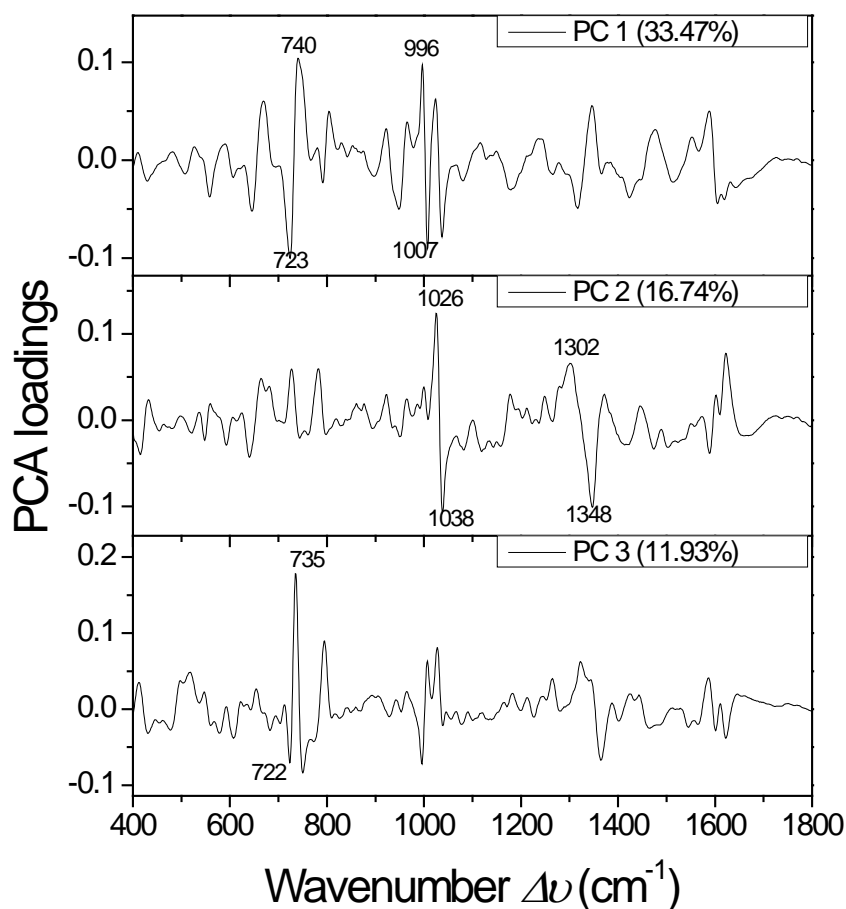


Figure B.1 PCA loading score plot based on the bacterial SERS spectra generated on pristine substrates which corresponds to the PCA plot in Figure 6.1B. The large absolute value on the y-axis suggests heavier weight in the analysis. The SERS peaks with heavy weight in each PC are numbered and the percentages associated with each PC represent the variances explained with that PC.

Table B.1 Literature summary on the use of chemometric analysis to differentiate bacteria based on SERS technique.

Chemometric methods	SERS Substrates	Bacterial samples	Number of bacteria	Results and Conclusions	Ref
DFA-HCA; PCA	Silver Colloid	Clinical bacterial isolates from patients with UTI ( <i>Escherichia coli</i> ; <i>Klebsiella oxytoca</i> ; <i>Klebsiella pneumoniae</i> ; <i>Citrobacter freundii</i> ; <i>Enterococcus spp.</i> and <i>Proteus mirabilis</i> )	6 species, 5 strains	Discriminate between different species, and discriminate <i>Escherichia coli</i> on strain level	(1)
PCA, HCA, and DFA based on the “barcoding method”	Au-nanoparticle-covered SiO <sub>2</sub> substrate	<i>Bacillus thuringiensis</i> ; <i>Bacillus cereus</i> ; <i>Bacillus anthracis</i> ; <i>Bacillus licheniformis</i> ; <i>Mycobacterium smegmatis</i> ; <i>Mycobacterium fortuitum</i> ; <i>Escherichia coli</i> ; <i>Salmonella typhimurium</i>	8 species	Species and strains separation	(2)
PCA, HCA, and PLS-DA	AgNR	<i>Mycoplasma pneumonia</i> and clinical throat swab	1 specie, 3 strains	The throat swab samples spiked with <i>Mycoplasma. pneumonia</i> and true clinical throat swab samples were correctly classified	(3)
PCA	Internal deposition of silver nanoparticles	<i>Staphylococcus epidermidis</i> , <i>Escherichia coli</i> O157:H7	2 species	Differentiate <i>Staphylococcus. epidermidis</i> , <i>Escherichia coli</i> O157:H7, and their 1:1 ratio mixer	(4)
PCA	Au ion doped SiO <sub>2</sub> sol-gel	<i>Klebsiella pneumoniae</i> , <i>Escherichia coli</i> , <i>Pseudomonas. aeruginosa</i> , <i>Enterococcus faecalis</i> , <i>Staphylococcus. aureus</i> ,	4 species, 2 strains	Discriminate SERS spectra of different bacteria and the culture media in which they are grown	(5)
PCA and SVM	Silver colloid incorporates with microfluidic device	<i>Escherichia coli</i>	9 strains	Classification between strains with high correct rate	(6)
PCA	Silver nanoparticles	<i>Enterococcus faecalis</i> ; <i>Streptococcus pyogenes</i> ; <i>Acinetobacter baumannii</i> ; <i>Klebsiella pneumoniae</i>	4 species	Discrimination between G+ and G- bacterial genera	(7)

Table B.1 continued

PCA, LDA, and HCA	Roughened gold coated glass slides	<i>Arthrobacter</i> strains	14 strains	Distinct molecular differences on the surface of fourteen closely related <i>Arthrobacter</i> strains; liquid and solid cultures are distinguished	(8)
PCA	Magnetic–plasmonic Fe <sub>3</sub> O <sub>4</sub> –Au core–shell nanoparticles (Au-MNPs)	<i>Acinetobacter. calcoaceticus</i> , <i>Escherichia coli</i> K12, and <i>Pseudomonas. aeruginosa</i>	3 species	Discriminate between species	(9)
PCA and HCA	Gold nanoparticles	<i>Salmonella typhimurium</i> ATCC 50013, <i>Salmonella</i> O7HZ10, <i>Shigella boydii</i> CMCC51514, <i>Shigella sonnei</i> CMCC51529, <i>Shigella dysenteriae</i> CMCC51252, <i>Citrobacter freundii</i> ATCC43864, and <i>Enterobacter sakazakii</i> 154	6 species, 2 strains	Discriminate between species and serotypes	(10)
PCA	AgNR	Generic <i>Escherichia coli</i> ; <i>Escherichia coli</i> O157:H7 ; <i>Staphylococcus aureus</i> ; <i>Salmonella typhimurium</i> 1925-1 poultry isolate , and <i>Escherichia. coli</i> DH 5a	3 species, 3 serotypes	Distinguish between different species, differentiate pure cell samples from mixed cell samples, and classify different bacteria strains.	(11)
PCA and PLS-DA	Vancomycin coated AgNR	<i>Salmonella</i> Anatum, <i>Salmonella</i> Cubana, <i>Salmonella</i> Stanley, <i>Salmonella</i> Enteritidis, <i>Escherichia coli</i> O157:H7, and <i>Staphylococcus epidermidis</i>	3 species, 4 serotypes	Differentiate between species and serotypes in mung bean sprout samples	(12)

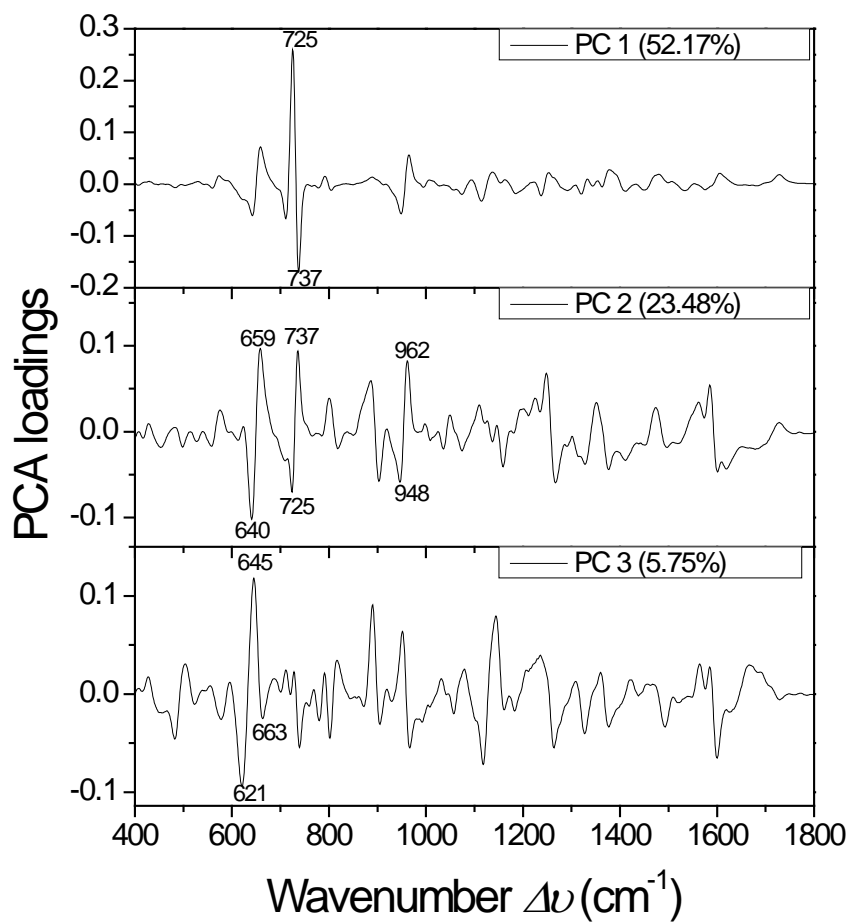


Figure B.2 PCA loading score plot based on the bacterial SERS spectra generated on VAN AgNR substrates which corresponds to the PCA plot in Figure 6.2B. The large absolute value on the y-axis suggests heavier weight in the analysis. The SERS peaks with heavy weight in each PC are numbered and the percentages associated with each PC represent the variances explained with that PC.

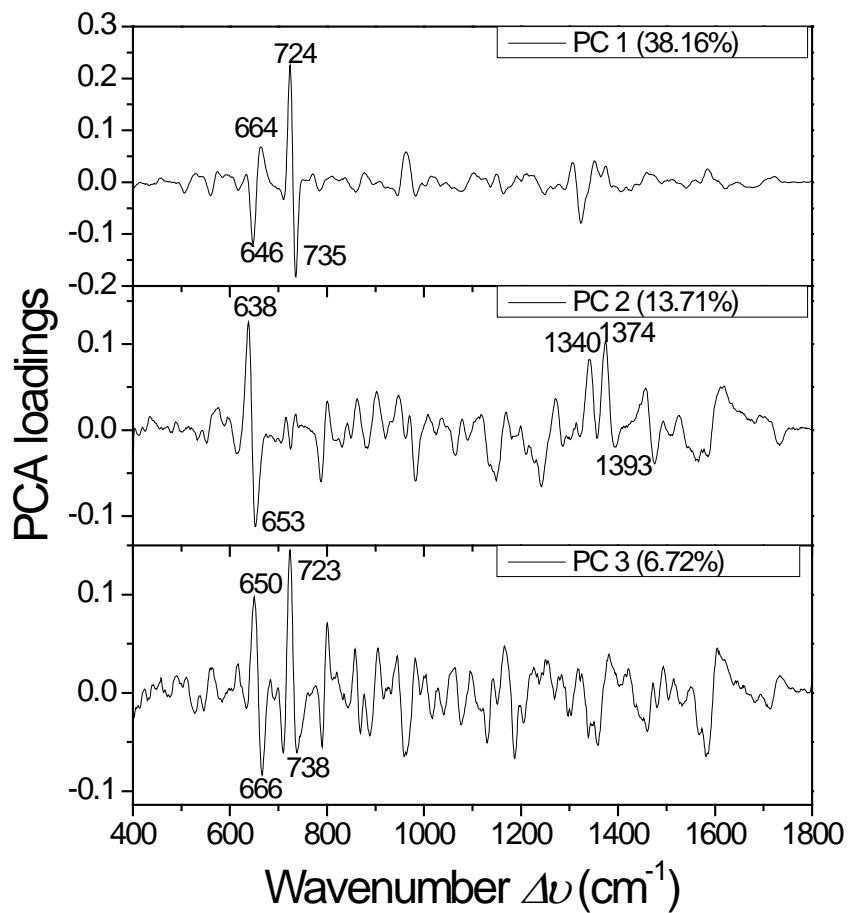


Figure B.3 PCA loading score plot based on the bacterial SERS spectra of five different serotypes of *Salmonella* species generated on VAN AgNR substrates which corresponds to the PCA plot in Figure 6.4A. The large absolute value on the y-axis suggests heavier weight in the analysis. The SERS peaks with heavy weight in each PC are numbered and the percentages associated with each PC represent the variances explained with that PC.

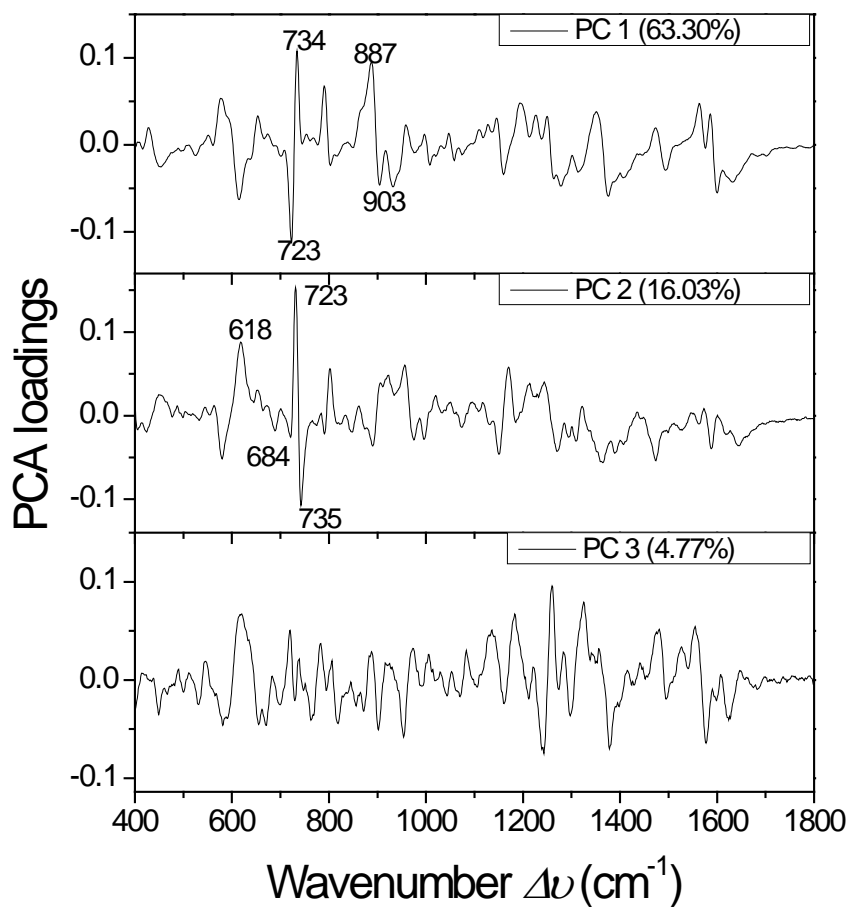


Figure B.4 PCA loading score plot based on the bacterial SERS spectra of five different strains of *Staphylococcus aureus* (SA) generated on VAN AgNR substrates which corresponds to the PCA plot in Figure 6.5A. The large absolute value on the y-axis suggests heavier weight in the analysis. The SERS peaks with heavy weight in each PC are numbered and the percentages associated with each PC represent the variances explained with that PC.

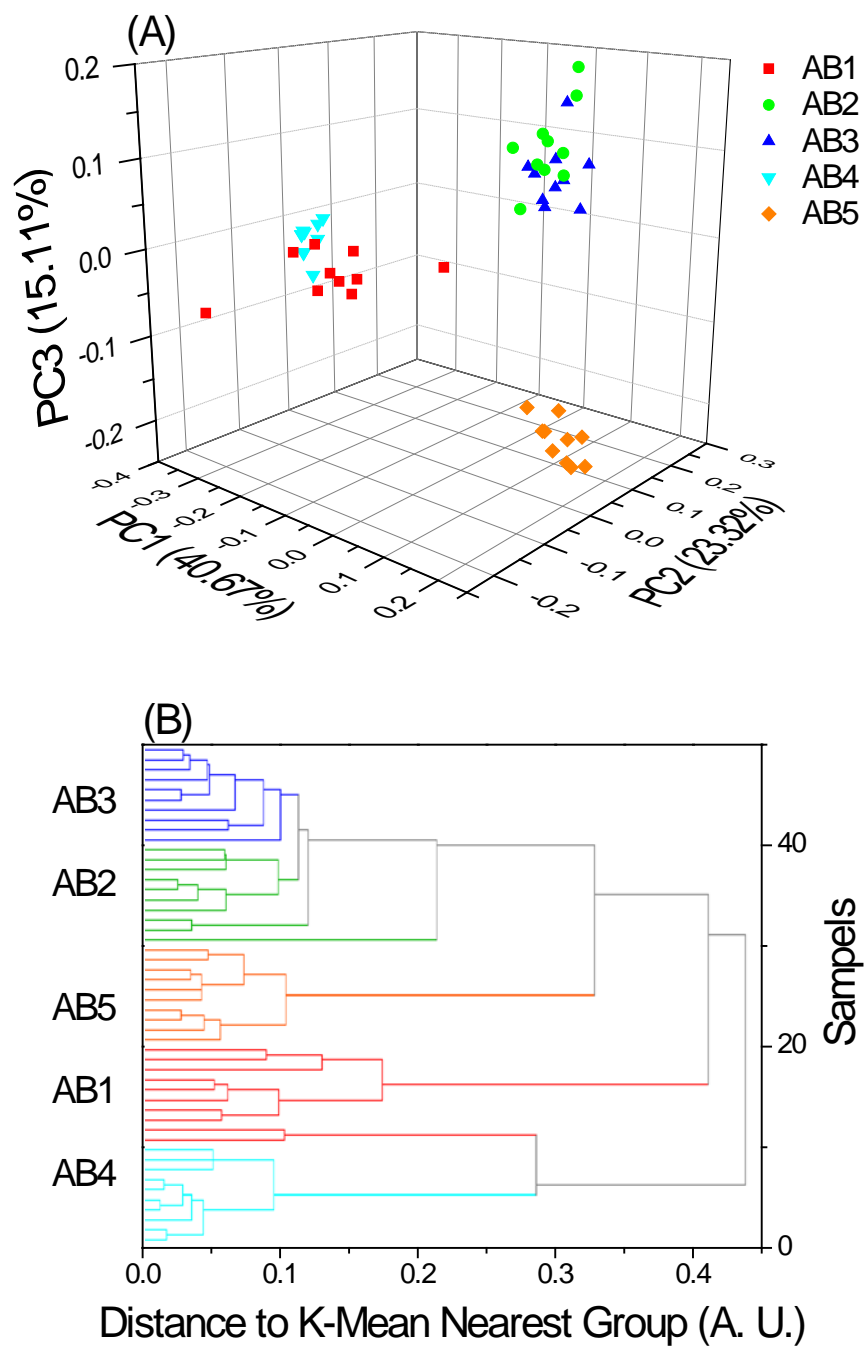


Figure B.5 Differentiation of five different strains of *Acinetobacter baumannii* (AB) based on the chemometric analysis of the SERS spectra generated on the VAN AgNR substrates. (A) The 3D PCA score plot and (B) HCA plot.

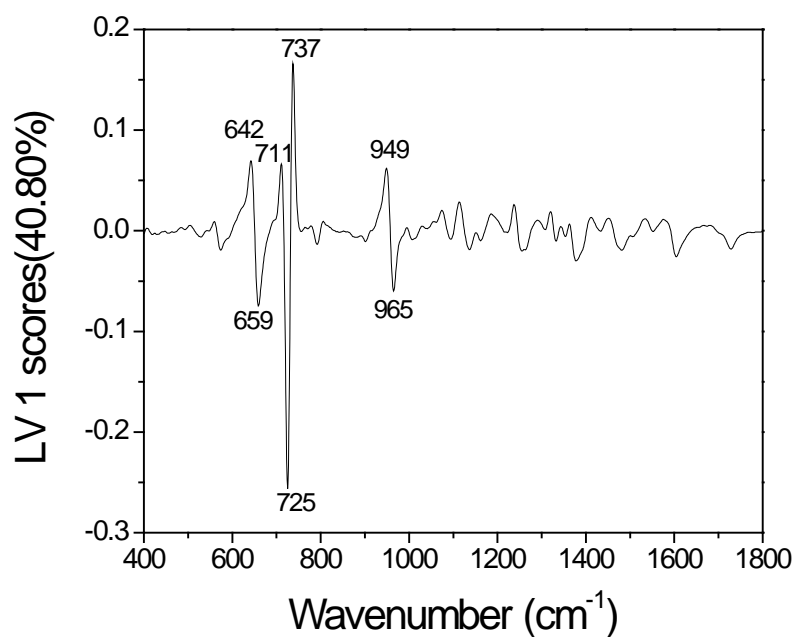


Figure B.6 PLS-DA loading score plot for classification between G+ and G- bacteria based on the spectra generated on VAN AgNR substrates which corresponds to the PLS-DA plot in Figure 6.6B. The large absolute value on the y-axis suggests heavier weight in the analysis. The SERS peaks with heavy weight are numbered.

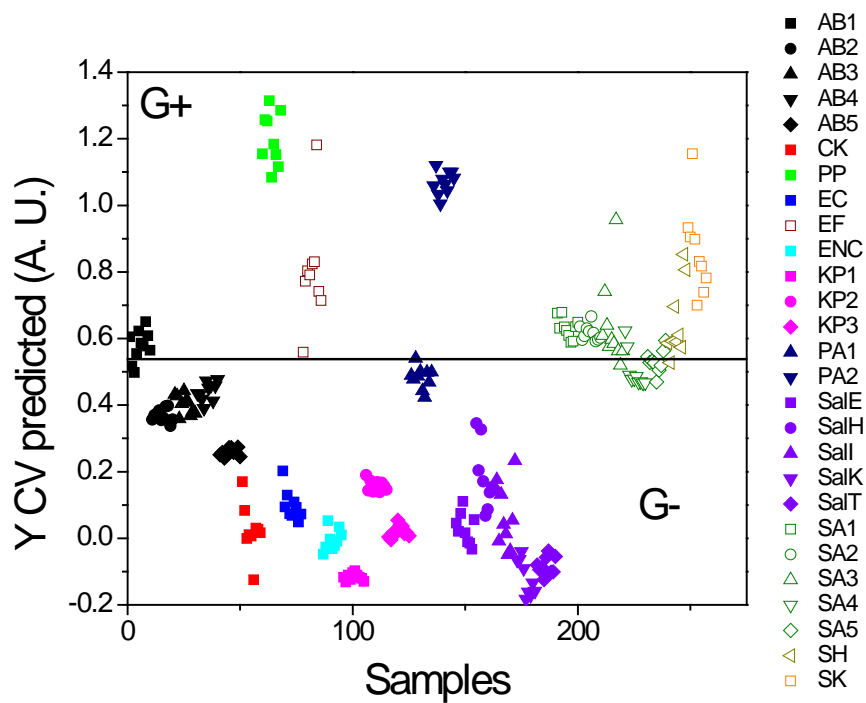


Figure B.7 PLS-DA based on the bacterial SERS spectra generated on the pristine AgNR substrates. G+ bacteria are indicated as unfilled symbols and the G- bacteria are indicated as filled symbols. Bacteria of the same species, regardless of the strains and serotypes, are represented by symbols of the same color. Black horizontal line indicates the threshold generated by the model to discriminate G+ and G- bacteria.

## References

1. **Jarvis RM, Goodacre R.** 2004. Discrimination of Bacteria Using Surface-Enhanced Raman Spectroscopy. *Analytical Chemistry* **76**:40-47.
2. **Patel IS, Premasiri WR, Moir DT, Ziegler LD.** 2008. Barcoding bacterial cells: a SERS-based methodology for pathogen identification. *J. Raman Spectrosc.* **39**:1660-1672.
3. **Neyrolles O, Hennigan SL, Driskell JD, Dluhy RA, Zhao Y, Tripp RA, Waites KB, Krause DC.** 2010. Detection of *Mycoplasma pneumoniae* in Simulated and True Clinical Throat Swab Specimens by Nanorod Array-Surface-Enhanced Raman Spectroscopy. *PLoS ONE* **5**:e13633.
4. **Fan C, Hu Z, Mustapha A, Lin M.** 2011. Rapid detection of food- and waterborne bacteria using surface-enhanced Raman spectroscopy coupled with silver nanosubstrates. *Appl Microbiol Biotechnol* **92**:1053-1061.
5. **Premasiri WR, Gebregziabher Y, Ziegler LD.** 2011. On the Difference Between Surface-Enhanced Raman Scattering (SERS) Spectra of Cell Growth Media and Whole Bacterial Cells. *Appl. Spectrosc.* **65**:493-499.
6. **Walter A, Marz A, Schumacher W, Rosch P, Popp J.** 2011. Towards a fast, high specific and reliable discrimination of bacteria on strain level by means of SERS in a microfluidic device. *Lab Chip* **11**:1013-1021.
7. **Prucek R, Ranc V, Kvitek L, Panacek A, Zboril R, Kolar M.** 2012. Reproducible discrimination between Gram-positive and Gram-negative bacteria using surface enhanced Raman spectroscopy with infrared excitation. *Analyst* **137**:2866-2870.

8. **Stephen KE, Homrighausen D, DePalma G, Nakatsu CH, Irudayaraj J.** 2012. Surface enhanced Raman spectroscopy (SERS) for the discrimination of *Arthrobacter* strains based on variations in cell surface composition. *Analyst* **137**:4280-4286.
9. **Zhang L, Xu J, Mi L, Gong H, Jiang S, Yu Q.** 2012. Multifunctional magnetic–plasmonic nanoparticles for fast concentration and sensitive detection of bacteria using SERS. *Biosensors and Bioelectronics* **31**:130-136.
10. **Xie Y, Xu L, Wang Y, Shao J, Wang L, Wang H, Qian H, Yao W.** 2013. Label-free detection of the foodborne pathogens of Enterobacteriaceae by surface-enhanced Raman spectroscopy. *Analytical Methods* **5**:946-952.
11. **Chu H, Huang Y, Zhao Y.** 2008. Silver Nanorod Arrays as a Surface-Enhanced Raman Scattering Substrate for Foodborne Pathogenic Bacteria Detection. *Appl. Spectrosc.* **62**:922-931.
12. **Wu X, Xu C, Tripp RA, Huang Y-w, Zhao Y.** 2013. Detection and differentiation of foodborne pathogenic bacteria in mung bean sprouts using field deployable label-free SERS devices. *Analyst* **138**:3005-3012.